Chapter – 6 (A)

Synthesis and study of antimicrobial, anti-tubercular and anticancer activities of

(E)-2-Aryl-4-[{N'-(6-bromo-/6-chloro-2-methylquinolin-4-yl)hydrazono}methyl]-5-methyl-1,3-oxazole and their docking study.

6.1 Introduction

In continuation with our interest in the synthesis of new heterocyclic compounds inclusive of the 1,3-oxazole unit, in this part of the chapter, several new compounds having 1,3-oxazole heterocycle linked with quinoline moiety via the hydrazine linkage have been prepared. All the newly synthesized compounds are screened for their biological activities including antimicrobial, anti-tubercular and anticancer activities.

Cancer may result in malicious diseases that may distress different parts of the body. Fast and uncontrolled formation of abnormal cells, which may accumulate together to form a tumour or disseminate all through the body creating anomalous growth at other sites are the distinguished characteristics of this malignant disease.[1] This process may lead to death of the patient if it is not controlled. With respect to their mechanism of action, anticancer agents can be classified such as DNA-interactive agents, hormones, anti-tubulin agents, monoclonal antibodies, antimetabolites, molecular targeting agents and other biological agents.[1]

An anticancer drug acts by killing cancer cells and stopping its multiplication or its growth at some point in their life cycle.[2] An ideal anticancer drug is expected to kill or inhibit the growth of cancer cells without distressing the normal cells.[2] As this ideal condition is challenging to accomplish, the important aspect of the ongoing research to synthesise or modify known drugs is continued. Therefore to develop and design novel scaffold as potential chemotherapeutic agent for the treatment of cancer is a sustained need now a days.

One of the biggest threats still at present to the human is tuberculosis (TB), which is mainly caused by *Mycobacterium tuberculosis* (MTB) and is a sort of lung infection.[3] With the appearance of multi-drug resistant (MDR-TB) and the extensively drug resistant (XDR-TB) strains, the TB situation may become even worst.[4] Even though the existing method of treatment is highly effective against tuberculosis, the side effects, the long duration of treatment and the potential for drug-drug interactions are issues that highlight the requirement of new anti-TB drugs.[5] Moreover *M. tuberculosis* is resistant to some of the first and second line drugs and hence some novel efficient drugs and advanced strategies are essential to treat tuberculosis.[6]

For the development of a new drug it is always beneficial to modify a known pharmacophore; the hybrid molecules are the most popular chemical entities to work upon for developing modified scaffolds with much enhanced and remarkable properties in the area of biology as well as medicinal science and that could be accomplished by the combination of structural features of two differently active moieties.[7–9]

It is thought that the existence of two or more pharmacophores in a single unit synergise their biological effects and may also increase their ability to inhibit more than one biological targets.[10]

It is well known that heterocyclic entities play an important role in designing a new class of structurally diverse molecules for medicinal applications.[11] Because of the broad spectrum of biological activities among all the heterocyclic compounds, quinoline and its derivatives are pharmacologically important.[12–16] Quinoline derivatives are important key building blocks for many naturally occurring bioactive compounds,[17] specially quinoline alkaloids which are found in many different plants[18–20] and hence quinoline derivatives have attracted much attention from chemists as well as biologists.

Quinoline containing compounds display a wide range of biological activities including insecticidal,[21] antimicrobial,[22] antimalarial,[23] anti-amoebic,[24] antiasthmatic,[25] analgesic,[26] vasorelaxing,[27] antidiabetic,[28] antimicobcterial,[29,30] anticancer,[31,32] anti-inflammatory,[33] antihypertensive,[34] antiulcer[35] and anti-HIV[36] activities.

Some of the quinoline based clinically used drug molecules are presented in **Figure 6.1**.

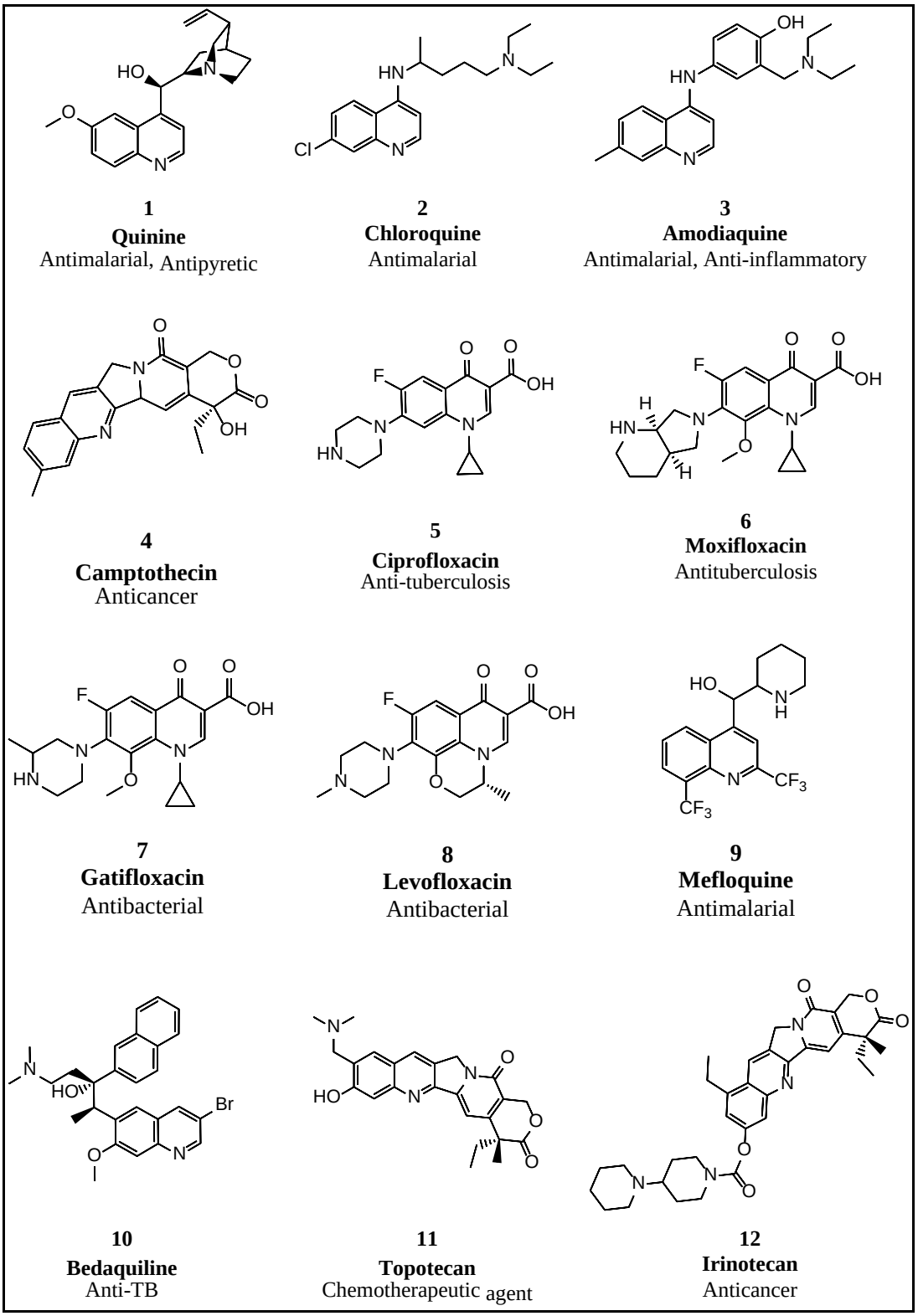

1
Quinine
Antimalarial, Antipyretic

2
Chloroquine
Antimalarial

3
Amodiaquine
Antimalarial, Anti-inflammatory

4
Camptothecin
Anticancer

5
Ciprofloxacin
Anti-tuberculosis

6
Moxifloxacin
Antituberculosis

7
Gatifloxacin
Antibacterial

8
Levofloxacin
Antibacterial

9
Mefloquine
Antimalarial

10
Bedaquiline
Anti-TB

11
Topotecan
Chemotherapeutic agent

12
Irinotecan
Anticancer

Figure 6.1 ***Clinically used quinoline based drugs.***

Structural Requirements For Quinoline Compounds To Act As Anti-tubercular And Anticancer Agents[37,38]

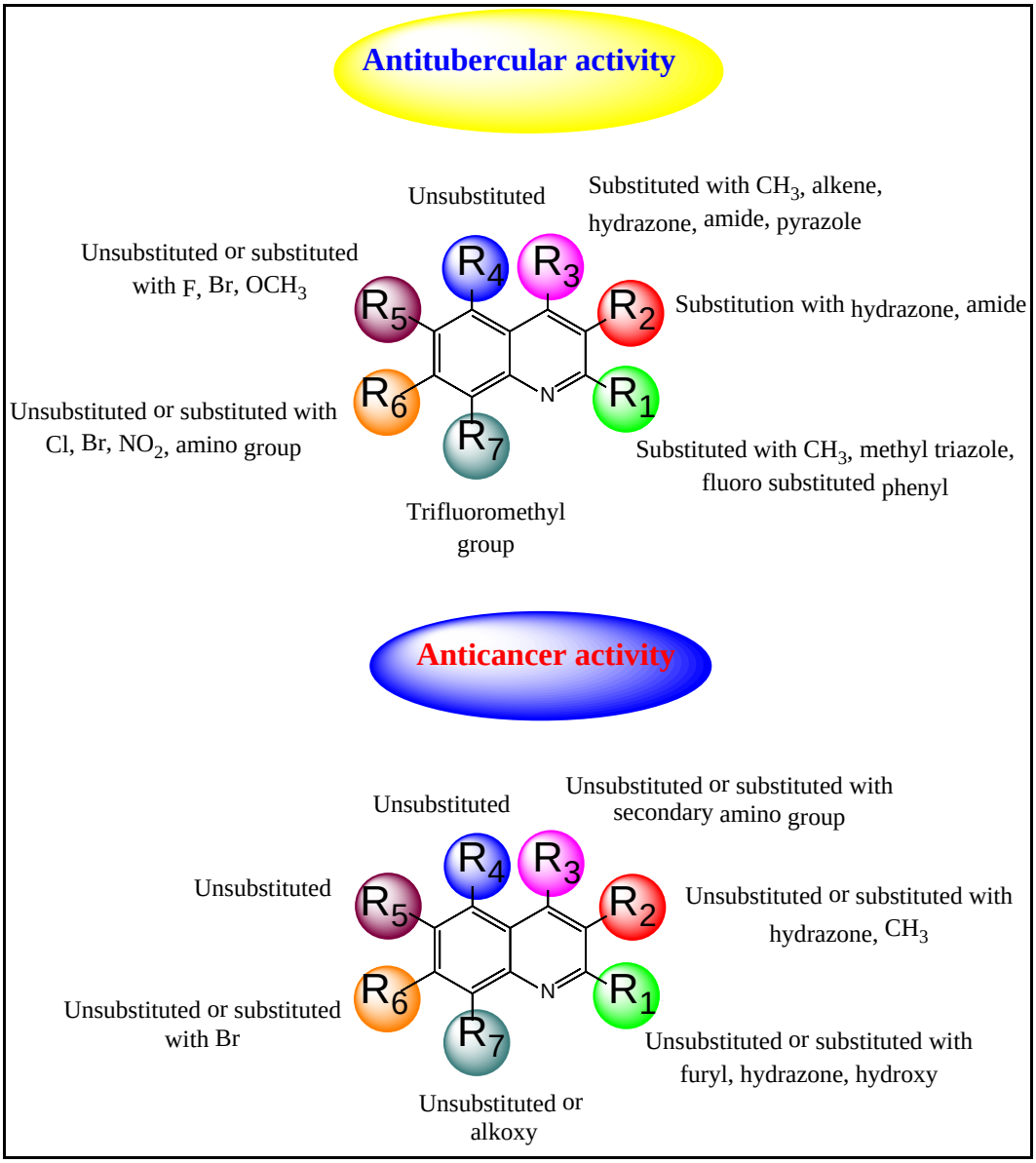

Figure 6.2 ***Structural requirements around quinoline nucleus for anti-TB and anticancer activity.***

According to the recent literature study, it is observed that differently substituted quinoline at the all positions have resulted in effective anti-TB and anticancer activities. Unsubstituted or R_1-position substituted with heterocyclic aromatic groups exhibits a good activity. Similarly, it is observed that unsubstituted R_4 and R_5-position of the quinoline along with the other conditions improve the anticancer activity (**Figure 6.2**).

The unsubstituted or substitution of secondary amino, alkyl or hydrazone group at R_2 or R_3-position of quinoline improves anticancer activity (**Figure 6.2**). The R_6 or R_7-position unsubstituted or substituted with halogen such as Br and R_7 position unsubstituted facilitate anticancer activity (**Figure 6.2**).

The unsubstituted R_4-position of the quinoline improves the anti-TB activity. Substitution of alkyl or bulky aromatic groups at R_1-position exhibits a good anti-TB activity (**Figure 6.2**). The substitution of functional groups like halogens, alkene linker, hydrazones, and amide derivatives or heteroaryl groups at R_2 or R_3-position of the quinoline show encouraging anti-TB activity (**Figure 6.2**). The positions R_5 or R_6-of quinoline may be unsubstituted or substituted with various functional groups like halogens, nitro, amino, 5-nitrofuran, dialkylamino, 4-fluorophenoxy, dimethylamino groups. The quinoline with trifluoro methyl ($-CF_3$) group at R_7 position shows a good anti-TB activity (**Figure 6.2**).

A wide spectrum of biological activities of quinoline and its derivatives have been reviewed.[39,40] A series of biologically important 7-chloro-4-quinolinylhydrazone derivatives (**13)** (**Figure 6.3**) were prepared and evaluated for their anti-tuberculosis activity.[41] A series of fluorine containing novel quinoline hydrazone derivatives (**14)** (**Figure 6.3**) were prepared and screened for their anti-tuberculosis activity.[42] New 4-hydroxy-8-trifluoromethyl-quinoline derivatives (**15)** (**Figure 6.3**) were synthesized and screened for their anti-TB activity against various strains of Mycobacterium.[43]

A novel series of aryl methylidine derivatives of quinoline-thiazolidinone hybrid **16** (**Figure 6.3**) were synthesized and evaluated for their *in vitro* antimalarial activity.[44] A series of new triazolyl-quinoline hybrid derivatives **17** (**Figure 6.3**) were synthesized and evaluated against *L. donovani* for their *in vitro* anti-leishmanial activity.[45] Some new quinoline-pyrazole hybrid scaffolds **18** (**Figure 6.3**) were synthesized and evaluated for their anti-inflammatory activity.[46] A series of new sulfonamide and sulfonate derivatives of quinoline **19** (**Figure 6.3**) were prepared and studied for their potent β-glucuronidase inhibitory activity.[47] Several quinoline derivatives with different linkers to ancillary phenyl ring **20** (**Figure 6.3**) were synthesized and evaluated for *in vitro* anti-HIV-1 activity.[48]

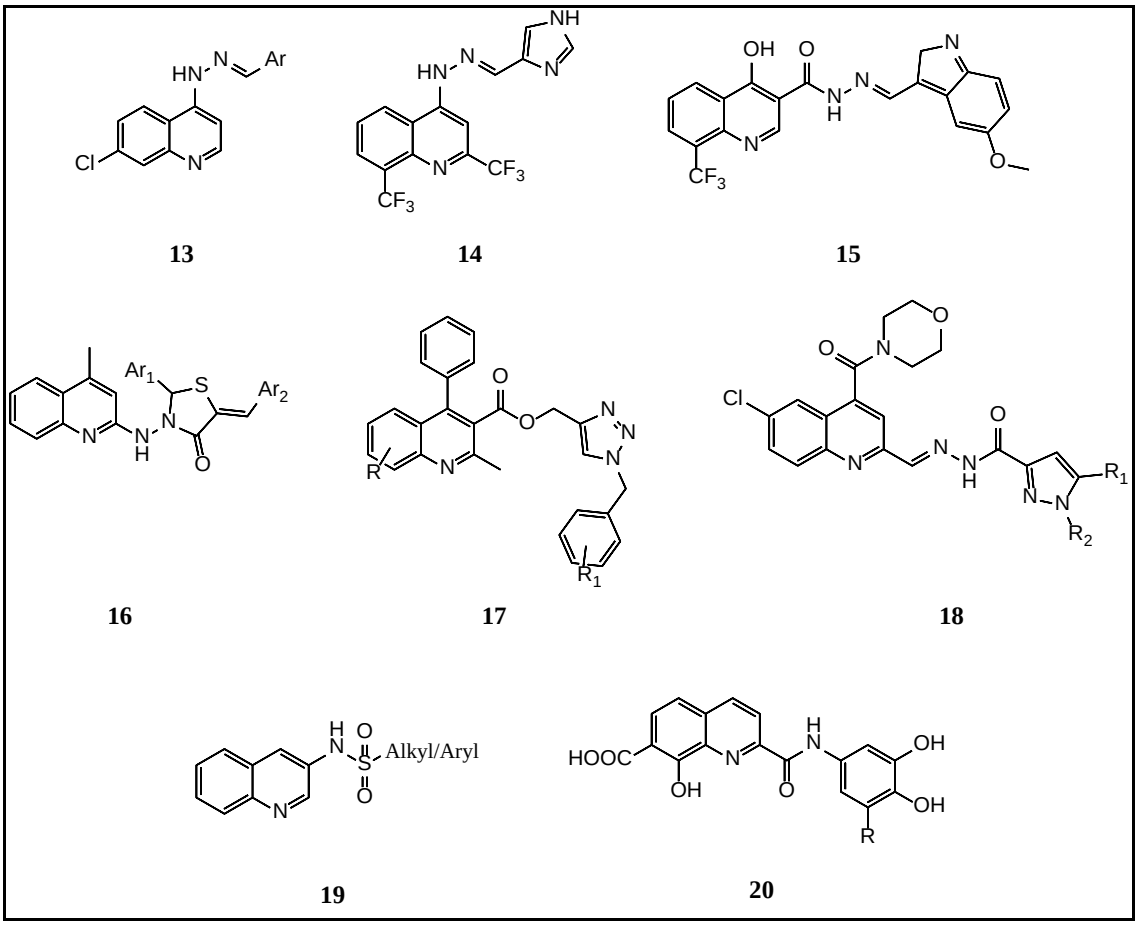

Figure 6.3 ***Biologically active Quinoline compounds.***

Several tetrahydroquinoline derivatives (**21)** (**Figure 6.4**) possessing hydrazone linkage were synthesized and evaluated for their anti-cancer activity against breast cancer MCF7 cell line.[49] Some new quinoline containing hydrazone derivatives (**22)** (**Figure 6.4**) were prepared and evaluated as anticancer agents.[50] Several new quinoline-based thiosemicarbazones (**23)** (**Figure 6.4**) were prepared and evaluated for their antitumor activity.[51] Several new hydrazone bearing quinolines (**24)** (**Figure 6.4**) were synthesized and studied as anticancer agents.[52] Some thiazolyl quinoline hydrazones (**25)** (**Figure 6.4**) were prepared and screened for their anticancer activity.[53]

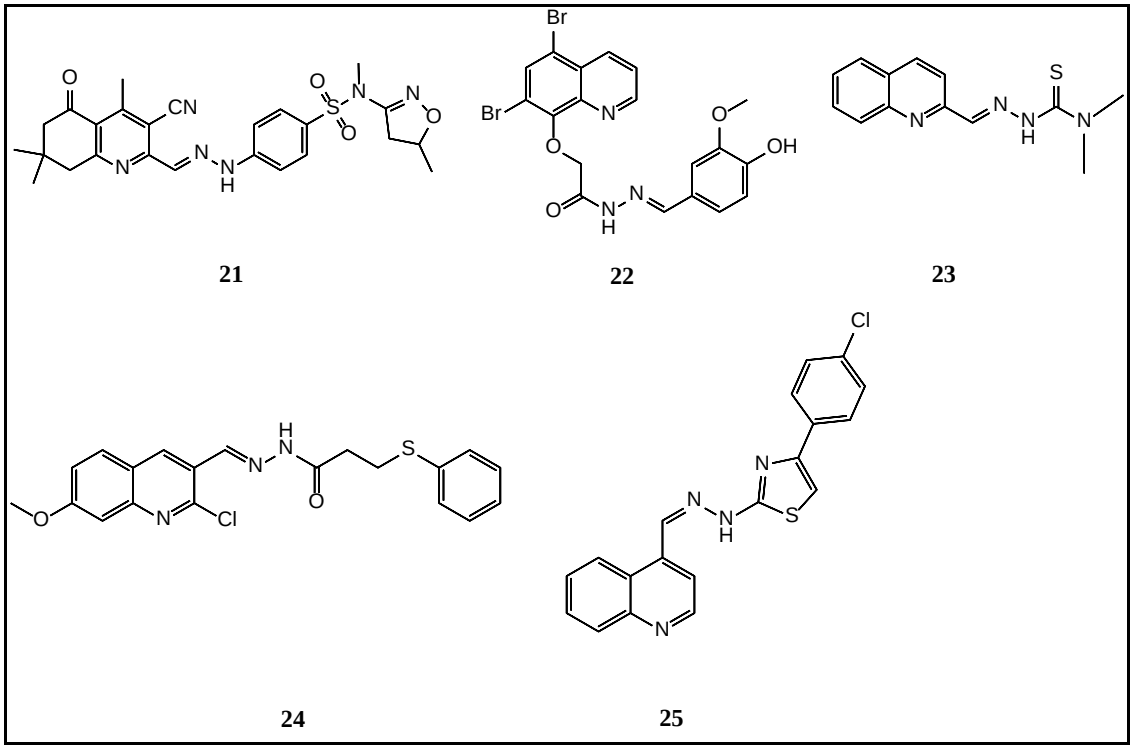

Figure 6.4 ***Quinoline hydrazones as anticancer agents.***

6.2 Results and Discussion

Since past few decades, the synthesis of hybrid molecules and their evaluation as pharmacological agents and as potent drugs have been under constant growth. Keeping in mind the medicinal importance of the quinoline compounds and hydrazone linked heterocycles in the field of medicinal chemistry, it is decided to synthesize and study some new target hybrid molecules possessing two pharmacophores with an intention to obtain enhanced biological activities.

In this part of the chapter, some oxazolyl quinoline hydrazones are prepared from 6-bromo/6-chloro-2-methyl-quinolin-4-yl-hydrazines **29a/b** and 2-aryl-5-methyl-1,3-oxazole-4-carbaldehydes **30a-f** and are evaluated for their biological activities.

The synthesis of the desired compounds started with the preparation of 6-bromo/6-chloro-2-methyl-quinolin-4-yl-hydrazines **29a/b** from the corresponding 4-bromo/chloro anilines **26** on reaction with ethyl acetoacetate in the presence of polyphosphoric acid.[54,55] (**Scheme 6.1**). The structures of the quinolyl hydrazines were confirmed with the help of spectroscopic techniques and by comparing the melting points with the reported ones.[56]

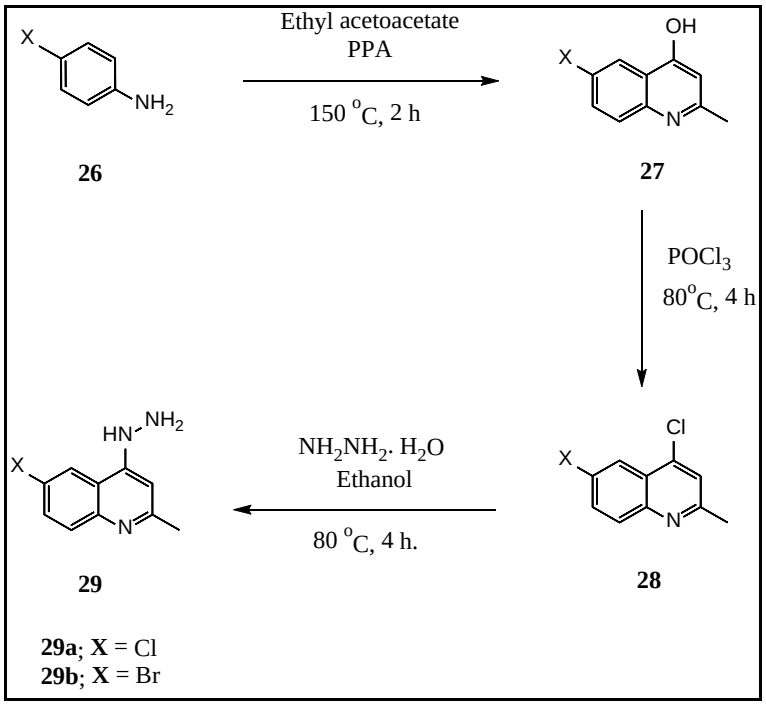

Scheme 6.1 ***Synthesis of quinolyl hydrazines.***

Some of the 2-(phenyl)-5-methyl-1,3-oxazole-4-carbaldehydes were reported earlier using some other synthetic routs as patents and were not fully characterized.[57–61]

To synthesize the final target molecules 2-aryl-4-[{2-(6-bromo-2-methylquinolin-4-yl)hydrazono}methyl]-5-methyl-1,3-oxazoles **31a-l,** the reaction between 2-aryl-5-methyl-1,3-oxazole-4-carbaldehydes **30a-f** and 6-bromo/6-chloro-2-methyl-quinolin-4-yl-hydrazine **29a/29b** was carried out in ethanol as a solvent[54,55] (**Scheme 6.2**).

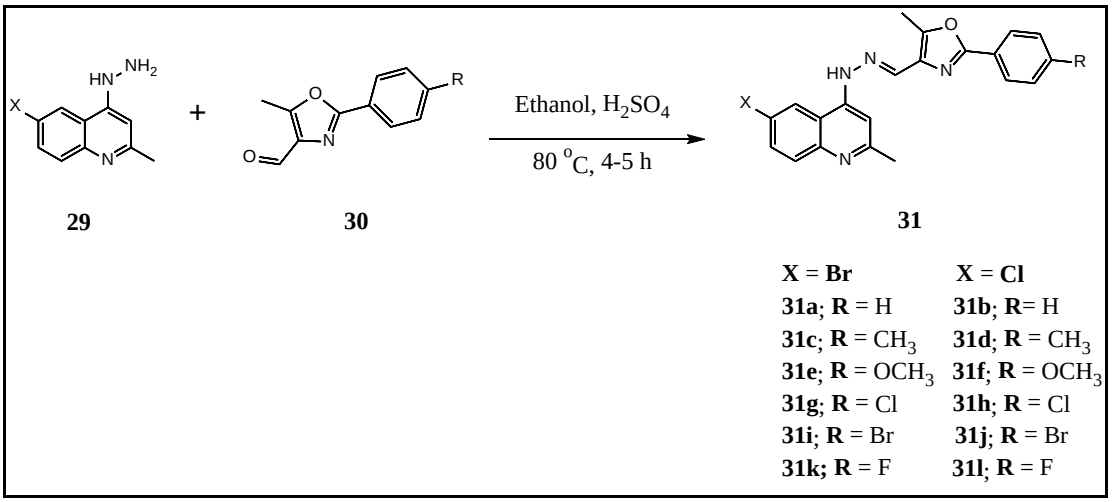

Scheme 6.2 ***Synthesis of oxazolyl quinoline hydrazones.***

6.2.1 Spectral Characterization

All the newly synthesized aryl-6-bromo/6-chloro-methylquinolinyl-hydrazono-1,3-oxazoles **31a-l** are characterized using various spectroanalytical techniques and the results are in full agreement with their proposed structures.

In the IR spectra of aryl-6-bromo/6-chloro-methylquinolinyl-hydrazono-1,3-oxazoles **31a-l** the characteristic N–H stretching is observed at ~3200-3295 cm^{-1}. Stretching band of C=N is observed as a strong to medium intensity band between ~1554-1560 cm^{-1}. The bands at ~1500 cm^{-1} and ~1600 cm^{-1} are for aromatic C=C stretching frequency. For all the compounds C-O stretching frequencies are observed at ~1260 cm^{-1} and ~1070 cm^{-1}. C-Cl and C-Br stretching for compound possessing (R_1 = Cl) and (R_1 = Br) as a substituents are observed at ~850 cm^{-1} and ~770 cm^{-1}.

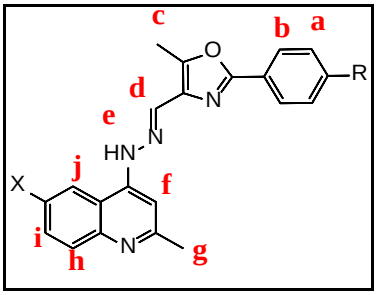

Figure 6.5 ***Compound 31 with proton labels.***

The newly synthesized quinolinyl-hydrazino-oxazoles **31a-l** (**Figure 6.5**) show characteristic ^{1}H NMR signals with distinct chemical shifts for different kinds of protons. For all the compounds methyl protons **c** on oxazole ring observed at δ 2.68 ppm and the methyl protons **g** of quinoline methyl group are found at δ 2.69 ppm. For compounds **31e** (R_2 = OCH_3) and **31f** (R_2 = OCH_3) the –OCH_3 protons appear at δ 3.8 ppm. The methylene proton **d** of imine linkage (-N═CH-) is observed as a singlet between δ 7.2-7.3 ppm and N–H proton **e** of the hydrazine group is observed most downfield between δ 12.0-14.0 ppm as a singlet. The aromatic protons **a** and **b** are observed at δ 7.6 ppm and δ 7.9 ppm respectively as a doublet with the coupling constant J = 8.4 Hz. The aromatic protons **h** and **i** of the quinoline ring are observed at δ 7.8 and δ 8.1 ppm as doublets with the coupling constant J = 8.8 Hz. While the aromatic protons **f** and **j** of quinoline ring are observed at δ 8.4-8.5 and δ 8.6-8.7 ppm as singlets.

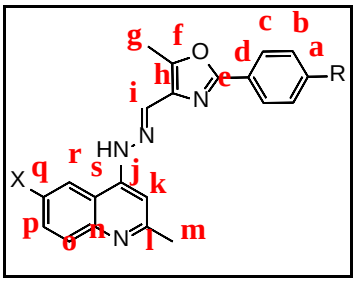

Figure 6.6 ***Carbon labels on compound 31.***

In ^{13}C NMR spectra of the hybrid molecules **31a-l** (**Figure 6.6**) oxazole ring methyl carbon **g** (-CH_3) gives signal at δ 10.9 ppm and the methyl carbon **m** is observed at δ 20.7 ppm. For the compound having an additional (-CH_3) group as a substitution, gives signal at δ 21 ppm. The –OCH_3 carbon of compounds (**31e** and **31f,** R = -OCH_3)

appear at δ 55.8 ppm. The imine carbon **i** (-C=N) is observed at δ 150.7 ppm. The aromatic carbon signals are observed in between δ 100 to 162 ppm.

All the final aryl-6-bromo/6-chloro-methylquinolinyl-hydrazono-1,3-oxazoles **31a-l** are analyzed with the help of Waters' Xevo G2-XS QToF mass spectrometer. The molecular ion peaks were observed as $(M)^+$ accompanied with $(M+H)^+$ for most of the compounds. Due to the presence of bromine, M: M+2 mass peaks were observed having intensity ratio ~1:1. And the presence of chlorine confirmed by the 3:1 intensity ratio of the mass peaks M: M+2.

Table 6.1 ***Experimental data (final step yield, mp) of the final new compounds.***

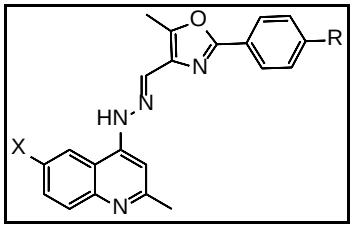

ID	Substitution		Molecular formula	Yield	mp
	X	R			
31a	-Br	-H	$C_{21}H_{17}BrN_4O$	80 %	204 ^oC
31b	-Cl	-H	$C_{21}H_{17}ClN_4O$	79 %	190 ^oC
31c	-Br	$-CH_3$	$C_{22}H_{19}BrN_4O$	82 %	210 ^oC
31d	-Cl	$-CH_3$	$C_{22}H_{19}ClN_4O$	80 %	202 ^oC
31e	-Br	$-OCH_3$	$C_{22}H_{19}BrN_4O_2$	78 %	192 ^oC
31f	-Cl	$-OCH_3$	$C_{22}H_{19}ClN_4O_2$	76 %	184 ^oC
31g	-Br	-Cl	$C_{21}H_{16}BrClN_4O$	80 %	194 ^oC
31h	-Cl	-Cl	$C_{21}H_{16}Cl_2N_4O$	76 %	188 ^oC
31i	-Br	-Br	$C_{22}H_{19}BrN_4O$	80 %	208 ^oC
31j	-Cl	-Br	$C_{21}H_{16}BrClN_4O$	78 %	198 ^oC
31k	-Br	-F	$C_{21}H_{16}BrFN_4O$	82 %	206 ^oC
31l	-Cl	-F	$C_{21}H_{16}ClFN_4O$	80 %	200 ^oC

6.2.2 Anti-tubercular Activity Study

As discussed in the beginning, quinoline compounds possessing hydrazone moiety are known to possess a good anticancer and anti-tubercular activities. With this back ground, anti-tubercular activity of all the newly synthesized 6-bromo/6-chloro-methylquinolinyl-hydrazono-aryl-1,3-oxazoles **31a-l** was studied against *Mycobacterium tuberculosis* H37Rv. Isoniazid was used as a reference drug standard. The standard experimental procedure was followed as discussed earlier in chapter-V.

Results of the *in vitro* anti-tubercular activity are summarised in **Table 6.2** and graphically presented as **Figure 6.7**.

Table 6.2 ***Anti-tubercular activity results.***

Entry	X	R	Inhibition (%) (at 250 µg/mL)	MIC (µg/mL)
31a	-Br	-H	**94**	**25**
31b	-Cl	-H	**95**	**25**
31c	-Br	$-CH_3$	**93**	**50**
31d	-Cl	$-CH_3$	**95**	**50**
31e	-Br	$-OCH_3$	**92**	**50**
31f	-Cl	$-OCH_3$	**97**	**25**
31g	-Br	-Cl	**92**	**50**
31h	-Cl	-Cl	86	100
31i	-Br	-Br	**96**	**25**
31j	-Cl	-Br	**93**	**50**
31k	-Br	-F	**91**	**50**
31l	-Cl	-F	82	----
Isoniazide			99	0.1

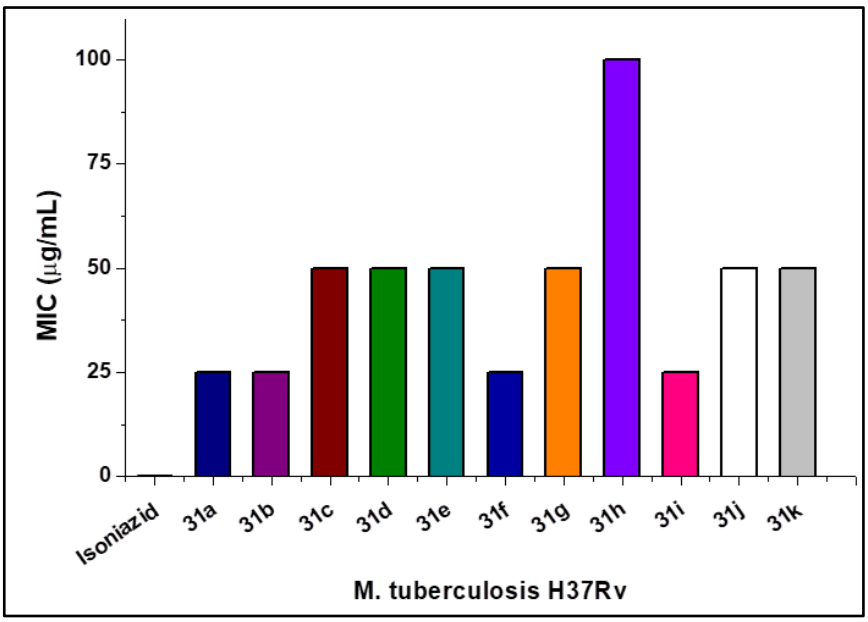

Figure 6.7 *Anti-tubercular activity (MIC) results.*

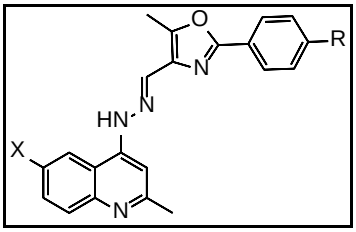

Figure 6.8 ***General structure of compound 31.***

Most of the aryl-6-bromo/6-chloro-methylquinolinyl-hydrazono- 1,3-oxazoles **31a-l** except **31h** (X/R = Cl) (MIC = 100 μg/mL) displayed significant inhibition activity against *M. tuberculosis* H37Rv with MIC ≤ 50 μg/mL (**Table 6.2** and **Figure 6.7**). Among them four compounds **31a** (X = Br, R = H), **31b** (X = Cl, R = H) **31f** (X = Cl, R = OCH_3), **31i** (X = Br, R = Br) are the most active compounds with MIC = 25 μg/mL (**Figure 6.7**). the remaining active compounds **31a**, **31d**, **31c**, **31g**, **31j** and **31k** show moderate activity with MIC = 50 μg/mL.

6.2.3 Molecular Docking Study

Molecular modelling studies of synthesized compounds were performed in order to recognize the feasible binding mode of the compounds. Considering enoyl-ACP reductase as the target receptor, docking studies was performed to determine the best in silico conformation. The native crystal structure of enoyl-ACP reductase downloaded

from Protein Data Bank with the (**PDB ID2H7M**). Docking simulation was done with the aid of Schrödinger Maestro-11.5. The protein structures obtained from the protein data bank (PDB) were initially subjected to various processes such as removal of water molecules and removal of heteroatoms etc. using the Protein Preparation Wizard of Schrödinger 2015. All the compounds (Ligands) were filtered by specifying options for screening like remove molecules that have a molecular weight of greater than 650 remove molecules with too many H-bond acceptor and donor atoms acceptor groups >3, Donor groups >3, Energy minimization was done by choosing a Ligprep (OPLS) module of Schrodinger. The docking of receptor enoyl-ACP reductase with newly prepared active molecule ligands showed interaction with one or more amino acids in the receptor active pocket. Docking score, π–H and π–π interaction of the ligand with the protein were used to prepare docking results. The best docking poses of the representative compounds in the active site of enzyme enoyl-ACP reductase are presented in **Figures 6.9**.

All the six compounds (**31b**, **31a**, **31f**, **31g**, **31h**, **31i**) displayed worthy docking score ranging from -6.67 to -10.97 (**Table 6.3**). The highest score was observed for the ligand **31b** (-10.97) (**Table 6.9)**. Compound **31f** (-7.10) showed π–π interactions with amino acid residues Phe 149 (**Figure 6.9**) while ligand **31h** (-6.71) and **31i** (-6.67) showed two common π–π interactions with amino acid residues Phe97 (**Figure 6.9**). Thus the anti-TB activity of the synthesized compounds could be due to their good interaction and inhibition activity against the MTB enzyme.

Table 6.3 ***Docking results of the active anti-TB compounds.***

ID	Docking score	Glide energy	Amino acids interacted with ligands
INH	-12.90	-52.248	Pro 193, Phe 149, Ala 157
31b	-10.97	-53.676	Ala 157, Met 155, Phe 149
31a	-7.119	-49.815	Met 199, Ala 157, Lys 165
31f	-7.10	-55.508	Met 199, Lys 165, Ala 157
31g	-6.79	-47.265	Phe 149, Met 199, Ala 157
31h	-6.71	-46.992	Phe 97, Ala 157, Pro 193
31i	-6.67	-41.105	Phe 97, Ala 157, Pro 193

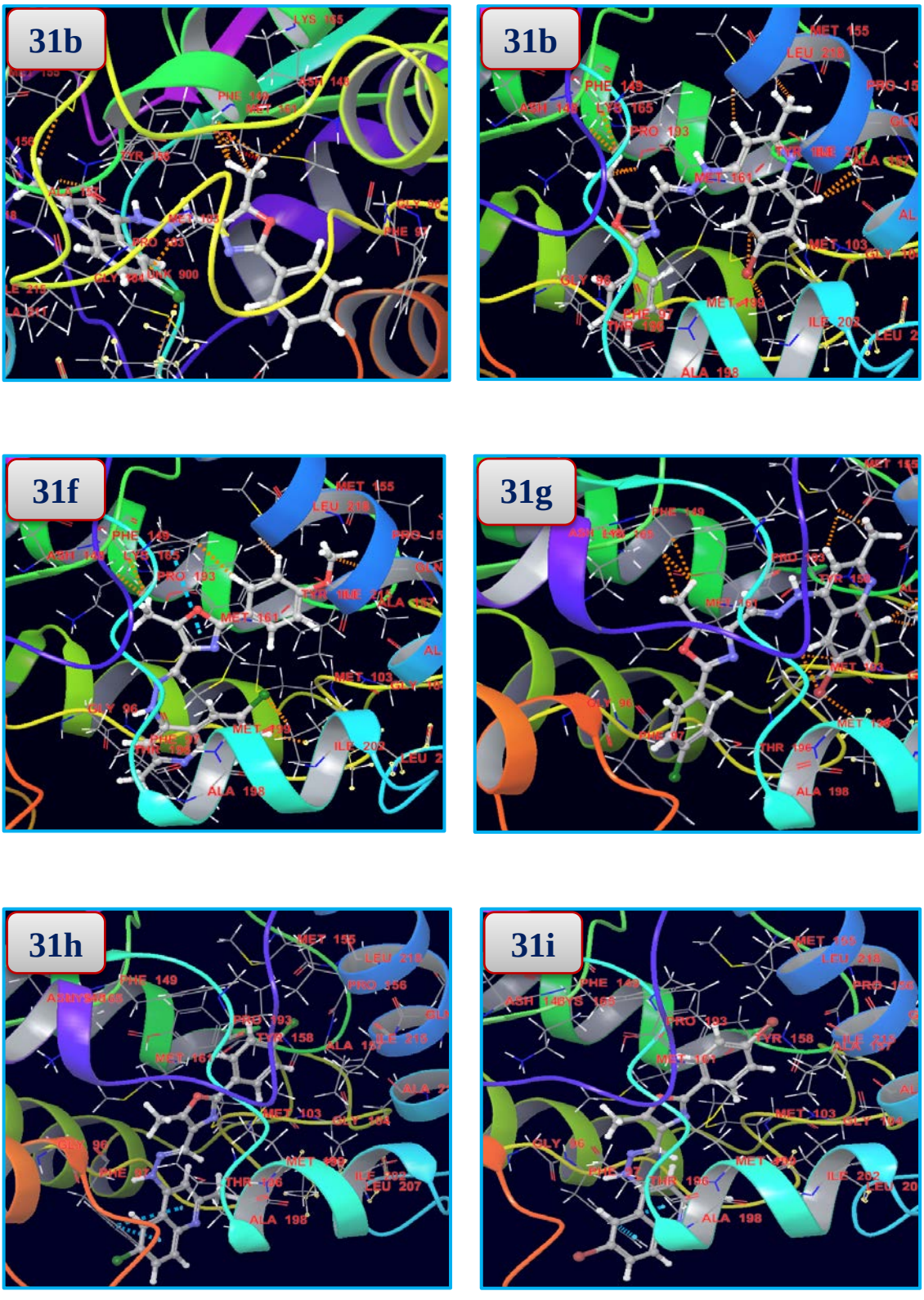

Figure 6.9 ***The docking pose of the compounds in the active pocket of enoyl-ACP reductase.***

6.2.4 Antimicrobial Activity Study

According to the literature survey, quinoline derivatives show good antimicrobial activity. To extend the study of biological activity of these compounds **31a-l,** antimicrobial activity study was carried out against (*Staphylococcus aureus* (MTCC 96), *Bacillus subtilis* (MTCC 619) as Gram positive bacteria, *Escherichia coli* (MTCC 739), *Pseudomonas aeruginosa* (MTCC 741) as Gram negative bacteria. For antifungal activity *Aspergillus niger* (MTCC 282) and *Candida albicans* (MTCC 183) were used and the paper disc diffusion technique was used. Zone of inhibition against all the six pathogenic strains were measured for all the twelve compounds and MIC were determined. Ciprofloxacin and gresiofulvin (100 µg/disc) were used as the reference compounds for antibacterial and antifungal activity respectively. Antimicrobial activity study was carried out at Microcare laboratory, Surat, Gujarat. Experimental procedure is same as discussed in Chapter-3.

Results of the *in vitro* antimicrobial activity are summarized in **Table 6.4** and are presented as graphical charts in **Figure 6.10** to **6.12**.

Table 6.4 ***Antimicrobial activity results.***

ID	Zone of inhibition in mm and (MIC in µg/mL)											
	Gram(+*ve*) bacteria				Gram(-*ve*) bacteria				Fungi			
	S. aureus		*B. subtilis*		*E. coli*		*P. aeruginosa*		*C. albicans*		*A. niger*	
	Zone (mm)	MIC (µg/mL)	Zone (mm)	MIC (µg/mL)	Zone (mm)	MIC (µg/mL)	Zone (mm)	MIC (µg/mL)	Zone (mm)	MIC (µg/mL)	Zone (mm)	MIC (µg/mL)
31a	23	25	**24**	**12.5**	**24**	**12.5**	21	100	22	50	**25**	**6.25**
31b	**26**	**6.25**	**25**	**12.5**	23	25	**24**	**12.5**	**25**	**12.5**	19	125
31c	21	100	23	25	20	100	22	50	23	25	22	50
31d	**24**	**12.5**	22	50	21	100	20	100	**24**	**12.5**	20	100
31e	23	25	22	50	**25**	**12.5**	**25**	**12.5**	23	25	**24**	**12.5**
31f	19	125	**24**	**12.5**	22	50	23	25	22	50	**25**	**6.25**
31g	**26**	**6.25**	**25**	**12.5**	23	25	**26**	**6.25**	23	25	**24**	**12.5**
31h	**27**	**6.25**	**26**	**6.25**	21	100	19	100	**25**	**12.5**	19	125
31i	20	100	21	100	**24**	**12.5**	19	125	**24**	**12.5**	23	25
31j	23	25	22	50	21	100	23	25	21	100	**24**	**12.5**
31k	22	50	**24**	**12.5**	**25**	**12.5**	**24**	**12.5**	23	25	20	100
31l	**24**	**12.5**	23	25	23	25	21	100	**24**	**12.5**	**25**	**6.25**
Ciprof-loxacin	**33**	**<3.12**	**30**	**<3.12**	**32**	**<3.12**	**31**	**<3.12**	-----		----	
Griseo-fulvin	----		----		----		----		**31**	**<3.12**	**30**	**<3.12**
DMSO	----		----		----		----		----		----	

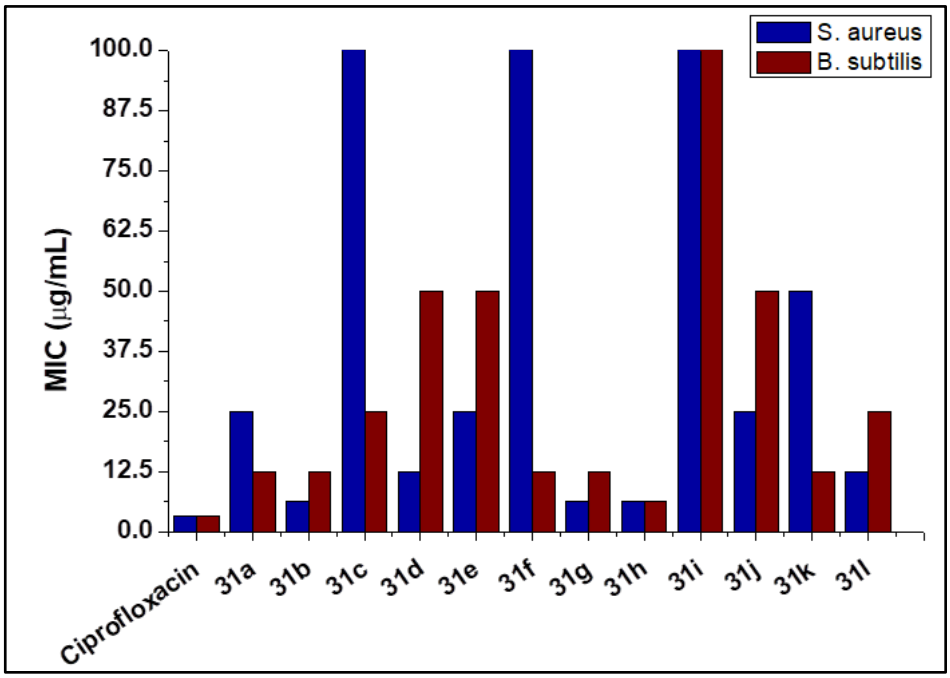

Figure 6.10 ***Antibacterial (Gram +ve) activity results.***

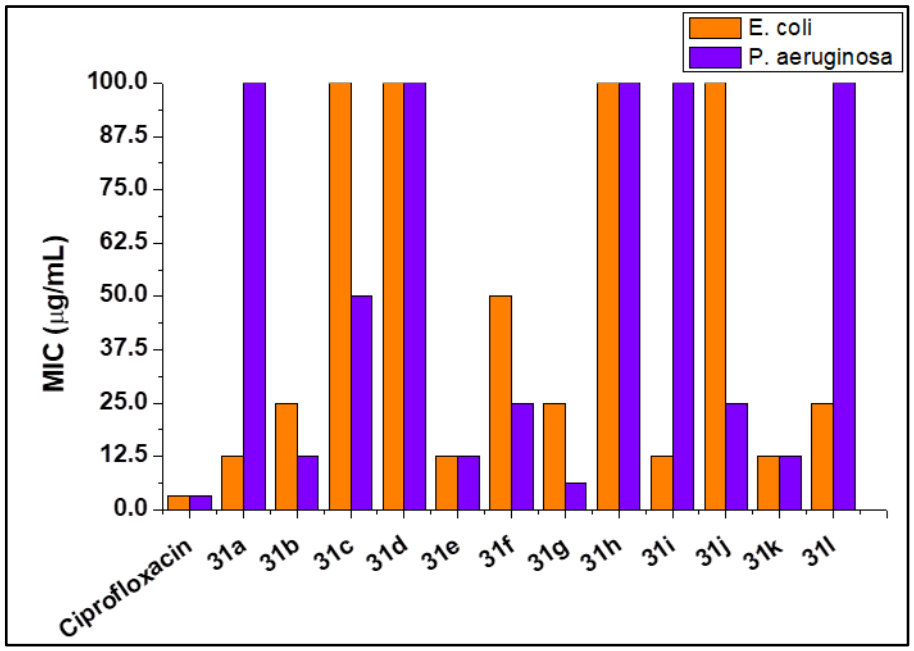

Figure 6.11 ***Antibacterial (Gram -ve) activity results.***

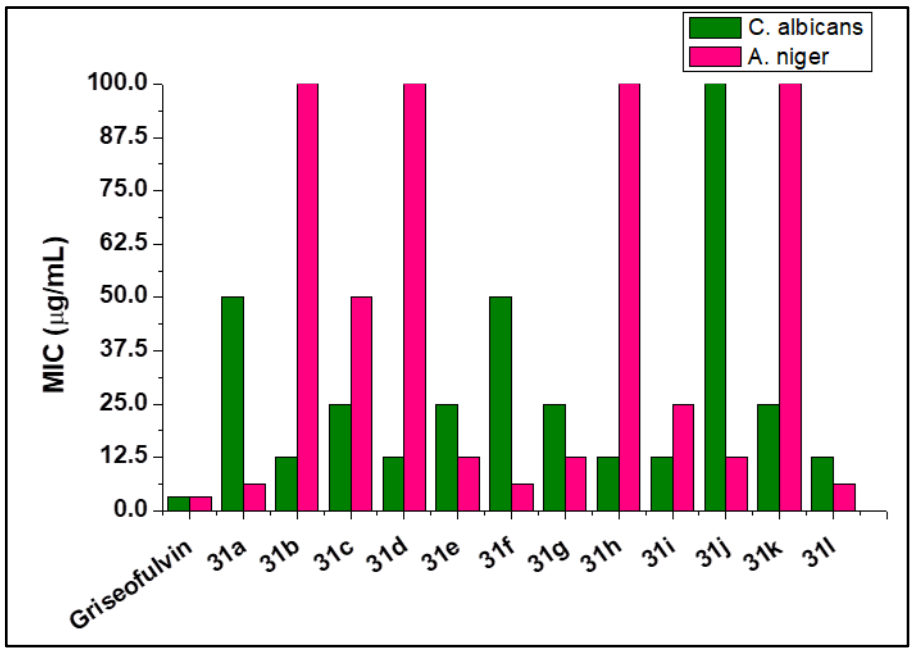

Figure 6.12 ***Antifungal activity results.***

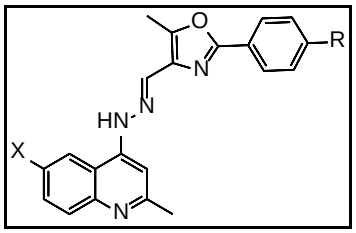

Figure 6.13 ***General structure of 31.***

The quinoline-oxazole hydrazones **31a-l** show good to excellent antimicrobial activity. For Gram *+ve* bacteria compounds **31b** (X = Br, R = H), **31g** (X = Br, R = Cl) and **31h** (X = Cl, R = Cl) displayed highest % inhibition against *S. aureus* with MIC = 6.25 µg/mL while compounds **31d** (X = Cl, R = CH_3) and **31l** (X = Cl, R = Br) showed good inhibition activity with MIC = 12.5 µg/mL (**Figure 6.10**). Against *B. subtilis* compounds **31a** (X = Br, R = H), **31b** (X = Cl, R = H), **31f** (X = Cl, R = OCH_3), **31g** (X = Br, R = Cl), **31h** (X = Cl, R = Cl), **31k** (X = Br, R = F) displayed good % inhibition and MIC 12.5 µg/mL (**Figure 6.10**). In case of Gram *-ve* bacteria, compounds **31a** (X = Br, R = H), **31e** (X = Br, R = OCH_3), **31i** (X = Br, R = Br), **31k** (X = Br, R = F) have MIC = 12.5 µg/mL with good inhibition activity against *E. coli* (**Figure 6.11**). Against *P. aeruginosa*, compound **g** showed an outstanding % inhibition with MIC = 6.25µg/mL and compounds **31b** (X = Cl, R = H), **31e** (X = Cl, R = OCH_3), **31k** (X =

Br, R = F) displayed MIC = 12.5 µg/mL against the same (**Figure 6.11**). Compounds **31b** (X = Cl, R = H), **31d** (X = Cl, R = CH_3), **31h** (X = Cl, R = Cl), **31i** (X = Br, R = Br), **31l** (X = Cl, R = F) showed an excellent activity and highest % inhibition against the fungal strain *C. albicans* while compounds **31c** (X = Br, R = CH_3), **31e** (X = Br, R = OCH_3), **31g** (X = Br, R = Cl), **31k** (X = Br, R = F) displayed moderate to good % inhibition and MIC = 25 µg/mL (**Figure 6.12**). In case of *A. niger* compounds **31a** (X = Br, R = H), **31f** (X = Cl, R = H), **31l** (X = Br, R = F) showed an outstanding % inhibition with MIC = 6.25 µg/mL and compounds **31e** (X = Br, R = OCH_3), **31g** (X = Br, R = Cl) and **31j** (X = Br, R = Br) showed good inhibition of the fungal strain with MIC = 12.5 µg/mL (**Figure 6.12**). From the antimicrobial activity data, it can be observed that all the synthesized compounds displayed outstanding antibacterial as well as antifungal activity. All the compounds showed higher inhibition against Gram +ve bacterial strains than that of Gram -ve bacterial strains. Compounds in which (X = Br) showed better activity than that of X = -Cl. It was observed that the compounds having R = -H, -Br, -Cl, -F show enhanced activity.

6.2.5 Anticancer Activity Study

All the new 6-bromo/6-chloro-methylquinolinyl-hydrazono-aryl-1,3-oxazoles **31a-l** were offered to NCI, USA for the study of their anticancer activity under the screening project at the National Cancer Institute (NCI), USA. Ten of the synthesized compounds were selected for *in vitro* single dose anticancer assay against full NCI 60 cell line panels.

Primary *in vitro* single dose anticancer assay was performed at a single dose (10 µM) and data for all the ten selected compounds **31(a-j)** and results are reported as mean graph of the percent growth of the treated cells compared to untreated control cells.

The complete results of the single dose anticancer screening (**Sheet 21-30**) of all the selected compounds in form of one dose mean graphs are included in **Appendix** at the end of the thesis.

Results of single dose study in terms of % lethality for the nine compounds which were later **selected for five dose anticancer study** are highlighted as **Figure 6.14A and 6.14B.**

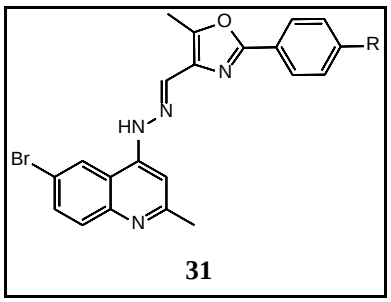

31

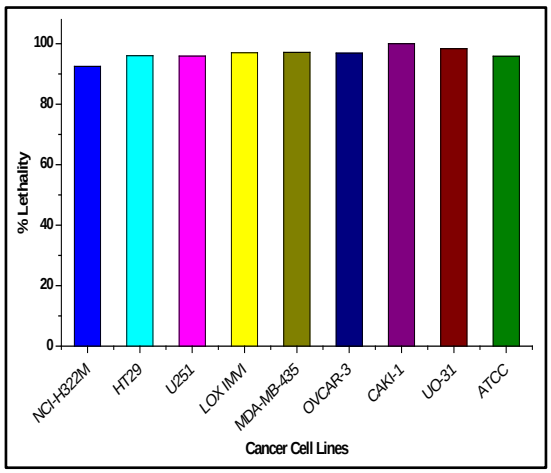

Compound 31a, R = H

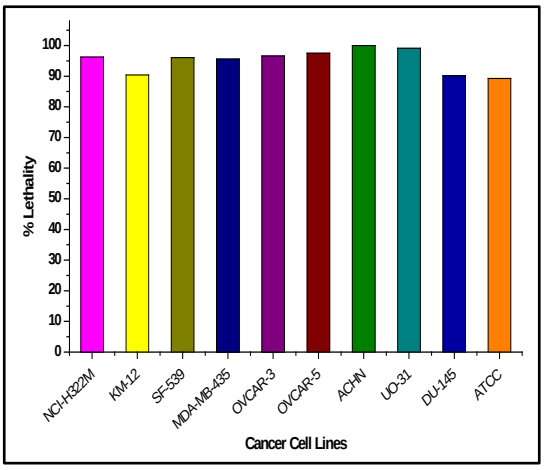

Compound 31c, R = CH_3

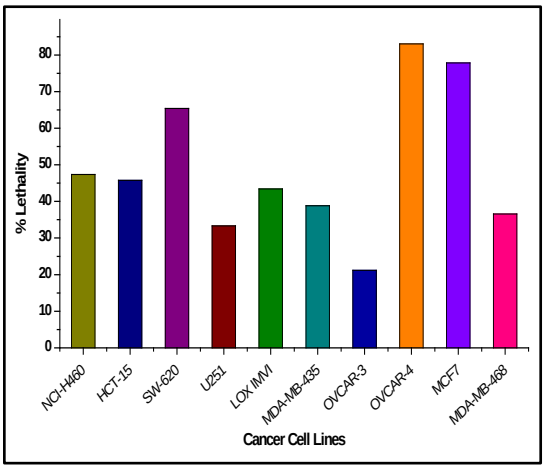

Compound 31e, R = OCH_3

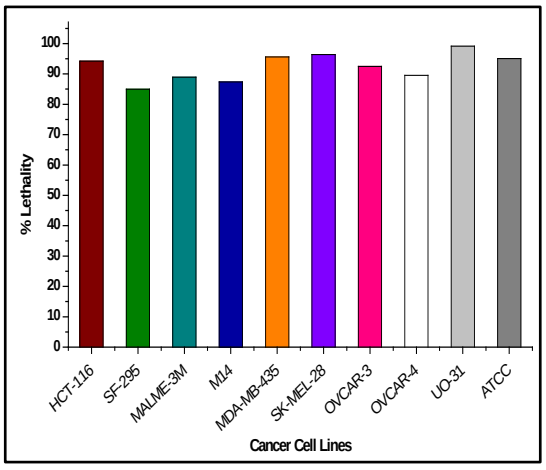

Compound 31g, R = Cl

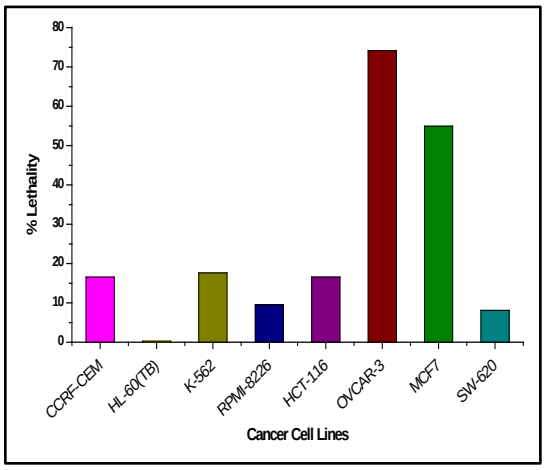

Compound 31i, R = Br

Figure 6.14A ***Single dose anticancer screening results of 31 (R_1 = Br) in terms of % lethality.***

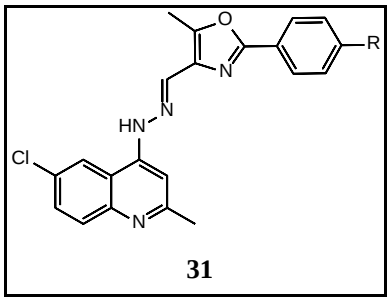

31

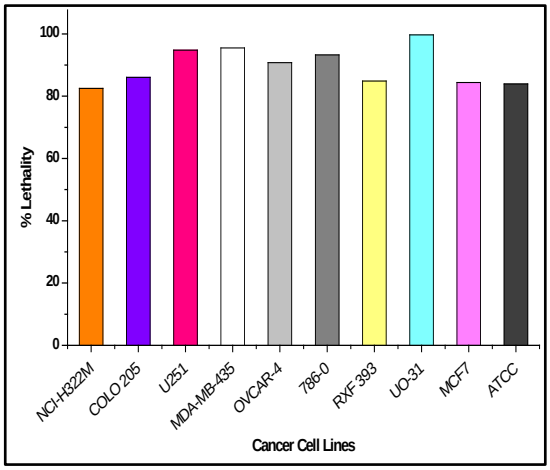

Compound 31b, R = H

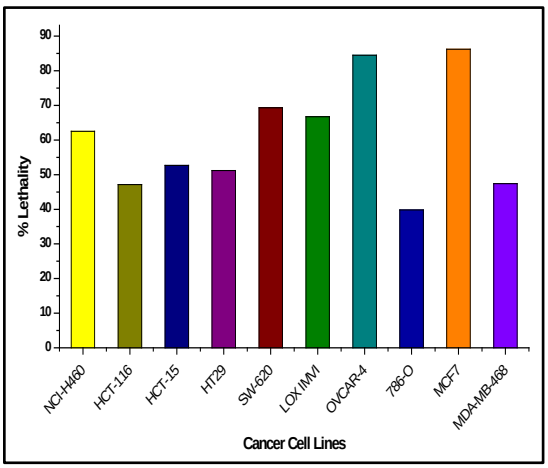

Compound 31d, R = CH_3

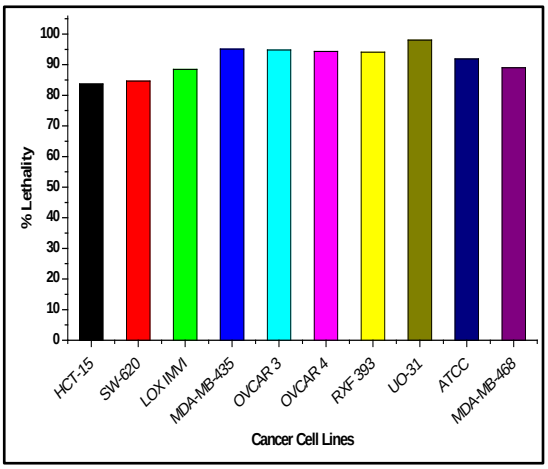

Compound 31h, R = Cl

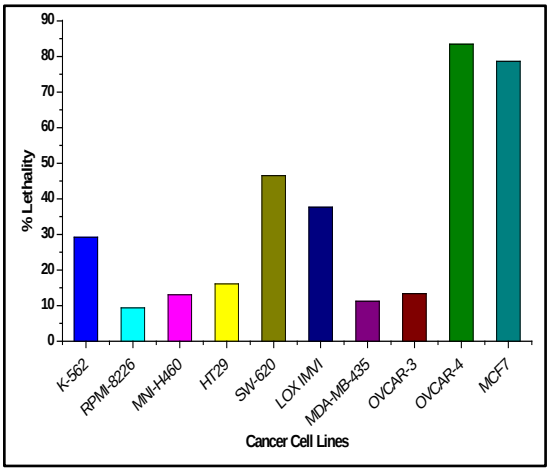

Compound 31j, R = Br

Figure 6.14B ***Single dose anticancer screening results of 31 (R_1 = Cl) in terms of % lethality.***

One Dose Study Results: Discussion

Out of the ten submitted compounds for preliminary one dose anticancer activity, nine compounds showed outstanding results as presented in **Figure 6.14A** and **Figure 6.14B**. Compound **31a (**X = Br, R = H**)** displayed excellent activity against various cancer cell lines having % lethality greater than 90% for more than ten cancer cell lines namely non-small lung cancer (NCI-H322M), colon cancer (HT29), CNS cancer (U251), melanoma cancer (LOX IMVI), ovarian cancer (OVCAR-3), renal cancer (CAKI-1), renal cancer (UO-31), breast cancer (ATCC) as presented in figures (**Figure 6.14A**). Compound **31b (**X = Cl, R = H**)**, **31c (**X = Br, R = CH_3**)**, **31g (**X = Br, R = Cl**)**, **31h (**X = Cl, R = Cl**)** which was least active against *M. tuberculosis* H37Rv showed good to outstanding activity with >85 % lethality for more than ten cancer cell lines as presented in **Figure 6.14B**. Compound **31e (**X = Br, R = OCH_3**)** showed 88% and 80% lethality against ovarian cancer (OVCAR-4) and breast cancer (MCF7) cell lines respectively (**Figure 6.14A**). Compound **31i (**X = Br, R = Br**)** displayed poor to moderate lethality with 74% and 54% lethality for ovarian cancer (OVCAR-3) and breast cancer (MCF7) cancer cell lines respectively (**Figure 6.14A**) and compound **31j (**X = Cl, R = Br**)** showed 84% lethality for ovarian cancer (OVCAR-4) and 79% lethality for breast cancer (MCF7) cell lines respectively (**Figure 6.14B**). Compounds, **31f** (X = Cl, R = OCH_3) (**Figure 6.14C**) showed moderate activity with a poor lethality on various cell lines at one dose level and was not selected for five dose study. The major inhibition % for some of the cancerous cell lines by this compound, if, are as presented in **Figure 6.14C**.

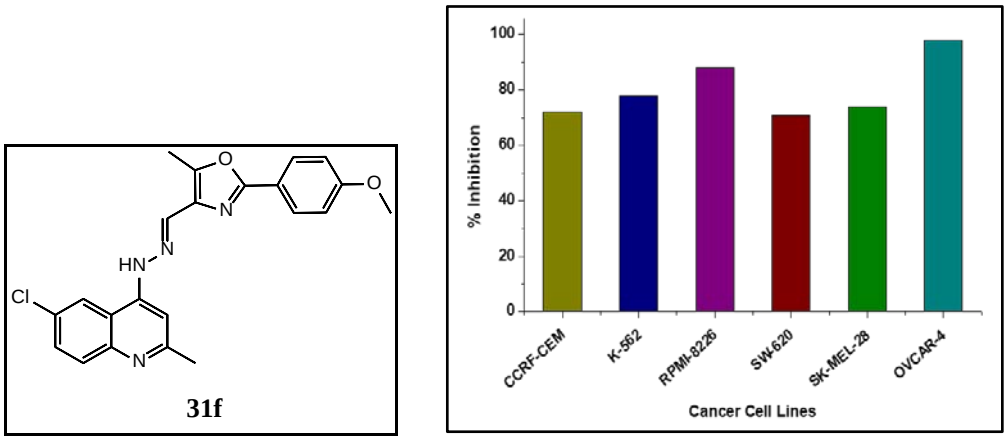

Figure 6.14C ***Single dose anticancer screening results for 31f in terms of % inhibition.***

Five Dose Study Results: Discussion

The compounds which fulfilled pre-determined criteria at a single dose of ($1x10^{-5}$ M) were selected for NCI full panel five dose study. Nine of the ten compounds except **31h** were further screened at five different concentrations (0.01, 0.1, 1, 10 & 100 μM) at the 10 fold dilution of the above concentration.

The results of the diluted solutions are presented in terms of three response parameters (GI_{50}, TGI & LC_{50}) for each cell line from log10 concentration verses % growth inhibition curves on nine different types of cancer. The GI_{50} value (growth inhibitory activity) represents the concentration of the compound which bring 50% decrease in net cell growth, the TGI value (cytostatic activity) is the concentration of the compound causing in total growth inhibition and LC_{50} value (cytotoxic activity) is the concentration of the compound which bring about net 50% loss of initial cells at the end of the incubation period of 48 h. The log molar concentration is also calculated of individual GI_{50}, TGI and LC_{50} and is represented as $log10GI_{50}$, log10TGI and $log10LC_{50}$ respectively. The results of the five dose anticancer activity screening in terms of log molar concentrations of response parameters ($log10GI_{50}$, log10TGI & $log10LC_{50}$) are included in **Appendix** from **Sheets 31 to 39**.

The dose response curve of the data package is generated by plotting the percentage growth against the log10 of the analogous concentration for every cell line. The cell line curves are clustered by sub panel. Horizontal lines are provided at the PG values of +50, 0 and -50. The concentrations matching to points where the curves cross these lines (+50, 0 & -50) are the GI_{50}, TGI and LC_{50}, correspondingly.

The dose response curves for all cell lines in the NCI 60 panel exposed to tested 2compounds are colour-coded by tissue of origin: red, Leukaemia cell line; blue, Lung cancer; green, Colon cancer; grey, CNS cancer; coral, Melanoma; purple, Ovarian cancer; gold, Renal cancer; turquoise, Prostate cancer and pink, Breast cancer (**Figure 6.15, 6.18, 6.21, 6.24, 6.27, 6.30, 6.33, 6.36, 6.39**).

The dose response curves (% growth verses sample concentration at NCI fixed protocol, μM) for all cell lines with different sub panel are obtained from the NCI against a diverse panel of 60 human tumour cell lines in a culture derived from nine cancer diseases of the tested active compounds. These dose response curves of each

tested compound for each cell line were measured at five dose concentrations and the cell lines with original tissue colour coded, shapes are indicative of growth percentage inhibition at the concentration of the tested compounds are shown in **Figure 6.16, 6.19, 6.22, 6.25, 6.28, 6.31, 6.34, 6.37, 6.40**.

The mean graph was generated from a set of GI_{50}, TGI and LC_{50} values to highlight the degree of difference of activity of the compounds on various human cancer cell lines and to simplify visual scanning of data for potential patterns of selectivity for specific cell lines or for precise subpanels with respect to a designated response parameter.

The log of molar concentration of the tested compounds was also calculated of individual GI_{50}, TGI and LC_{50} and presented as log10GI_{50}, log10TGI, log10LC_{50} respectively and obtained values are presented in **Figure 6.17, 6.20, 6.23, 6.26, 6.29, 6.32, 6.35, 6.38, 6.41**.

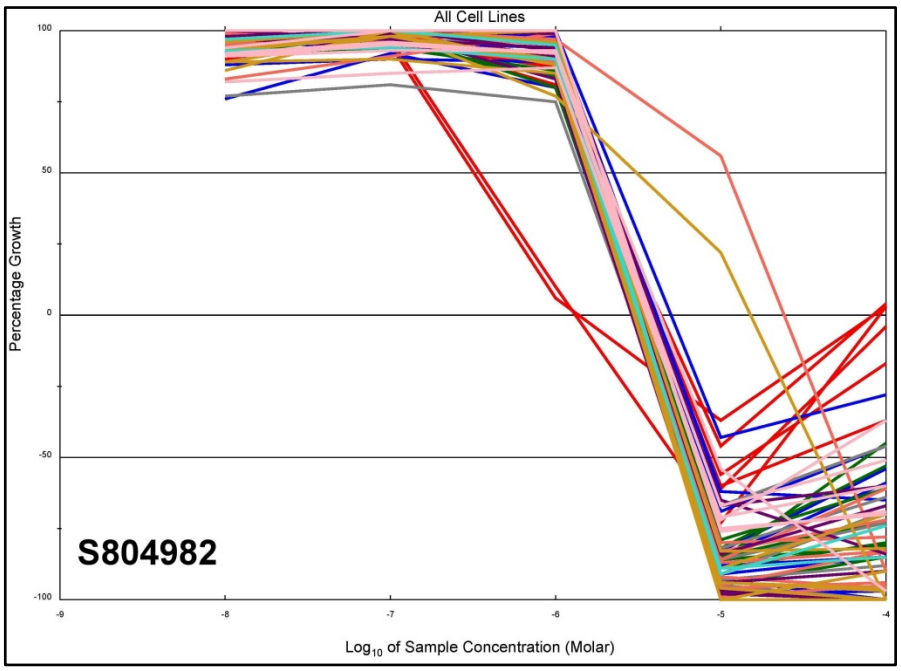

Figure 6.15 ***Dose response curves for all cell lines in the NCI 60 panel exposed to compound 31a with tissue originated colours and shapes.***

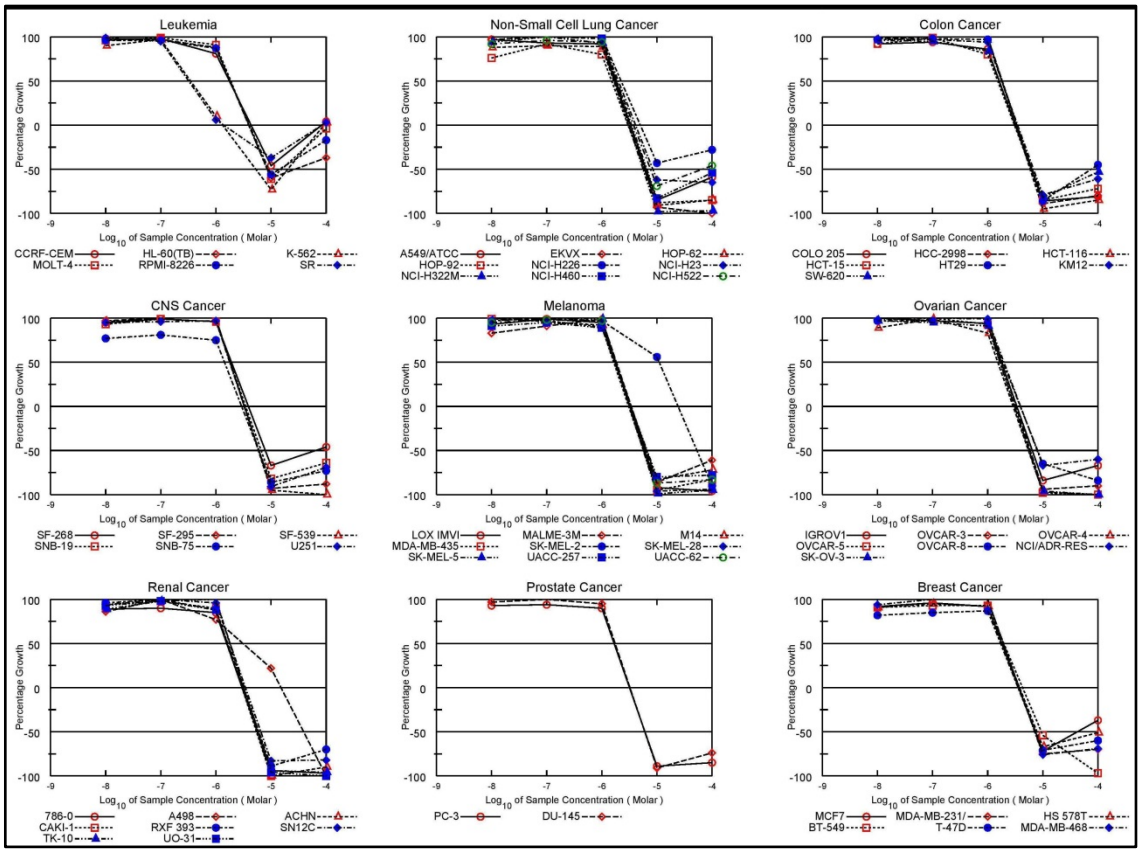

Figure 6.16 ***Dose response curves (% growth verses sample concentration) for all cell lines with different subpanel obtained from the NCI's in vitro human cancer cells line of compound 31a on nine types of cancer.***

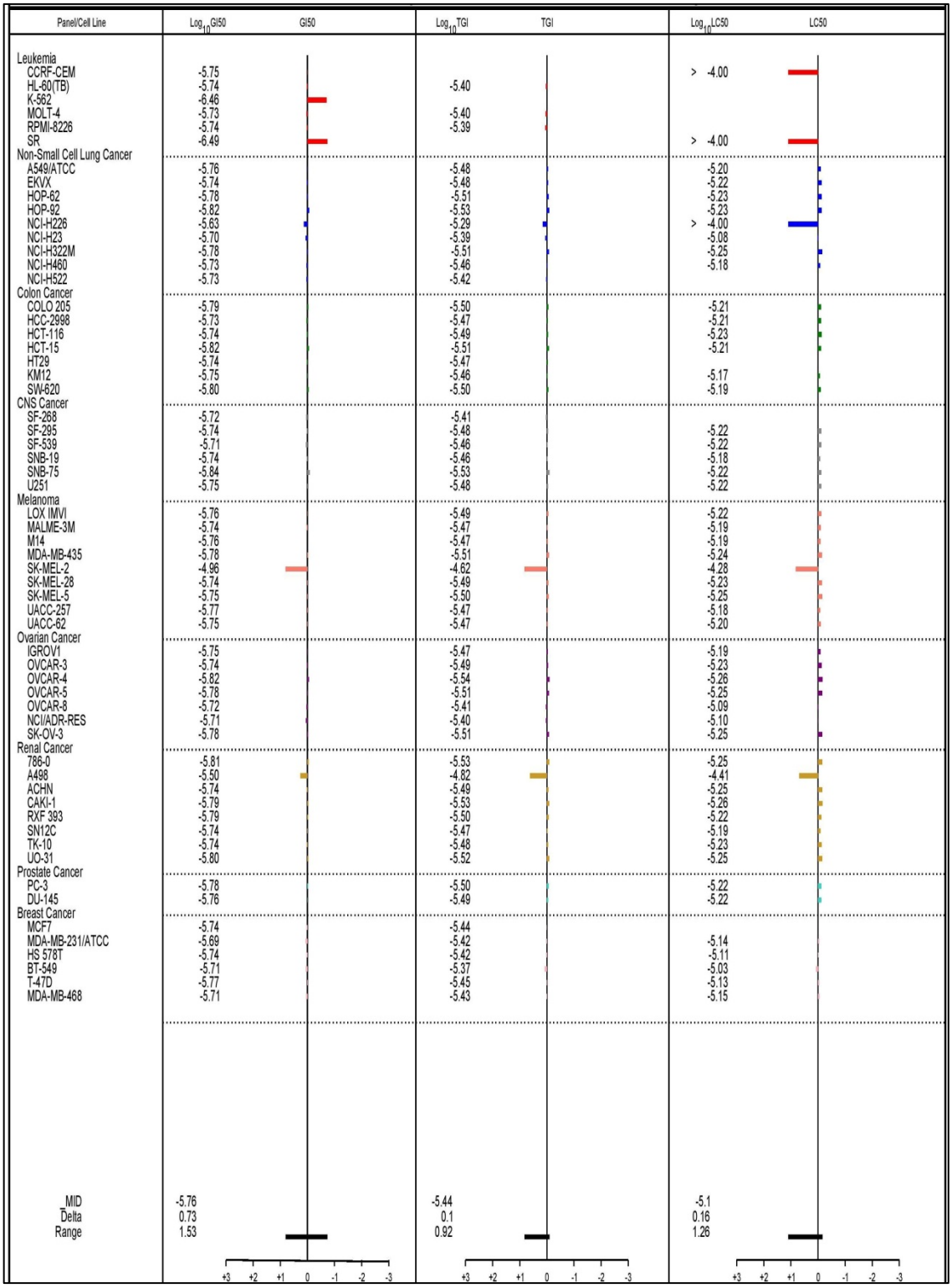

Figure 6.17 ***Values of log molar concentration of response parameters (log_{10}GI50, log_{10}TGI & log_{10}LC50) of compound 31a.***

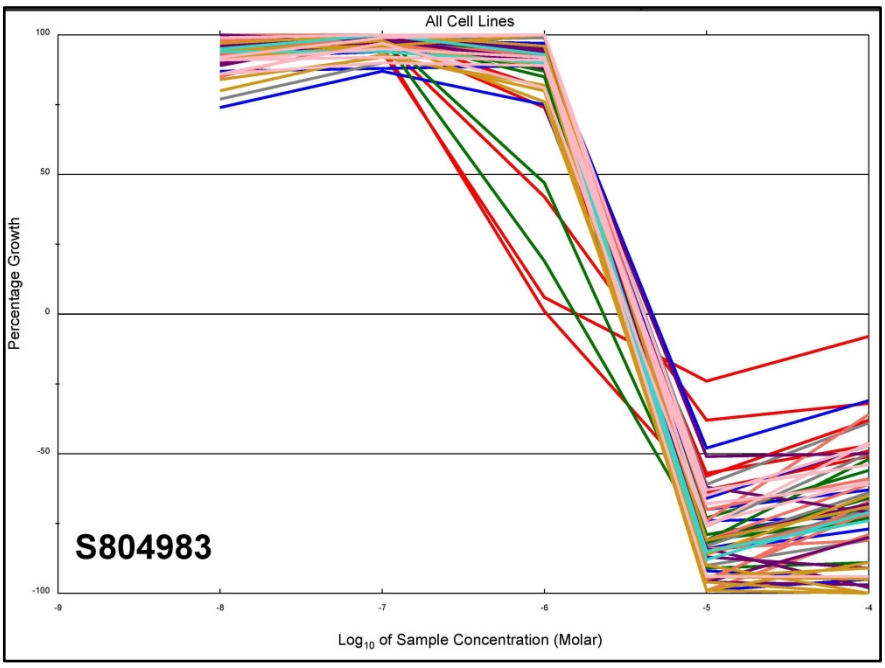

Figure 6.18 ***Dose response curves for all cell lines in the NCI60 panel exposed to compound 31b with tissue originated colours and shapes.***

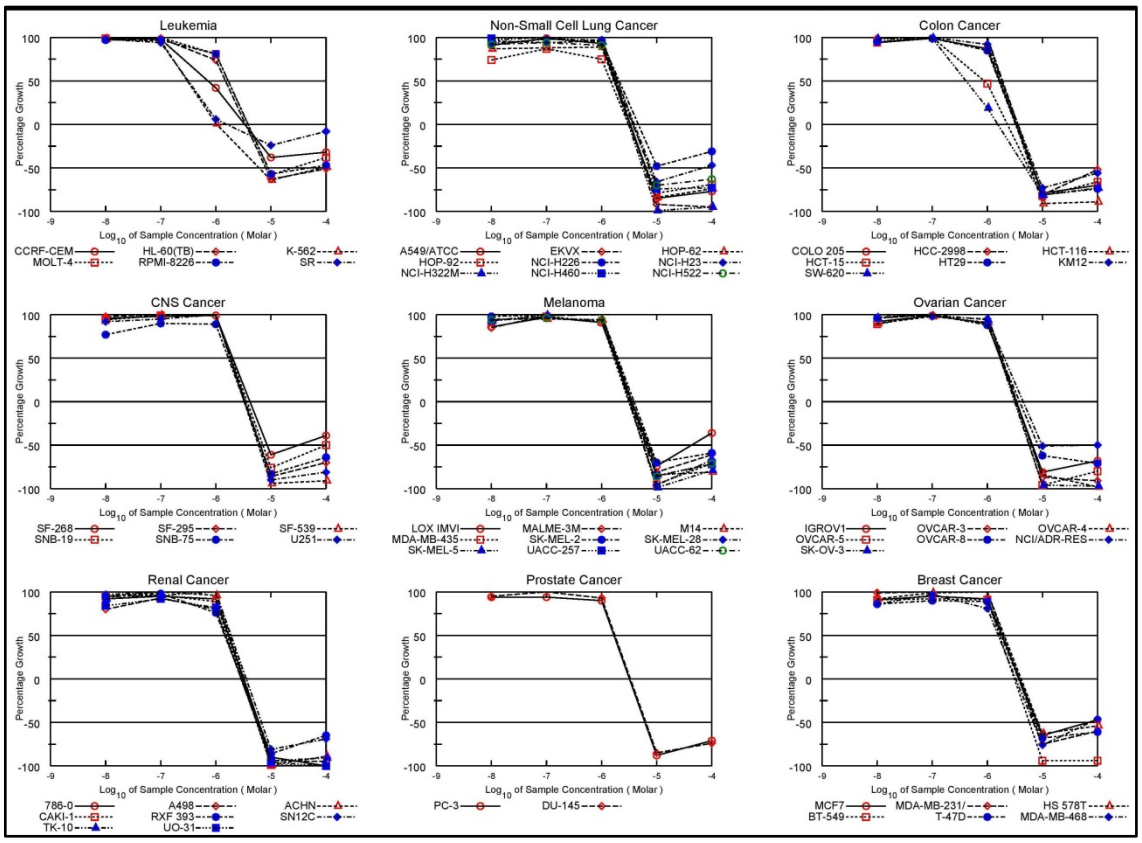

Figure 6.19 ***Dose response curves (% growth verses sample concentration) for all cell lines with different subpanel obtained from the NCI's in vitro disease-oriented human cancer cells line of compound 31b on nine types of cancer.***

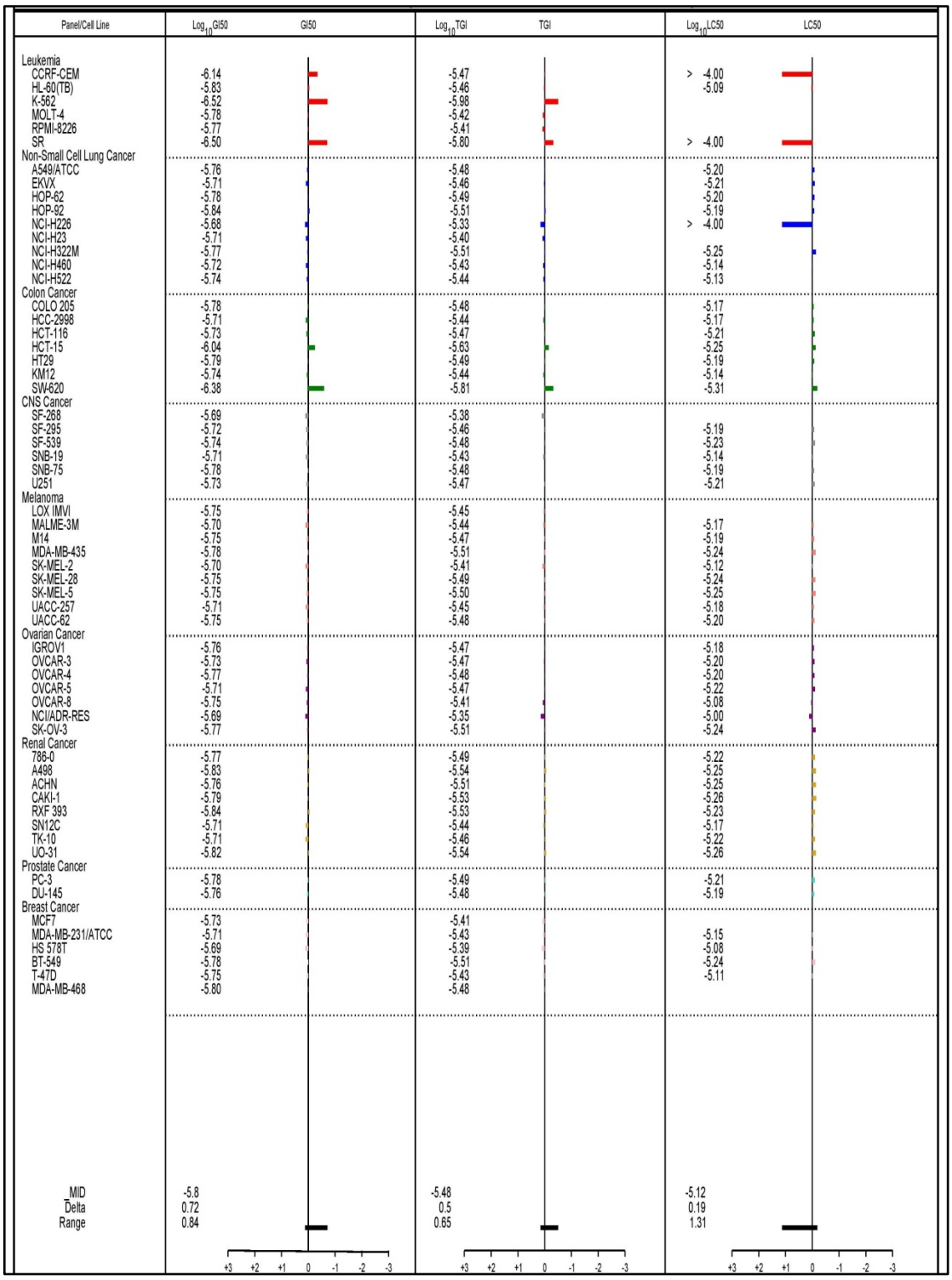

Figure 6.20 ***Values of log molar concentration of response parameters (log_{10}GI50, log_{10}TGI & log_{10}LC50) of compound 31b.***

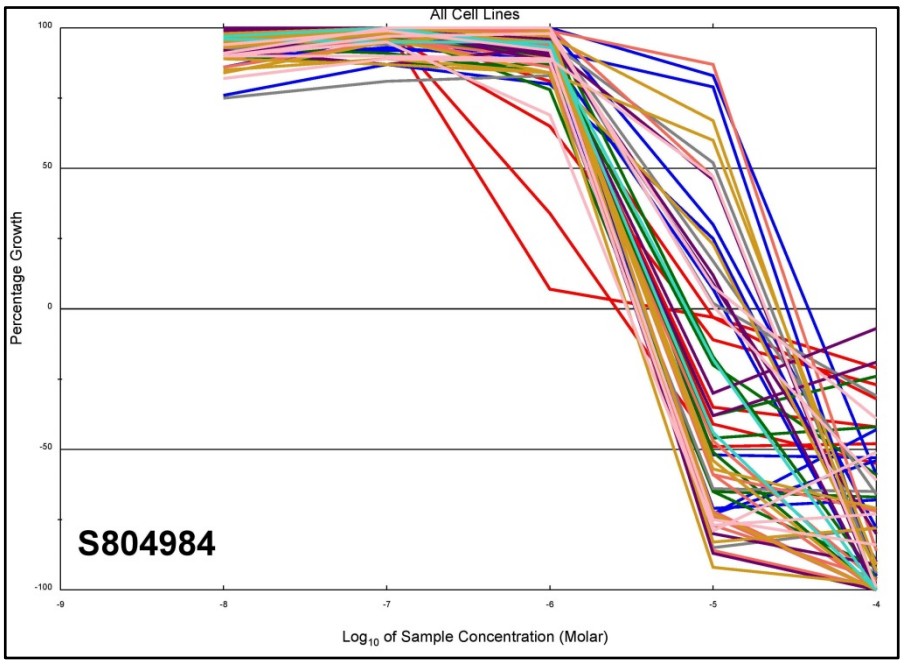

Figure 6.21 ***Dose response curves for all cell lines in the NCI60 panel exposed to compound 31c with tissue originated colours and shapes.***

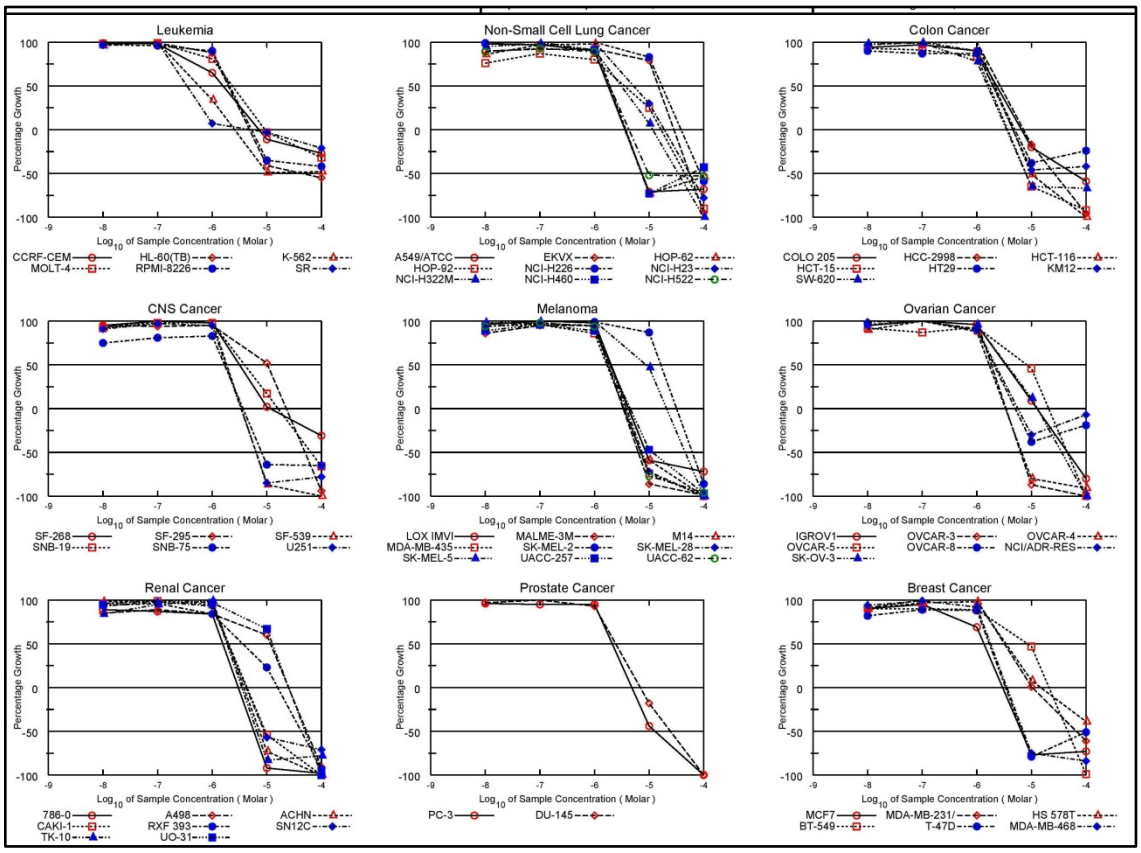

Figure 6.22 ***Dose response curves (% growth verses sample concentration) for all cell lines with different subpanel obtained from the NCI's in vitro disease-oriented human cancer cells line of compound 31c on nine types of cancer.***

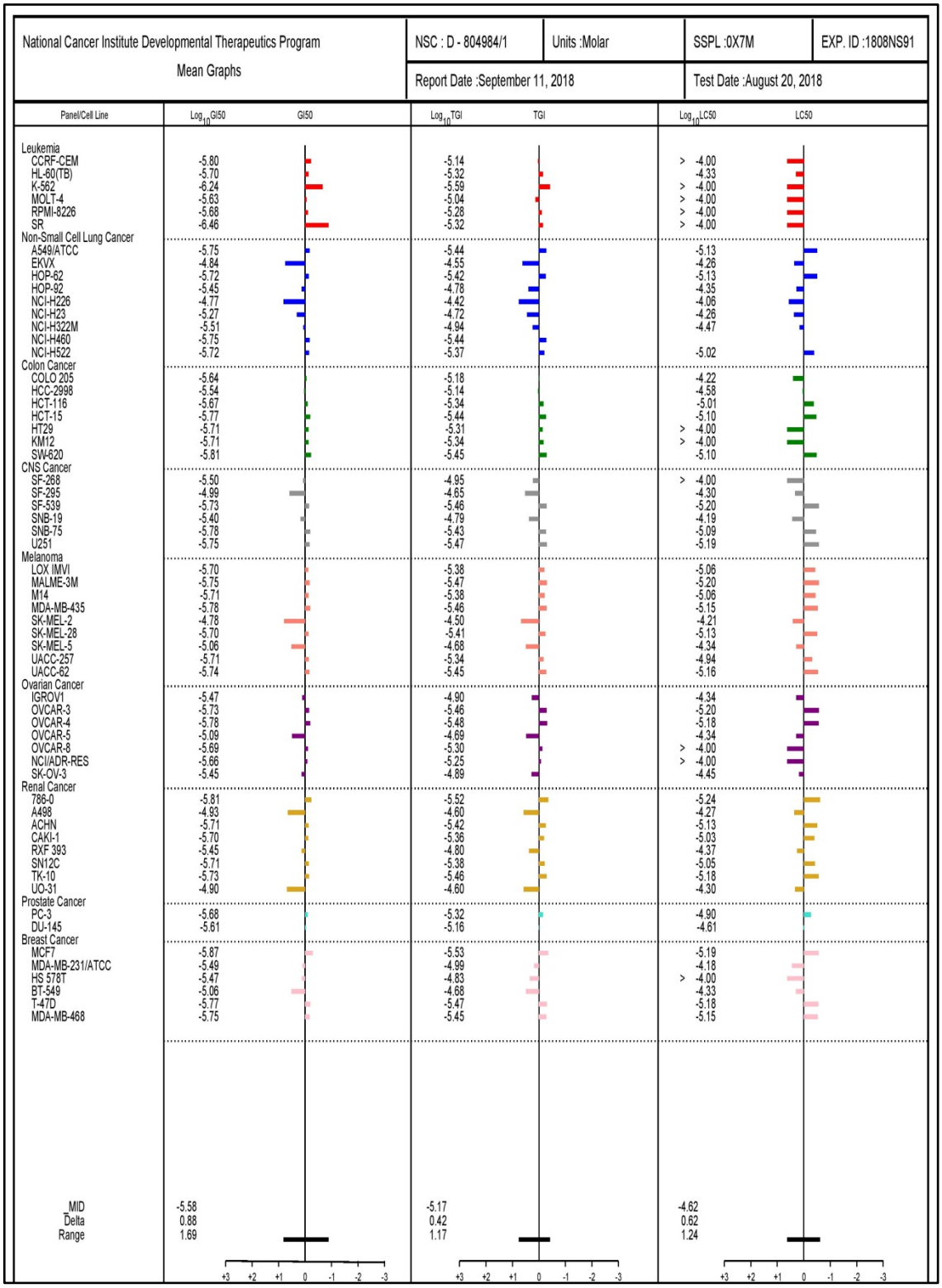

Figure 6.23 ***Values of log molar concentration of response parameters (log_{10}GI50, log_{10}TGI & log_{10}LC50) of compound 31c.***

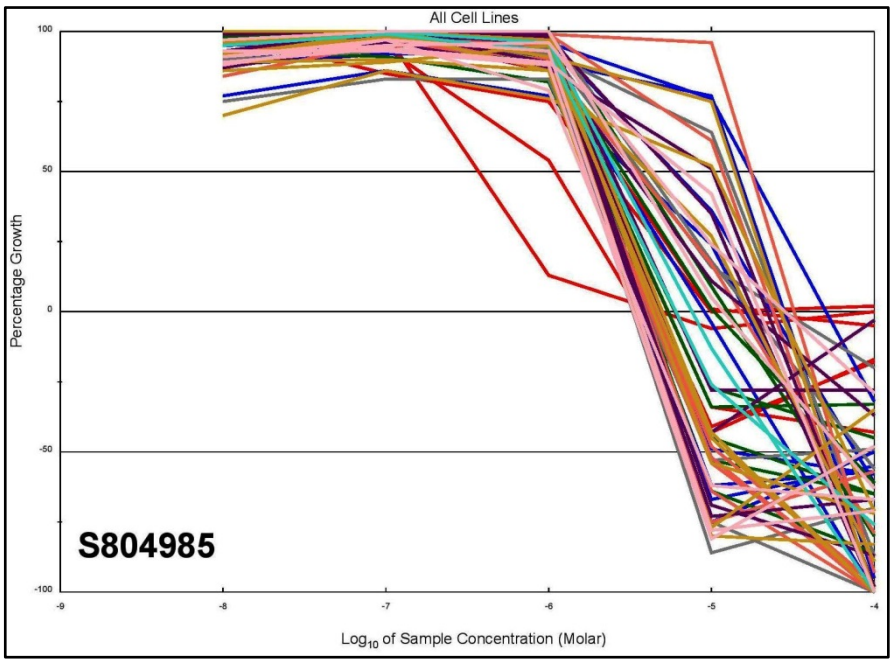

Figure 6.24 ***Dose response curves for all cell lines in the NCI60 panel exposed to compound 31d with tissue originated colours and shapes.***

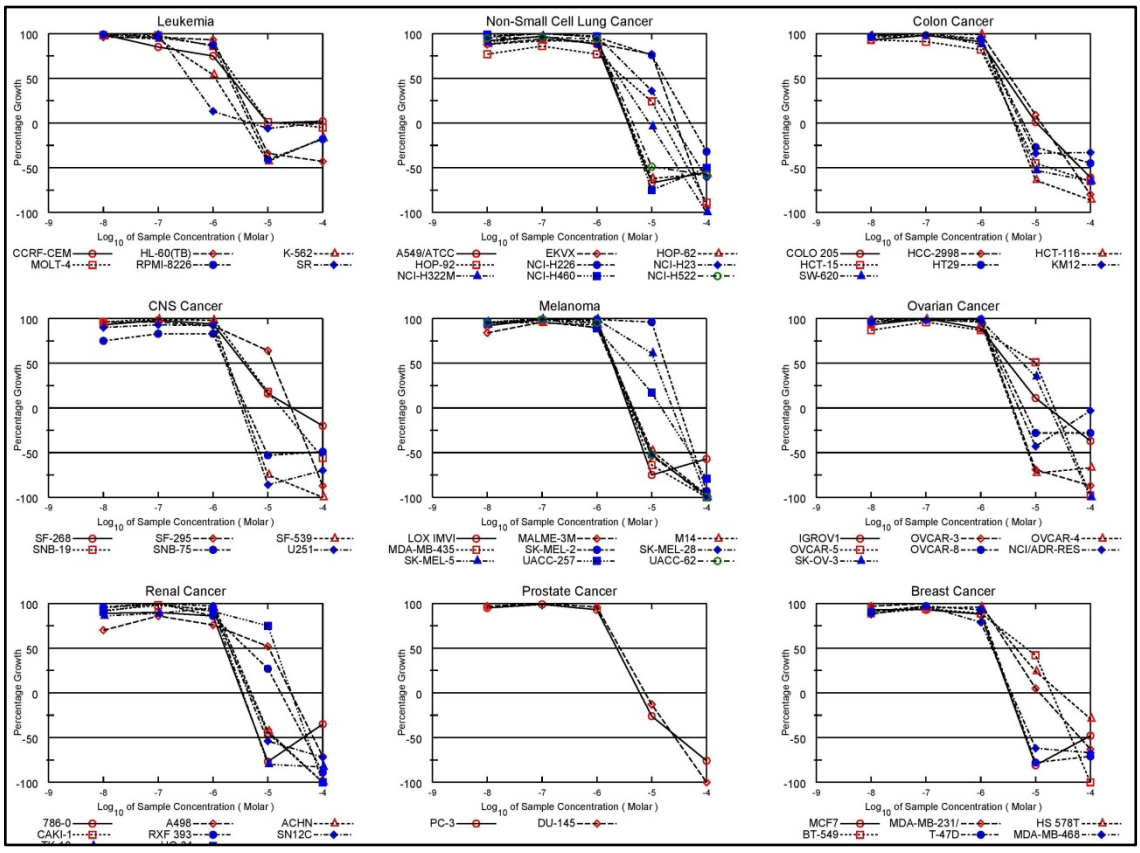

Figure 6.25 ***Dose response curves (% growth verses sample concentration) for all cell lines with different subpanel obtained from the NCI's in vitro disease-oriented human cancer cells line of compound 31d on nine types cancer.***

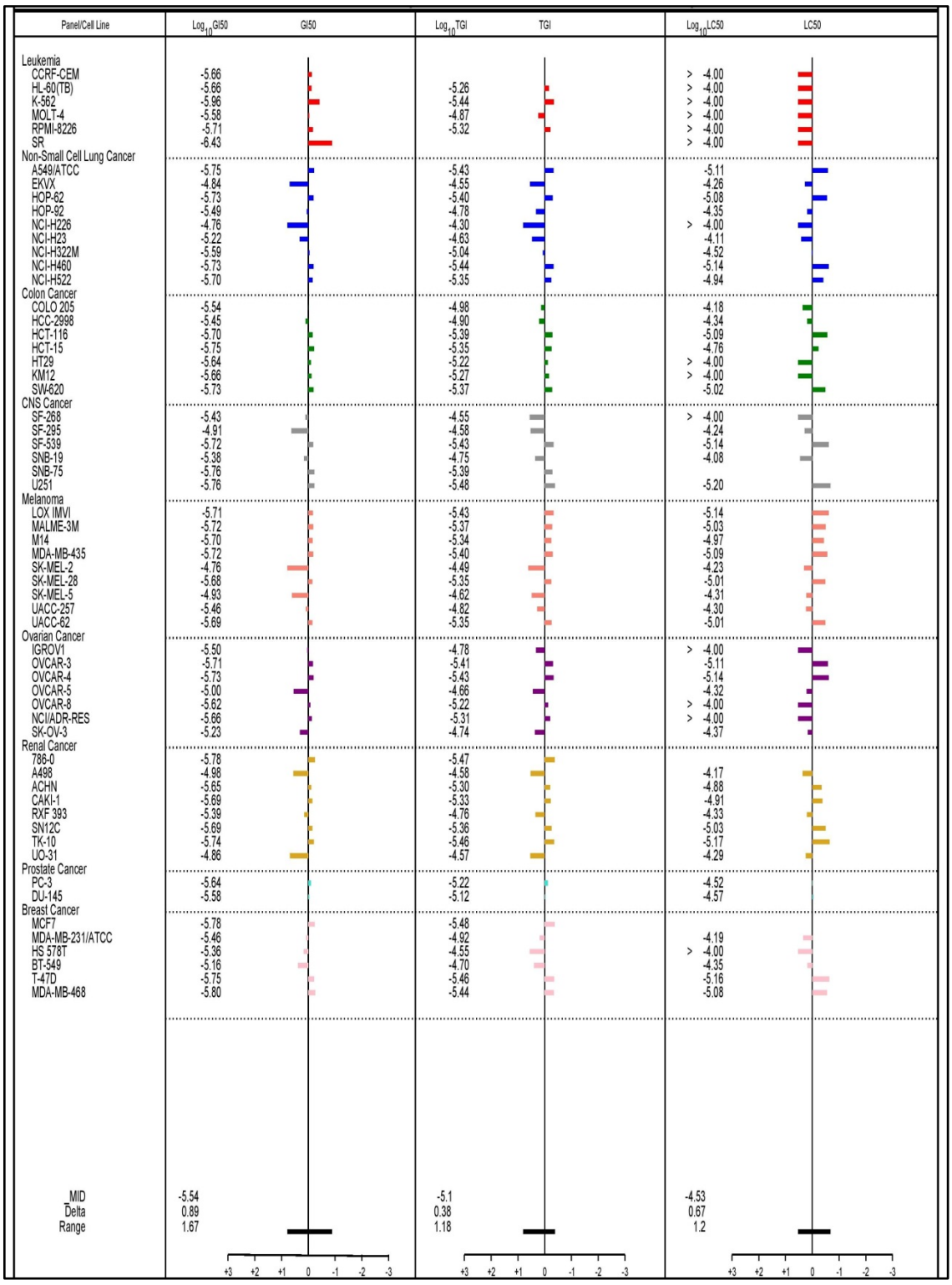

Figure 6.26 ***Values of log molar concentration of response parameters (log_{10}GI50, log_{10}TGI & log_{10}LC50) of compound 31d.***

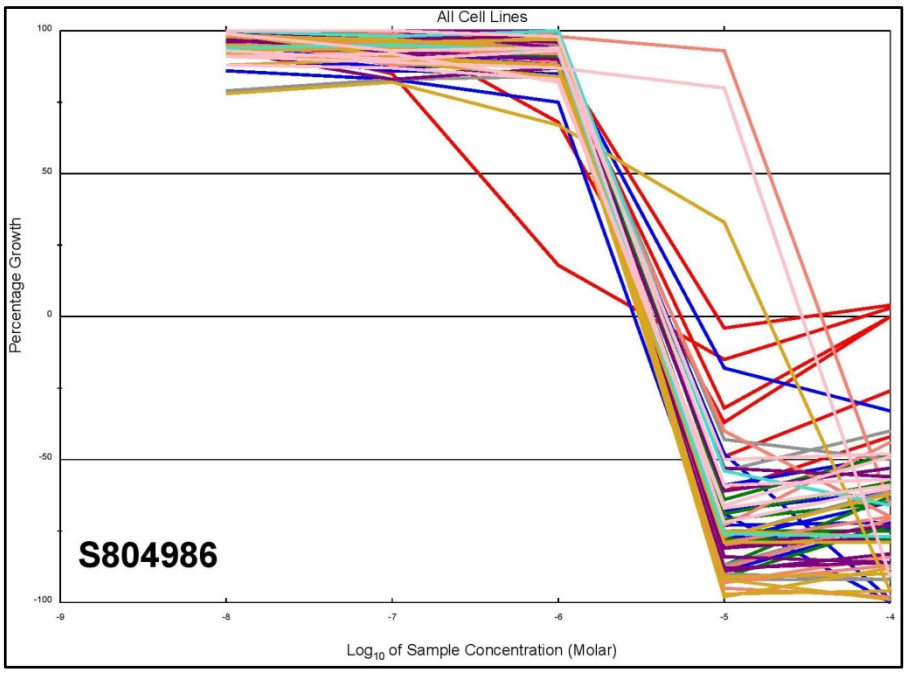

Figure 6.27 ***Dose response curves for all cell lines in the NCI60 panel exposed to compound 31e with tissue originated colours and shapes.***

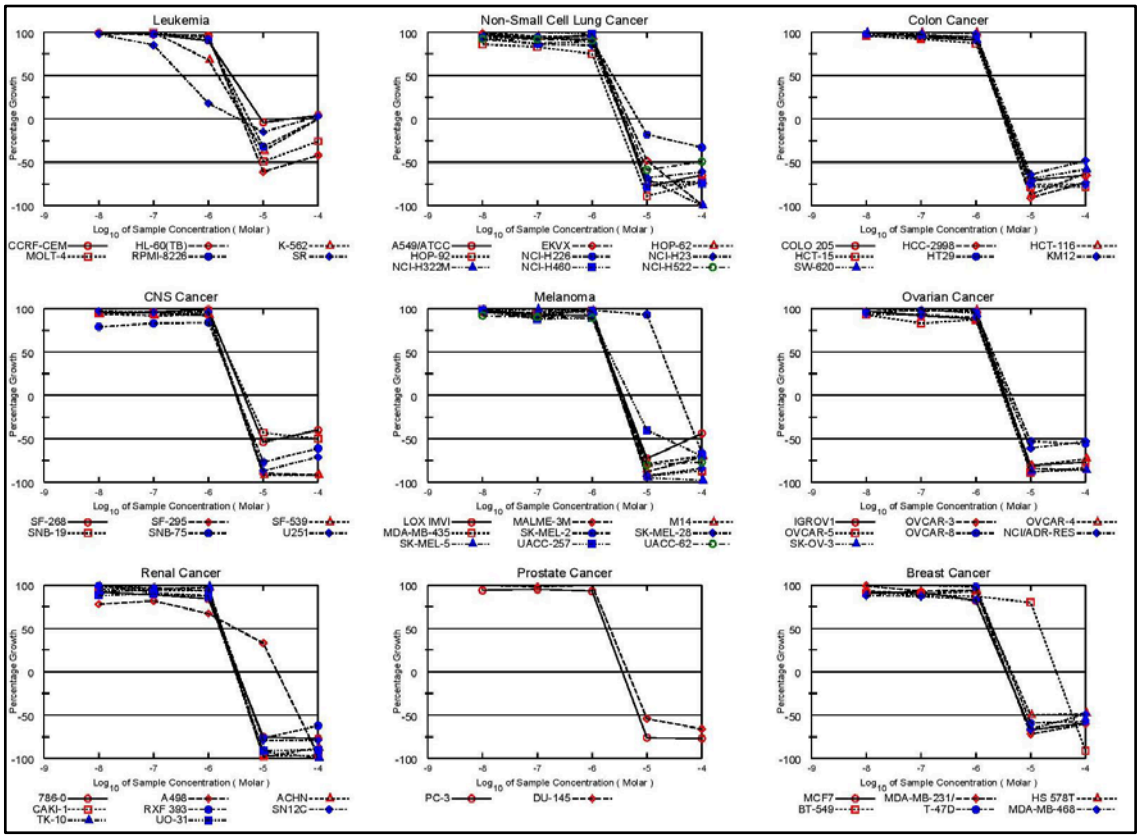

Figure 6.28 ***Dose response curves (% growth verses sample concentration) for all cell lines with different subpanel obtained from the NCI's in vitro disease-oriented human cancer cells line of compound 31e on nine types cancer.***

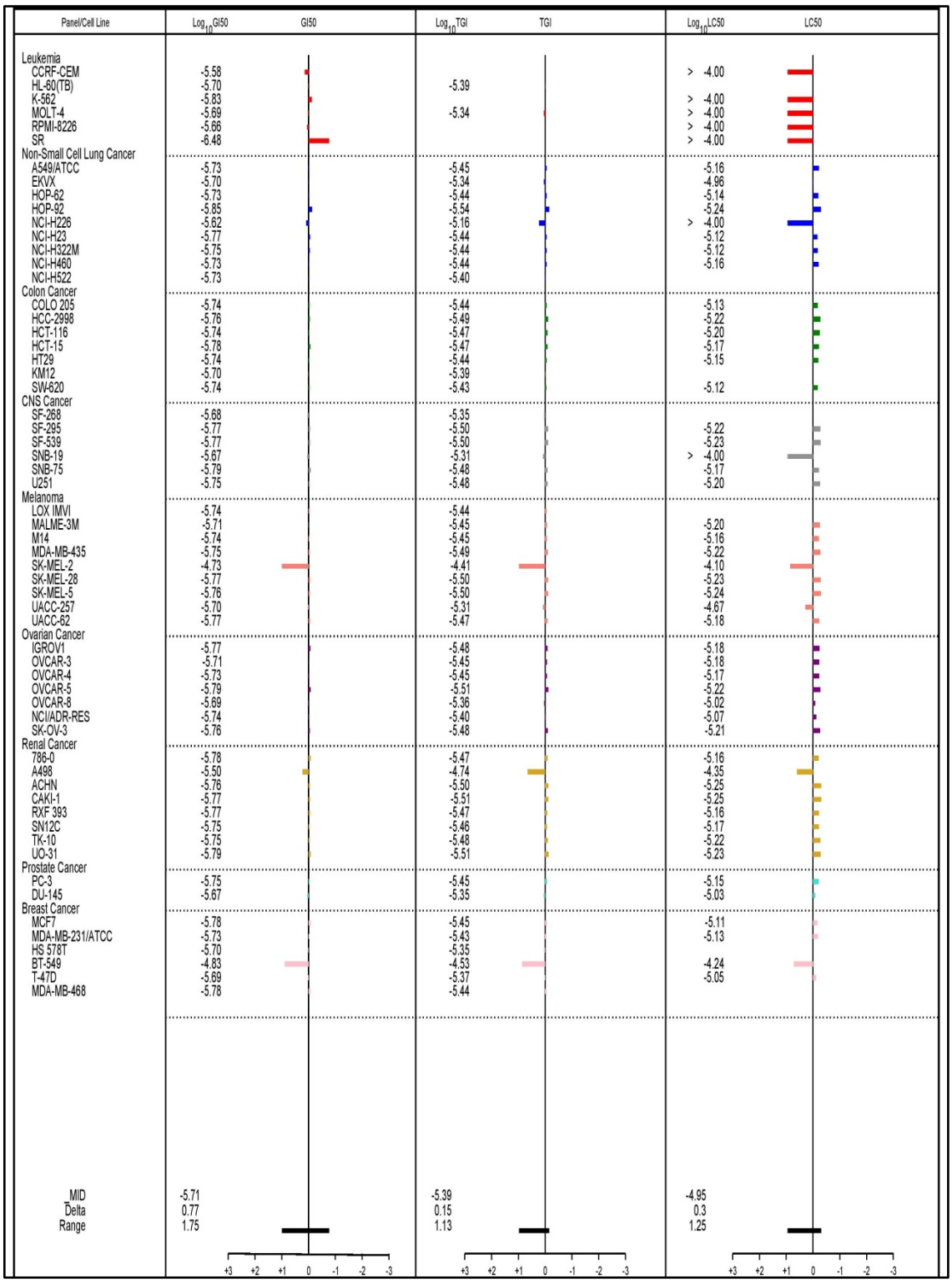

Figure 6.29 ***Values of log molar concentration of response parameters (log_{10}GI50, log_{10}TGI & log_{10}LC50) of compound 31e.***

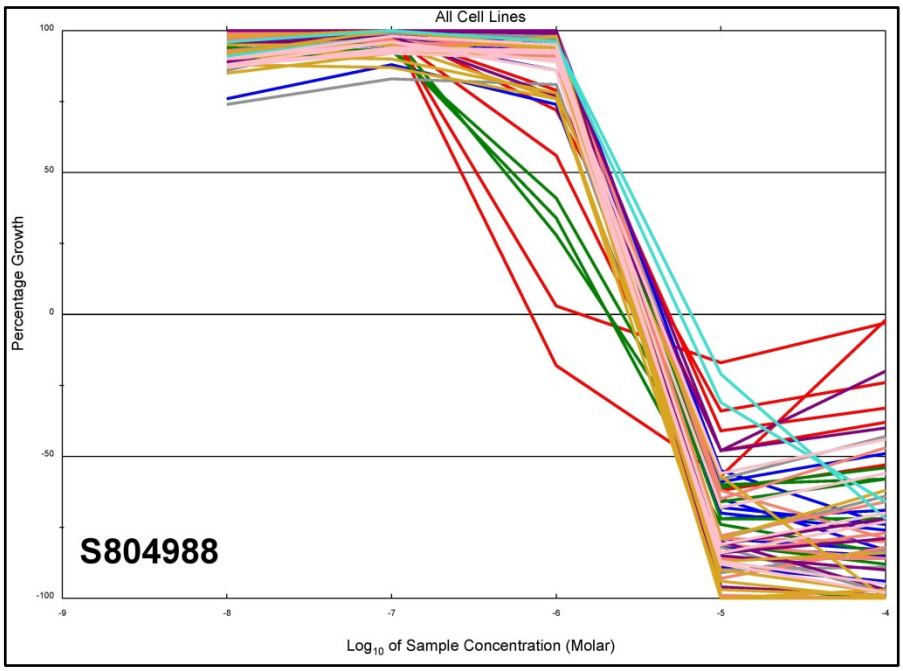

Figure 6.30 ***Dose response curves for all cell lines in the NCI60 panel exposed to compound 31g with tissue originated colours and shapes.***

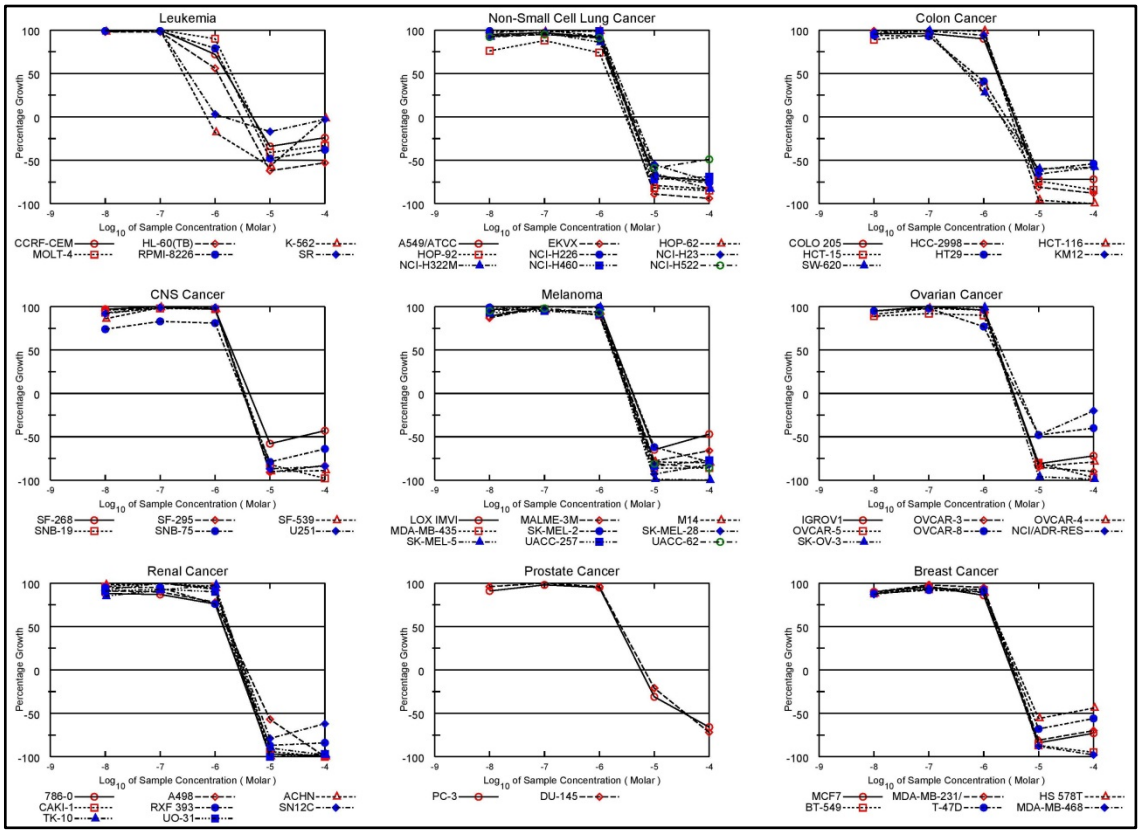

Figure 6.31 ***Dose response curves (% growth verses sample concentration) for all cell lines with different subpanel obtained from the NCI's in vitro disease-oriented human cancer cells line of compound 31g on nine types of cancer.***

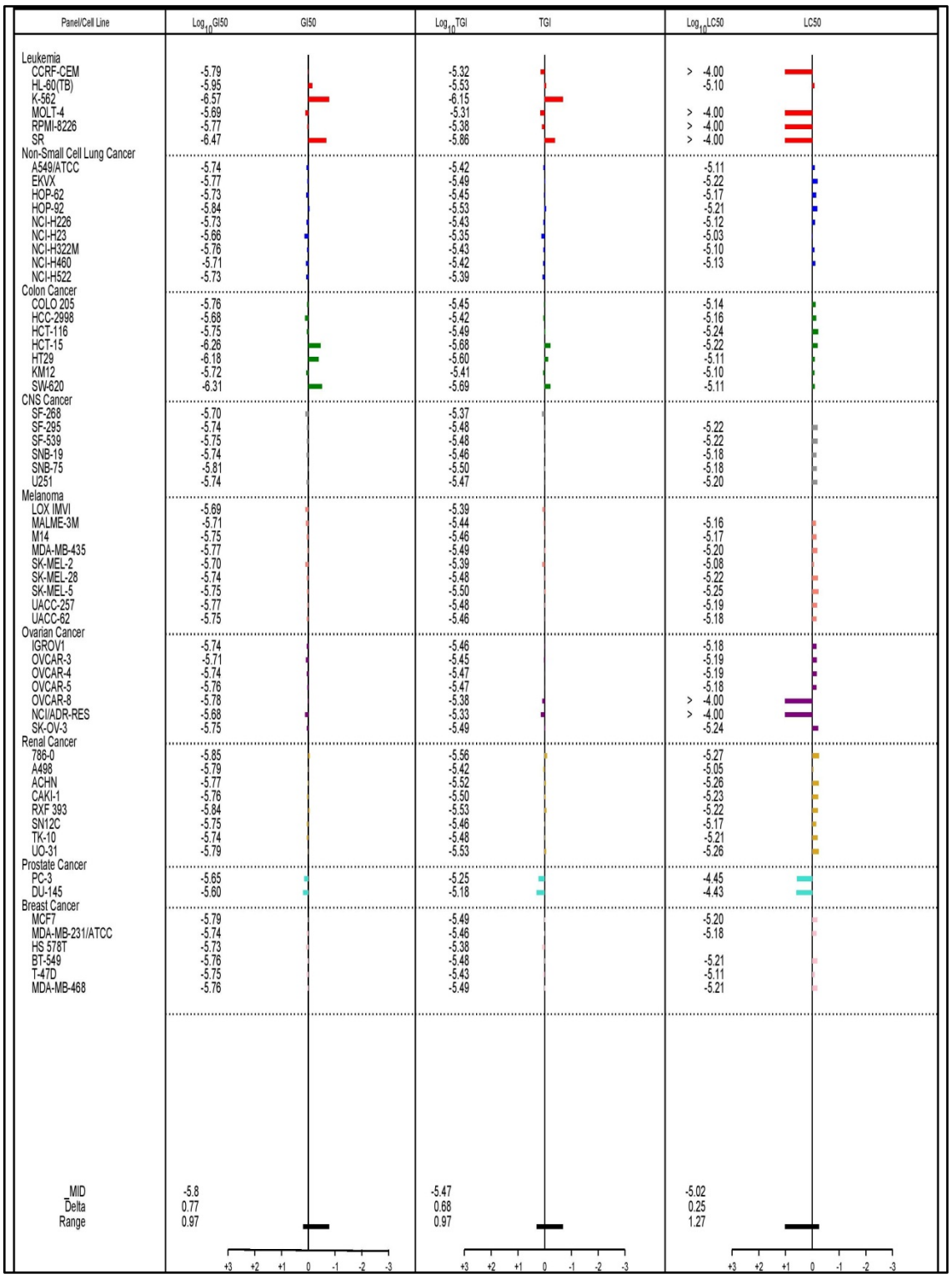

Figure 6.32 ***Values of log molar concentration of response parameters (log_{10}GI50, log_{10}TGI & log_{10}LC50) of compound 31g.***

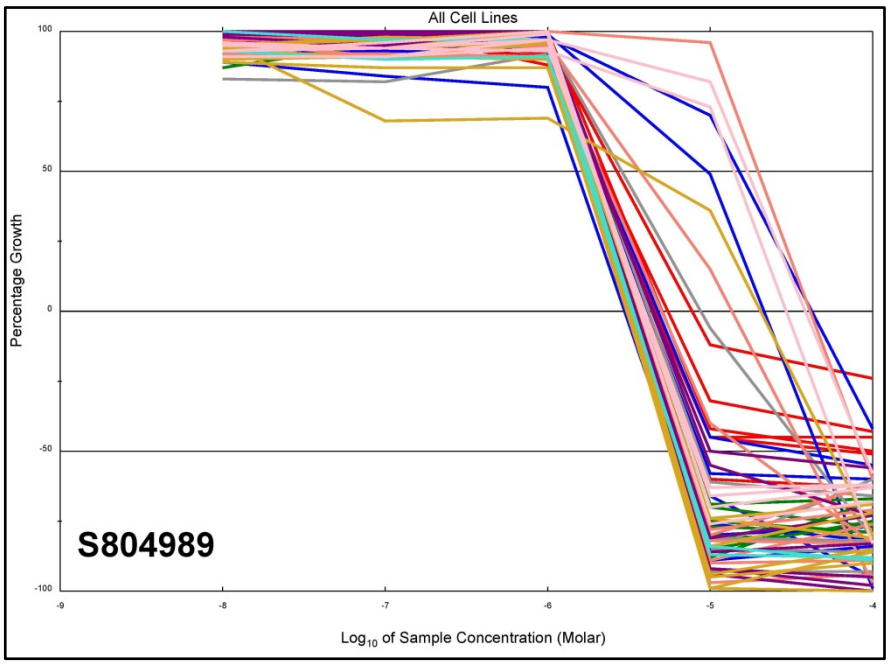

Figure 6.33 ***Dose response curves for all cell lines in the NCI60 panel exposed to compound 31h with tissue originated colours and shapes.***

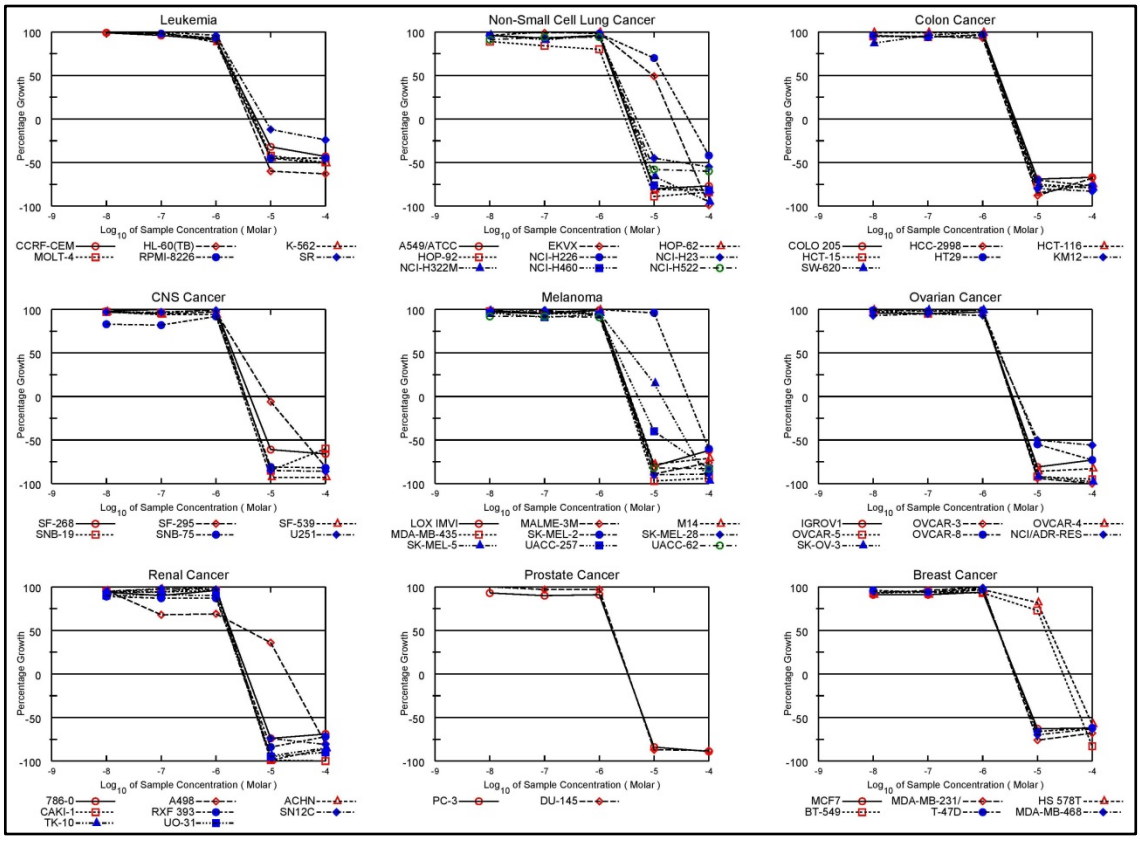

Figure 6.34 ***Dose response curves (% growth verses sample concentration) for all cell lines with different subpanel obtained from the NCI's in vitro disease-oriented human cancer cells line of compound 31h on nine types of cancer.***

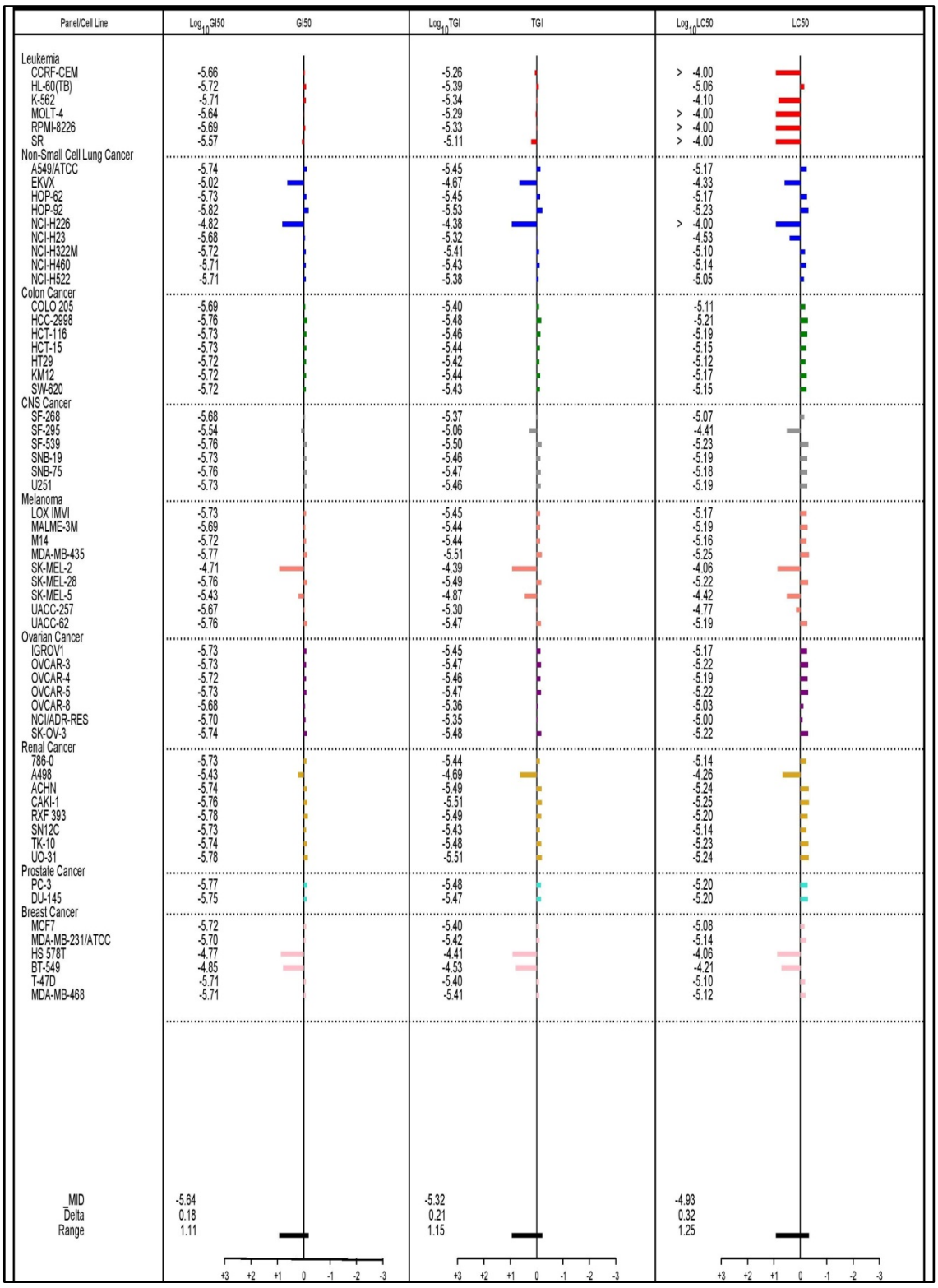

Figure 6.35 ***Values of log molar concentration of response parameters (log_{10}GI50, log_{10}TGI & log_{10}LC50) of compound 31h.***

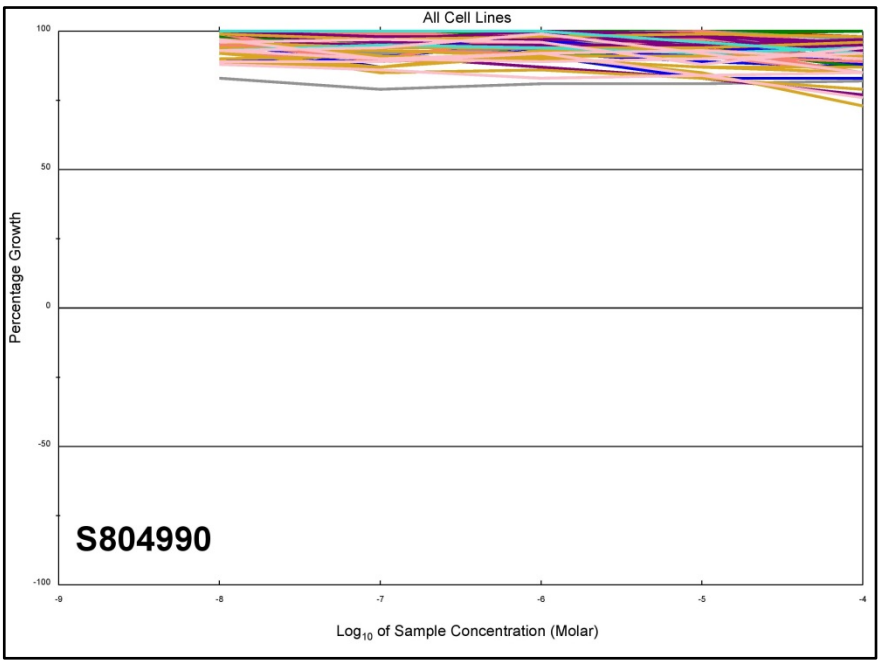

Figure 6.36 ***Dose response curves for all cell lines in the NCI60 panel exposed to compound 31i with tissue originated colours and shapes.***

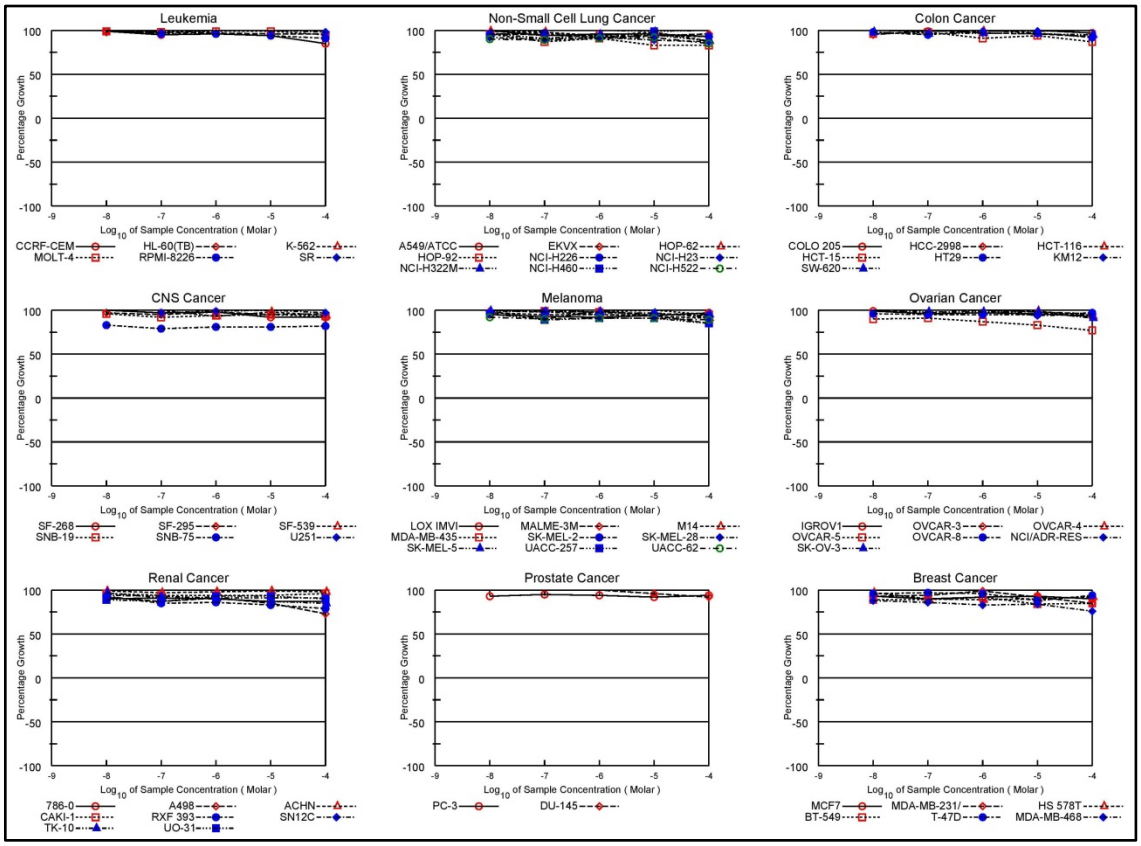

Figure 6.37 ***Dose response curves (% growth verses sample concentration) for all cell lines with different subpanel obtained from the NCI's in vitro disease-oriented human cancer cells line of compound 31i on nine types of cancer.***

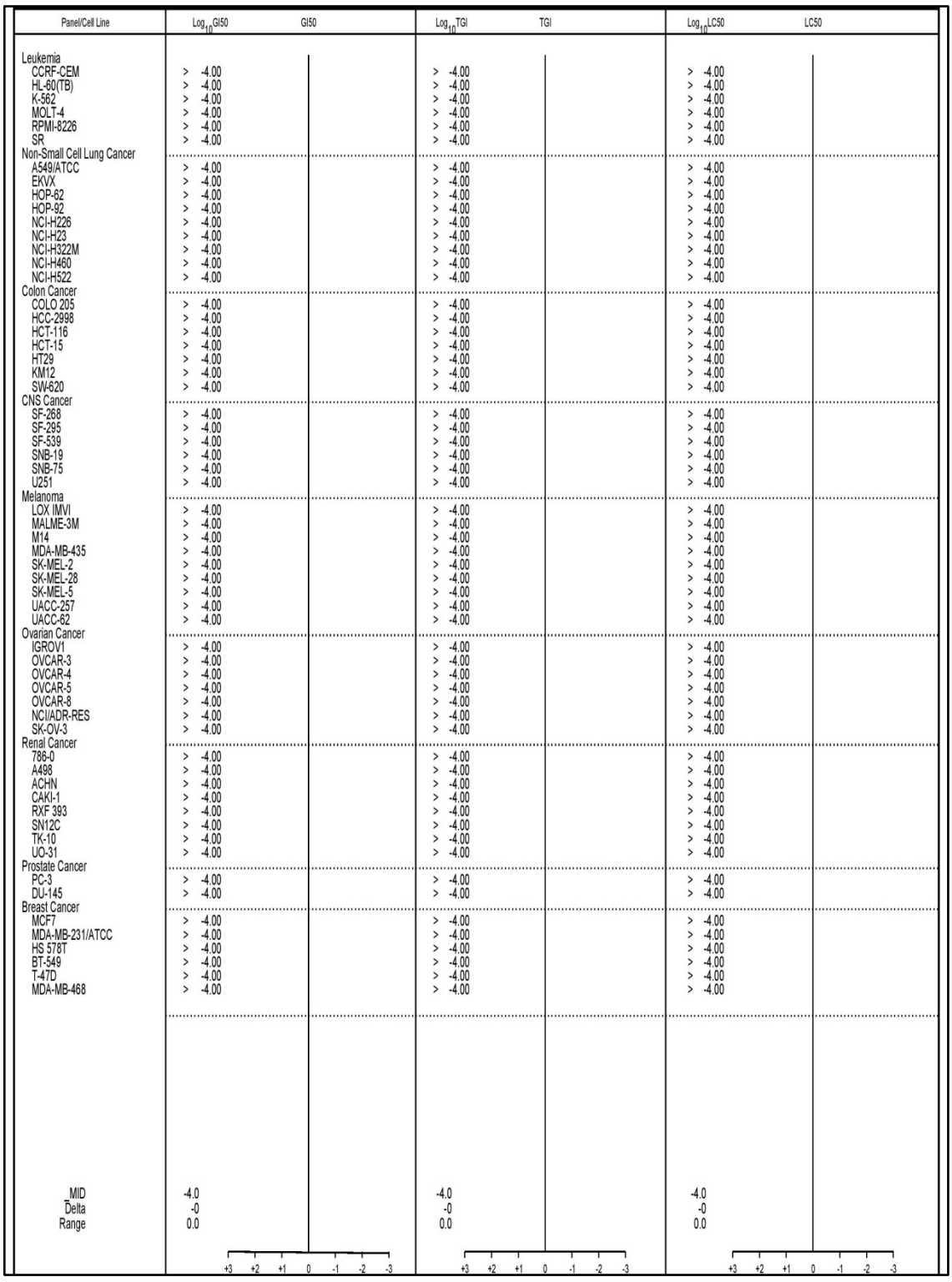

Figure 6.38 ***Values of log molar concentration of response parameters (log_{10}GI50, log_{10}TGI & log_{10}LC50) of compound 31i.***

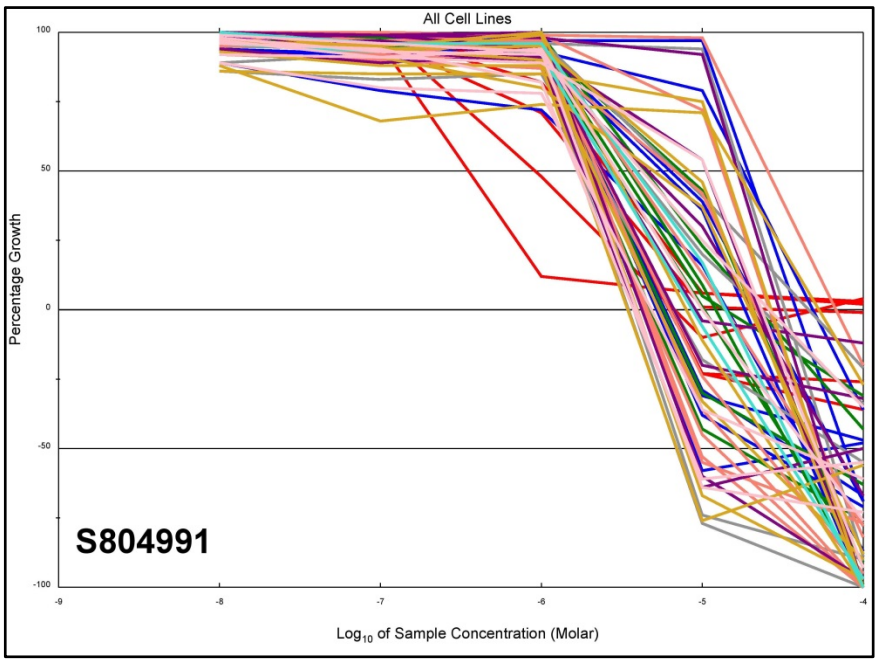

Figure 6.39 ***Dose response curves for all cell lines in the NCI60 panel exposed to compound 31j with tissue originated colours and shapes.***

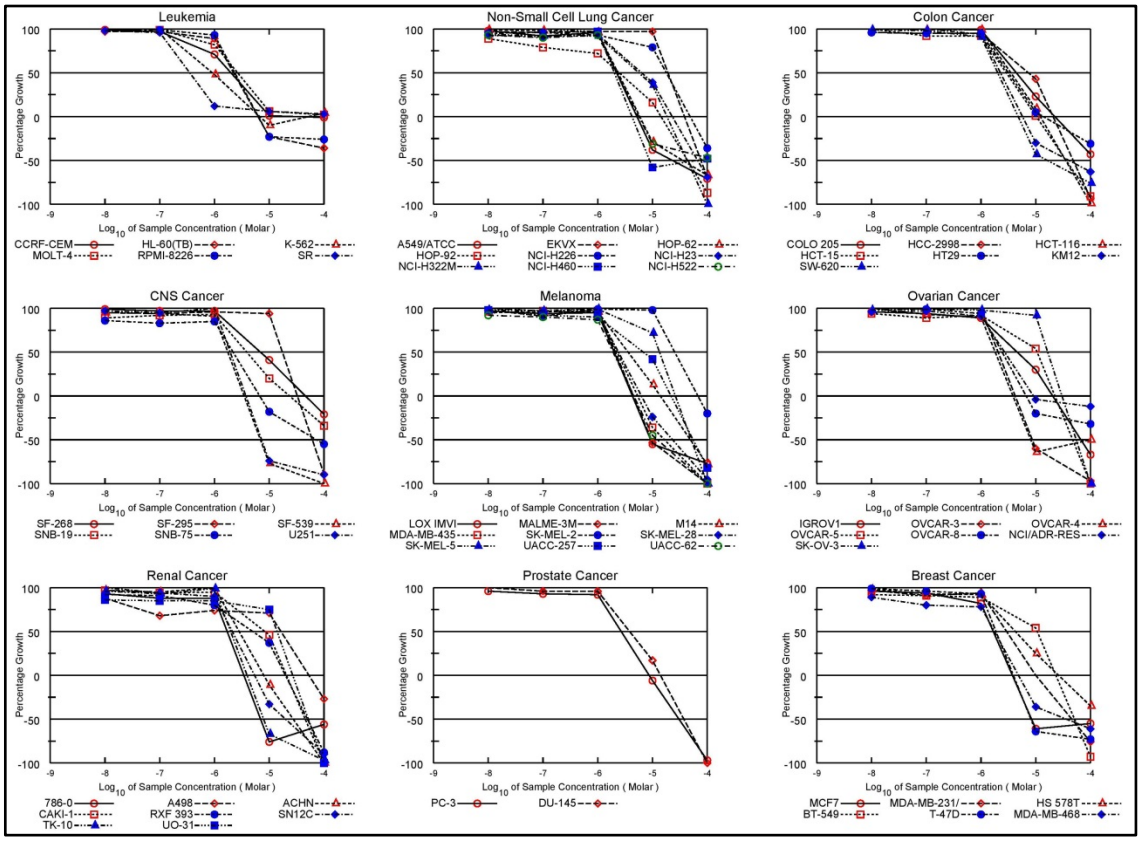

Figure 6.40 ***Dose response curves (% growth verses sample concentration) for all cell lines with different subpanel obtained from the NCI's in vitro disease-oriented human cancer cells line of compound 31j on nine types of cancer.***

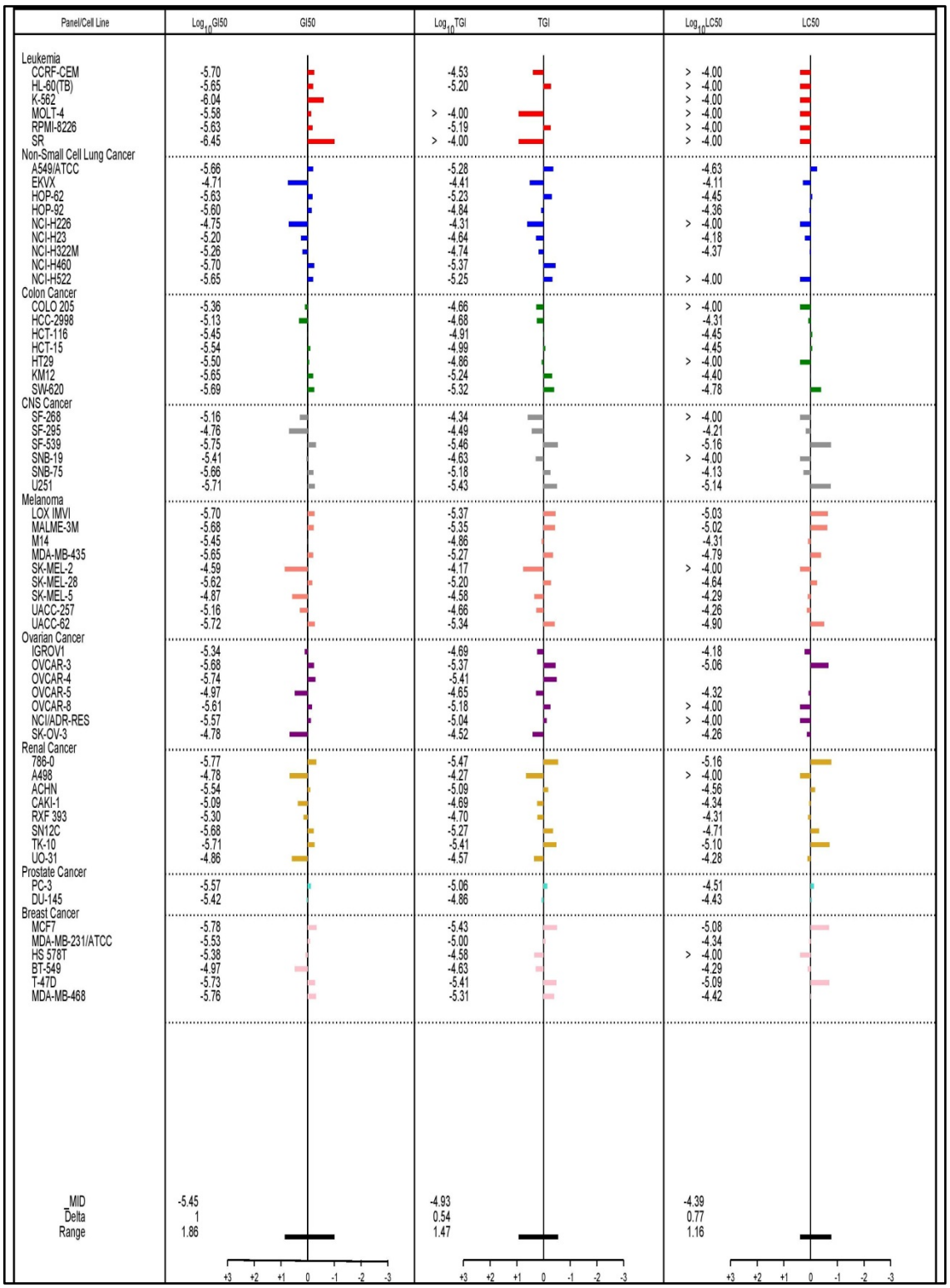

Figure 6.41 ***Values of log molar concentration of response parameters (log_{10}GI50, log_{10}TGI & log_{10}LC50) of compound 31j.***

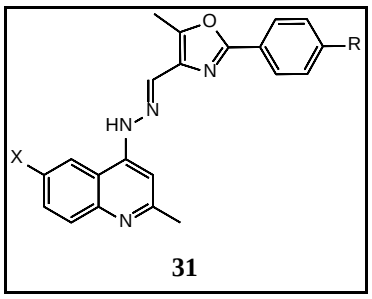

31

Figure 6.42

Compound **31a** (X = Br, R = H) showed remarkable anticancer activity against most of the tested cell lines representing nine different subpanels with GI_{50} value 3.21 x 10^{-7} to 1.6 x 10^{-6} M, TGI value 3.84 x 10^{-6} to 1.52 x 10^{-5} M and LC_{50} value ranging in between 9.4 x10^{-6} to >1 x 10^{-4} M. Leukemia (K-562) and leukemia (SR) were found to be the most sensitive cell line against compound **31a** with GI_{50} values of 3.45 x 10^{-7} and 3.21 x 10^{-7} respectively. Compound **31b** (X = Cl, R = H) displayed noteworthy anticancer activity with GI_{50} value 3.15 x 10^{-7} – 1.32 x 10^{-6} M, TGI value 3.88 – 1.04 x 10^{-6} M and LC_{50} value 8.07 x 10^{-6} - > 1 x 10^{-4} M. Leukemia (SR) and colon cancer (SW-620) were found to be the most sensitive cell line against compound **31b** with GI_{50} values of 3.15 x 10^{-7} and 4.15 x 10^{-7} respectively. The values for compound **31c** (X = Br, R = CH_3) are GI_{50} value 3.44 x 10^{-7} – 1.59 x 10^{-6} M, TGI value 9.11-1.15 x 10^{-6} M and LC_{50} value 9.08 x 10^{-6} - 1.0 x 10^{-4} M. Leukemia (K-562) and leukemia (SR) were found to be the most sensitive cell line against compound **31c** with GI_{50} values of 5.71 x 10^{-7} and 3.44 x 10^{-7} respectively. The GI_{50}, TGI and LC_{50} values for compound **31d** (X = Cl, R = CH_3) are 3.73 x 10^{-7} to 1.1 x 10^{-6} M, 3.6-1.35 x 10^{-6} M, 8.1 x 10^{-6} to >1.0 x 10^{-4} M respectively. Leukemia (SR) was found to be the most sensitive cell line against compound **31d** with GI_{50} values of 3.73 x 10^{-7}. Compound **31e** (X = Br, R = OCH_3) displayed outstanding anticancer activity with GI_{50}, TGI and LC_{50} values 3.32 x 10^{-7} to 1.70 x 10^{-6} M, 4.53-3.34 x 10^{-6} M and 6.92 x 10^{-6} to > 1.0 x 10^{-4} M respectively. Leukemia (SR) was found to be the most sensitive cell line against compound **31e** with GI_{50} values of 3.32 x 10^{-7}. Compound **31g** (X = Br, R = Cl) displayed good anticancer activity with GI_{50}, TGI and LC_{50} values 2.67 x 10^{-7} to 1.69 x 10^{-6} M, 4.81- 1.39 x 10^{-6} M and 6.21 x 10^{-6} to >1.00 x 10^{-4} M respectively. Leukemia (K-562) and leukemia (SR) were found to be the most sensitive cell lines against compound **31g** with GI_{50} values of 2.67 x 10^{-7} and 3.39 x 10^{-7} respectively. For compound **31h** (X = Cl, R = Cl)

the GI_{50}, TGI and LC_{50} values are 2.17-1.50 x 10^{-6} M, 5.10 x 10^{-6} to 2.14x 10^{-5} M and 8.62 x 10^{-6} to >1.0 x 10^{-4} M respectively. Non-small cell lung cancer (HOP-92) was found to be the most sensitive cell line against compound **31h** with GI_{50} values of 1.50 x 10^{-6} M. The GI_{50}, TGI and LC_{50} values for compound **31i** (X = Br, R = Br) are >1 x 10^{-4} M showed poor to moderate anticancer activity. The values of GI_{50}, TGI and LC_{50} for compound **31j** (X = Cl, R = Br) are 3.55 x 10^{-7} to 1.07 x 10^{-6} M, 4.22 x 10^{-6} to >1.0 x 10^{-4} and 6.95 x 10^{-6} to >1.0 x 10^{-4} M respectively. Leukemia (K-562) and leukemia (SR) were found to be the most sensitive cell lines against compound **31c** with GI_{50} values of 9.04 x 10^{-7} M and 3.55 x 10^{-7} M respectively.

6.3 Conclusion

In the present study, some new oxazole containing quinolyl hydrazones were prepared from 6-Bromo/6-chloro-2-methyl-quinolin-4-yl-hydrazine and 2-aryl-5-methyl-1,3-oxazole-4-carbaldehydes connecting both the heterocyclic moieties together via an important hydrazone linkage. All the synthesised compounds are characterized by various spectroanalytical techniques. Anti-tubercular activity against *M. tuberculosis* H37Rv is carried out for all the new compounds. Some of the synthesized compounds exhibit good antitubecular activity. Molecular modelling study revealed that the anti-TB activity of these compounds could be due to their interaction and inhibition activity against the MTB enzyme enoyl-ACP reductase. All the twelve new compounds are also screened for antimicrobial activity using two fungal and four bacterial strains. Some of the compounds show outstanding activity. Further, *in vitro* anticancer activity (single dose as well as five dose assay) on 60 different cancer cell lines is carried out at NCI, USA. Out of ten submitted compounds, nine compounds displayed an outstanding anticancer activity with lethality value ranging from 10% to 100% for several cancer cell lines at the single dose level. All the selected nine compounds exhibit an excellent anticancer activity at five dose levels as well having GI_{50} value up to 0.3 μM against some of the cancer cell lines.

6.4 Experimental

General

The chemicals were used as received from local companies without further purification. Organic solvents were purified by distillation prior to use.

Column chromatography was carried out using silica gel (60-120 mesh). Thin layer chromatography was performed on the pre-coated silica gel 60 F_{254} aluminium sheets. Melting points are determined in open capillary and are uncorrected.

FT-IR spectra were recorded on Bruker Alpha FTIR spectrometer between 4000-400 cm^{-1} in solid state as KBr discs. The NMR spectra were recorded on 400 MHz Bruker Avance-III instrument and chemical shifts are given in parts per million. In the NMR data for ^{19}F decoupled ^{1}H NMR experiments, the data for the affected signals only are included. ^{19}F chemical shift values are of ^{1}H decoupled ^{19}F signals.

ESI mass spectra of all the new compounds were recorded on Waters' Xevo G2-XS QToF mass spectrometer at Zydus Research Centre, Ahmedabad.

General Procedure for the Synthesis of 6-Bromo/6-chloro-2-methyl-quinolin-4-yl-hydrazine 29.

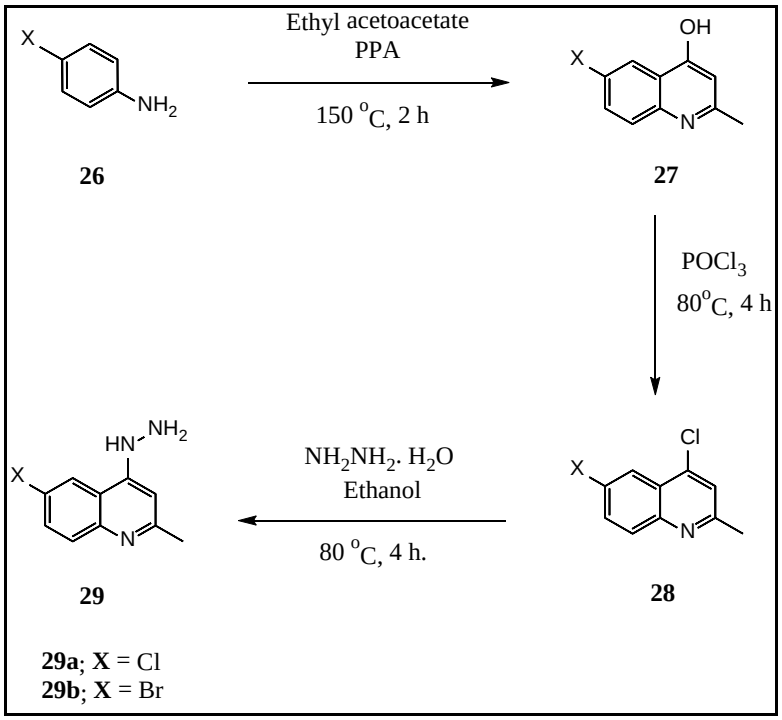

6-Bromo/6-chloro-2-methyl-quinolin-4-yl-hydrazine **29a**/**29b** was prepared following a known procedure.[54,55] To an equimolar quantity mixture of 4-chloro/bromo aniline **26** (78.3 mmol) and ethyl acetoacetate (78.3 mmol), polyphosphoric acid (50g, 5 w/w) was added and the reaction mixture was heated with stirring for 2h at 150 ^{o}C. After the completion of the reaction (as monitored by TLC), the reaction mixture was poured slowly into ice water with vigorous stirring. The precipitated solid was filtered and dried in vacuum oven to get the crude 6-bromo/6-chloro-2-methyl-quinolin-4-yl-hydrazine **27** as yellow solid. The crude product was pure enough and was used for the next step without further purification.

A mixture of **27** (25.82 mmol) and phosphorous oxychloride (28 mL) was heated at 80 ^{o}C for 4 h. The reaction was monitored by TLC. After completion of the reaction, excess $POCl_3$ was distilled off. The residue thus obtained was stirred with ice water for 15 min. After this, the separated precipitates were filtered and dried to obtain 6-bromo/-chloro-4-chloro-2-methyl hydrazine **28**.

Compound **28** (32.0 mmol) and hydrazine hydrate (20 mL) in ethanol (20 mL) were heated under reflux at 90 ^{o}C for 4 h. Completion of the reaction was monitored by TLC. The reaction mixture was concentrated and allowed to cool. The solid product obtained was filtered, washed with water and dried. Yield: 72-75%. 6-Bromo/6-chloro-2-methyl-quinolin-4-yl-hydrazine **29** were found to have melting points matching with that of the reported ones.[56]

General Procedure for the Synthesis of 2-aryl-4-[{N'-(6-bromo/6-chloro-2-methyl-quinolin-4-yl)hydrazono}methyl]- 5-methyl-1,3-oxazole 31.[54,55]

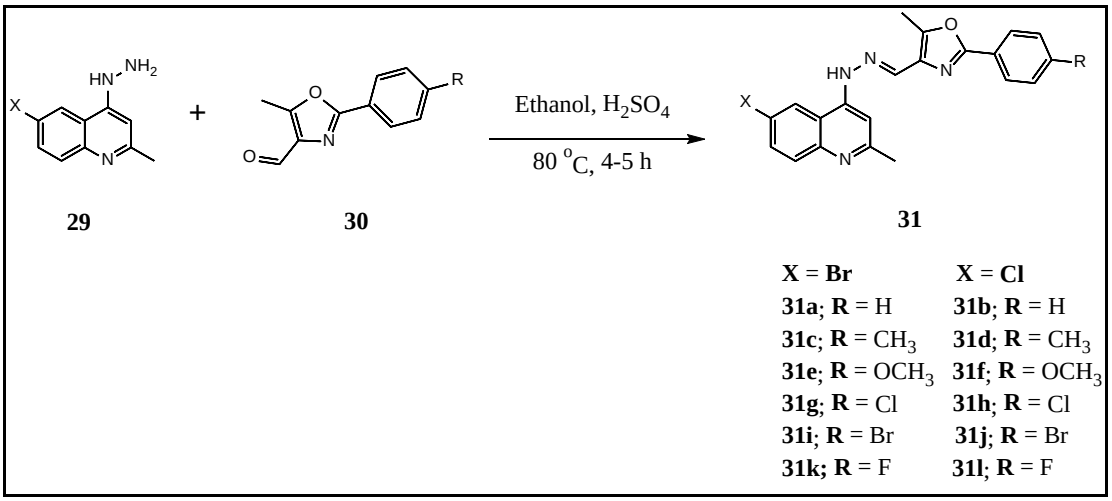

29 **30** **31**

X = **Br**	**X** = **Cl**
31a; **R** = H	**31b**; **R** = H
31c; **R** = CH_3	**31d**; **R** = CH_3
31e; **R** = OCH_3	**31f**; **R** = OCH_3
31g; **R** = Cl	**31h**; **R** = Cl
31i; **R** = Br	**31j**; **R** = Br
31k; R = F	**31l**; **R** = F

5-Methyl-2-aryl-1,3-oxazole-4-carbaldehydes **30a-f** (0.46 mmol) and 6-bromo/6-chloro-2-methyl-quinolin-4-yl-hydrazine **29a/29b** (0.46 mmol) were dissolved in ethanol (5 mL) and a catalytic amount of concentrated sulphuric acid was added. The resulting mixture was stirred at 80 ^{o}C for 4-5 h, and then kept the reaction mixture at room temperature for overnight. The solid separated was filtered, washed with chilled ethanol and recrystallized from ethanol to afford the pure final compounds **31a-l**. Yield: 76-82%.

4-[{N'-(6-Bromo-2-methylquinolin-4-yl)hydrazono}methyl]-5-methyl-2-phenyl-1,3-oxazole 31a.

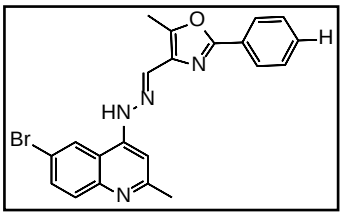

Compound **31a** was prepared following the general procedure described above by treating 2-(4-phenyl)-5-methyl-1,3-oxazole-4-carbaldehyde **30a** (0.1g, 0.53 mmol) in ethanol with 6-bromo-2-methyl-quinolin-4-yl-hydrazine **29a** (0.11g, 0.53 mmol) using H_2SO_4 as a catalyst. Yield = 0.17g, 80%; Yellow Solid; M.P. = 204 °C; **IR (KBr) cm^{-1}**: 3291, 2985, 1602, 1262, 1054, 776; **^{1}H NMR (400 MHz, DMSO-d$_6$, δ ppm)**: 2.68 (3H, s, -CH_3), 2.69 (3H, s, -CH_3), 7.34 (1H, s, -N=CH-), 7.62 (3H, m, Ar-H), 7.78 (1H, d, *J* = 9.2 Hz, Qui-H), 7.87 (1H, s, Qui-H), 8.04 (2H, d, *J* = 8.0 Hz, Ar-H,), 8.11 (1H, d, *J* = 8.8 Hz, Qui-H), 8.17 (1H, s, Qui-H), 13.38 (1H, s, -NH); **^{13}C NMR (100 MHz, DMSO-d$_6$, δ ppm)**: 10.9 (-**C**H_3), 20.7 (-**C**H_3), 61.7, 101.2, 115.5, 116.1, 117.0, 120.7, 124.0, 126.5, 129.9, 130.7, 131.7, 132.2, 135.6, 136.0, 137.0, 155.1, 159.2, 160.3; **Mass (TOF MS ES+)**: m/z 420.82 $(M+H)^+$, 422.81 $(MH+2)^+$ for M = $C_{21}H_{17}BrN_4O$.

4-[{N'-(6-Chloro-2-methylquinolin-4-yl)hydrazono}methyl]-5-methyl-2-phenyl-1,3-oxazole 31b.

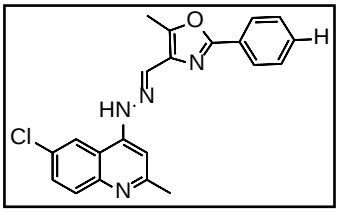

Compound **31b** was prepared following the general procedure described above by treating 2-(4-phenyl)-5-methyl-1,3-oxazole-4-carbaldehyde **30a** (0.1g, 0.53 mmol) in ethanol with 6-chloro-2-methyl-quinolin-4-yl-hydrazine **29b** (0.092g, 0.53 mmol) using H_2SO_4 as a catalyst. Yield = 0.15g, 79%; Yellow Solid; M.P. = 190 °C; **IR (KBr) cm^{-1}**: 3291, 2979, 1595, 1251, 1186, 956; **^{1}H NMR (400 MHz, DMSO-d$_6$, δ ppm)**: 2.68 (3H, s, -CH_3), 2.73 (3H, s, -CH_3), 7.32 (1H, s, -N=CH-), 7.56 (3H, t(b), *J* = 6.4 Hz, Ar-H), 7.88 (1H, d, *J* = 8.8 Hz, Qui-H), 8.00 (3H, m, Ar-H), 8.56 (1H, s, Qui-H), 8.63 (1H, s, Qui-H), 12.20 (1H, s, -NH); **^{13}C NMR (100 MHz, DMSO-d$_6$, δ ppm)**: 11.6 (-**C**H3), 20.5 (-**C**H3), 62.3, 101.1, 115.1, 122.0, 122.2, 126.1, 126.3, 129.6, 131.5, 131.6, 134.1, 137.2, 142.6, 150.9, 152.4, 155.2, 160.1; **Mass (TOF MS ES+)**: m/z 377.08 $(M+H)^+$, 379.51 $(MH+2)^+$ for M = $C_{21}H_{17}ClN_4O$.

4-[{N'-(6-Bromo-2-methylquinolin-4-yl)hydrazono}methyl]-5-methyl-2-(4-methyl-phenyl)-1,3-oxazole 31c.

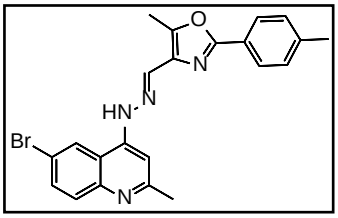

Compound **31c** was prepared following the general procedure described above by treating 2-(4-methylphenyl)-5-methyl-1,3-oxazole-4-carbaldehyde **30b** (0.1g, 0.49 mmol) in ethanol with 6-bromo-2-methyl-quinolin-4-yl-hydrazine **29a** (0.10g, 0.46 mmol) using H_2SO_4 as a catalyst. Yield = 0.17g, 82%; Yellow Solid; M.P. = 210 °C; **IR (KBr) cm^{-1}**: 3211, 2939, 1603, 1263, 1183, 777; **^{1}H NMR (400 MHz, DMSO-d$_6$, δ ppm)**: 2.33 (3H, s, -CH_3), 2.60 (3H, s, -CH_3), 2.63 (3H, s, -CH_3), 7.18 (1H, s, -N=CH-), 7.29 (2H, d, *J* = 8.0 Hz, Ar-H), 7.70 (2H, t(b), *J* = 8.8 Hz, Qui-H), 7.76 (2H, d, *J* = 8.0 Hz, Ar-H), 7.94 (1H, s, Qui-H), 8.01 (1H, d, *J* = 9.2 Hz, Qui-H), 13.18 (1H, s, -NH); **^{13}C NMR (100 MHz, DMSO-d$_6$, δ ppm)**: 10.9 (-**C**H_3), 20.8 (-**C**H_3), 21.6, 61.8, 100.5, 115.4, 120.1, 120.7, 122.2, 123.5, 126.3, 130.3, 130.5, 136.7, 142.5, 149.6, 154.7, 156.0, 159.3; **Mass (TOF MS ES+)**: m/z 434.83 $(M+H)^+$, 436.83 $(MH+2)^+$ for M = $C_{22}H_{19}BrN_4O$.

4-[{N'-(6-Chloro-2-methylquinolin-4-yl)hydrazono}methyl]-5-methyl-2-(4-methyl-phenyl)-1,3-oxazole 31d.

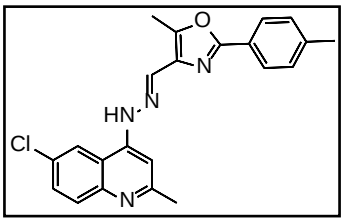

Compound **31d** was prepared following the general procedure described above by treating 2-(4-methylphenyl)-5-methyl-1,3-oxazole-4-carbaldehyde **30b** (0.1g, 0.49 mmol) in ethanol with 6-chloro-2-methyl-quinolin-4-yl-hydrazine **29b** (0.085g, 0.49 mmol) using H_2SO_4 as a catalyst. Yield = 0.15g, 80%; Yellow Solid; M.P. = 202 °C; **IR (KBr) cm^{-1}**: 3205, 2981, 1597, 1248, 1017, 776; **^{1}H NMR (400 MHz, DMSO-d$_6$, δ ppm)**: 2.36 (3H, s, -CH_3), 2.64 (3H, s, -CH_3), 2.70 (3H, s, -CH_3), 7.30 (1H, s, -N=CH-), 7.33 (2H, d, *J* = 8.0 Hz, Ar-H), 7.85 (3H, d(b), *J* = 8.0 Hz, Ar-H), 7.97 (1H, d, *J* = 9.2 Hz, Qui-H), 8.50 (1H, s, Qui-H), 8.58 (1H, s, Qui-H), 12.20 (1H, s, -NH); **^{13}C NMR (100 MHz, DMSO-d$_6$, δ ppm)**: 11.7 (-**C**H_3), 20.8 (-**C**H_3), 21.6, 61.8, 101.0, 115.4, 122.6, 123.8, 126.4, 130.2, 131.4, 131.5, 134.3, 137.9, 141.4, 143.0, 150.9, 152.0, 155.9, 160.2; **Mass (TOF MS ES+)**: m/z 390.89 $(M+H)^+$, 392.89 $(MH+2)^+$ for M = $C_{22}H_{19}ClN_4O$.

4-[{N'-(6-Bromo-2-methylquinolin-4-yl)hydrazono}methyl]-2-(4-methoxyphenyl)-5-methyl-1,3-oxazole 31e.

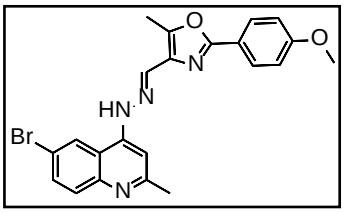

Compound **31e** was prepared following the general procedure described above by treating 2-(4-methoxyphenyl)-5-methyl-1,3-oxazole-4-carbaldehyde **29c** (0.1g, 0.46 mmol) in ethanol with 6-bromo-2-methyl-quinolin-4-yl-hydrazine **30a** (0.1g, 0.46 mmol) using H_2SO_4 as a catalyst. Yield = 0.16g, 78%; Yellow Solid; M.P. = 192 °C; **IR (KBr) cm^{-1}**: 3243, 2950, 1601, 1400, 1175, 861; **^{1}H NMR (400 MHz, DMSO-d$_6$, δ ppm)**: 2.62 (3H, s, -CH_3), 2.71 (3H, s, -CH_3 protons), 3.82 (3H, s, -OCH_3), 7.05 (2H, d, *J* = 8.4 Hz, Ar-H), 7.24 (1H, s, -N=CH-), 7.76 (1H, d, *J* = 9.2 Hz, Qui-H), 7.87 (2H, d, *J* = 8.4 Hz, Ar-H), 8.06 (1H, d, *J* = 8.8 Hz, Qui-H), 8.49 (1H, s, Qui-H), 8.70 (1H, s, Qui-H), 12.13 (1H, s, -NH); **^{13}C NMR (100 MHz, DMSO-d$_6$, δ ppm)**: 11.8 (-**C**H_3), 20.7 (-**C**H_3), 55.8 (-O**C**H_3), 61.7, 100.9, 115.0, 115.7, 119.0, 119.7, 122.3, 128.2, 131.4, 136.8, 143.2, 150.7, 151.8, 155.2, 160.1, 161.7; **Mass (TOF MS ES+)**: m/z 450.81 $(M+H)^+$, 452.81 $(MH+2)^+$ for M = $C_{22}H_{19}BrN_4O_2$.

4-[{N'-(6-Chloro-2-methylquinolin-4-yl)hydrazono}methyl)]-2-(4-methoxyphenyl) -5-methyl-1,3-oxazole 31f.

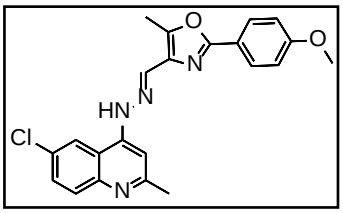

Compound **31f** was prepared following the general procedure described above by treating 2-(4-methoxyphenyl)-5-methyl-1,3-oxazole-4-carbaldehyde **29c** (0.1g, 0.46 mmol) in ethanol with 6-chloro-2-methyl-quinolin-4-yl-hydrazine **30b** (0.079g, 0.46 mmol) using H_2SO_4 as a catalyst. Yield = 0.14g, 76%; Yellow Solid; M.P. = 184 °C; **IR (KBr) cm^{-1}**: 3288, 2976, 1594, 1250, 855, 778; **^{1}H NMR (400 MHz, DMSO-d$_6$, δ ppm)**: 2.61 (3H, s, -CH_3), 2.70 (3H, s, -CH_3), 3.81 (3H, s, -OCH_3), 7.04 (2H, d, *J* = 8.4 Hz, Ar-H), 7.23 (1H, s, -N=CH-), 7.85 (2H, d, *J* = 9.6 Hz, Qui-H), 7.95 (2H, d, *J* = 8.4 Hz, Ar-H), 8.48 (1H, s, Qui-H), 8.55 (1H, s, Qui-H), 12.11 (1H, s, -NH); **^{13}C NMR (100 MHz, DMSO-d$_6$, δ ppm)**: 11.8 (-**C**H_3), 20.7 (-**C**H_3), 55.8 (-O**C**H_3), 61.7, 100.8, 144.9, 115.2, 119.0, 122.3, 128.1, 131.4, 134.1, 137.3, 143.2, 150.7, 151.7, 155.2, 160.1, 161.6; **Mass (TOF MS ES+)**: m/z 407.14 $(M+H)^+$,409.39 $(MH+2)^+$ for M = $C_{22}H_{19}ClN_4O_2$.

4-[{N'-(6-Bromo-2-methylquinolin-4-yl)hydrazono}methyl]-2-(4-chlorophenyl)-5-methyl-1,3-oxazole 31g.

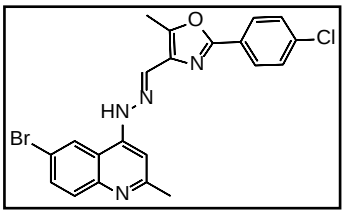

Compound **31g** was prepared following the general procedure described above by treating 2-(4-chlorophenyl)-5-methyl-1,3-oxazole-4-carbaldehyde **29d** (0.1g, 0.45 mmol) in ethanol with 6-bromo-2-methyl-quinolin-4-yl-hydrazine **30a** (0.098g, 0.45 mmol) using H_2SO_4 as a catalyst. Yield = 0.16g, 80%; Yellow Solid; M.P. = 194 °C; **IR (KBr) cm^{-1}**: 3204, 2983, 1596, 1250, 1187, 1017, 921; **^{1}H NMR (400 MHz, DMSO-d$_6$, δ ppm)**: 2.68 (3H, s, -CH_3), 2.72 (3H, s, -CH_3), 7.30 (1H, s, -N=CH-), 7.62 (2H, d, *J* = 8.4 Hz, Ar-H), 7.80 (1H, d, *J* = 8.8 Hz, Qui-H), 7.98 (2H, d, *J* = 8.4 Hz, Ar-H), 8.01 (1H, d, *J* = 8.8 Hz, Qui-H), 8.55 (1H, s, Qui-H), 8.76 (1H, s, Qui-H), 12.21 (1H, s, -NH); **^{13}C NMR (100 MHz, DMSO-d$_6$, δ ppm)**: 11.9 (-**C**H_3), 20.8 (-**C**H_3), 61.7, 101.1, 115.7, 119.7, 122.4, 125.3, 125.5, 128.1, 129.7, 131.8, 136.0, 136.8, 143.0, 150.7, 152.5, 155.5, 159.1; **Mass (TOF MS ES+)**: m/z 454.76 $(M+H)^+$, 456.76 $(MH+2)^+$ for M = $C_{21}H_{16}BrClN_4O$.

4-[{N'-(6-Chloro-2-methylquinolin-4-yl)hydrazono}methyl]-2-(4-chlorophenyl)-5-methyl-1,3-oxazole 31h.

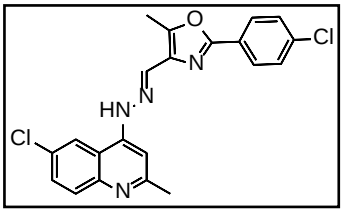

Compound **31h** was prepared following the general procedure described above by treating 2-(4-chlorophenyl)-5-methyl-1,3-oxazole-4-carbaldehyde **30d** (0.1g, 0.45 mmol) in ethanol with 6-chloro-2-methyl-quinolin-4-yl-hydrazine **29b** (0.078g, 0.45 mmol) using H_2SO_4 as a catalyst. Yield = 0.14g, 76%; Yellow Solid; M.P. = 188 °C; **IR (KBr) cm^{-1}**: 3204, 2983, 1576, 1240, 1019, 921; **^{1}H NMR (400 MHz, DMSO-d$_6$, δ ppm)**: 2.68 (3H, s, -CH_3), 2.73 (3H, s, -CH_3), 7.30 (1H, s, -N=CH-), 7.61 (2H, d, *J* = 8.4 Hz, Ar-H), 7.88 (1H, d, , *J* = 8.8 Hz, Qui-H), 7.98 (2H, d, *J* = 8.4 Hz, Ar-H), 8.01 (1H, d, , *J* = 2.0 Hz, Qui-H), 8.55 (1H, s, Qui-H), 8.62 (1H, s, Qui-H), 12.19 (1H, s, -NH); **^{13}C NMR (100 MHz, DMSO-d$_6$, δ ppm)**: 11.9 (-**C**H_3), 20.7 (-**C**H_3), 61.7, 100.8, 115.2, 122.3, 125.2, 128.0, 129.7, 131.5, 131.8, 134.2, 136.0, 137.3, 143.0, 150.7, 152.4, 155.3, 159.0; **Mass (TOF MS ES+)**: m/z 410.83 $(M+H)^+$, 412.82 $(MH+2)^+$ for M = $C_{21}H_{16}Cl_2N_4O$.

4-[{N'-(6-Bromo-2-methylquinolin-4-yl)hydrazono}methyl]-2-(4-bromophenyl)-5-methyl-1,3-oxazole 31i.

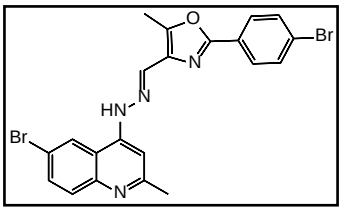

Compound **31i** was prepared following the general procedure described above by treating 2-(4-bromophenyl)-5-methyl-1,3-oxazole-4-carbaldehyde **30e** (0.1g, 0.37 mmol) in ethanol with 6-bromo-2-methyl-quinolin-4-yl-hydrazine **29a** (0.081g, 0.37 mmol) using H_2SO_4 as a catalyst. Yield = 0.15g, 80%; Yellow Solid; M.P. = 208 °C; **IR (KBr) cm^{-1}**: 3244, 2949, 1602, 1256, 1199, 1046, 795; **^{1}H NMR (400 MHz, DMSO-d$_6$, δ ppm)**: 2.66 (3H, s, -CH_3), 2.70 (3H, s, -CH_3), 7.31 (1H, s, -N=CH-), 7.74 (2H, d, *J* = 8.0 Hz, Ar-H), 7.78 (1H, d, *J* = 8.4 Hz, Qui-H), 7.90 (2H, d, *J* = 8.0 Hz, Ar-H), 8.09 (1H, d, *J* = 8.8 Hz, Qui-H), 8.52 (1H, s, Qui-H), 8.74 (1H, s, Qui-H), **^{13}C NMR (100 MHz, DMSO-d$_6$, δ ppm)**: 10.9 (-**C**H_3), 15.3 (-**C**H_3), 20.8, 21.6, 61.8, 100.5, 115.4, 120.1, 120.7, 122.2, 123.5, 126.3, 130.3, 130.5, 136.7, 142.5, 149.6, 154.7, 156.0, 159.3; **Mass (TOF MS ES+)**: m/z 498.70 $(M+H)^+$, 500.98 $(MH+2)^+$ for M = $C_{22}H_{19}BrN_4O$.

2-(4-Bromophenyl)-4-[{N'-(6-chloro-2-methylquinolin-4-yl)hydrazono}methyl]-5-methyl-1,3-oxazole 31j.

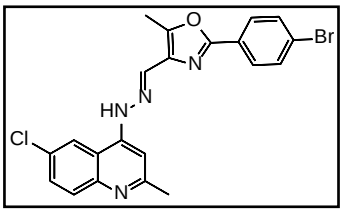

Compound **31j** was prepared following the general procedure described above by treating 2-(4-bromophenyl)-5-methyl-1,3-oxazole-4-carbaldehyde **30e** (0.1g, 0.37 mmol) in ethanol with 6-chloro-2-methyl-quinolin-4-yl-hydrazine **29b** (0.065g, 0.37 mmol) using H_2SO_4 as a catalyst. Yield = 0.13g, 78%; Yellow Solid; M.P. = 198 °C; **IR (KBr) cm^{-1}**: 3251, 2953, 1600, 1209, 1042, 778; **^{1}H NMR (400 MHz, DMSO-d$_6$, δ ppm)**: 2.63 (3H, s, -CH_3), 2.70 (3H, s, -CH_3), 7.24 (1H, s, -N=CH-), 7.68 (2H, d, *J* = 8.4 Hz, Ar-H), 7.80 (1H, d, *J* = 9.2 Hz, Qui-H), 7.83 (2H, d, *J* = 8.8 Hz, Ar-H), 7.94 (1H, d, *J* = 9.2 Hz, Qui-H), 8.46 (1H, s, Qui-H), 8.52 (1H, s, Qui-H), **^{13}C NMR (100 MHz, DMSO-d$_6$, δ ppm)**: 11.8 (-**C**H_3), 20.7 (-**C**H_3), 61.9, 100.8, 115.2, 122.3, 124.9, 125.5, 128.2, 131.5, 131.8, 132.6, 134.2, 137.3, 142.7, 144.4, 150.8, 152.5, 155.3, 159.2; **Mass (TOF MS ES+)**: m/z 454.7715 $(M+H)^+$,456.7677 $(M+2H)^+$ for M = $C_{21}H_{16}BrClN_4O$.

4-[{N'-(6-Bromo-2-methylquinolin-4-yl)hydrazono}methyl]-2-(4-fluorophenyl)-5-methyl-1,3-oxazole 31k.

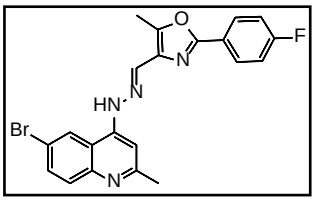

Compound **31k** was prepared following the general procedure described above by treating 2-(4-fluorophenyl)-5-methyl-1,3-oxazole-4-carbaldehyde **30f** (0.1g, 0.48 mmol) in ethanol with 6-bromo-2-methyl-quinolin-4-yl-hydrazine **29a** (0.10g, 0.48 mmol) using H_2SO_4 as a catalyst. Yield = 0.17g, 82%; Yellow Solid; M.P. = 206 ^oC; **IR (KBr) cm^{-1}**: 3264, 2977, 1644, 1250, 1089, 855; **^{1}H NMR (400 MHz, DMSO-d$_6$, δ ppm)**: 2.66 (3H, s, -CH_3), 2.71 (3H, s, -CH_3), 7.26 (1H, s, -N=CH-), 7.39 (3H, m, Ar-H), 7.80 (1H, d, *J* = 8.8 Hz, Qui-H), 8.05 (3H, m, Ar-H), 8.55 (1H, s, Qui-H), 8.76 (1H, s, Qui-H); **^{19}F NMR (376 MHz, $CDCl_3$, δ ppm)** : -108.8; **^{13}C NMR (100 MHz, DMSO-d$_6$, δ ppm)**: 11.8 (-**C**H_3), 20.7 (-**C**H_3), 61.9, 101.2, 116.7, 116.9 ($^2J_{CF}$ = 23 Hz), 119.4, 119.8, 122.3, 123.2, 125.7, 129.0, 131.6, 136.8, 142.9, 150.7, 152.6 ($^4J_{CF}$ = 183 Hz), 155.3, 159.8, 162.8, 165.1 ; **Mass (TOF MS ES+)**: m/z 439.01 $(M+H)^+$ calculated for M = $C_{21}H_{16}BrFN_4O$.

4-[{N'-(6-Chloro-2-methylquinolin-4-yl)hydrazono}methyl]-2-(4-fluorophenyl)-5-methyl-1,3-oxazole 31l.

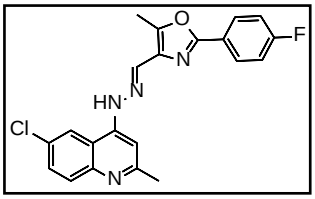

Compound **31l** was prepared following the general procedure described above by treating 2-(4-fluorophenyl)-5-methyl-1,3-oxazole-4-carbaldehyde **30f** (0.1g, 0.48 mmol) in ethanol with 6-chloro-2-methyl-quinolin-4-yl-hydrazine **29b** (0.085g, 0.48 mmol) using H_2SO_4 as a catalyst. Yield = 0.15g, 80%; Yellow Solid; M.P. = 200 ^oC; **IR (KBr) cm^{-1}**: 3251, 2984, 1642, 1230, 1071, 843; **^{1}H NMR (400 MHz, DMSO-d$_6$, δ ppm)**: 2.61 (3H, s, -CH_3), 2.70 (3H, s, -CH_3), 7.25 (1H, s, -N=CH-), 7.33 (2H, t(b), *J* = 7.6 Hz, Ar-H), 7.79 (1H, d, *J* = 8.4 Hz, Qui-H), 7.93 (3H, d(b), *J* = 6.4 Hz, Ar-H), 8.46 (1H, s, Qui-H), 8.51 (1H, s, Qui-H), 12.1 (1H, s, -NH) **^{19}F NMR (376 MHz, $CDCl_3$, δ ppm)** : -108.9; **^{13}C NMR (100 MHz, DMSO-d$_6$, δ ppm)**: 11.8 (-**C**H_3), 20.8 (-**C**H_3), 61.9, 100.9, 115.2, 116.7, 116.9 ($^2J_{CF}$ = 22 Hz), 122.2, 122.3, 132.1, 128.9, 128.98 ($^2J_{CF}$ = 8.7 Hz), 131.6, 131.64 ($^3J_{CF}$ = 3.6 Hz), 134.3, 137.2, 143.0, 150.9, 152.4 ($^4J_{CF}$ = 152 Hz), 155.3, 159.2, 162.7 ; **Mass (TOF MS ES+)**: m/z 394.86 $(M+H)^+$, 396.86 $(MH+2)^+$ for M = $C_{21}H_{16}ClFN_4O$.

6.5 Spectral Data

Compound 31a

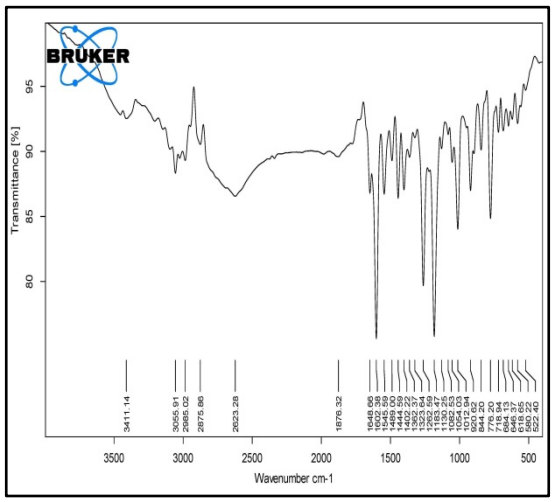

Spectrum 1. IR of compound 31a

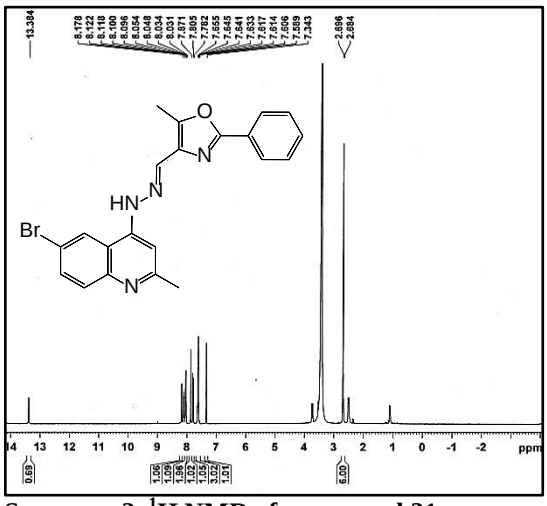

Spectrum 2. ^{1}H NMR of compound 31a

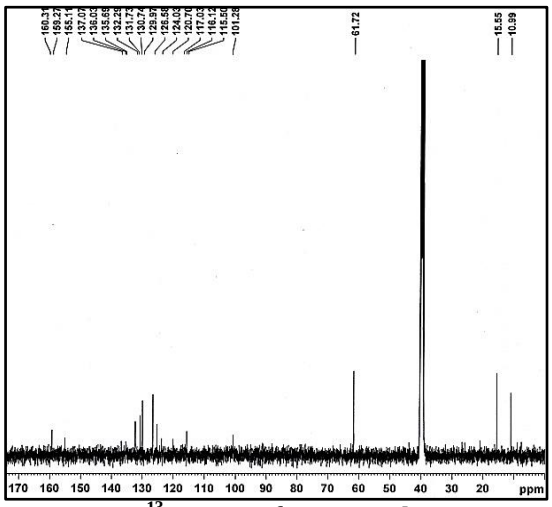

Spectrum 3. ^{13}C NMR of compound 31a

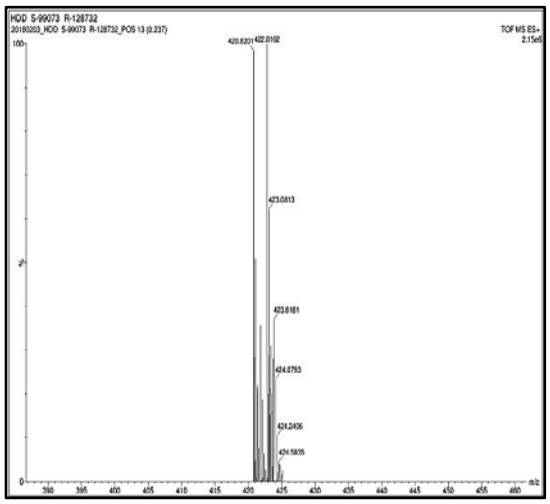

Spectrum 4. MASS of compound 31a

Compound 31b

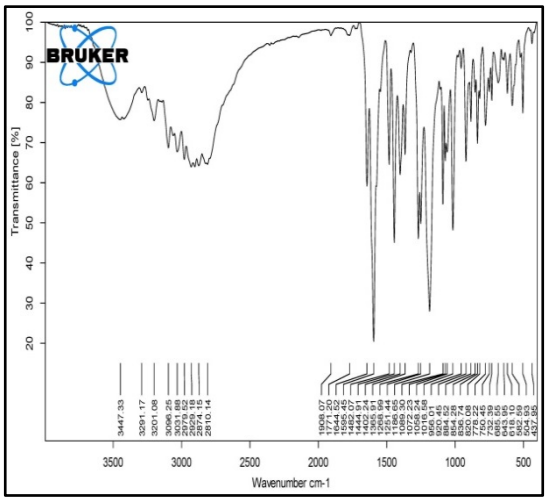

Spectrum 5. IR of compound 31b

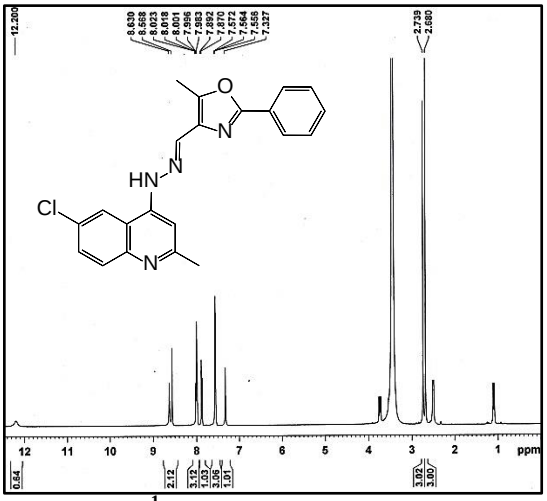

Spectrum 6. ^{1}H NMR of compound 31b

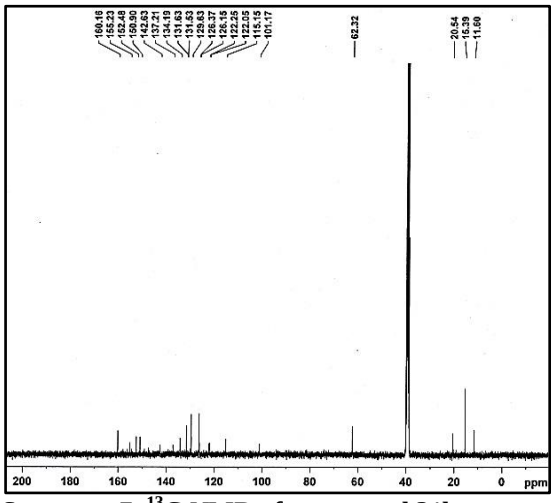

Spectrum 7. ^{13}C NMR of compound 31b

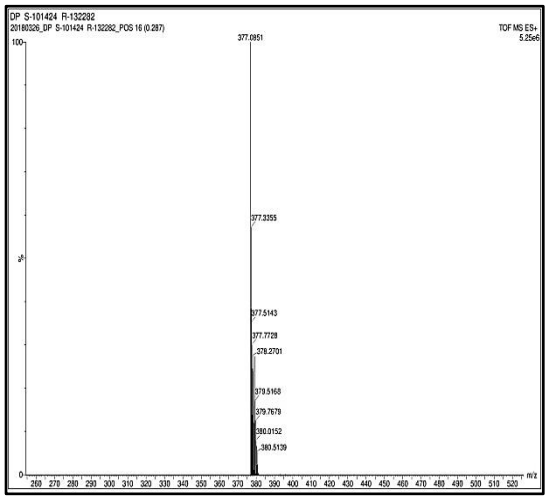

Spectrum 8. MASS of compound 31b

Compound 31c

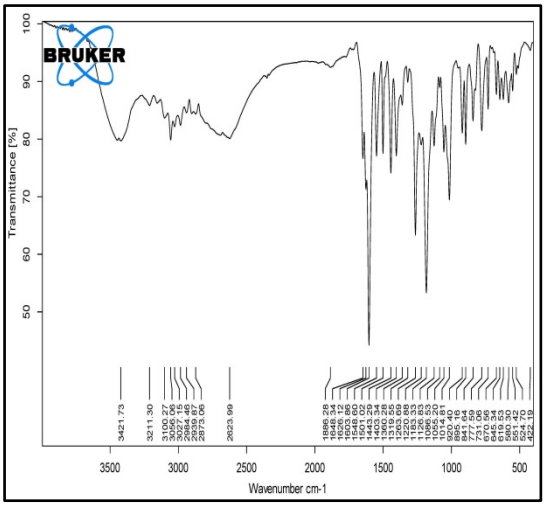

Spectrum 9. IR of compound 31c

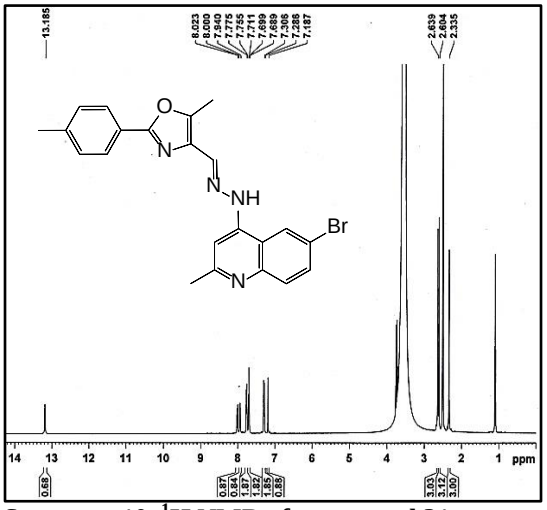

Spectrum 10. ^{1}H NMR of compound 31c

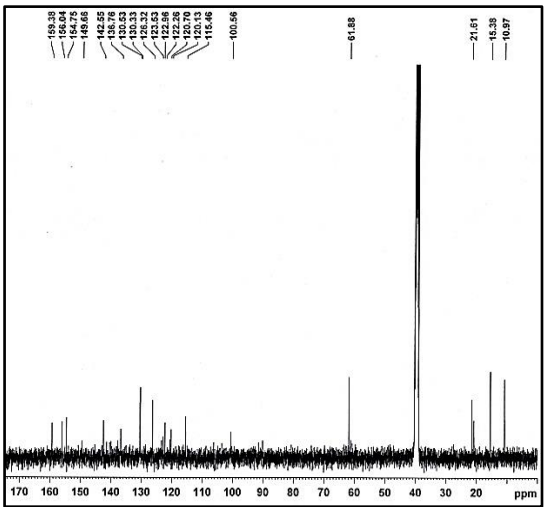

Spectrum 11. ^{13}C NMR of compound 31c

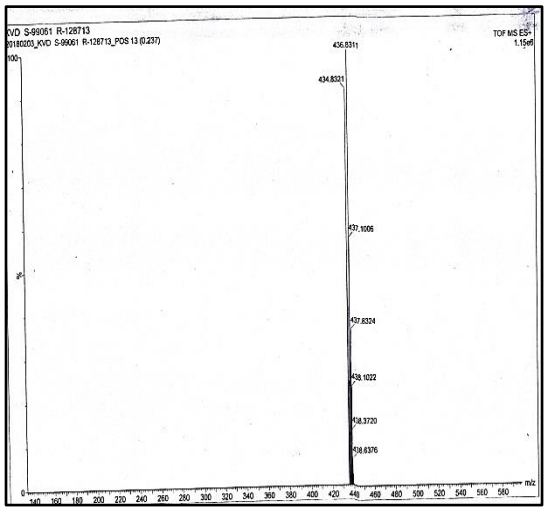

Spectrum 12. MASS of compound 31c

Compound 31d

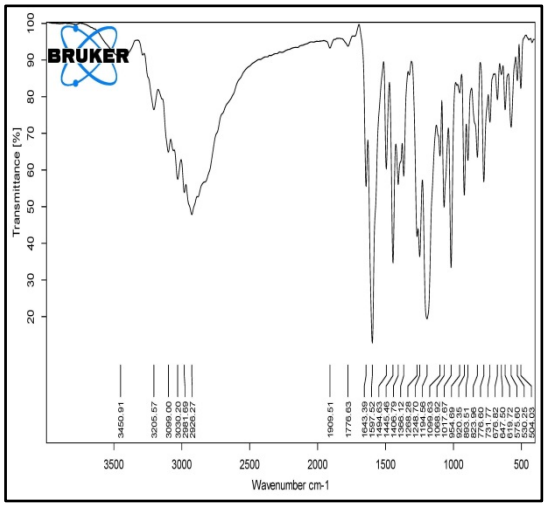

Spectrum 13. IR of compound 31d

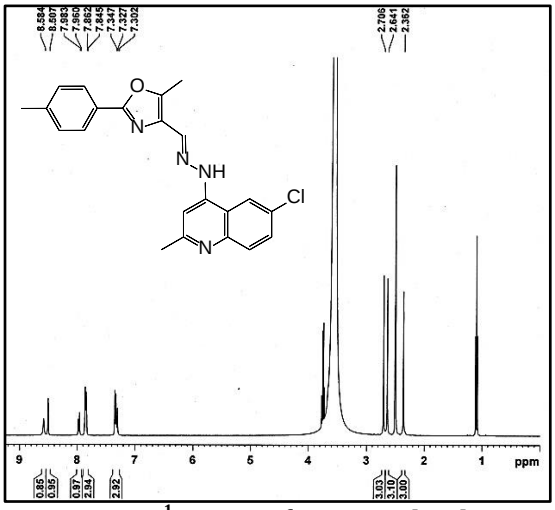

Spectrum 14. ^{1}H NMR of compound 31d

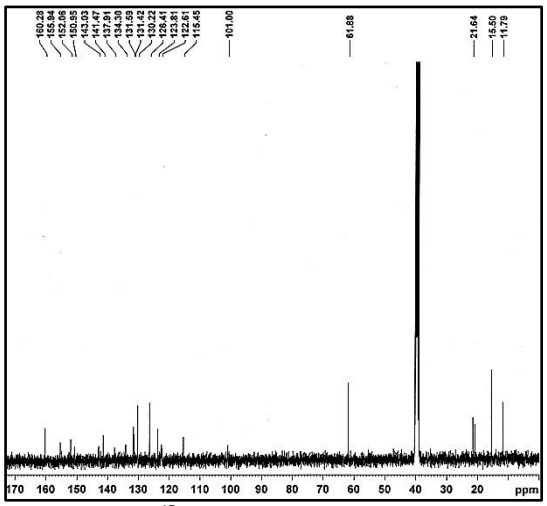

Spectrum 15. ^{13}C NMR of compound 31d

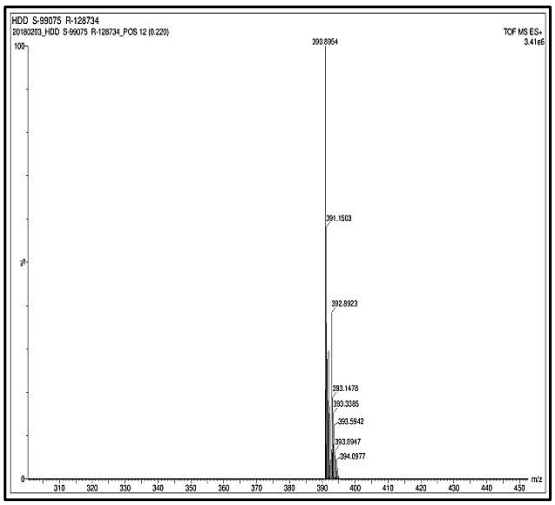

Spectrum 16. MASS of compound 31d

Compound 31e

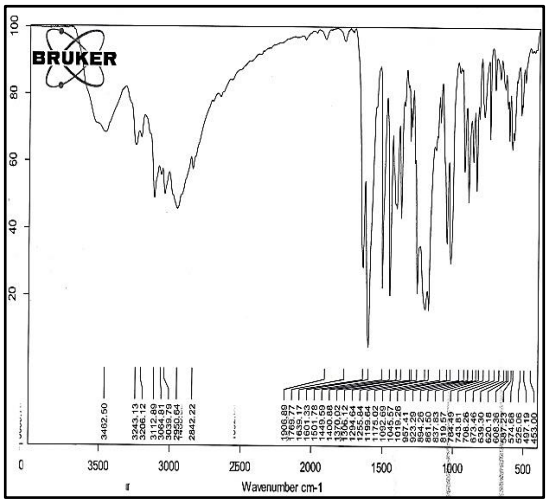

Spectrum 17. IR of compound 31e

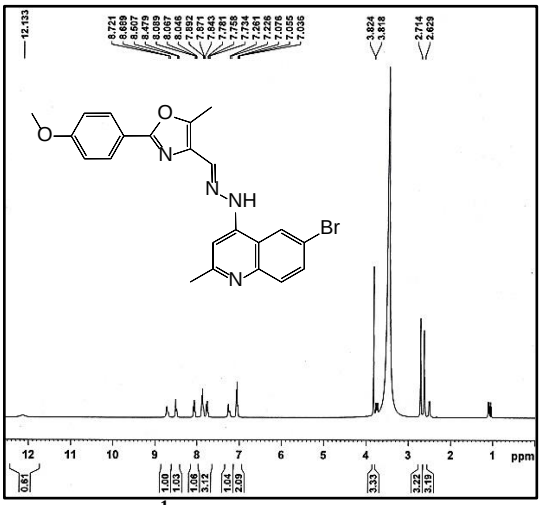

Spectrum 18. ^{1}H NMR of compound 31e

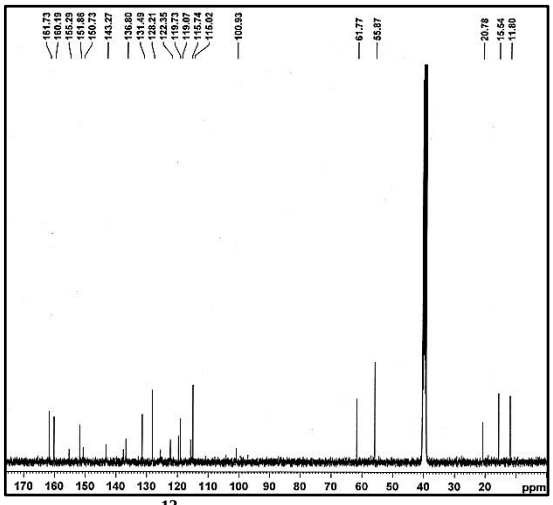

Spectrum 19. ^{13}C NMR of compound 31e

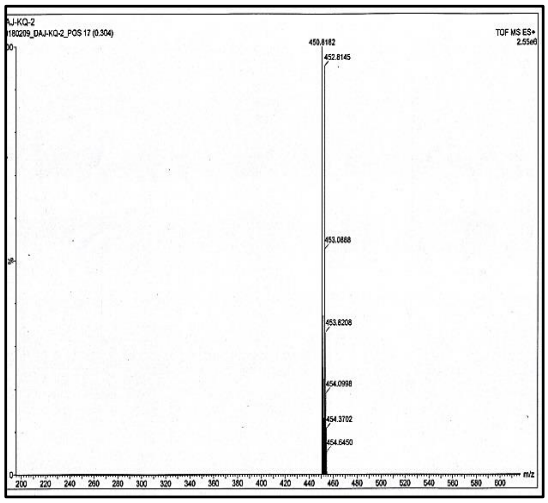

Spectrum 20. MASS of compound 31e

Compound 31f

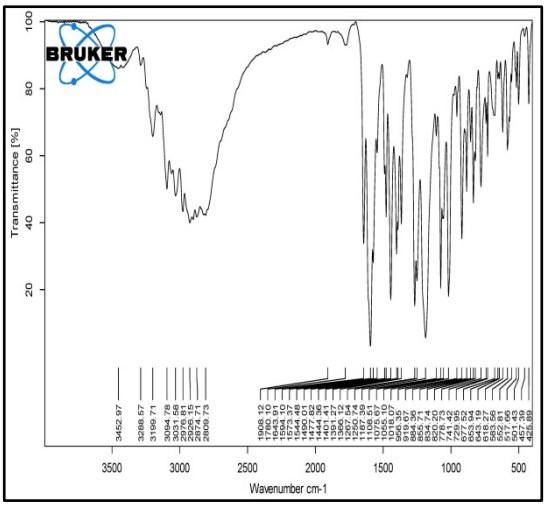

Spectrum 21. IR of compound 31f

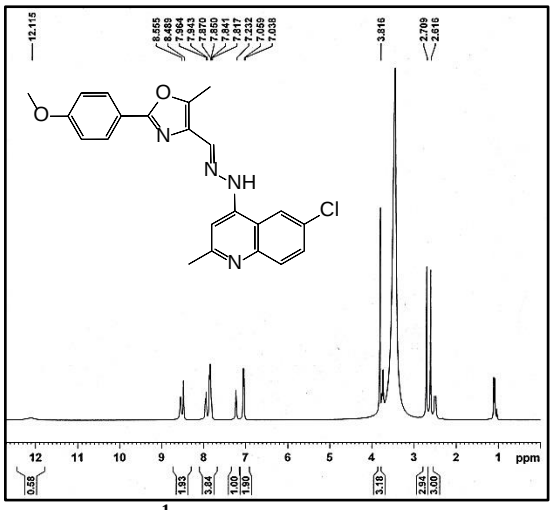

Spectrum 22. ^{1}H NMR of compound 31f

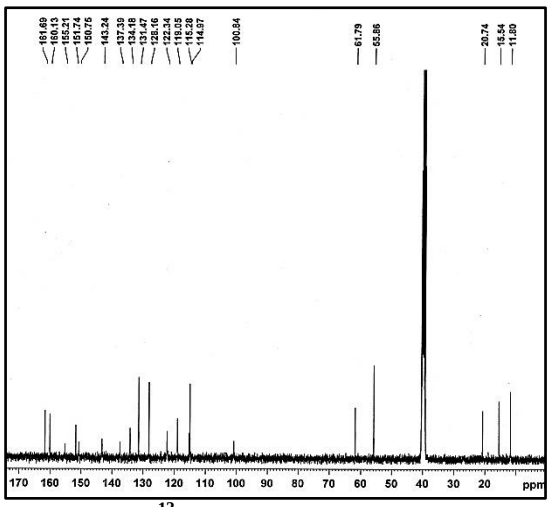

Spectrum 23. ^{13}C NMR of compound 31f

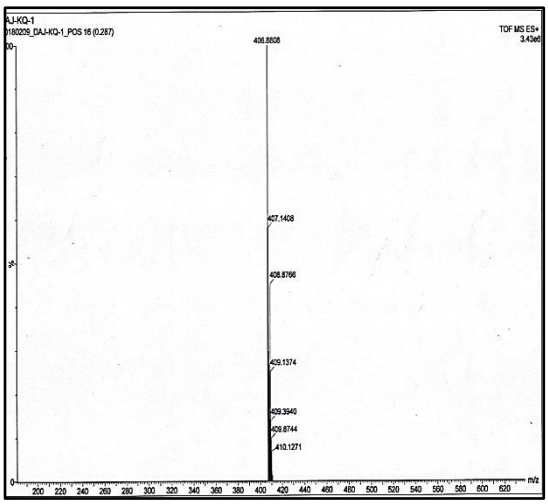

Spectrum 24. MASS of compound 31f

Compound 31g

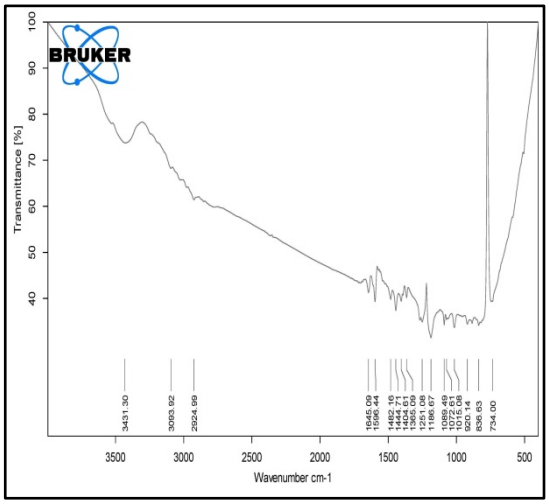

Spectrum 25. IR of compound 31g

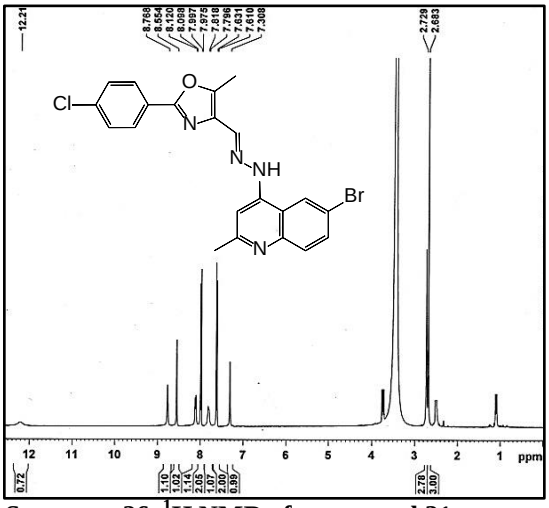

Spectrum 26. ^{1}H NMR of compound 31g

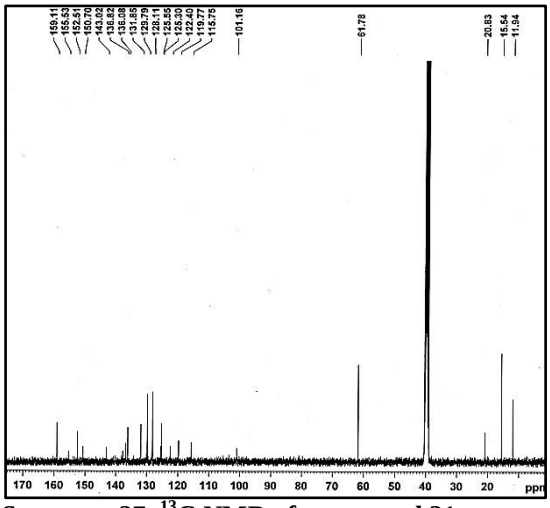

Spectrum 27. ^{13}C NMR of compound 31g

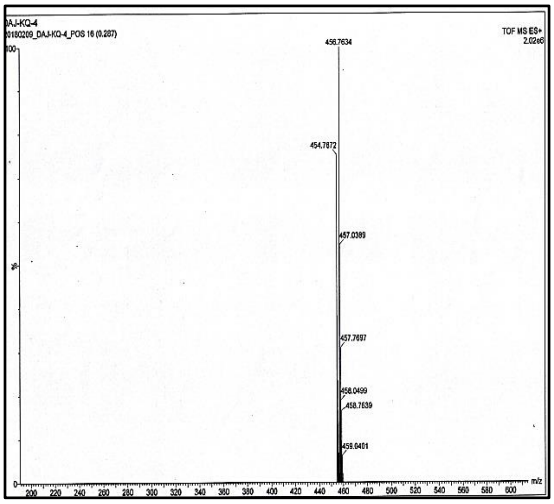

Spectrum 28. MASS of compound 31g

Compound 31h

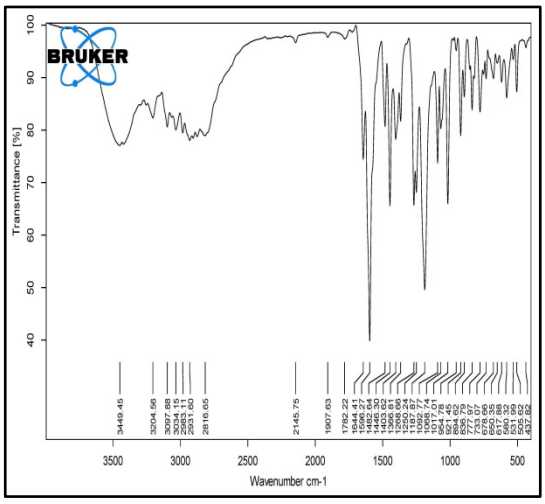

Spectrum 29. IR of compound 31h

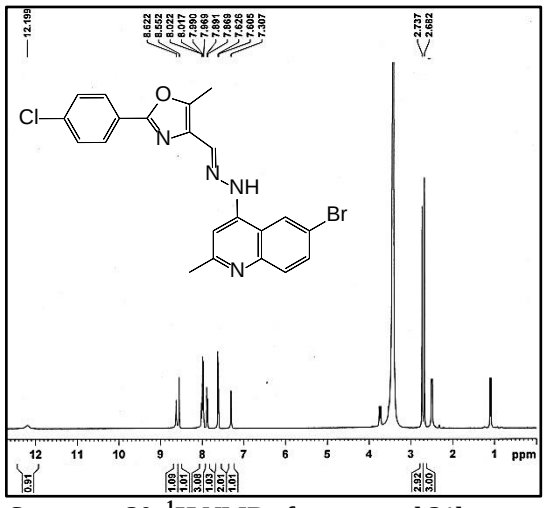

Spectrum 30. ^{1}H NMR of compound 31h

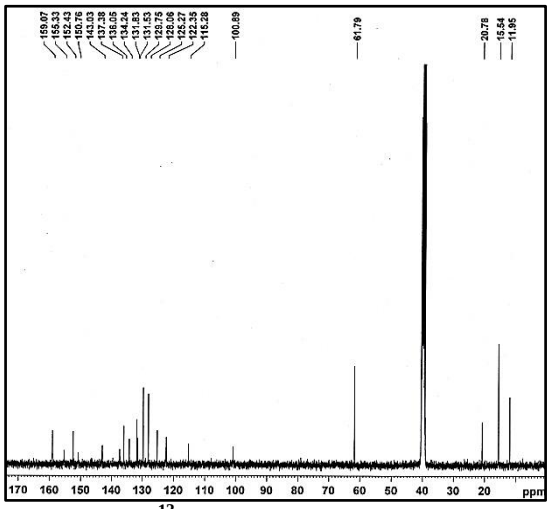

Spectrum 31. ^{13}C NMR of compound 31h

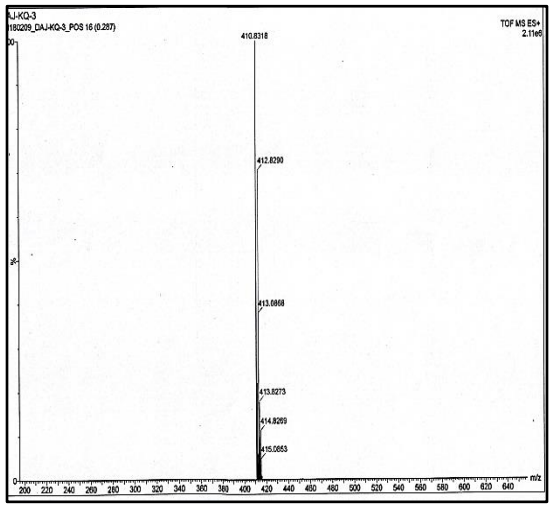

Spectrum 32. MASS of compound 31h

Compound 31i

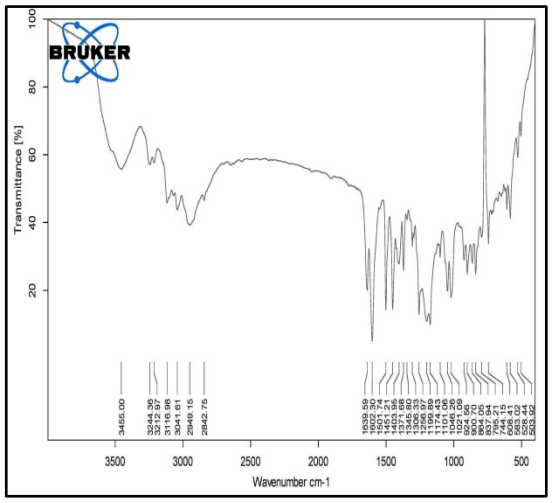

Spectrum 33. IR of compound 31i

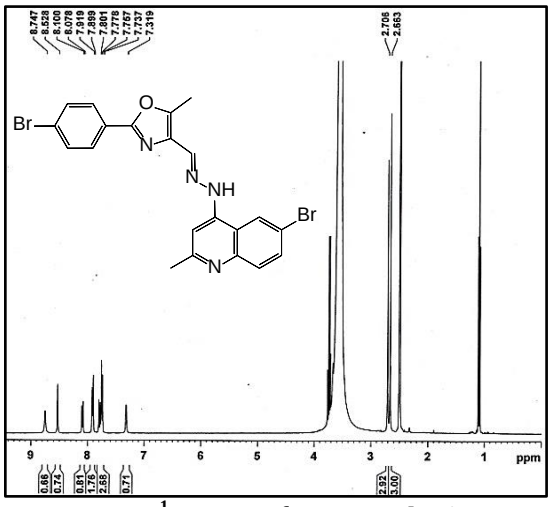

Spectrum 34. ^{1}H NMR of compound 31i

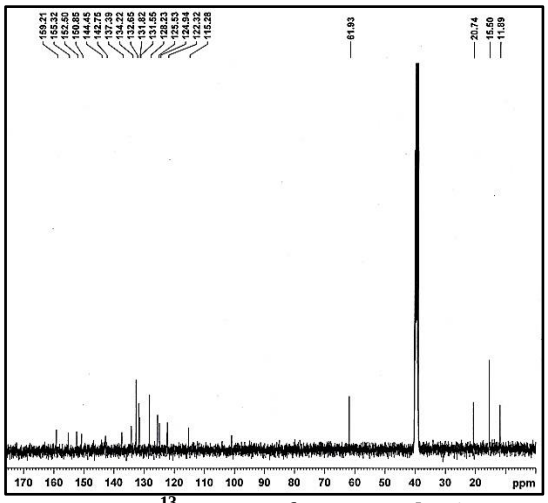

Spectrum 35. ^{13}C NMR of compound 31i

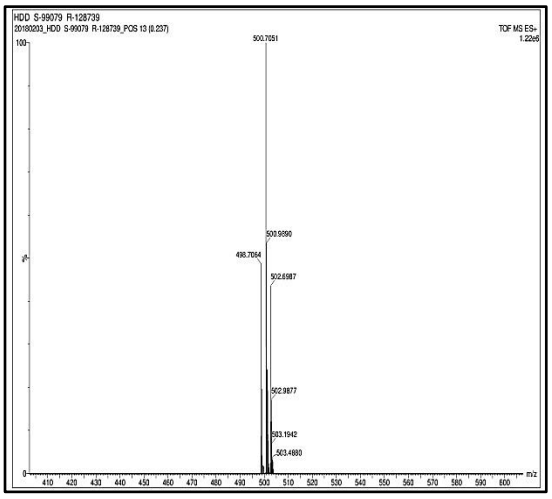

Spectrum 36. MASS of compound 31i

Compound 31j

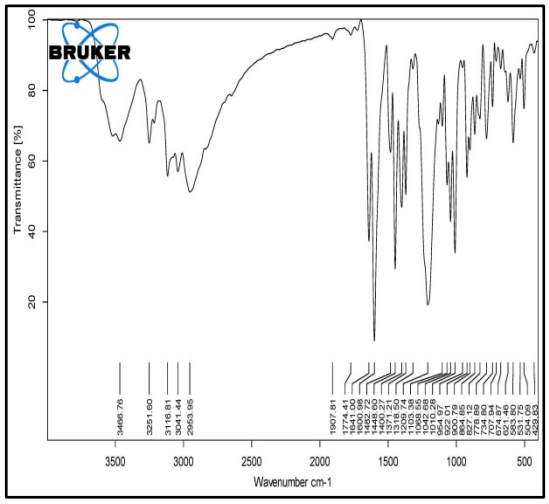

Spectrum 37. IR of compound 31j

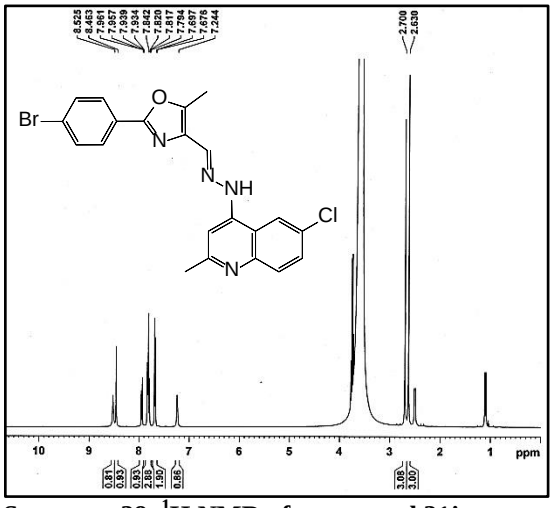

Spectrum 38. ^{1}H NMR of compound 31j

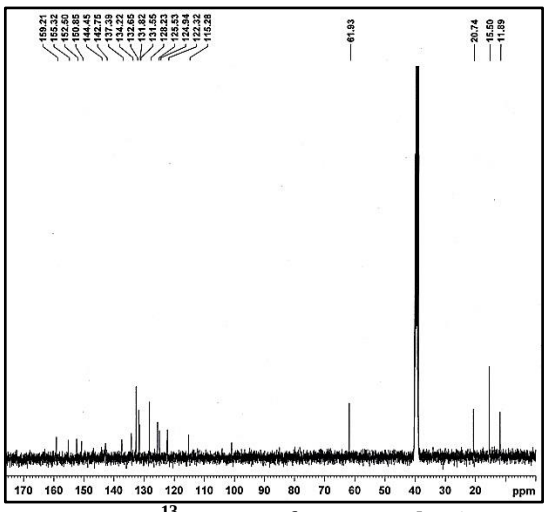

Spectrum 39. ^{13}C NMR of compound 31j

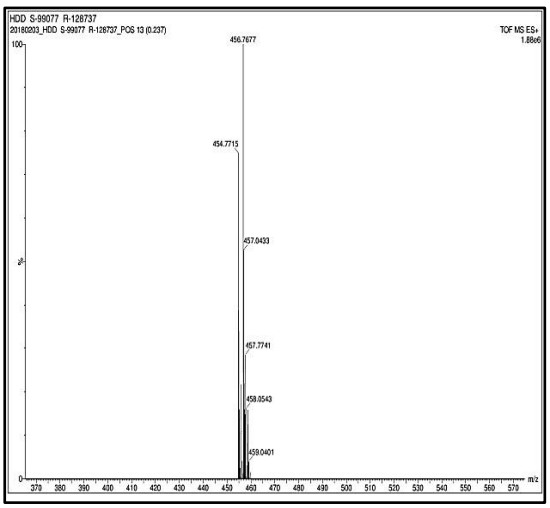

Spectrum 40. MASS of compound 31j

Compound 31k

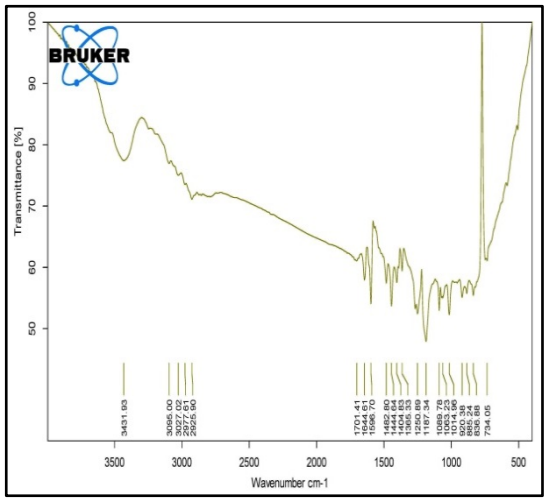

Spectrum 41. IR of compound 31k

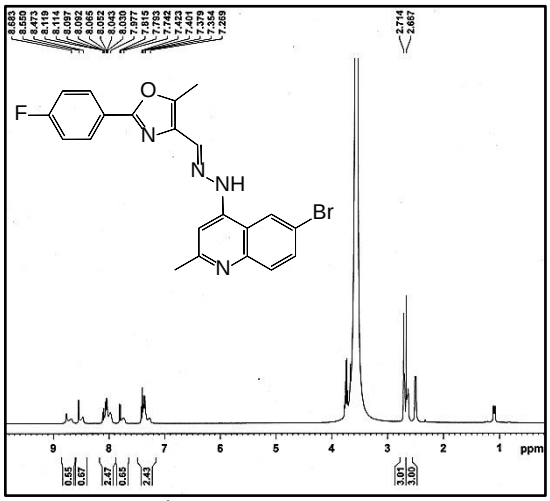

Spectrum 42. ^{1}H NMR of compound 31k

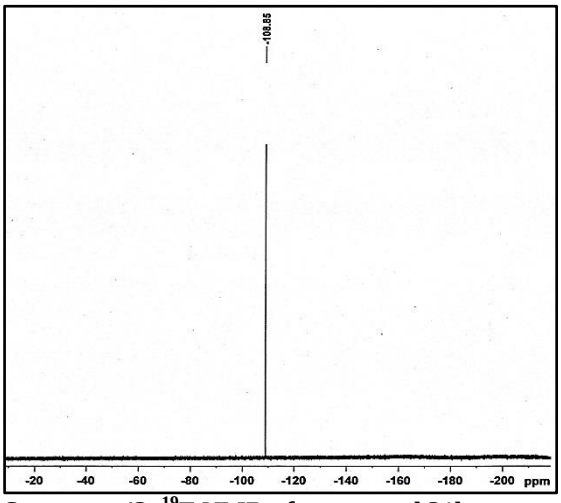

Spectrum 43. ^{19}F NMR of compound 31k

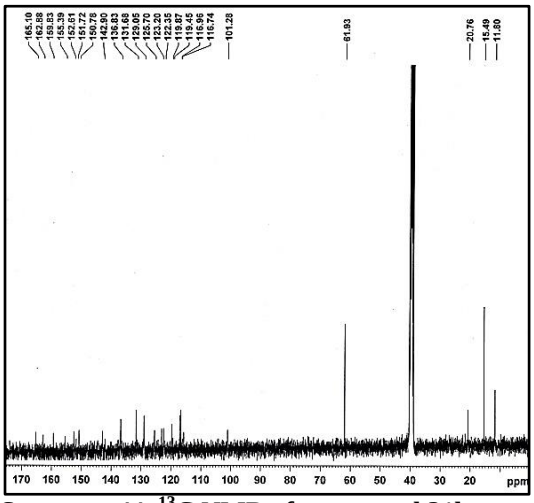

Spectrum 44. ^{13}C NMR of compound 31k

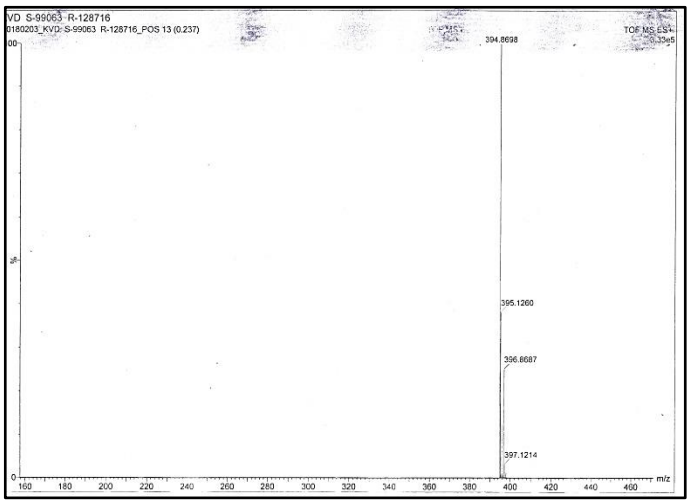

Spectrum 45. MASS of compound 31k

Compound 31l

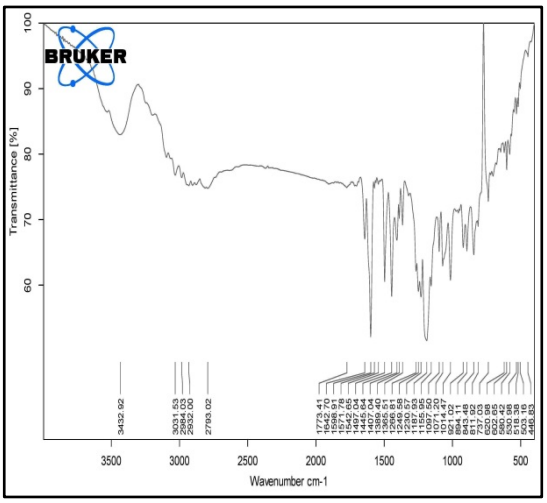

Spectrum 46. IR of compound 31l

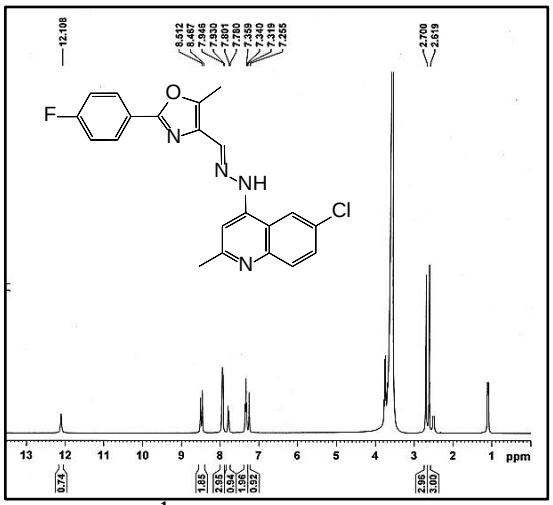

Spectrum 47. ^{1}H NMR of compound 31l

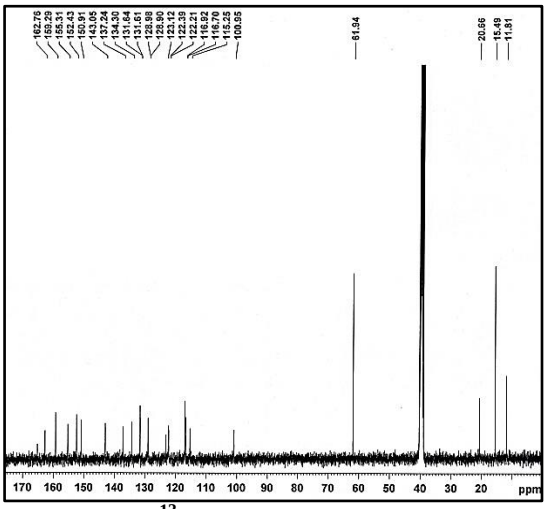

Spectrum 48. ^{13}C NMR of compound 31l

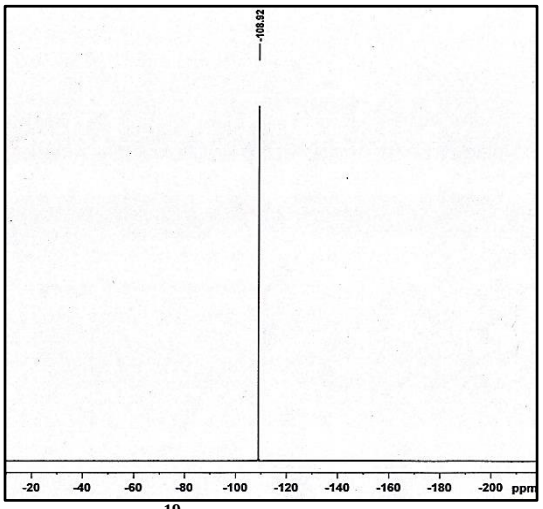

Spectrum 49. ^{19}F NMR of compound 31l

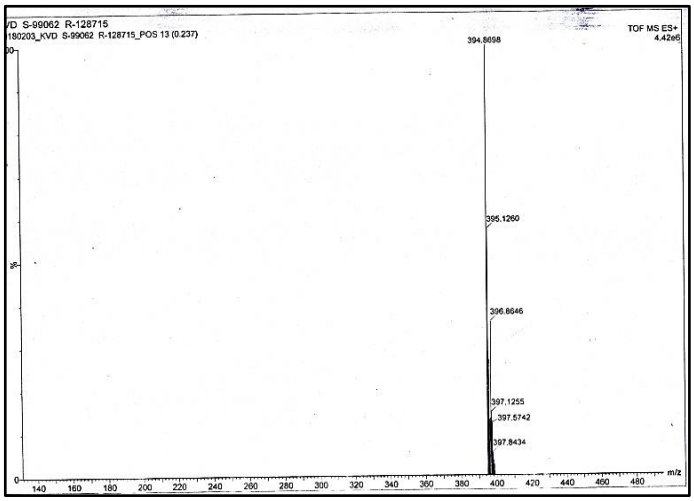

Spectrum 50. MASS of compound 31l

Chapter – 6 (B)

Synthesis and study of antimicrobial and anticancer activities of

(E)-4-{N'-Arylidene-hydrazinyl}-6-bromo-/6-chloro- 2-methylquinoline and their docking study.

6.6 Introduction

Keeping diverse biological activities of quinoline derivatives and of quinoline hydrazone derivatives in mind, several new quinoline hydrazones have been prepared using quinoline-4-hydrazine derivatives in this part of the chapter. Bioactivity study of these new quinoline hydrazones has been carried out.

For the synthesis of the new hydrazones, several alkoxy substituted aromatic aldehydes were prepared from the corresponding hydroxy aldehydes. 4-Alkoxy acetophenones were also prepared from 4-hydroxy acetophenone and were condensed with the quinoline hydrazines to yield the corresponding new hydrazones.

6.7 Results and Discussion

Synthesis of alkoxy substituted aromatic aldehydes and ketones was carried out with varying alkyl chain lengths to have different lipophilicity of the final compounds. The use of these compounds in preparation of new hydrazone derivatives is expected to result in different lipophilicity of the final compounds.

To prepare the new quinoline hydrazones, these alkoxy substituted aromatic aldehydes and 4-alkoxy acetophenones were condensed with 6-bromo/6-chloro-2-methyl-quinolin-4-yl-hydrazine to get the final targeted new hydrazones.

The 4-alkyloxybenzaldehydes were prepared by reacting 4-hydroxy benzaldehyde and alkyl halides with chain length varying from 2 to 8 carbons in the presence of K_2CO_3 as a base in acetone[56,62] (**Scheme 6.3**).

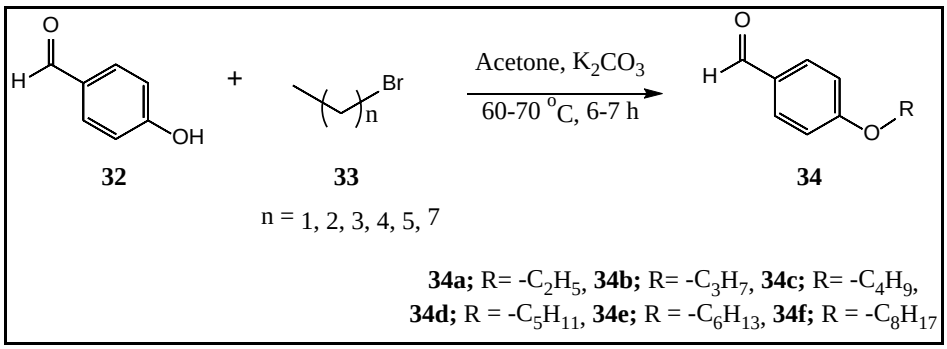

Scheme 6.3 ***Synthesis of 4-alkoxy benzaldehydes***.

Similarly, 3,4-bis-octyloxy benzaldehyde and 3,4,5-tris-octyloxy benzaldehyde were prepared from 3,4-dihydroxy benzaldehyde and 3,4,5-trihydroxybenzaldehyde respectively by reacting 3,4-hydroxy aldehyde and 3,4,5-trihydroxybenzaldehyde with 1-bromooctane in dry DMF using K_2CO_3 as a base to afford 3,4-bis-octyloxy benzaldehyde and 3,4,5-tris-octyloxy benzaldehyde[63,64] (**Scheme 6.4**).

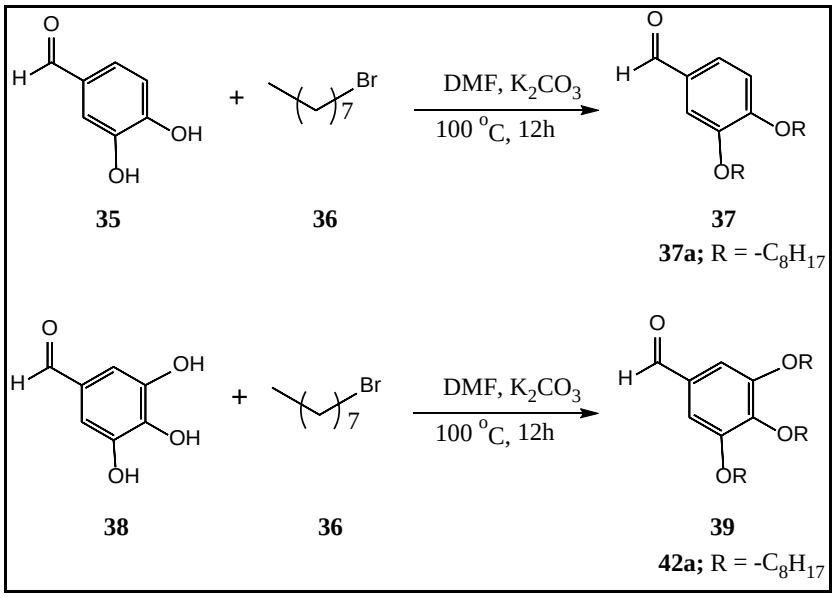

Scheme 6.4 ***Synthesis of 3,4-bisoctyloxy and 3,4,5-trisoctyloxy benzaldehydes***.

4-Alkoxy acetophenones were prepared from 4-hydroxy acetophenone by reacting it with three different n-alkyl bromides in dry DMF using K_2CO_3 as a base to afford the corresponding 4-alkoxy acetophenones[65] (**Scheme 6.5**).

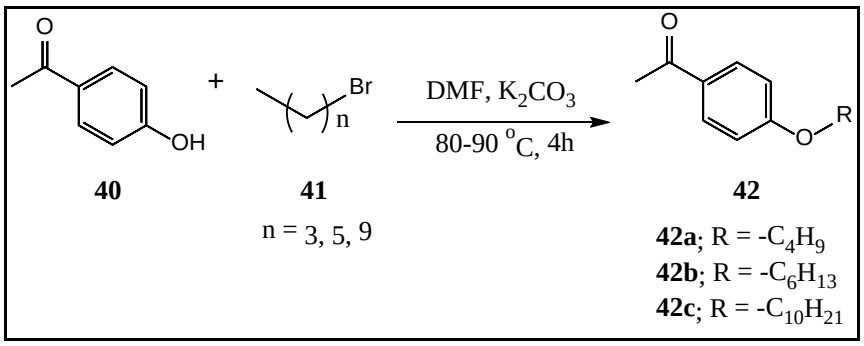

Scheme 6.5 ***Synthesis of 4-alkoxy acetophenones***.

Boiling points of all the synthesized alkoxy aldehydes and alkoxy acetophenones were in agreement with that of the reported ones.[65]

To synthesize the final quinolyl hydrazones, the alkoxy benzaldehydes and alkoxy acetophenones prepared were reacted with 6-bromo/6-chloro-2-methyl-quinolin-4-yl-hydrazine in ethanol using a catalytic amount of sulphuric acid[54] (**Scheme 6.6**).

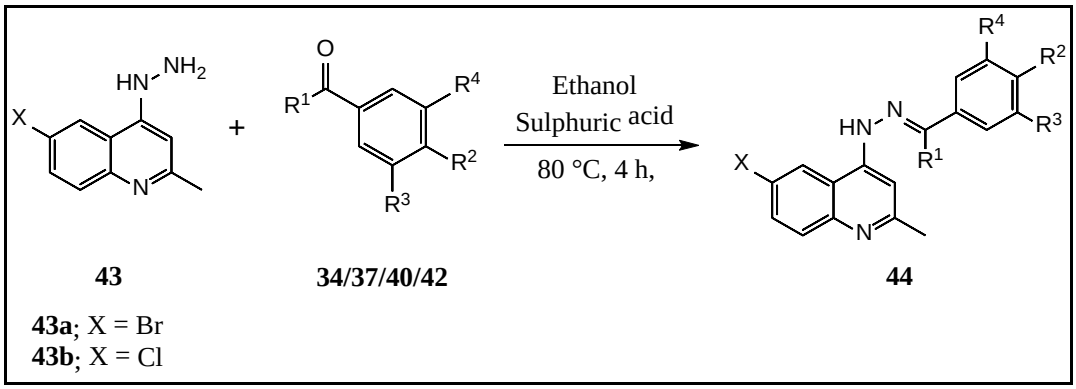

Scheme 6.6 ***Synthesis of quinolyl hydrazones*****.**

6.7.1 Spectral Characterization

All the newly synthesized quinolyl hydrazones (**44a-u**) are characterized using various spectroanalytical techniques and the spectral characteristics of the new compounds are well in agreement with the proposed structures.

In infrared spectra of quinolyl hydrazones (**44a-u**), the characteristic N–H stretching is observed between 3270-3200 cm^{-1}. The presence of alkyl chains is marked by the C–H stretching observed at ~2977 cm^{-1}. The strong bands observed at ~1605 cm^{-1} and ~1571 cm^{-1} are corresponding to the aromatic C=C stretching. Stretching band near ~1643 cm^{-1} is due to C=N stretching. Stretching bands at ~1388 cm^{-1} and ~1535 cm^{-1} showed the presence of $-NO_2$ in (**44r**). Bands at ~1045 cm^{-1} and ~1245 cm^{-1} are due to C-O stretching of aromatic-alkyl ether. Strong bands at frequency range ~850 cm^{-1} and ~770 cm^{-1} are due to the presence of C-Cl and C-Br stretching.

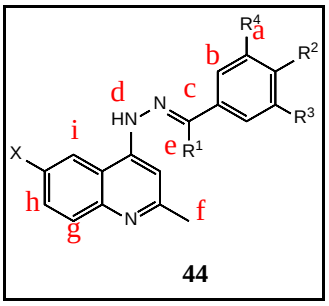

Figure 6.46A ***Compound 44 with proton labels.***

In proton NMR of the quinolyl hydrazones (**44a-u**) (**Figure 6.46A**), the terminal methyl protons are found most upfield near δ 0.9-1.1 ppm as a quartet with coupling constant J = 7.2 Hz. The –CH_3 protons on quinoline ring observed at δ 2.73 ppm as a singlet. For compounds (**44a/44b,** R_3 = -C_2H_5), –OCH_2 protons are observed at δ 4.1 ppm as a quartet with coupling constant J = 7.2 Hz while for other compounds –OCH_2 protons appears as triplet with coupling constant J = 6.4 Hz. The methylene proton of imine linkage (-N═CH-) is observed as a singlet at δ 7.5 ppm for the compounds derived from aldehydes. The –NH proton is observed most downfield at δ 13.0-14.0 ppm as a singlet. The other aromatic protons are observed in between δ 7.0-8.8 ppm value as per the substitution pattern at various positions of the aromatic ring.

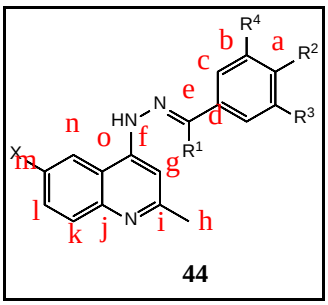

44

Figure 6.46B ***Compound 44 with carbon labels.***

In ^{13}C NMR of the new quinolyl hydrazones (**44a-u**) (**Figure 6.46B**) the most downfield carbon is hydrazone carbon **e** observed near δ 160 ppm while the other aromatic carbons are observed between δ 152 to 100 ppm and for alkoxy hydrazones oxygen attached carbon is observed near δ 63 ppm and other aliphatic carbons are observed up field with the chemical shift value up to δ 15 ppm.

Mass spectral analysis of the newly synthesized quinolyl hydrazones (**44a-u**) was carried out to obtain the molecular ion peak using ESI technique on Waters' Xevo G2-XS QToF mass spectrometer. The molecular ion peaks for these compounds were observed as $(M+H)^+$ in all the cases. The presence of the molecular ion peaks ratio with 1:1 intensity 3:1 ratio indicate the presence of Br and Cl in the synthesized compounds.

The melting points and yields of the quinolyl hydrazones **32** are summarized in **Table 6.5**.

Table 6.5 ***Physical data (yield, mp) of the newly synthesized compounds.***

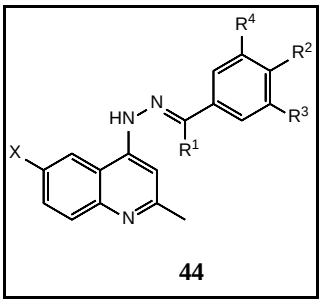

44

ID	Substitution					Molecular formula	Yield	mp
	X	R_1	R_2	R_3	R_4			
44a	-Br	-H	$-OC_2H_5$	-H	-H	$C_{19}H_{18}BrN_3O$	82 %	202 °C
44b	-Cl	-H	$-OC_2H_5$	-H	-H	$C_{19}H_{18}ClN_3O$	74 %	210 °C
44c	-Br	-H	$-OC_3H_7$	-H	-H	$C_{20}H_{20}BrN_3O$	78 %	204 °C
44d	-Cl	-H	$-OC_3H_7$	-H	-H	$C_{20}H_{20}ClN_3O$	74 %	200 °C
44e	-Br	-H	$-OC_4H_9$	-H	-H	$C_{21}H_{22}ClN_3O$	76 %	198 °C
44f	-Cl	-H	$-OC_4H_9$	-H	-H	$C_{21}H_{22}BrN_3O$	80 %	186 °C
44g	-Br	-H	$-OC_5H_{11}$	-H	-H	$C_{22}H_{24}BrN_3O$	68 %	194 °C
44h	-Cl	-H	$-OC_5H_{11}$	-H	-H	$C_{22}H_{24}ClN_3O$	72 %	190 °C
44i	-Br	-H	$-OC_6H_{13}$	-H	-H	$C_{23}H_{26}BrN_3O$	74 %	194 °C
44j	-Cl	-H	$-OC_6H_{13}$	-H	-H	$C_{22}H_{24}ClN_3O$	76 %	188 °C
44k	-Br	-H	$-OC_8H_{17}$	-H	-H	$C_{25}H_{30}ClN_3O$	82 %	186 °C
44l	-Cl	-H	$-OC_8H_{17}$	-H	-H	$C_{25}H_{30}ClN_3O$	79 %	182 °C
44m	-Br	-H	$-OC_8H_{17}$	-H	$-OC_8H_{17}$	$C_{33}H_{46}BrN_3O_2$	78 %	184 °C
44n	-Cl	-H	$-OC_8H_{17}$	-H	$-OC_8H_{17}$	$C_{33}H_{46}ClN_3O_2$	71 %	182 °C
44o	-Br	-H	$-OC_8H_{17}$	$-OC_8H_{17}$	$-OC_8H_{17}$	$C_{41}H_{62}ClN_3O_3$	74 %	180 °C
44p	-Cl	-H	$-OC_8H_{17}$	$-OC_8H_{17}$	$-OC_8H_{17}$	$C_{41}H_{62}BrN_3O_3$	72 %	178 °C
44q	-Br	$-CH_3$	-H	-H	-H	$C_{18}H_{16}ClN_3$	56 %	137 °C
44r	-Br	$-CH_3$	$-NO_2$	-H	-H	$C_{18}H_{15}BrN_4O_2$	83 %	143 °C
44s	-Br	$-CH_3$	$-OC_4H_9$	-H	-H	$C_{22}H_{24}BrN_3O$	81 %	132 °C
44t	-Br	$-CH_3$	$-OC_6H_{13}$	-H	-H	$C_{24}H_{28}BrN_3O$	87 %	141 °C
44u	-Br	$-CH_3$	$-OC_{10}H_{21}$	-H	-H	$C_{28}H_{36}BrN_3O$	76 %	138 °C

6.7.2 Antimicrobial Activity Study

All the newly synthesized quinolyl hydrazones (**44a-u**) were screened for their *in vitro* antimicrobial activity against *S. aureus* (MTCC 96) and *B. subtilis* (MTCC 619) as Gram positive bacteria and *E. coli* (MTCC 739), *P. aeruginosa* (MTCC 741) as Gram negative bacteria and antifungal activity was carried out on *A. niger* (MTCC 282) and *C. albicans* (MTCC 183) with the help of Microcare laboratory, Surat, Gujarat using

paper disc diffusion technique. Zone of inhibition against all the six pathogenic strains were measured for all the new compounds and MIC were determined. Ciprofloxacin and gresiofulvin (100 μg/disc) were used as reference drugs for antibacterial and antifungal activity respectively. Results of the *in vitro* antimicrobial activity are summarised in **Table 6.6** and graphically presented as **Figure 6.44** (results against Gram+ve bacterial strains)**, Figure 6.45 (**results against Gram+ve bacterial strains**),** and in **Figure 6.46 (**results against fungal strains**)**.

Table 6.6 ***Antimicrobial activity results.***

ID	Zone of inhibition in mm and (MIC in μg/mL)											
	Gram(+*ve*) bacteria				Gram(-*ve*) bacteria				Fungi			
	S. aureus		*B. subtilis*		*E. coli*		*P. aeruginosa*		*C. albicans*		*A. niger*	
	Zone (mm)	MIC (μg/mL)	Zone (mm)	MIC (μg/mL)	Zone (mm)	MIC (μg/mL)	Zone (mm)	MIC (μg/mL)	Zone (mm)	MIC (μg/mL)	Zone (mm)	MIC (μg/mL)
44a	21	100	**25**	**12.5**	22	50	19	100	24	25	**25**	**12.5**
44b	24	25	24	25	19	125	24	25	19	125	20	100
44c	**25**	**12.5**	21	100	24	25	18	125	**25**	**12.5**	24	25
44d	21	100	23	25	20	100	22	50	21	100	20	100
44e	22	50	**25**	**12.5**	20	100	24	25	**25**	**12.5**	21	100
44f	20	100	21	100	18	125	19	125	20	100	24	25
44g	**25**	**12.5**	22	50	21	100	19	100	24	25	**25**	**12.5**
44h	24	25	17	125	20	125	22	50	18	125	17	100
44i	**26**	**12.5**	**25**	**12.5**	**27**	**6.25**	**25**	**12.5**	22	50	**25**	**12.5**
44j	**25**	**12.5**	24	25	24	25	23	25	**25**	**12.5**	23	25
44k	23	25	22	50	**26**	**12.5**	24	25	21	100	22	50
44l	24	25	**25**	**12.5**	24	25	**25**	**12.5**	24	25	**25**	**12.5**
44m	22	50	23	25	21	100	22	50	24	25	22	50
44n	24	25	**26**	**12.5**	**25**	**12.5**	23	25	**25**	**12.5**	23	25
44o	**25**	**12.5**	24	25	24	25	**26)**	**12.5**	23	25	24	25
44p	**28**	**6.25**	24	25	**26**	**12.5**	**27**	**6.25**	24	25	**25**	**12.5**
44q	19	125	**25**	**12.5**	24	25	17	125	21	100	19	125
44r	**26**	**12.5**	**26**	**12.5**	**28**	**6.25**	**25**	**12.5**	**25**	**12.5**	24	25
44s	22	50	20	100	**25**	**12.5**	20	100	19	125	21	100
44t	**25**	**12.5**	24	25	23	25	**25**	**12.5**	20	100	**25**	**12.5**
44u	24	25	23	25	24	25	23	25	24	25	19	125
Ciprof-loxacin	**33**	**<3.12**	**30**	**<3.12**	**32**	**<3.12**	**31**	**<3.12**	-----		----	
Griseo-fulvin	----		----		----		----		**31**	**<3.12**	**30**	**<3.12**
DMSO	----		----		----		----		----		----	

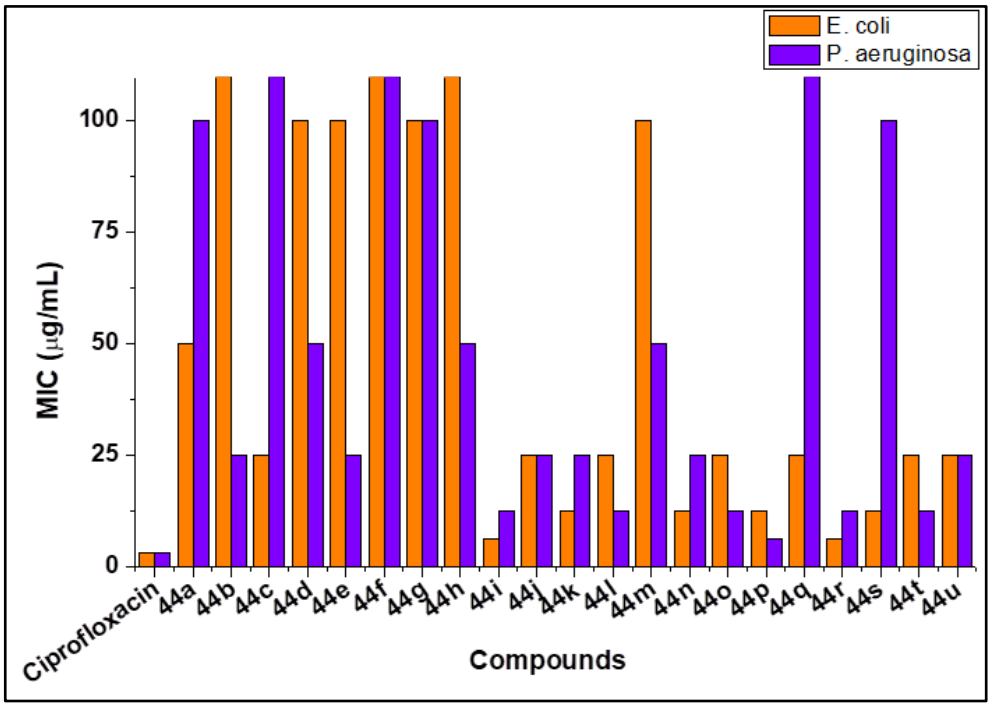

Figure 6.47 ***Antibacterial (Gram +ve) activity results.***

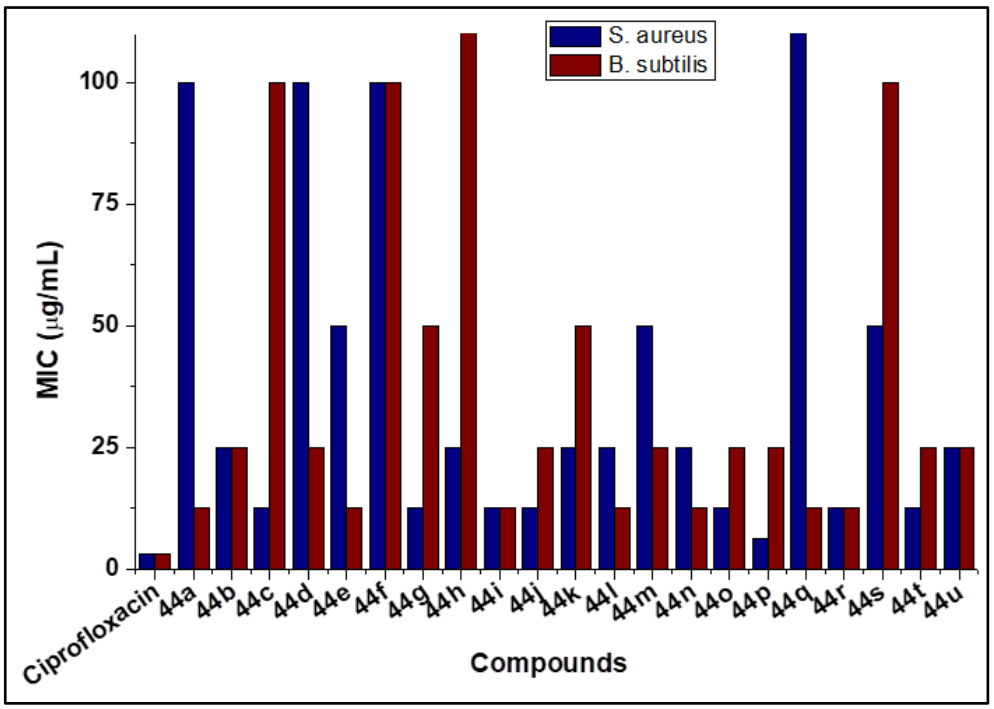

Figure 6.48 ***Antibacterial (Gram -ve) activity results.***

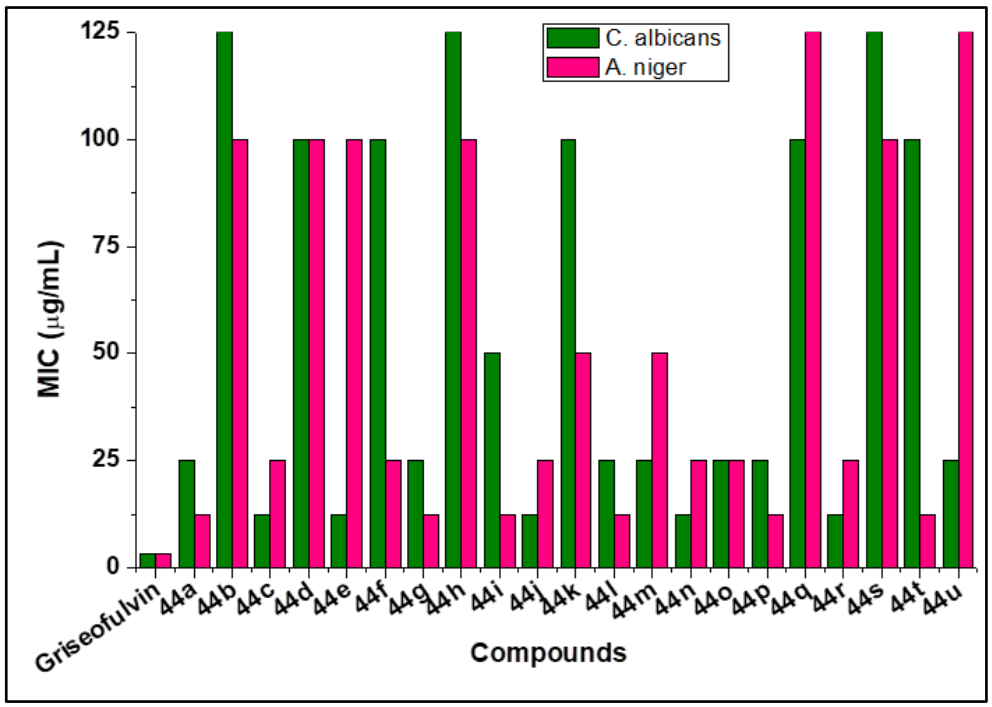

Figure 6.49 ***Antifungal activity results.***

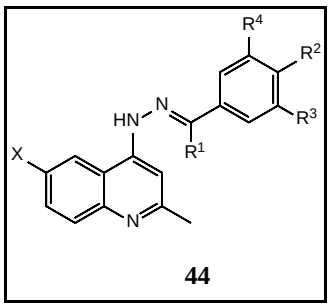

Figure 6.50 ***General structure of compound 44.***

The results of the *in vitro* antimicrobial study revealed that the newly synthesized compounds showed good to moderate activity. Among all the compounds **44p** (X = Cl, R_1 = H, R_2 = OC_8H_{17}, R_3 = OC_8H_{17}, R_4 = OC_8H_{17}) showed excellent inhibition activity (MIC = 6.25 µg/mL) against the Gram *+ve* bacteria *S. aureus* while compounds **44g** (X = Br, R_1 = H, R_2 = OC_5H_{11}, R_3 = H, R_4 = H), **44i** (X = Br, R_1 = H, R_2 = OC_6H_{13}, R_3 = H, R_4 = H), **44j** (X = Cl, R_1 = H, R_2 = OC_6H_{13}, R_3 = H, R_4 = H), **44o** (X = Br, R_1 = H, R_2 = OC_8H_{17}, R_3 = OC_8H_{17}, R_4 = OC_8H_{17}), **44t** (X = Br, R_1 = CH_3, R_2 = OC_6H_{13}, R_3 = H, R_4 = H) displayed significant inhibition with MIC = 12.5 µg/mL against the same strain (**Figure 6.47**). Against *B. subtilis* compounds **44a** (X = Br, R_1 = H, R_2 = OC_2H_5, R3 = H, R_4 = H), **44e** (X = Br, R_1 = H, R_2 = OC_4H_9, R_3 = H, R_4 = H), **44i** (X = Br, R_1 =

H, $R_2 = OC_6H_{13}$, R_3 = H, R_4 = H), **44l** (X = Cl, R_1 = H, $R_2 = OC_8H_{17}$, R_3 = H, R_4 = H), **44n** (X = Cl, R_1 = H, $R_2 = OC_8H_{17}$, R3 = H, $R_4 = OC_8H_{17}$), **44q** (X = Br, $R_1 = CH_3$, R2 = H, R_3 = H, R_4 = H), **44r** (X = Br, $R_1 = CH_3$, $R_2 = NO_2$, R_3 = H, R_4 = H) showed MIC = 12.5 µg/mL with remarkable inhibition activity (**Figure 6.47**). In case of Gram -*ve* bacteria *E. coli*, compounds **44i** (X = Br, R_1 = H, $R_2 = OC_6H_{13}$, R_3 = H, R_4 = H), **44k** (X = Br, R_1 = H, $R_2 = OC_8H_{17}$, R_3 = H, R_4 = H), **44n** (X = Cl, R_1 = H, $R_2 = OC_8H_{17}$, R_3 = H, $R_4 = OC_8H_{17}$), **44p** (X = Cl, R_1 = H, $R_2 = OC_8H_{17}$, $R_3 = OC_8H_{17}$, $R_4 = OC_8H_{17}$), **44r** (X = Br, $R_1 = CH_3$, R2 = NO_2, R_3 = H, R_4 = H), **44s** (X = Br, $R_1 = CH_3$, $R_2 = OC_2H_5$, R_3 = H, R_4 = H) have shown potent inhibitory activity as shown (**Figure 6.48**). Compounds **44i** (X = Br, R_1 = H, $R_2 = OC_6H_{13}$, R3 = H, R_4 = H), **44l** (X = Cl, R_1 = H, $R_2 = OC_8H_{17}$, R_3 = H, R4 = H), **44o** (X = Br, R1 = H, $R_2 = OC_8H_{17}$, $R_3 = OC_8H_{17}$, $R_4 = OC_8H_{17}$), **44p** (X = Cl, R_1 = H, $R_2 = OC_8H_{17}$, $R_3 = OC_8H_{17}$, $R_4 = OC_8H_{17}$), **44r** (X = Br, $R_1 = CH_3$, $R_2 = NO_2$, R_3 = H, R_4 = H), **44t** (X = Br, $R_1 = CH_3$, $R_2 = OC_6H_{13}$, R_3 = H, R_4 = H) displayed excellent inhibitory activity against *P. aeruginosa* with MIC = 12.5 µg/mL (**Figure 6.48**). Against the fungal strain *C. albicans,* compounds **44c** (X = Br, R_1 = H, $R_2 = OC_3H_7$, R3 = H, R_4 = H), **44e** (X = Br, R_1 = H, $R_2 = OC_4H_9$, R_3 = H, R_4 = H), **44j** (X = Cl, R_1 = H, $R_2 = OC_6H_{13}$, R_3 = H, R_4 = H), **44n** (X = Cl, R_1 = H, $R_2 = OC_8H_{17}$, R_3 = H, $R_4 = OC_8H_{17}$), **44r** (X = Br, $R_1 = CH_3$, $R_2 = NO_2$, R_3 = H, R_4 = H) showed potent inhibitory activity and compounds **44a** (X = Br, R_1 = H, $R_2 = OC_2H_5$, R_3 = H, R_4 = H), **44g** (X = Br, R_1 = H, $R_2 = OC_5H_{11}$, R_3 = H, R_4 = H), **44i** (X = Br, R_1 = H, $R_2 = OC_6H_{13}$, R_3 = H, R_4 = H), **44e** (X = Br, R_1 = H, $R_2 = OC_4H_9$, R_3 = H, R_4 = H), **44p** (X = Cl, R_1 = H, $R_2 = OC_8H_{17}$, $R_3 = OC_8H_{17}$, $R_4 = OC_8H_{17}$), **44t** (X = Br, R1 = CH_3, $R_2 = OC_6H_{13}$, R_3 = H, R_4 = H) displayed excellent activity by the inhibition of *A. niger* showed MIC = 12.5 µg/mL (**Figure 6.49**). Compound **44r** (X = Br, $R_1 = CH_3$, $R_2 = NO_2$, R_3 = H, R_4 = H) showed the significant activity against all six tested strains.

6.7.3 Molecular Docking Study

Antimicrobial activity data revealed that most of the compounds reported here exhibited good activity against the fungal strains. An attempt was made to study the binding modes of these compounds with a fungal enzyme. As sterol 14 alpha demethylase (CYP51) is one of the widely studied targets, it was chosen for docking purpose. The protein structure was downloaded from the protein data bank (**PDB id:**

1X8 V). Docking simulation was done with the aid of Schrödinger Maestro-11.5. The protein structures obtained from the protein data bank (PDB) were initially subjected to various processes such as removal of water molecules and removal of heteroatoms etc. using the Protein Preparation Wizard of Schrödinger 2015. All the compounds (Ligands) were filtered by specifying options for screening like remove molecules that have a molecular weight of greater than 650 remove molecules with too many H-bond acceptor and donor atoms acceptor groups >3, Donor groups >3, Energy minimization was done by choosing a Ligprep (OPLS) module of Schrodinger.

The results suggest that the compounds efficiently interact with the amino acid residues in the binding pocket of CYP51 (**Figure 6.51**). Except compound **44e,** in all other compounds namely **44n** (-10.79), **44a** (-9.34), **44c** (-9.12), **44i** (-7.51), **44l** (-7.40) the oxygen atom of the alkoxy chain is involved in common hydrogen bonding interactions with the amino acid residue Arg 96. Moreover, compound **44n** also shows additional hydrogen bond between other alkoxy oxygen atom and amino acid residue Arg 96 (**Figure 6.51**). Compound **44a** and **44c** showed π-π interactions with the amino acid residue Phe 78. Compound **44i** shows the hydrogen bonding with the amino acid residue Gln 72 (**Figure 6.51**). Compound **44e** (-8.83) interacts with the amino acid residue Phe 78 by hydrogen bonding (**Figure 6.51**). Compound **44l** also displays the hydrogen bonding between nitrogen of hydrazone linkage and amino acid residue Gln 72 (**Figure 6.51**). Based on these observations, the efficient interaction and binding with enzyme CYP51 supports good activity observed of newly synthesized compounds on the fungi studied.

Table 6.7 ***Docking results of the active compounds.***

ID	Docking score	Glide energy	Amino acids interacted with ligands
Griseofulvin	-11.80	-40.08	Arg 96, Ile 323, Gln 72, Phe 78
44n	-10.79	-60.31	Arg 96
44a	-9.34	-38.04	Phe 78, Arg 96
44c	-9.12	-41.67	Arg 96, Phe 78
44i	-7.51	-43.44	Arg 96, Ile 323, Gln 72
44e	-8.83	-41.19	Phe 78
44l	-7.40	-48.56	Arg 96, Gln 72

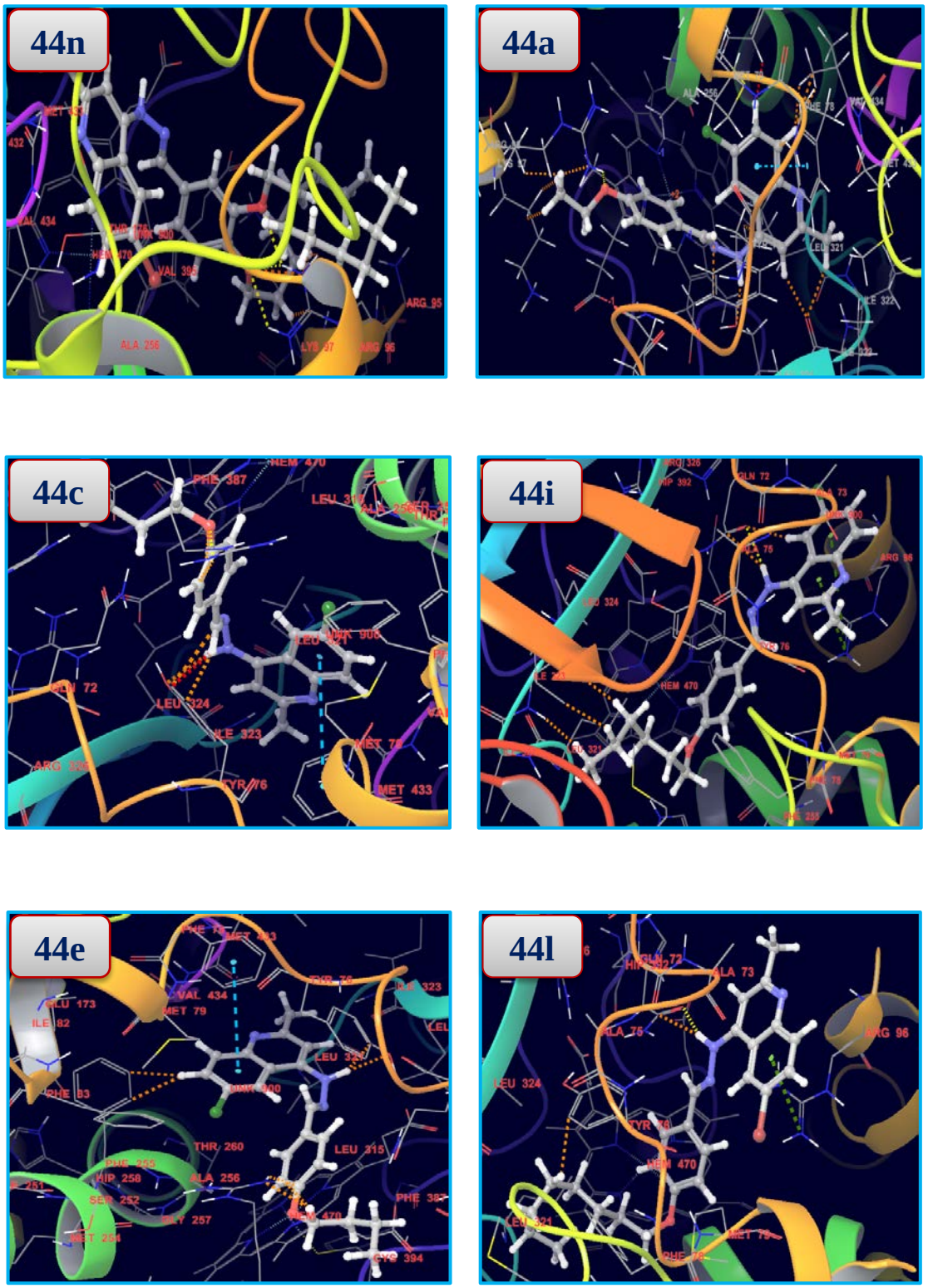

Figure 6.51 ***The docking pose of the compounds in the active pocket of InhA.***

6.7.4 Anticancer Activity Study

All the newly synthesized quinolyl hydrazones were presented for acceptance for single dose anticancer assay study against full NCI 60 cell lines panel under the screening project at the National Cancer Institute (NCI), USA. Twenty of the twenty one new compounds were selected for the single dose anticancer assay determination against full NCI 60 cell lines panel.

Primary *in vitro* single dose anticancer assay was performed at a single dose (10 μM) and data of all the nine selected compounds are presented as mean graph of the percent growth of the treated cells compared to untreated control cells.

The results of the single dose anticancer screening of all the selected compounds in form of one dose mean graphs are included in appendix from **Sheets 40 to 59** at the end of the thesis.

Nine of the compounds were selected for further detailed study at five different dilutions due to good positive results in the single dose study and found to be lethal to a greater extent.

Results of preliminary single dose anticancer activity for these nine compounds in terms of % lethality are presented as graph form in **Figure 6.52A** and **Figure 6.52B**.

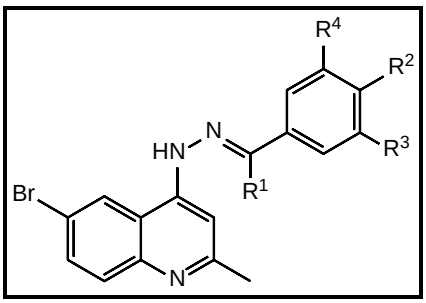

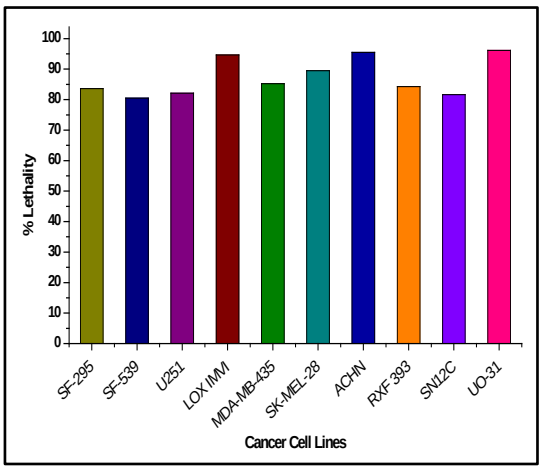

Compound 44e

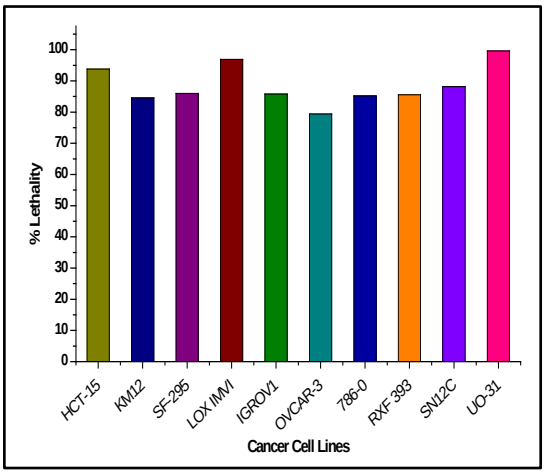

Compound 44g

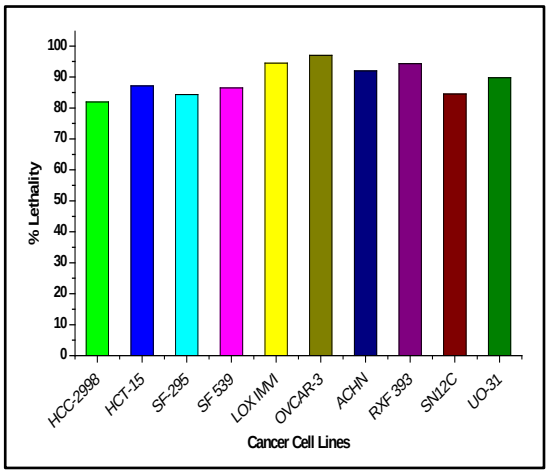

Compound 44i

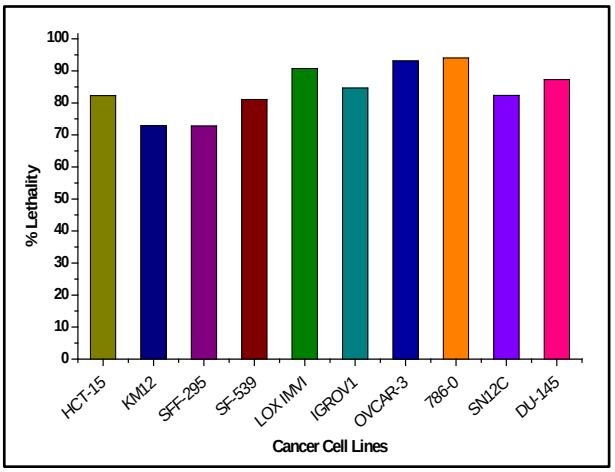

Compound 44k

Figure 6.52A ***Primary in vitro one dose anticancer screening results of compounds (X = Br) in terms of % lethality.***

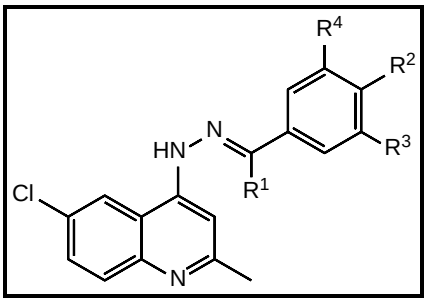

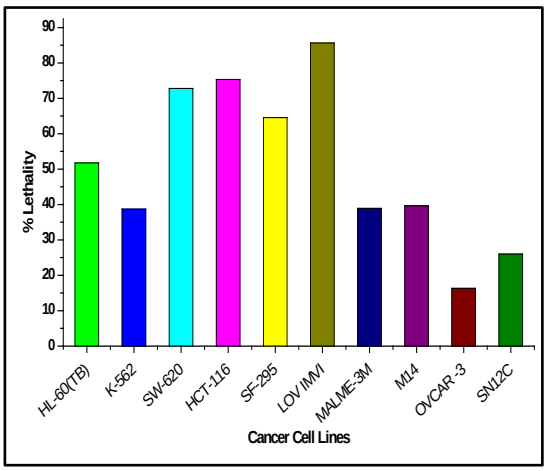

Compound 44b

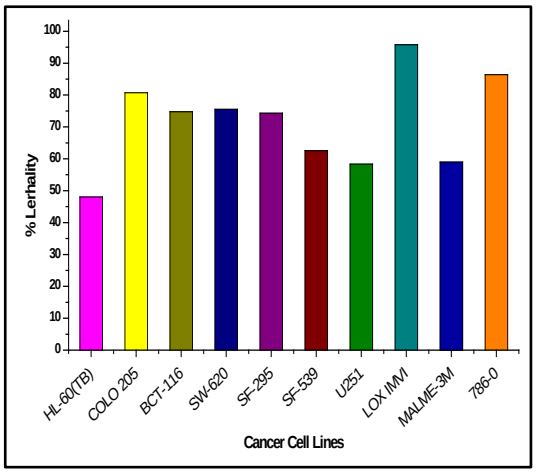

Compound 44d

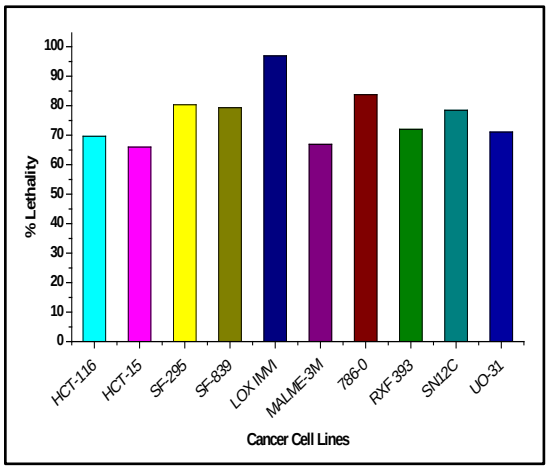

Compound 44f

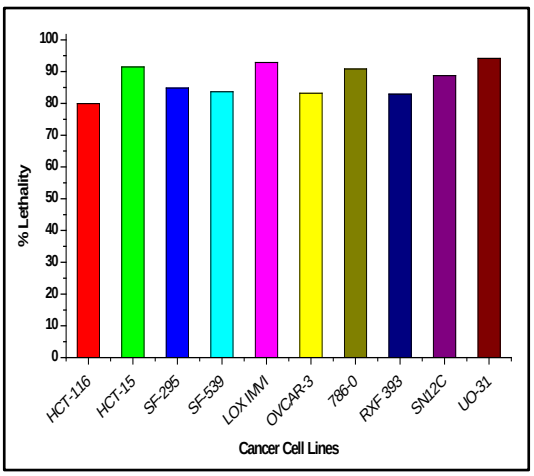

Compound 44h

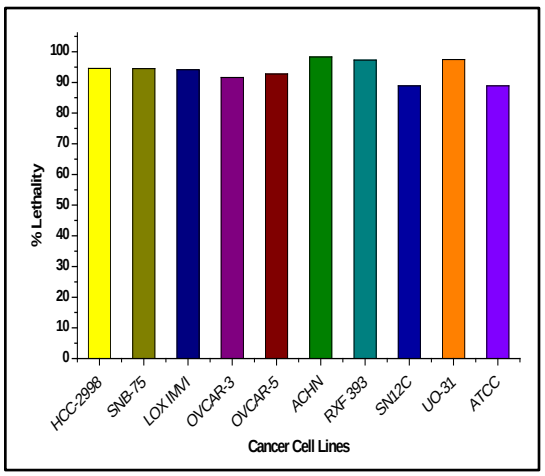

Compound 44j

Figure 6.52B ***Primary in vitro one dose anticancer screening results of compounds (X = Cl) in terms of % lethality.***

Single Dose Study Results: Discussion

All the selected compounds for five dose assay displayed significant anticancer activity in terms of % lethality against several cell lines as presented in **Figure 6.52A** and **Figure6.52B.** Compound **44b** showed a good anticancer activity by inhibiting various cancer cell lines with % lethality of 85%, 75% and 72% for melanoma (LOX IMVI), colon cancer (HCT-116) and colon cancer (SW-620) cell lines respectively (**Figure 6.52B**). Compound **44d** displayed an excellent anticancer activity with lethality 96% and 86% for melanoma cancer (LOX IMVI) and renal cancer (786-0) cell lines respectively and for several cancer cell lines it showed >40% lethality (**Figure 6.52B**). Compound **44e** showed lethality value >80% for the various cell lines including 94% lethality for melanoma (LOX IMVI), 95% lethality for renal cancer (ACHN) and 96% lethality for renal cancer (UO-31) as shown in **Figure 6.52A**. Compound **44f** displayed the highest lethality value 95% for melanoma (LOX IMVI) cell line as included in **Figure 6.52B**. While compound **44g** showed an excellent lethality for Colon Cancer (HCT-15) and renal cancer (UO-31) with the lethality values of 94% and 99% respectively as shown in **Figure 6.52A**. Greater than 80% lethality was observed for compound **44h** against a numerous cancer cell lines including colon cancer (HCT-15), melanoma (LOX IMVI), renal cancer (786-0) and renal cancer (UO-31) cell lines as shown in **Figure 6.52B**. Compound **44i** displayed the highest activity with 97% lethality for ovarian cancer (OVCAR-3) cell line and 94% lethality for melanoma (LOX IMVI) cancer cell line as can be observed in **Figure 6.52A**. Compound **44j** showed an excellent inhibition with lethality values >97% of renal cancer cell lines namely (786-0), (RXF 393), (UO-31) (**Figure 6.52B**) and compound **44k** displayed 93% and 94% lethality for ovarian cancer (OVCAR-3) and renal cancer (786-0) cell lines respectively as can be seen in **Figure 6.52A**. All the other compounds which were not selected for five dose assay showed good to moderate activity against various cancer cell lines.

Compound **44u** (X = Br, R = $-OC_{10}H_{21}$ an acetophenone hydrazone) was not selected for anticancer activity study by NCI. While the other eleven compounds (**44a**, **44c**, **44l**, **44m**, **44n**, **44o**, **44p**, **44q**, **44r**, **44s**, **44t**) (**Figure 6.53**) were screened only at a single dose concentration showing lethality on one or two types of cell lines.

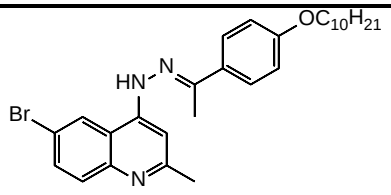

44u

Not selected for anticancer activity study

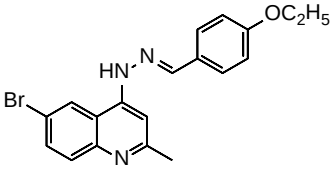

44a

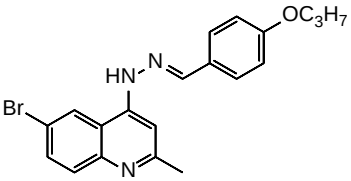

44c

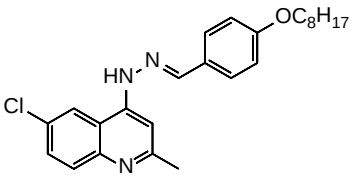

44l

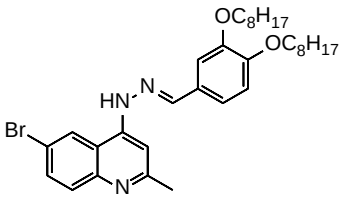

44m

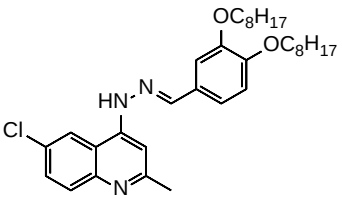

44n

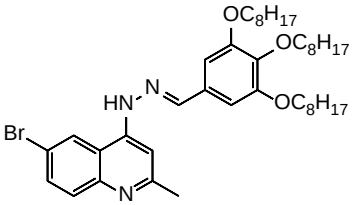

44o

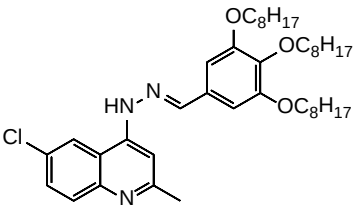

44p

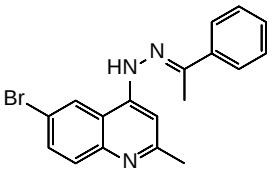

44q

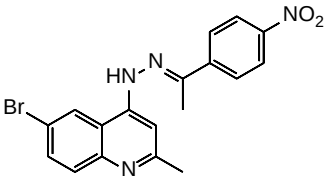

44r

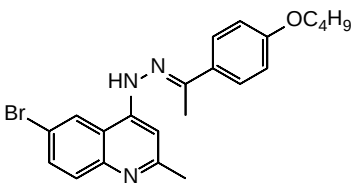

44s

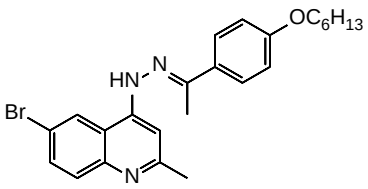

44t

Compounds which have been studied only at single dose

Figure 6.53

Five Dose Study Results: Discussion

From the selected twenty compounds, nine compounds (**44b, 44d, 44e, 44f, 44g, 44h, 44i, 44j, 44k**) exhibited excellent anticancer activity in terms of % lethality at single dose level. On the basis of these results, these compounds were screened at 10-fold dilutions of five different concentrations of the test compounds (0.01, 0.1, 1, 10 & 100 μM) against all the NCI 60 tested cell lines.

The results of the five dose anticancer activity screening in terms of log molar concentrations of response parameters ($log10GI_{50}$, log10TGI & $log10LC_{50}$) are presented in **Appendix** as **Sheets 60 to 68**.

The dose response curves for all the cell lines in the NCI 60 panel exposed to the compounds studied at five dose concentrations are presented as **Figures 6.53, 6.56, 6.59, 6.62, 6.65, 6.68, 6.71, 6.74,** and **6.77**.

The dose response curves (% growth verses sample concentration at NCI fixed protocol, μM) for all the cell lines with different subpanel obtained from the NCI's against a diverse panel of 60 human tumour cell lines were measured at five dose concentrations and the cell lines of NCI with original tissue colour cods are presented in **Figure 6.54, 6.57, 6.60, 6.63, 6.66, 6.69, 6.72, 6.75** and **6.78**.

The logs molar concentration of the tested compounds was also calculated of individual GI_{50}, TGI and LC_{50} and represented as $log10GI_{50}$, log10TGI, $log10LC_{50}$ respectively and the obtained values are presented in the **Figure 6.55, 6.58, 6.61, 6.64, 6.67, 6.70, 6.73, 6.76** and **6.79**.

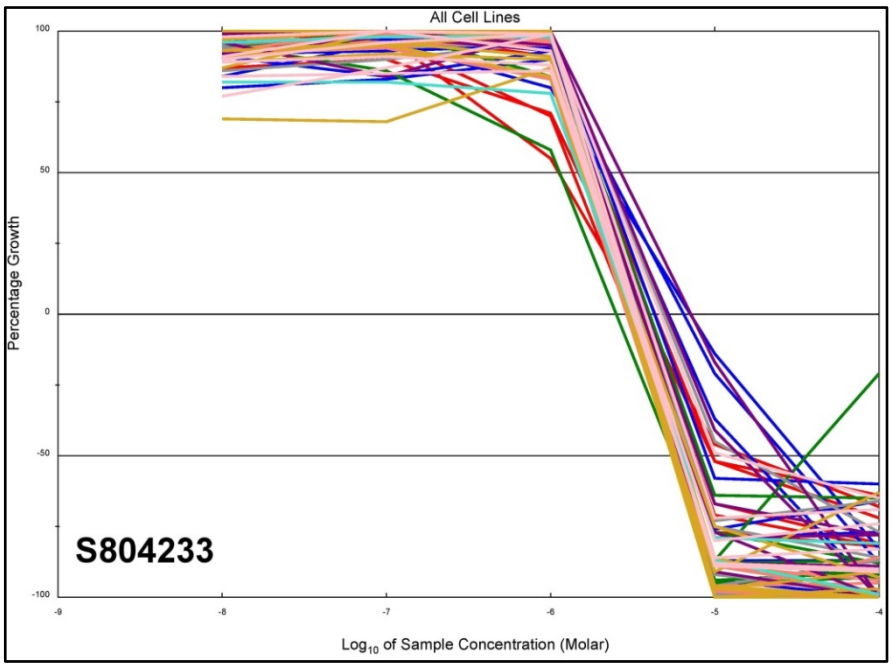

Figure 6.53 ***Dose response curves for all cell lines in the NCI 60 panel exposed to compound 44b with tissue originated colours and shapes.***

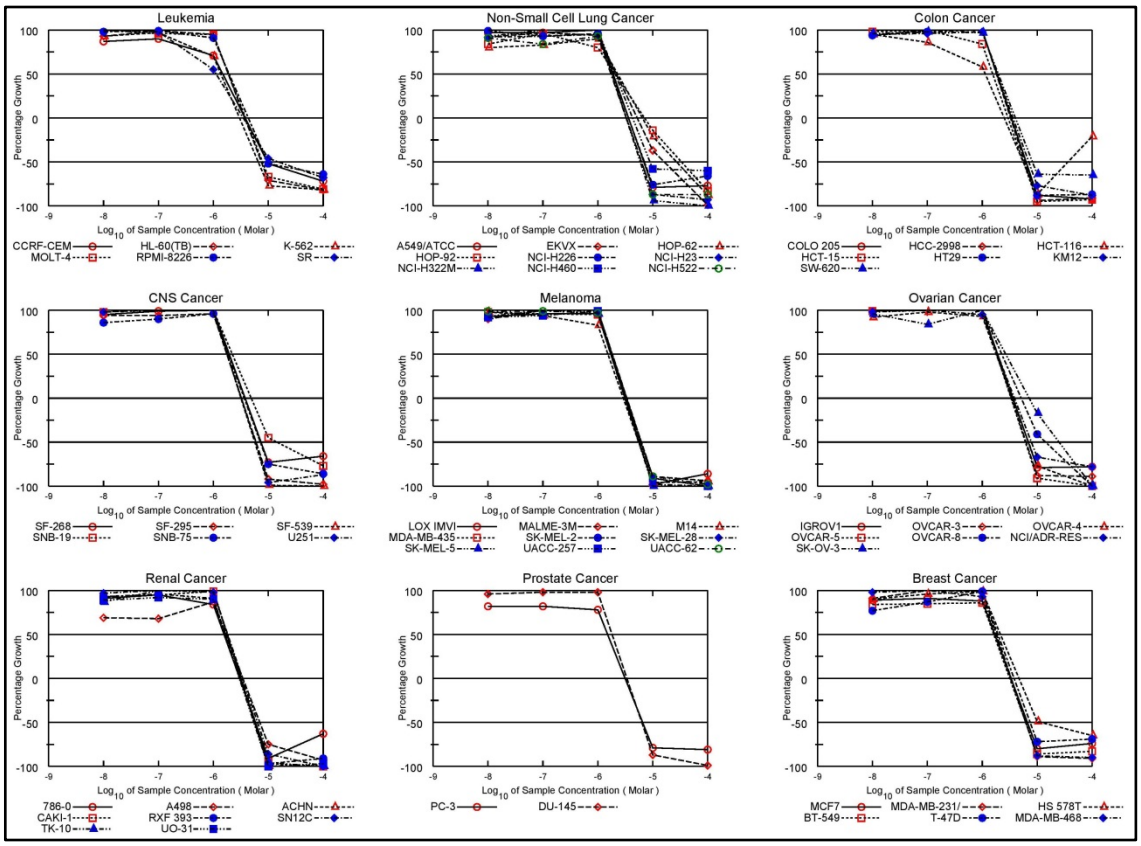

Figure 6.54 ***Dose response curves (% growth verses sample concentration) for all cell lines with different subpanel obtained from the NCI's in vitro disease-oriented human cancer cells line for compound 44b on nine types of cancer.***

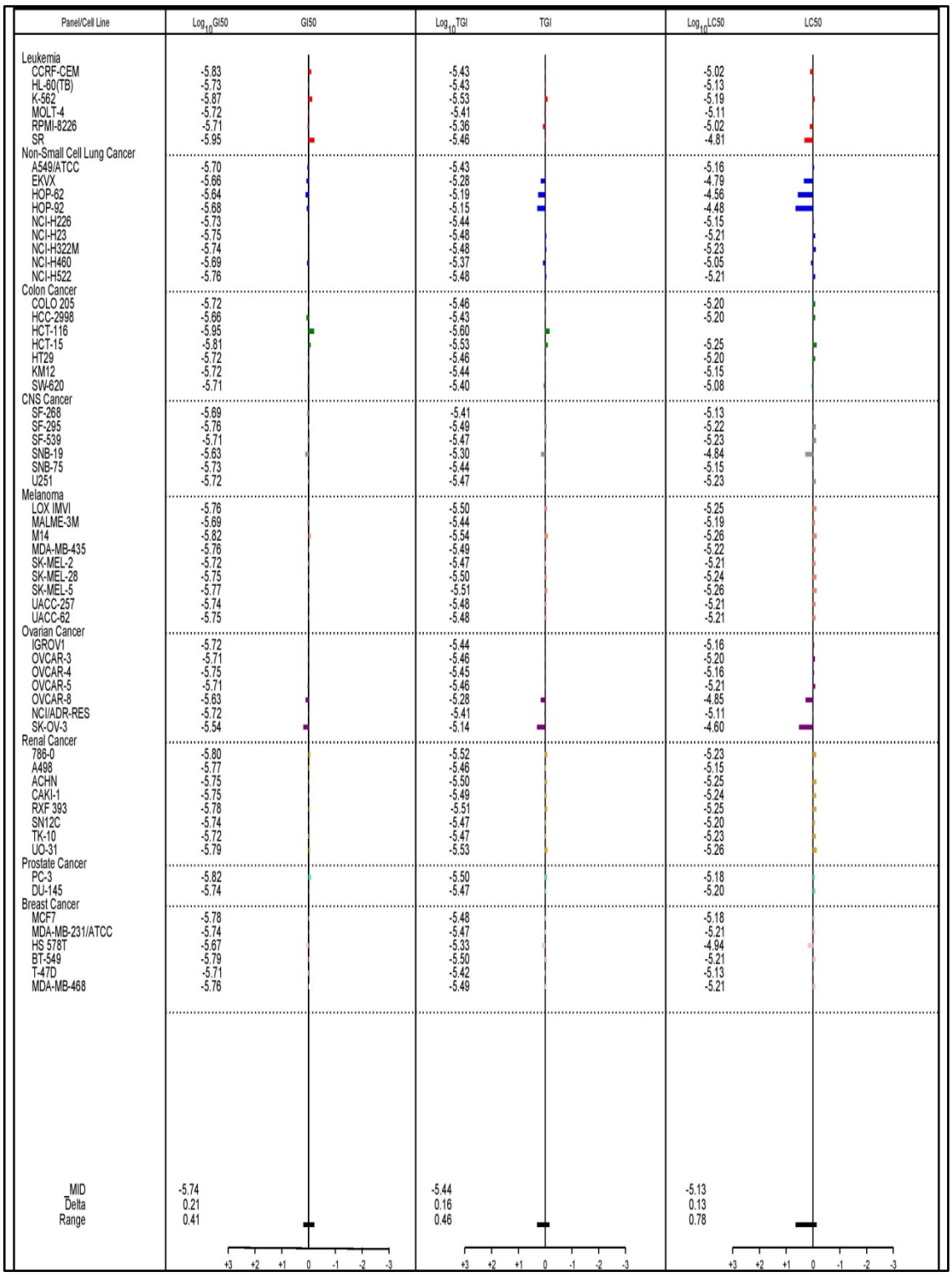

Figure 6.55 ***Values of log molar concentration of response parameters ($log_{10}GI50$, $log_{10}TGI$ & $log_{10}LC50$) for compound 44b.***

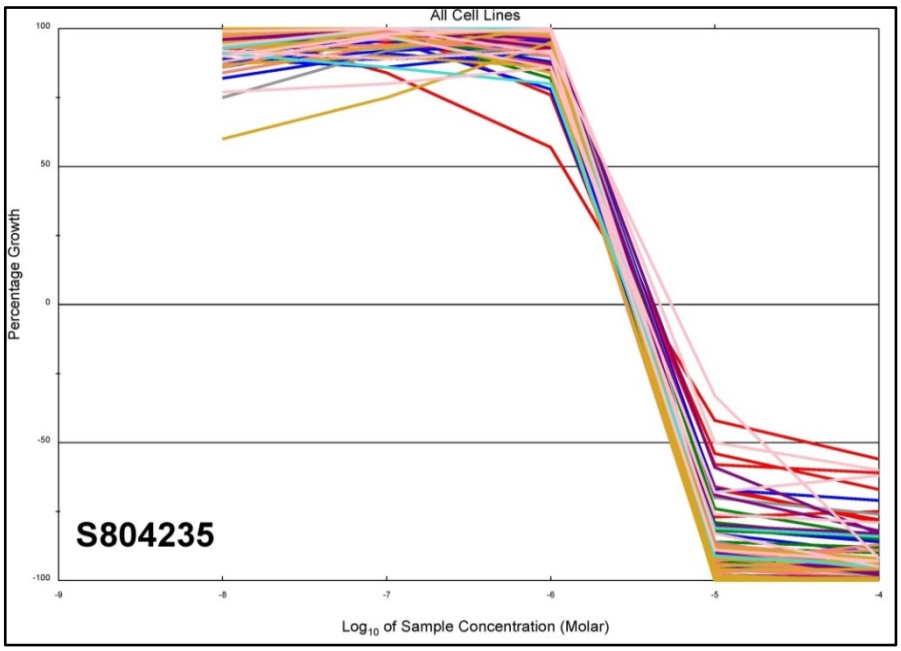

Figure 6.56 ***Dose response curves for all cell lines in the NCI 60 panel exposed to compound 44d with tissue originated colours and shapes.***

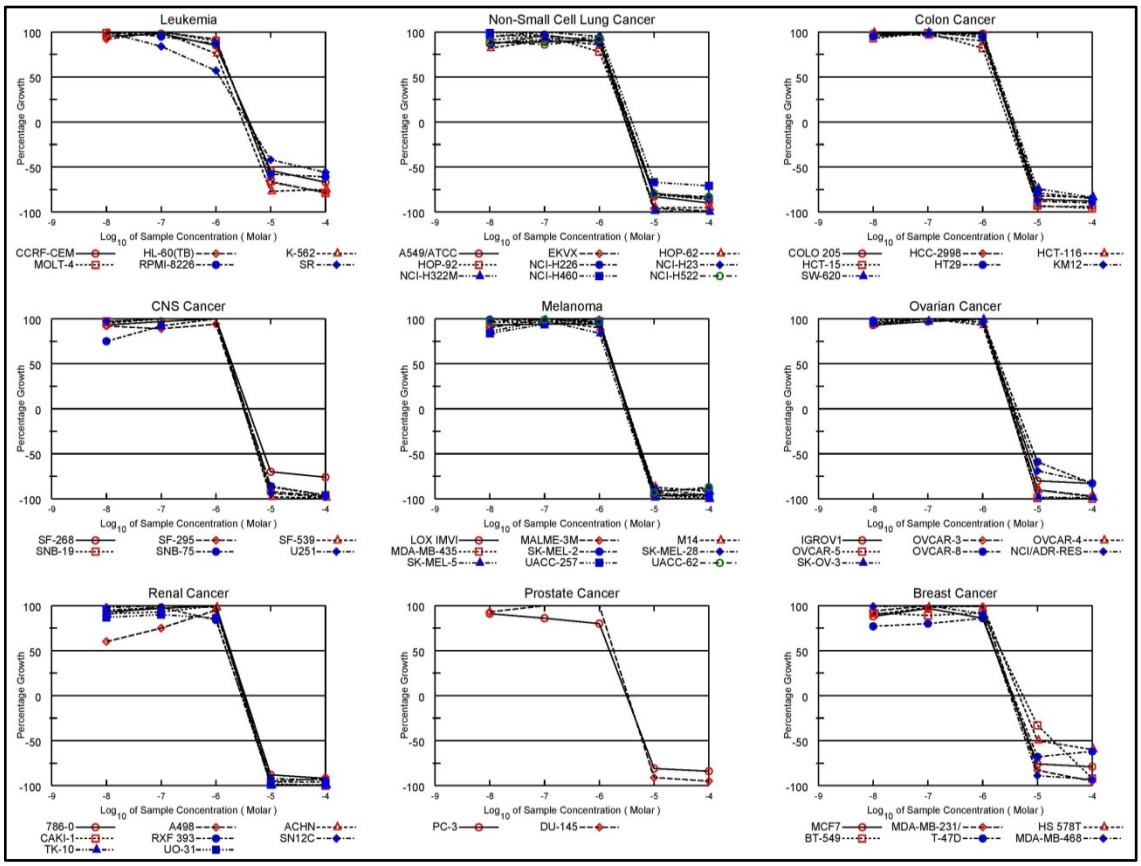

Figure 6.57 ***Dose response curves (% growth verses sample concentration) for all cell lines with different subpanel obtained from the NCI's in vitro disease-oriented human cancer cells line for compound 44d on nine types of cancer.***

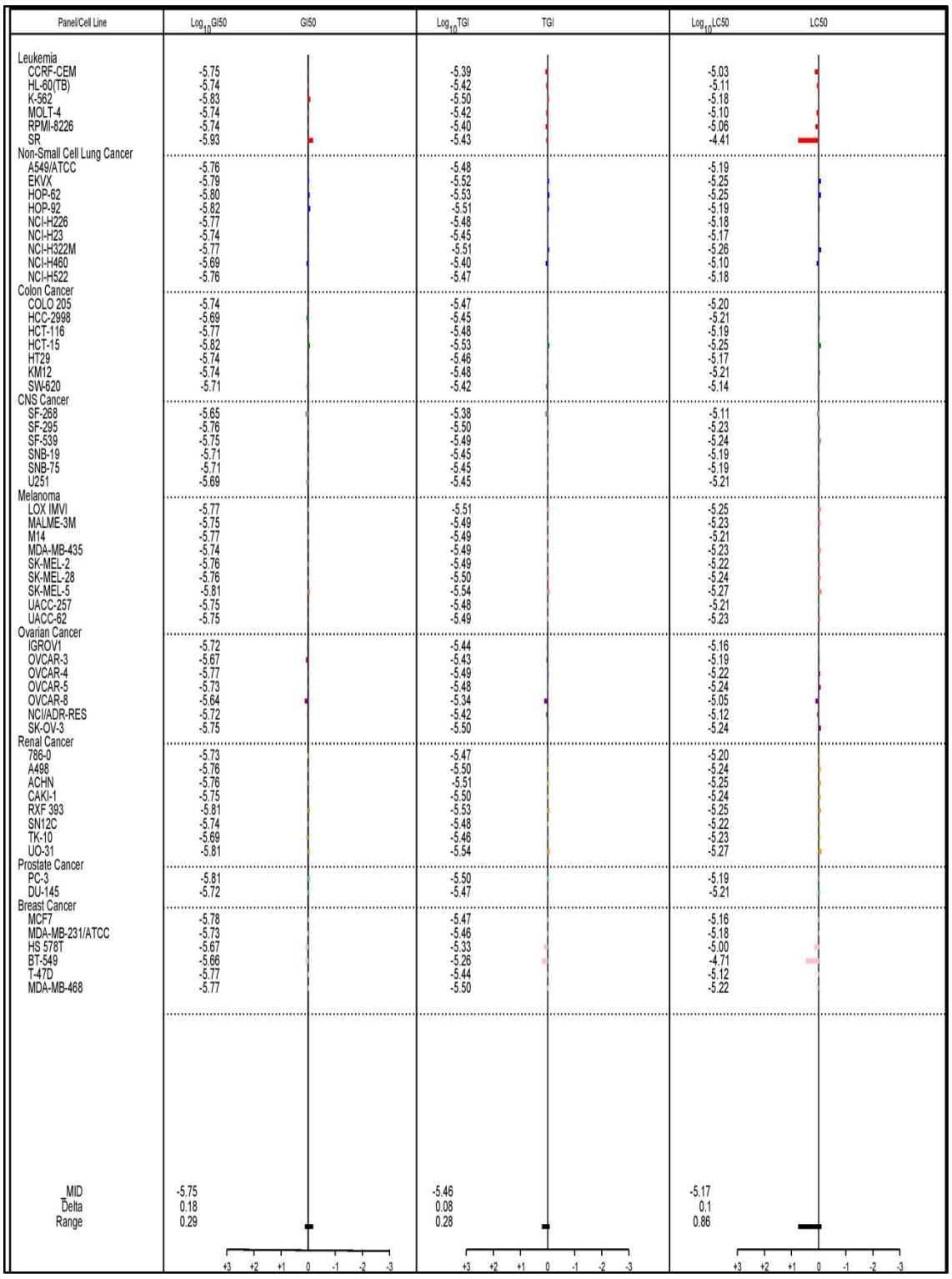

Figure 6.58 ***Values of log molar concentration of response parameters (log_{10}GI50, log_{10}TGI & log_{10}LC50) for compound 44d.***

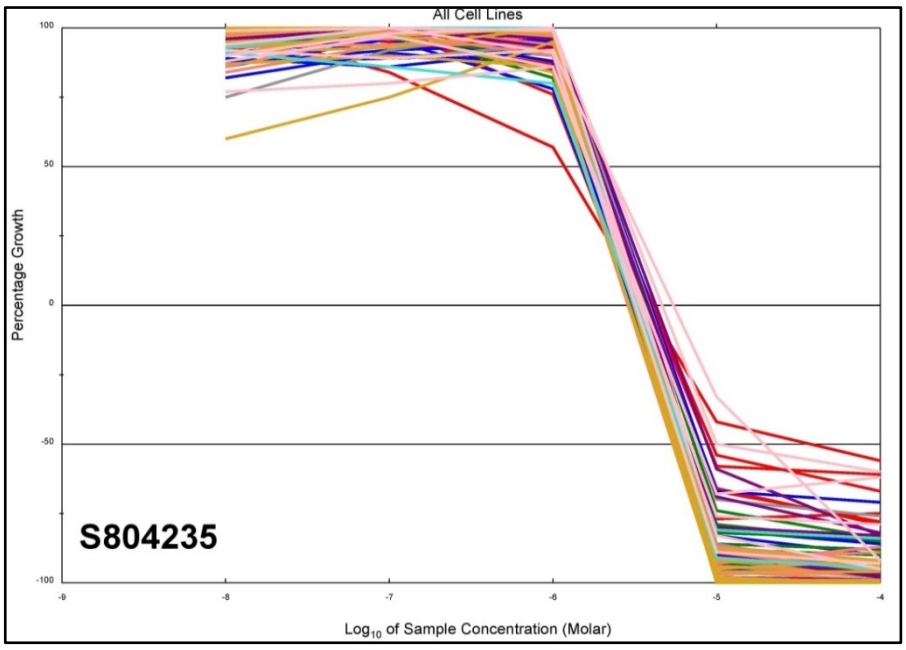

Figure 6.59 ***Dose response curves for all cell lines in the NCI 60 panel exposed to compound 44e with tissue originated colours and shapes.***

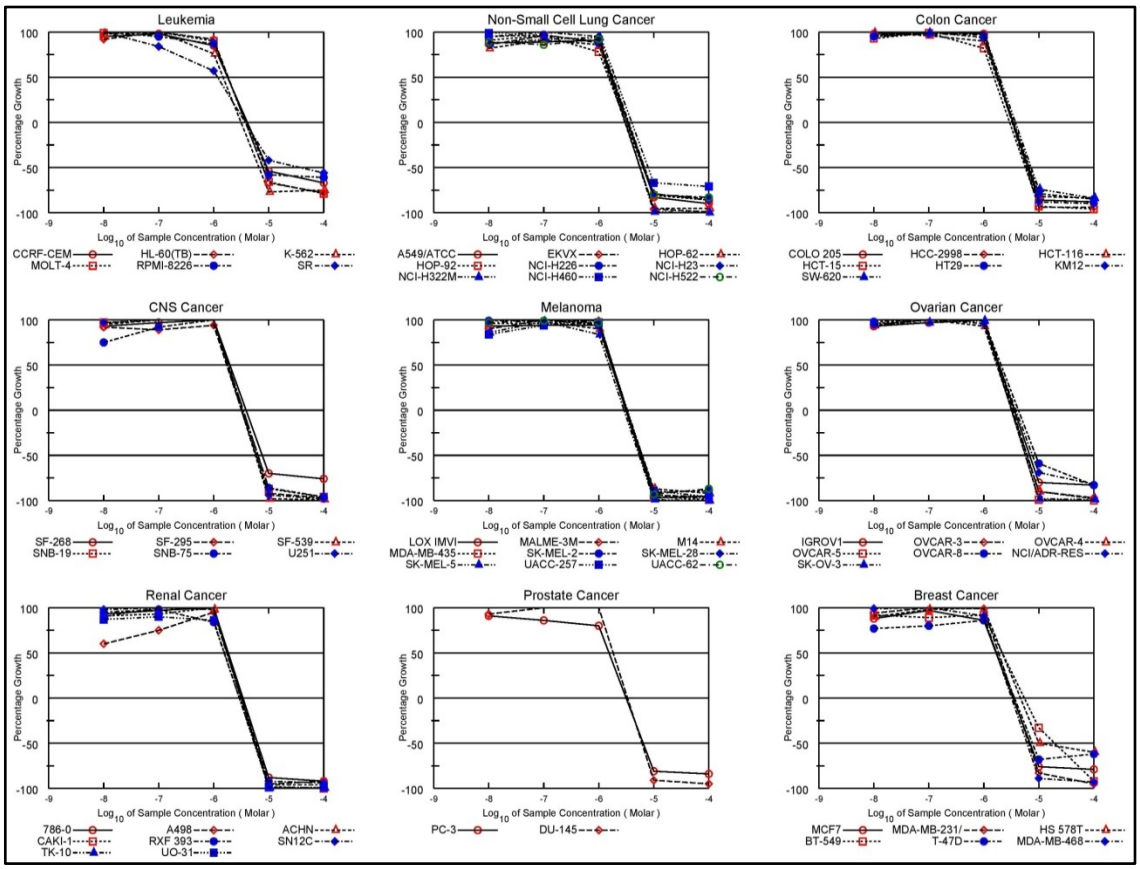

Figure 6.60 ***Dose response curves (% growth verses sample concentration) for all cell lines with different subpanel obtained from the NCI's in vitro disease-oriented human cancer cells line for compound 44e on nine types of cancer.***

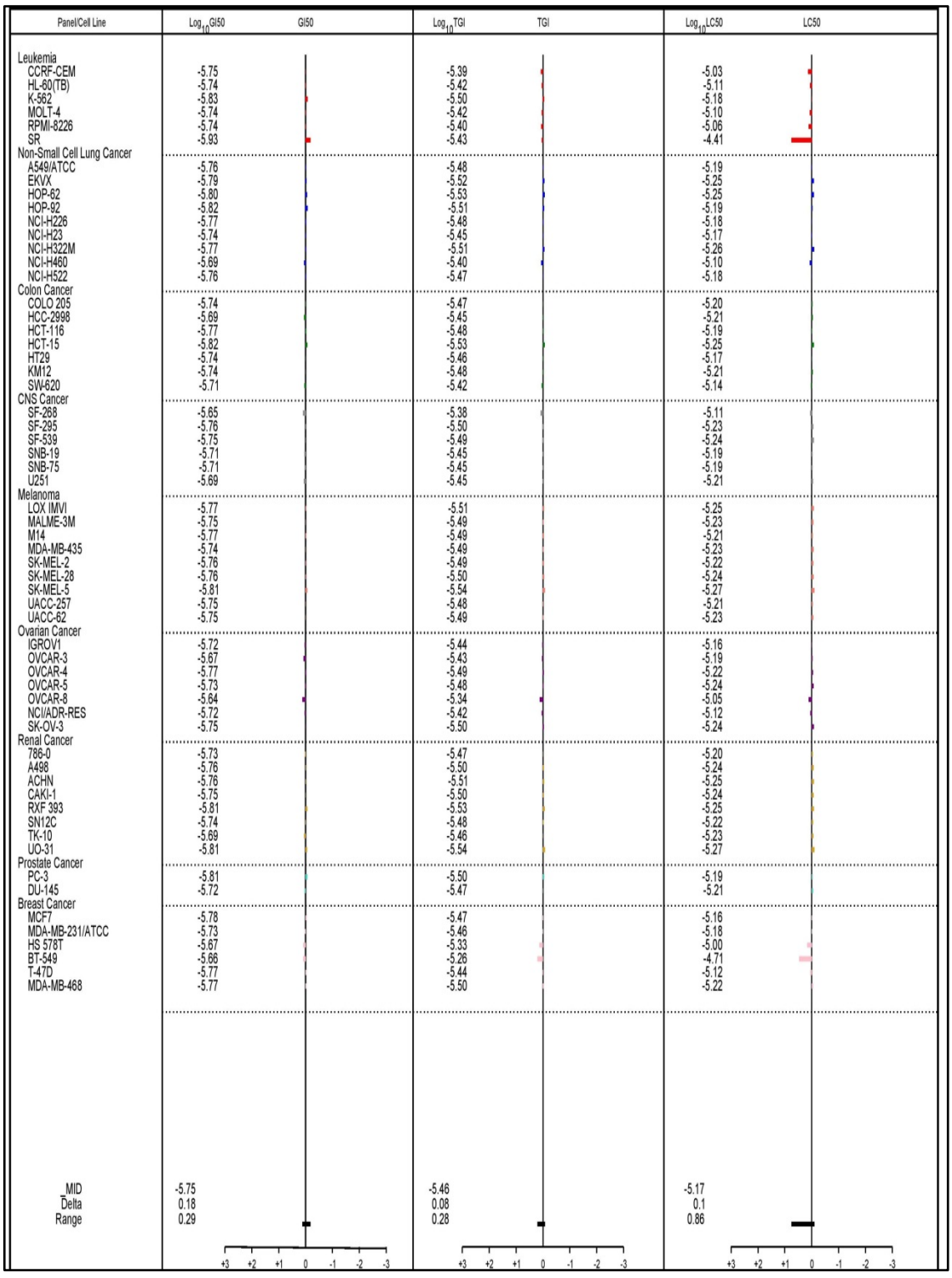

Figure 6.61 ***Values of log molar concentration of response parameters (log_{10}GI50, log_{10}TGI & log_{10}LC50) for compound 44e.***

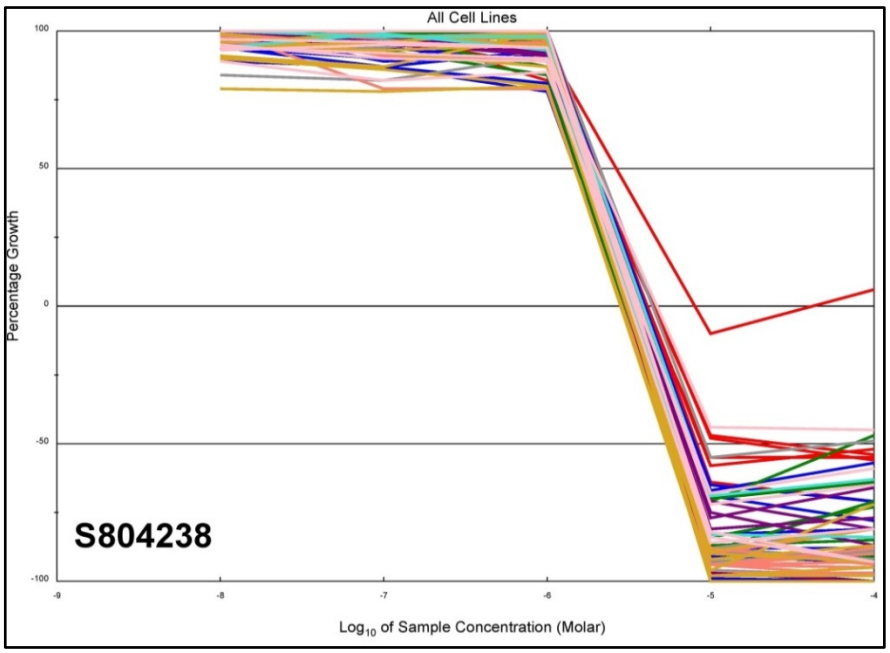

Figure 6.62 ***Dose response curves for all cell lines in the NCI60 panel exposed to compound 44f with tissue originated colours and shapes.***

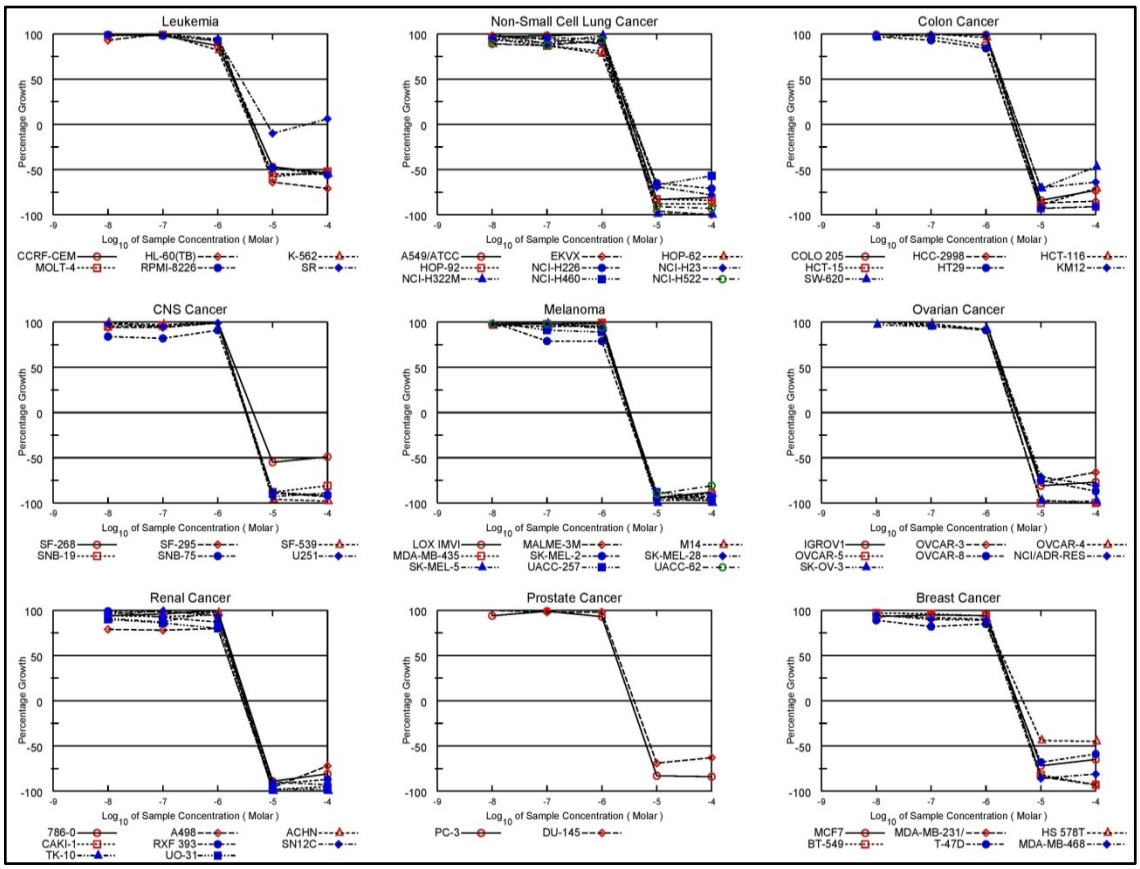

Figure 6.63 ***Dose response curves (% growth verses sample concentration) for all cell lines with different subpanel obtained from the NCI's in vitro disease-oriented human cancer cells line for compound 44f on nine types of cancer.***

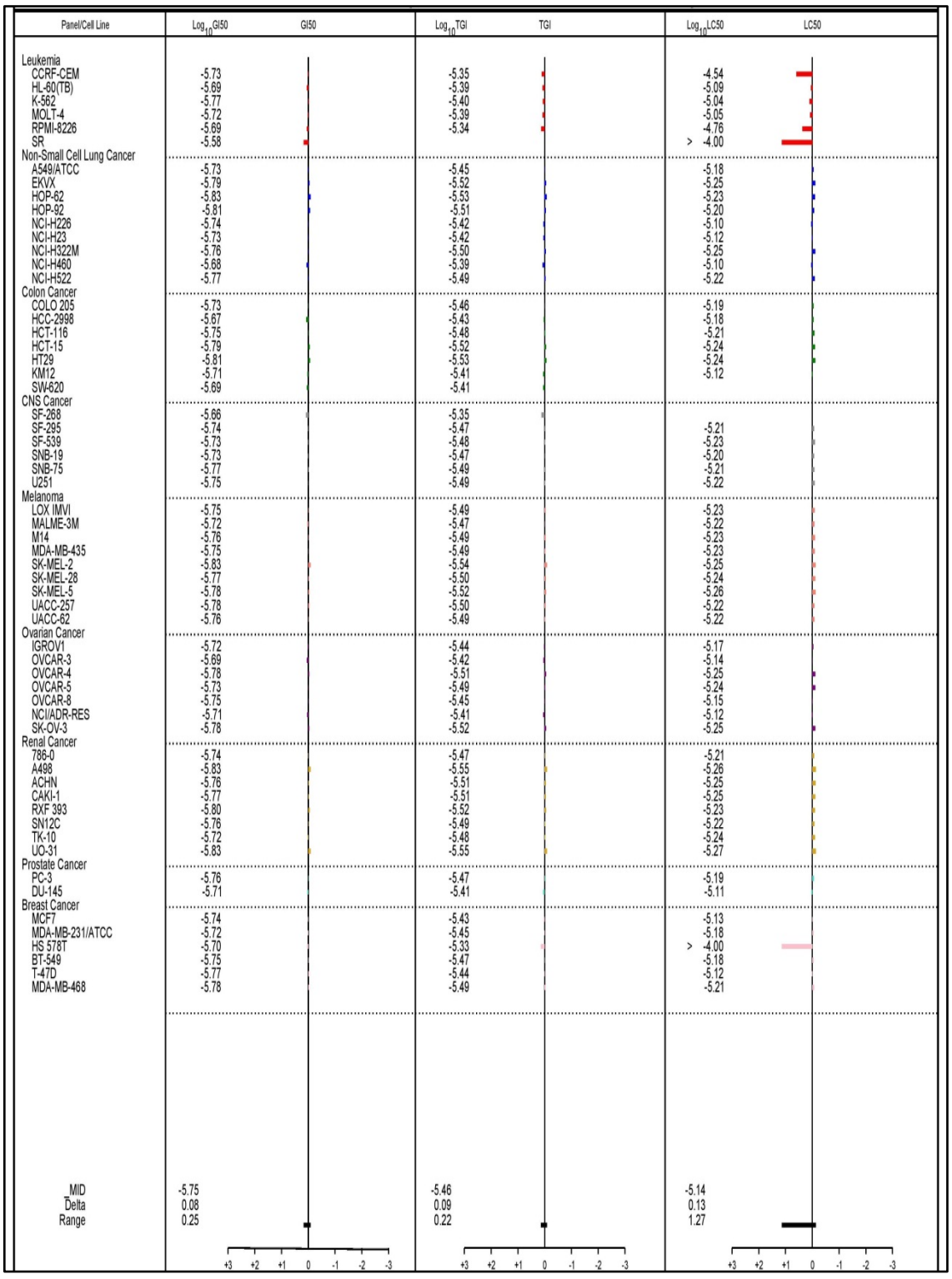

Figure 6.64 ***Values of log molar concentration of response parameters (log_{10}GI50, log_{10}TGI & log_{10}LC50) for compound 44f.***

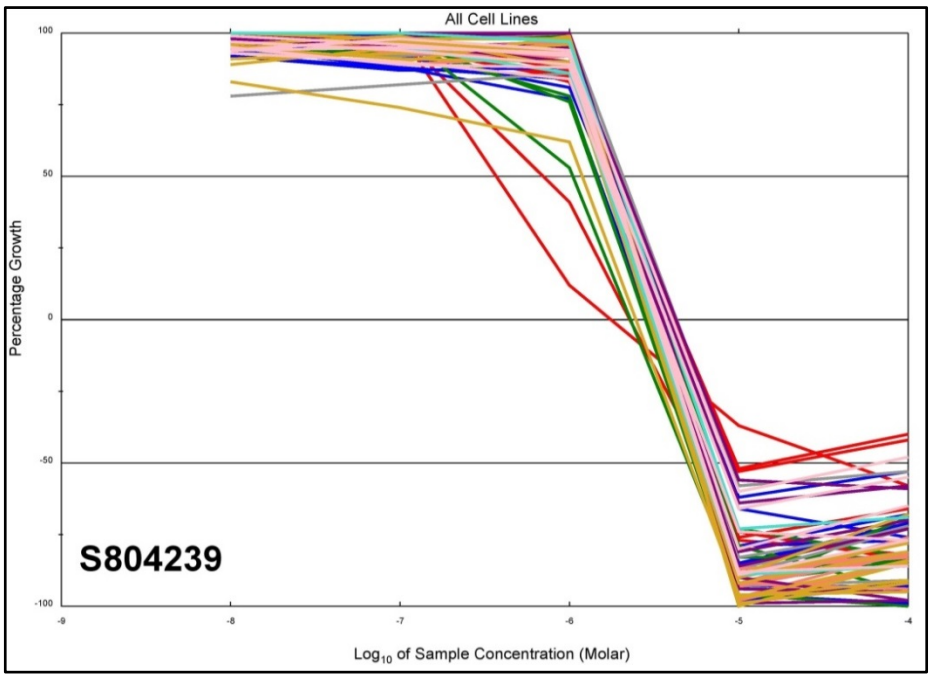

Figure 6.65 ***Dose response curves for all cell lines in the NCI60 panel exposed to compound 44g with tissue originated colours and shapes.***

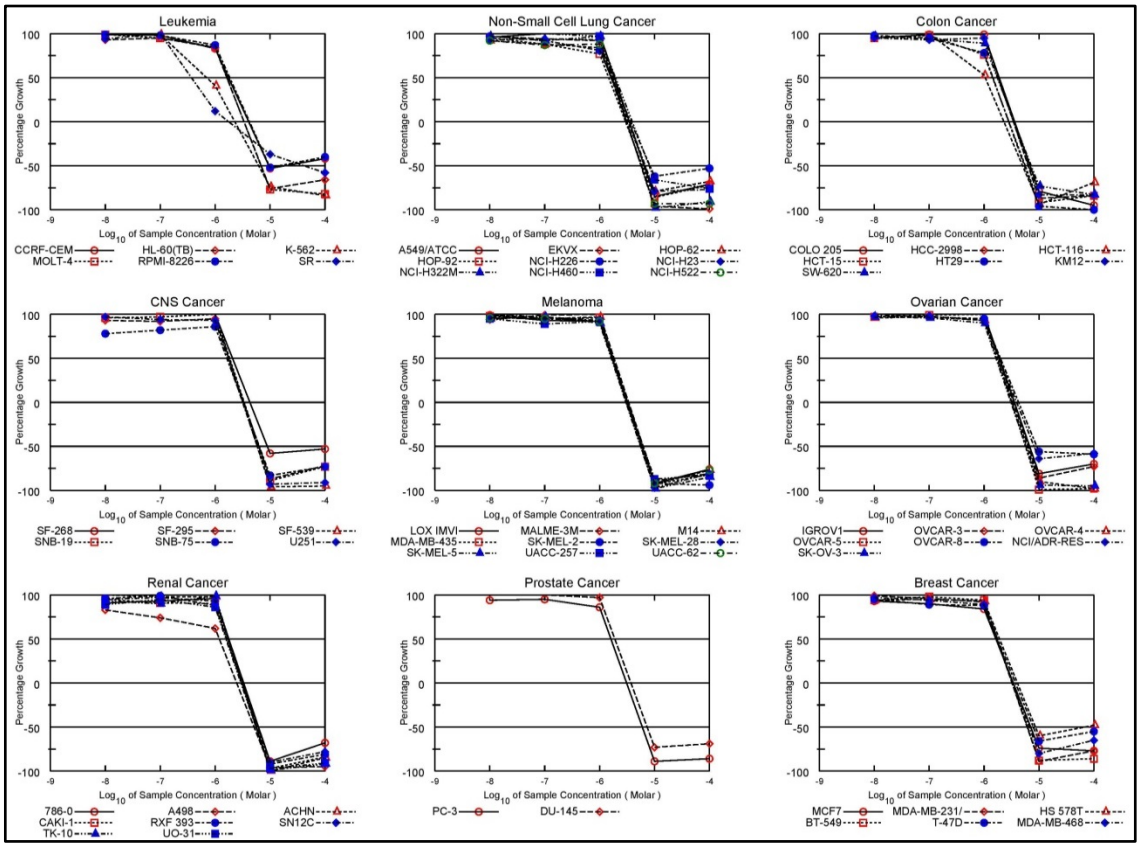

Figure 6.66 ***Dose response curves (% growth verses sample concentration) for all cell lines with different subpanel obtained from the NCI's in vitro disease-oriented human cancer cells line for compound 44g on nine types of cancer.***

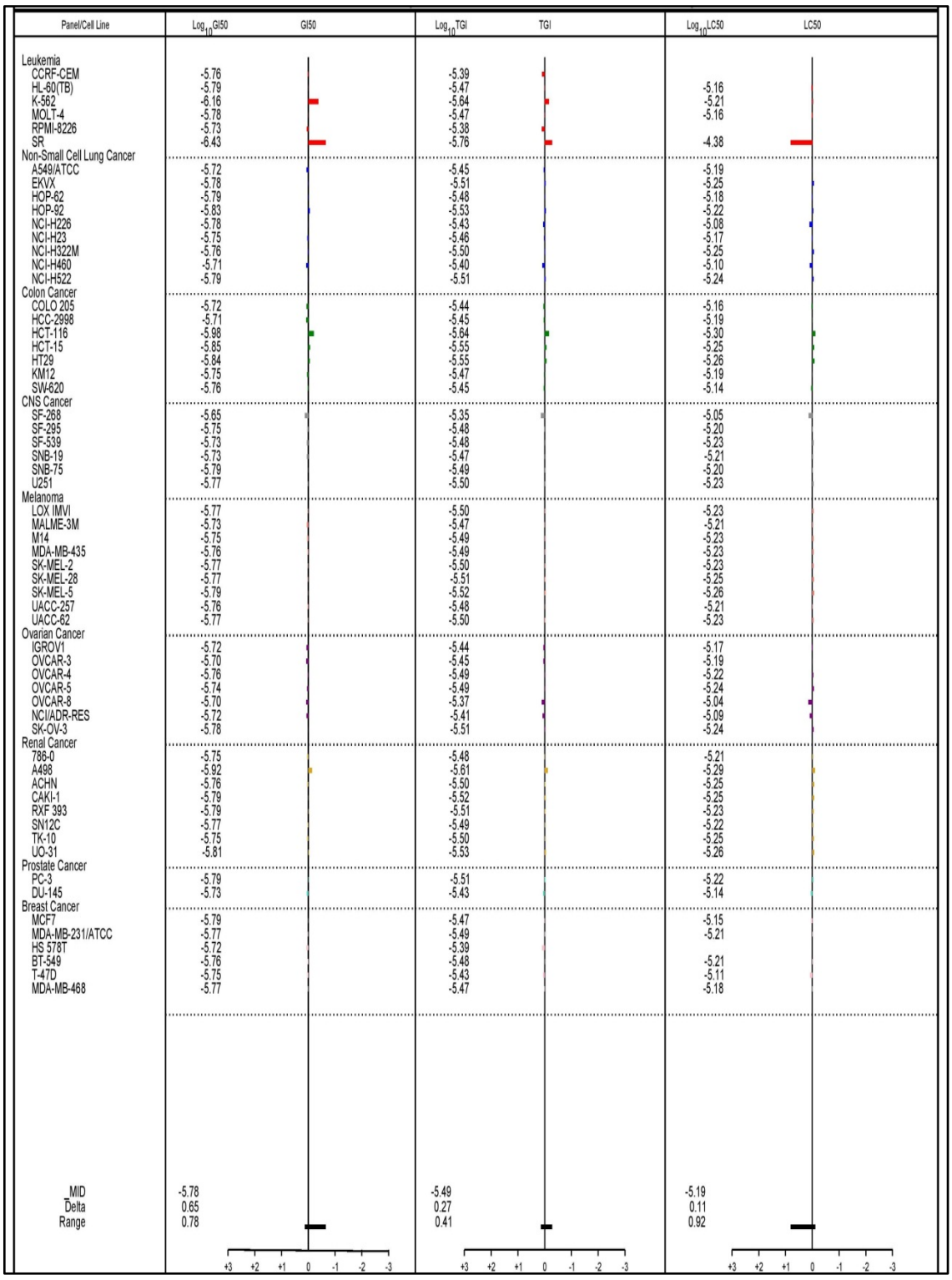

Figure 6.67 ***Values of log molar concentration of response parameters (log_{10}GI50, log_{10}TGI & log_{10}LC50) for compound 44g.***

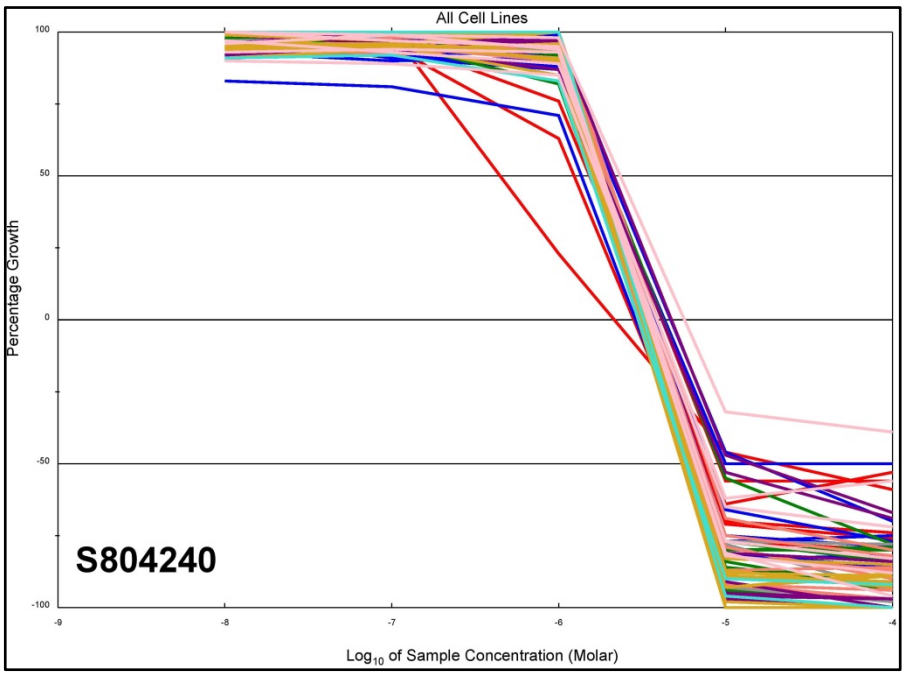

Figure 6.68 ***Dose response curves for all cell lines in the NCI60 panel exposed to compound 44h with tissue originated colours and shapes.***

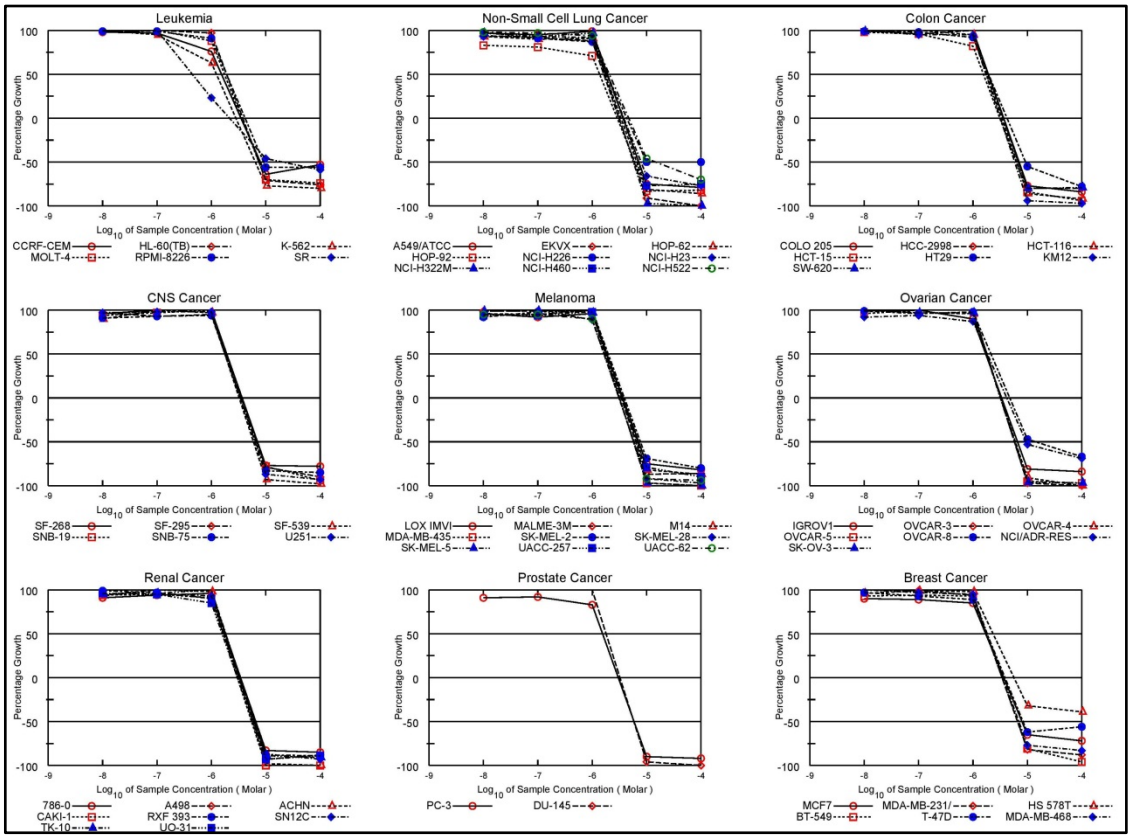

Figure 6.69 ***Dose response curves (% growth verses sample concentration) for all cell lines with different subpanel obtained from the NCI's in vitro disease-oriented human cancer cells line for compound 44h on nine types of cancer.***

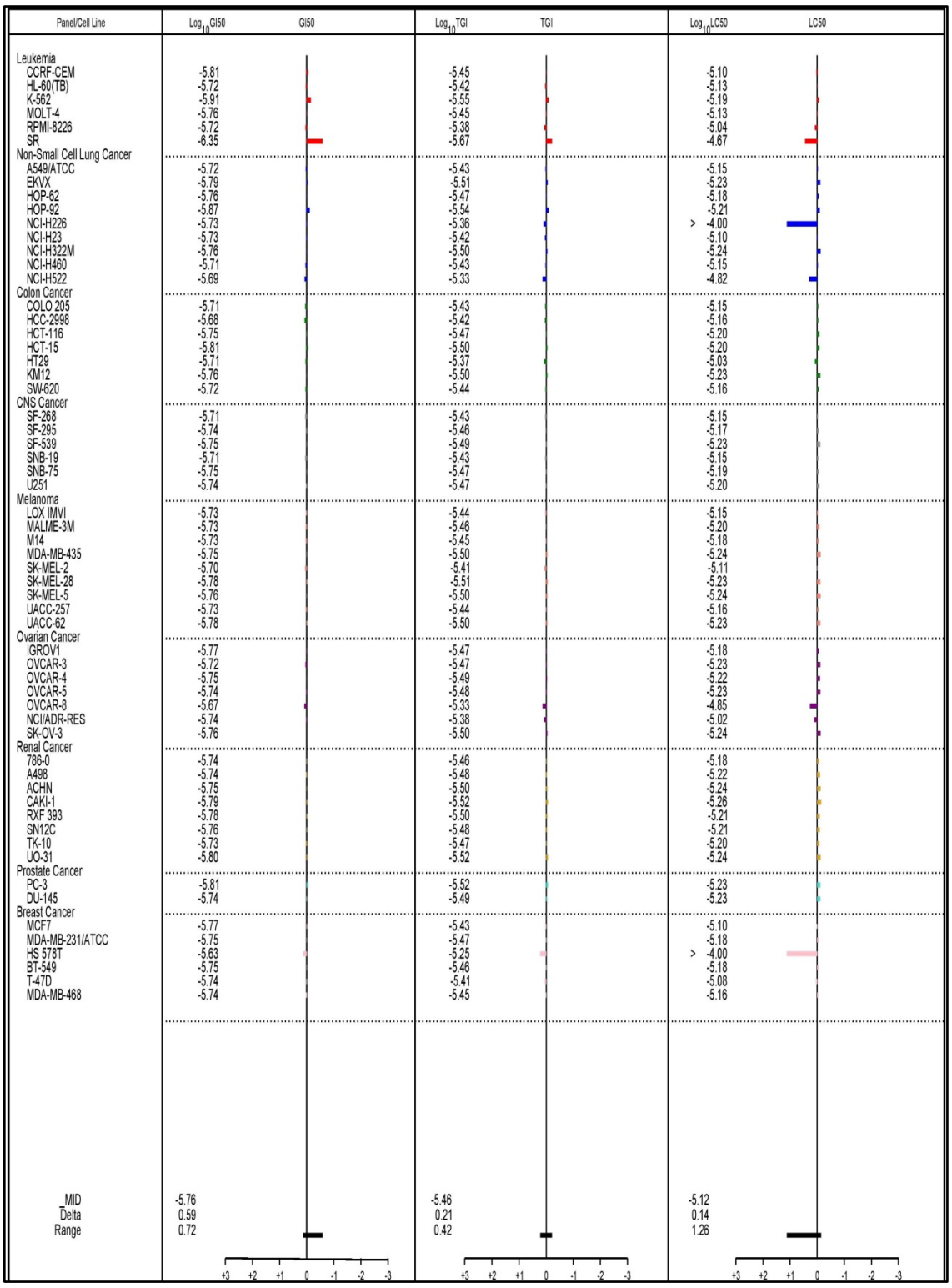

Figure 6.70 ***Values of log molar concentration of response parameters (log_{10}GI50, log_{10}TGI & log_{10}LC50) for compound 44h.***

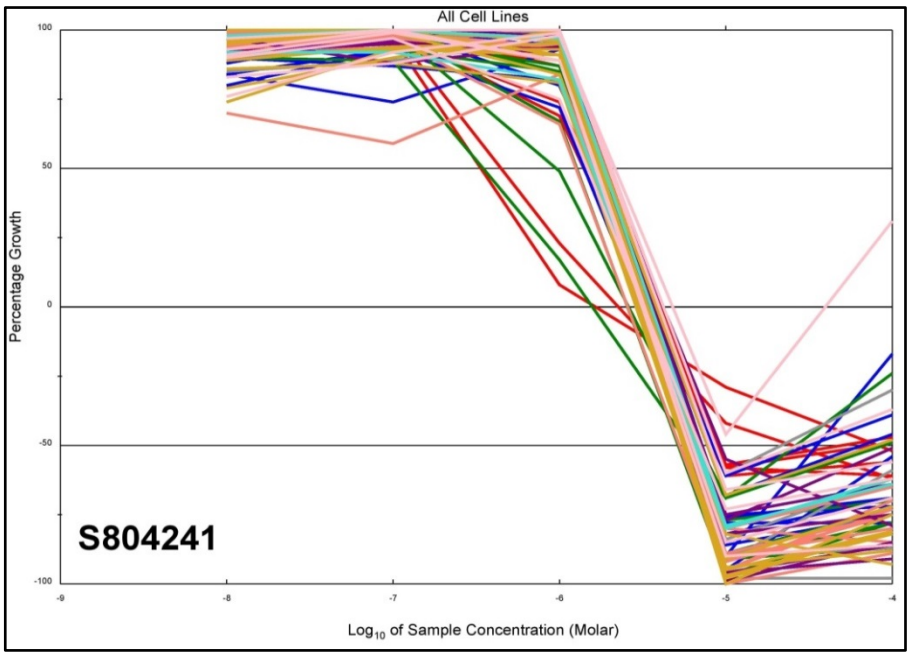

Figure 6.71 ***Dose response curves for all cell lines in the NCI60 panel exposed to compound 44i with tissue originated colours and shapes.***

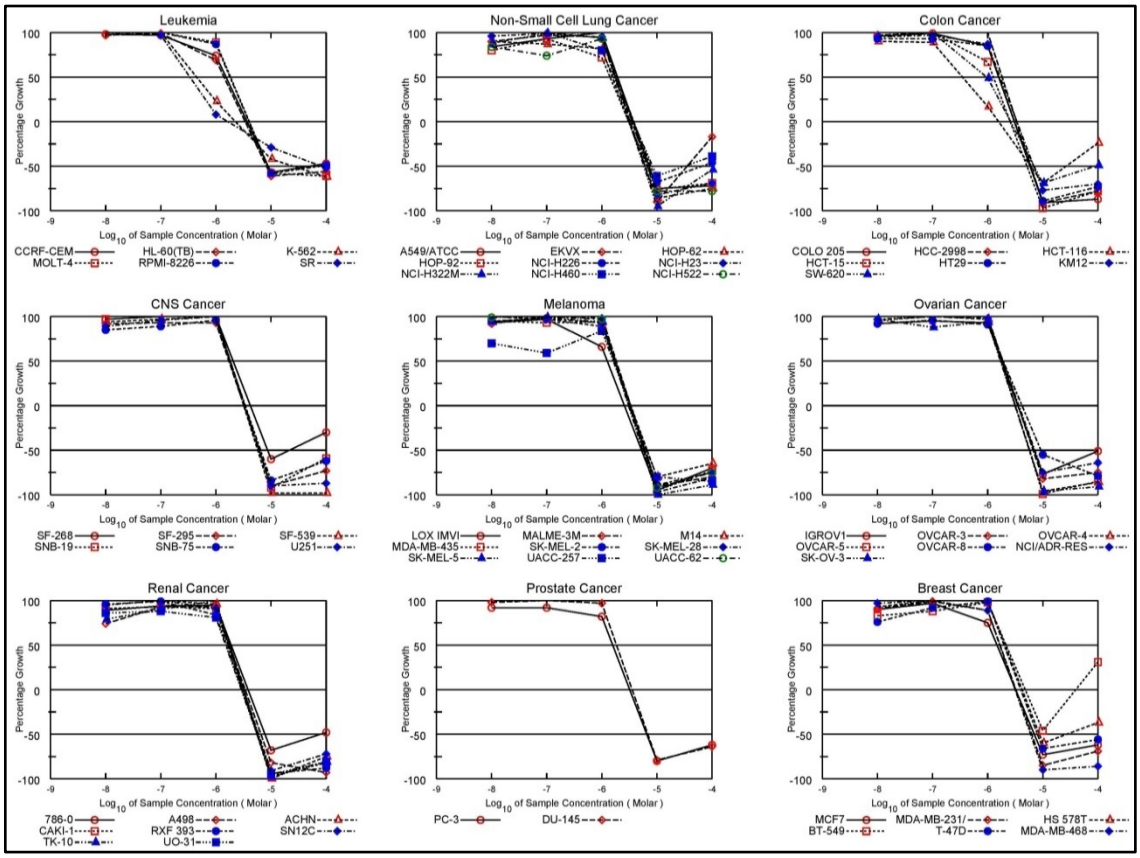

Figure 6.72 ***Dose response curves (% growth verses sample concentration) for all cell lines with different subpanel obtained from the NCI's in vitro disease-oriented human cancer cells line for compound 44i on nine types of cancer.***

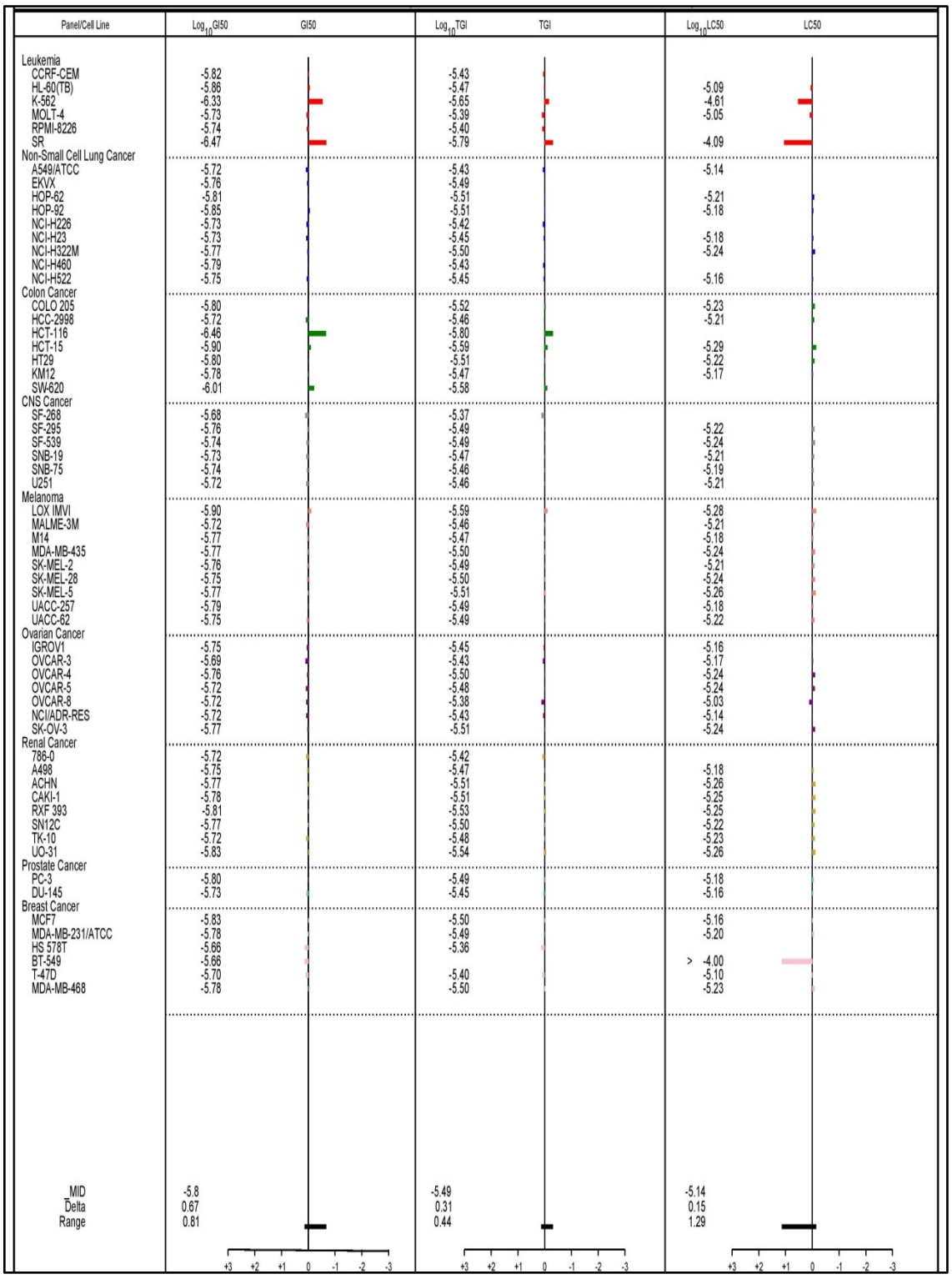

Figure 6.73 ***Values of log molar concentration of response parameters (log_{10}GI50, log_{10}TGI & log_{10}LC50) for compound 44i.***

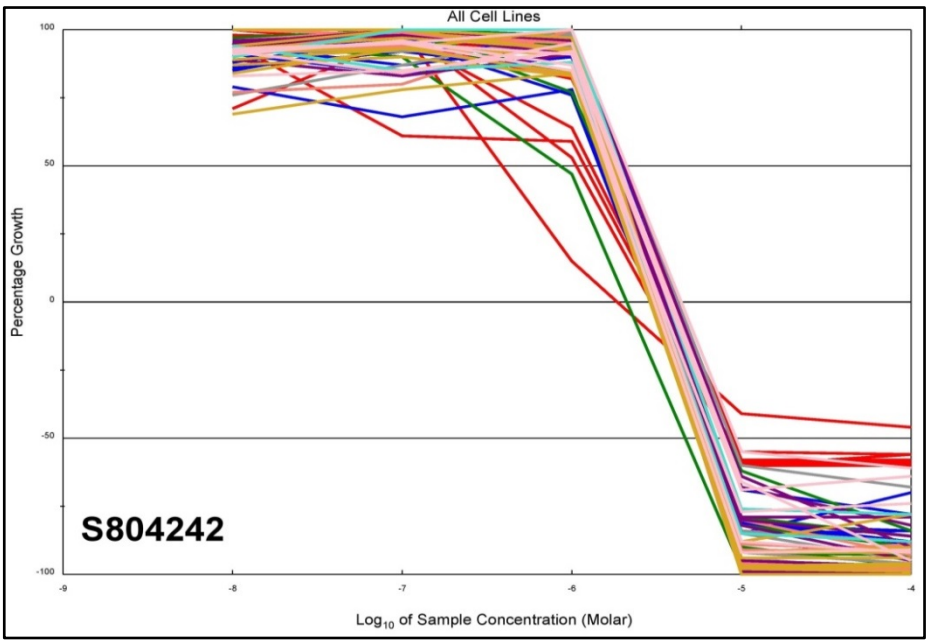

Figure 6.74 ***Dose response curves of 44j for all cell lines in the NCI60 panel exposed to compound with tissue originated colours and shapes.***

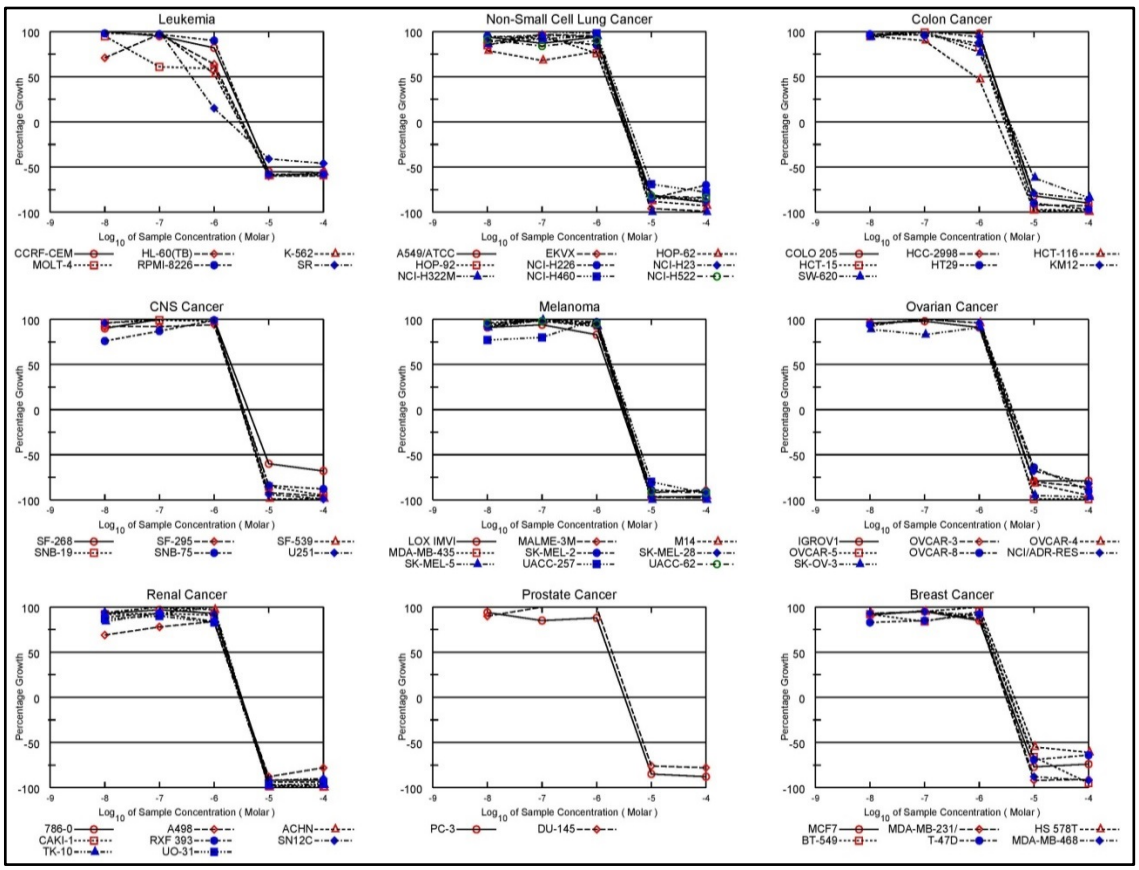

Figure 6.75 ***Dose response curves (% growth verses sample concentration) for all cell lines with different subpanel obtained from the NCI's in vitro disease-oriented human cancer cells line for compound 44j on nine types of cancer.***

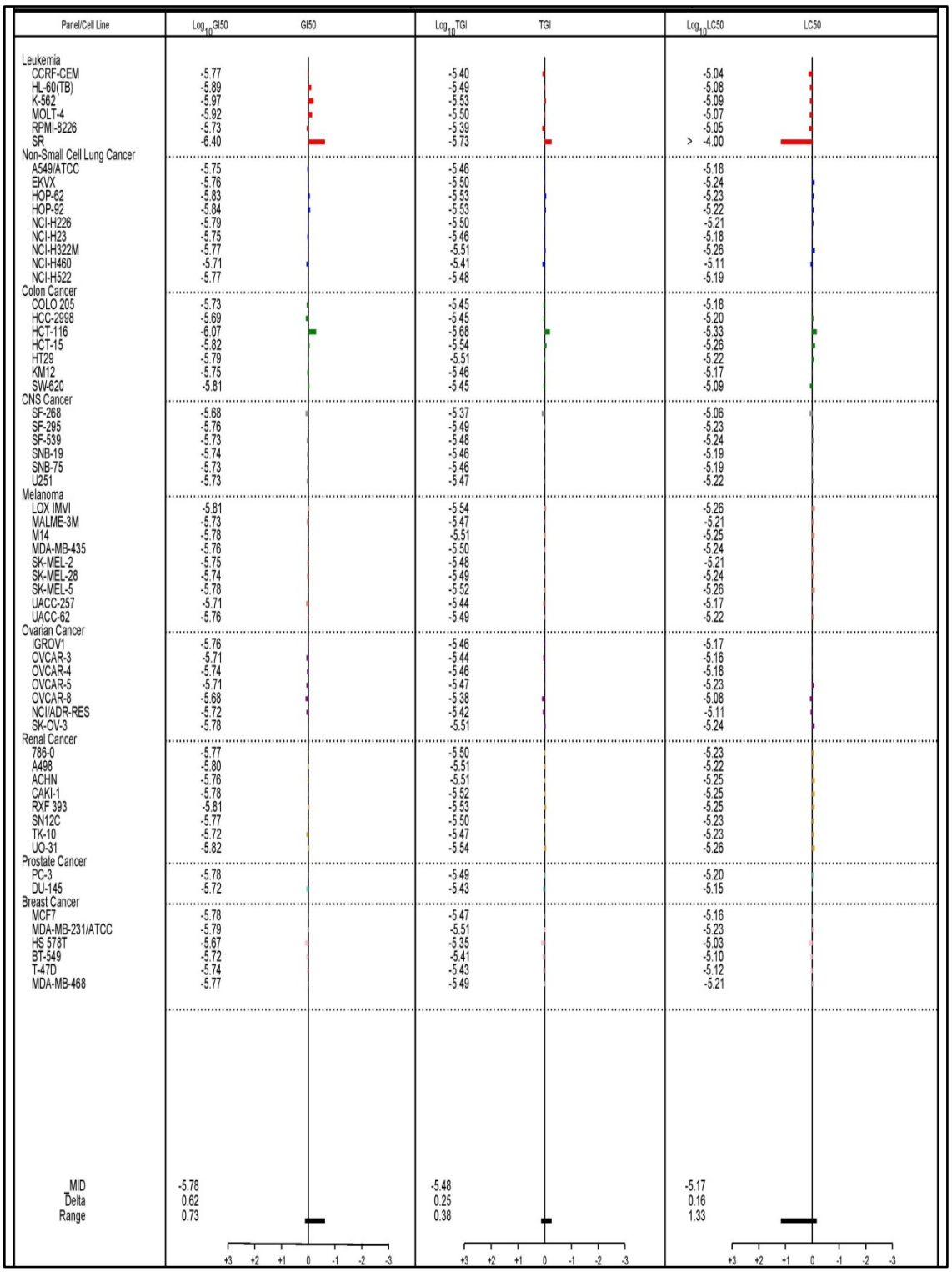

Figure 6.76 ***Values of log molar concentration of response parameters (log_{10}GI50, log_{10}TGI & log_{10}LC50) for compound 44j.***

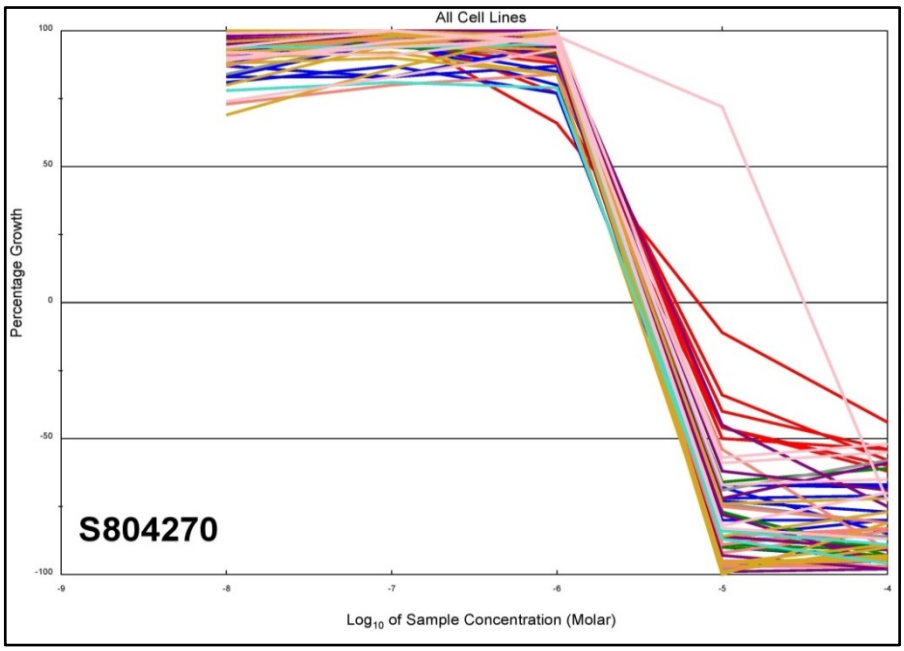

Figure 6.77 ***Dose response curves for all cell lines in the NCI60 panel exposed to compound 44k with tissue originated colours and shapes.***

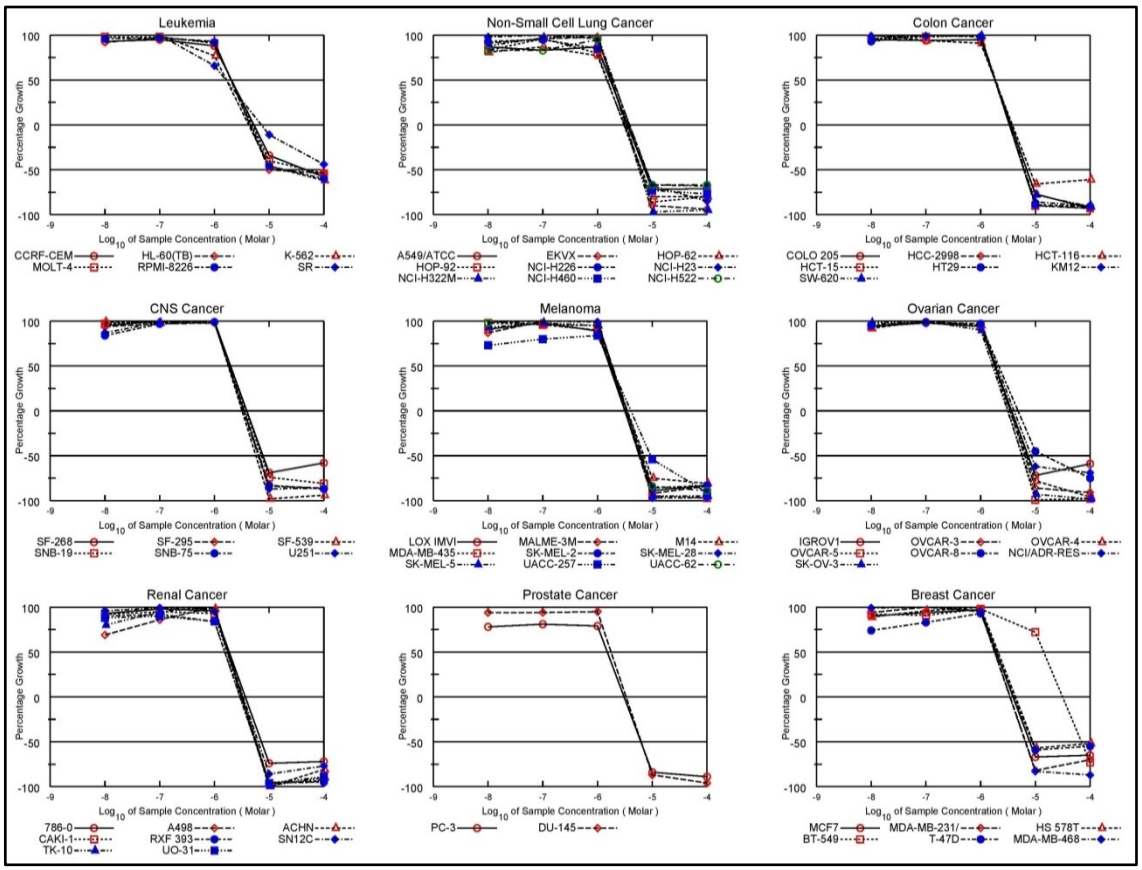

Figure 6.78 ***Dose response curves (% growth verses sample concentration) for all cell lines with different subpanel obtained from the NCI's in vitro disease-oriented human cancer cells line for compound 44k on nine types of cancer.***

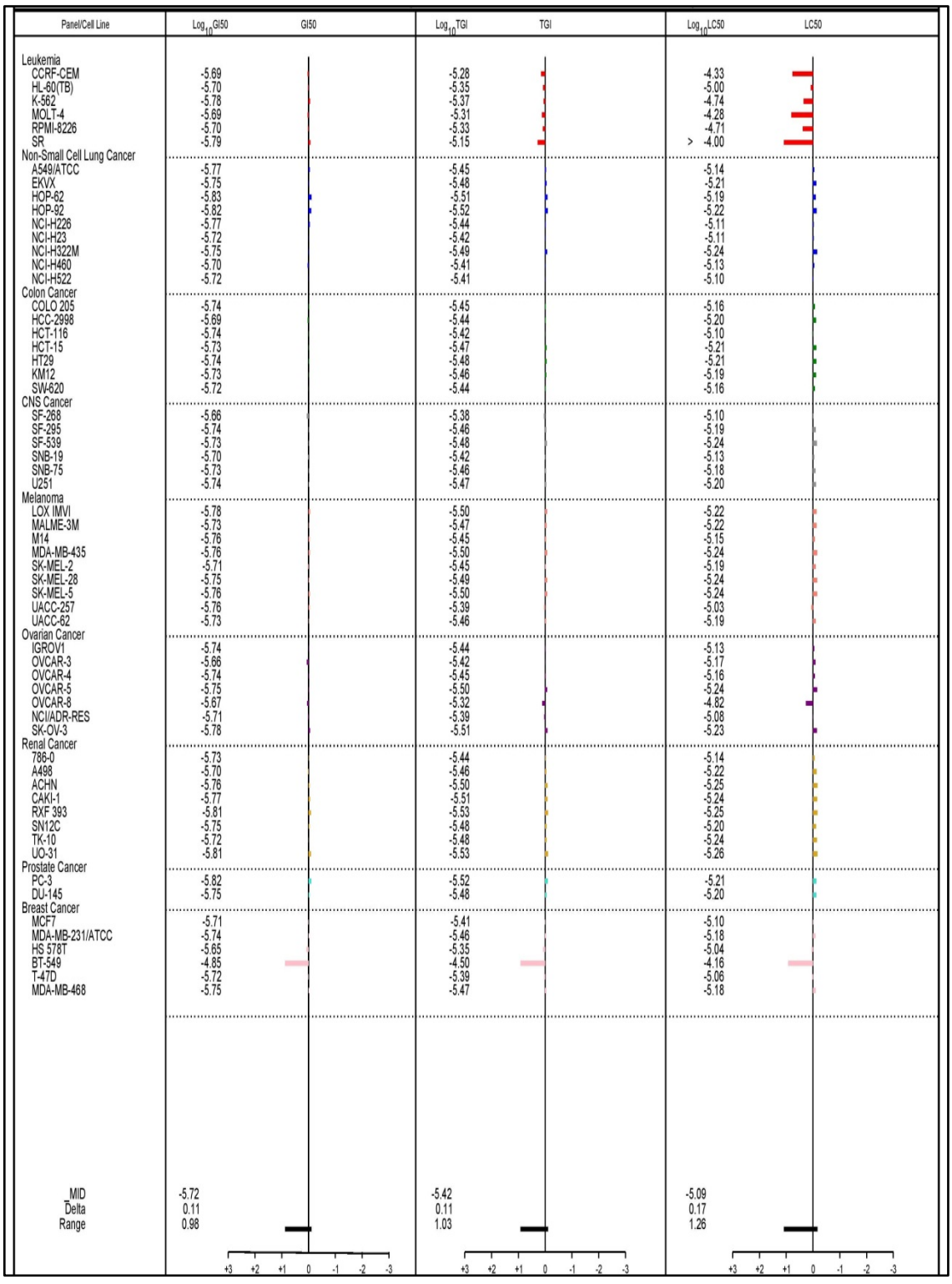

Figure 6.79 ***Values of log molar concentration of response parameters (log_{10}GI50, log_{10}TGI & log_{10}LC50) for compound 44k.***

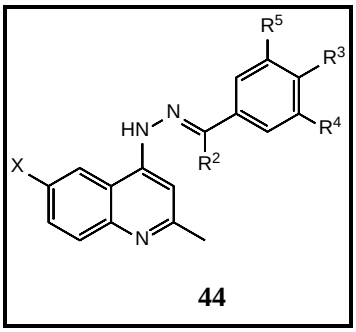

44

Compound **44b** under investigation exhibited a remarkable anticancer activity against most of the tested cell lines representing nine different subpanels with GI_{50} value 1.12 - 2.37 x 10^{-6} M, TGI value 2.95 - 7.29 x 10^{-6} M and LC_{50} value ranging in between 1.15 - 9.60 x10^{-6} M. Leukemia (SR) cell lines were found to be the most affected cell lines by the compound **44b** with GI_{50} values of 1.12 x 10^{-6} M. Compound **44d** showed noteworthy anticancer activity with GI_{50} value 1.17 - 2.31 x 10^{-6} M, TGI value 2.88 - 4.63 x 10^{-6} M and LC_{50} value 1.96 - 9.32 x 10^{-6} M. Leukemia (SR) cell lines were found to be the most affected cell line with compound **44d** with GI_{50} values of 1.17 x 10^{-6} M. The values for compound **44e** are GI_{50} value 1.43 x 10^{-6} - 5.01 x 10^{-7} M, TGI value 2.93 - 4.53 x 10^{-6} M and LC_{50} value 1.0 x 10^{-4} - 9.32 x 10^{-6} M. In this case also leukemia (SR) cell lines were the most affected cell lines with GI_{50} values of 5.01 x 10^{-7} M. The GI_{50}, TGI and LC_{50} values for compound **44f** are 2.71 – 2.12 x 10^{-6} M, 2.92 - 4.71 x 10^{-6} M, 1.0 x 10^{-6} – 6.20 x 10^{-6} M respectively. The compound **44f** was most active against renal cancer cell line (UO-31) with GI_{50} values of 1.48 x 10^{-6} M. Compound **44g** displayed outstanding anticancer activity with GI_{50}, TGI and LC_{50} values 3.69 x 10^{-7} – 1.43 x 10^{-6} M, 1.73- 4.23 x 10^{-6} M and 7.83 x 10^{-6} – 4.20 x 10^{-5} M respectively. Leukemia (SR) and leukemia (K-562) cancer cell lines were found to be the most affected cell lines by compound **44g** with GI_{50} values of 6.91 x 10^{-7} M and 3.69 x 10^{-7} respectively. Compound **44h** displayed an exceptional anticancer activity with GI_{50}, TGI and LC_{50} values 4.48 x 10^{-7} – 1.55 x 10^{-6} M, 3.11- 5.64 x 10^{-6} M and 7.99 x 10^{-6} – >1.00 x 10^{-4} M respectively. Compound **44h** was most active on leukemia (SR) cell lines with GI_{50} values of 4.48 x 10^{-7} M. For compound **44i** the GI_{50}, TGI and LC_{50} values are 3.36 x 10^{-7} – 1.27 x 10^{-6} M, 1.60 x 10^{-6} – 4.37 x 10^{-6} M and 1.0 x 10^{-4} – 9.28 x 10^{-6} M respectively. Leukemia (SR) and leukemia (K-562) cell lines were found to be the most affected cell lines with compound **44i** having GI_{50} values of 4.67 x 10^{-7} M and 3.36 x 10^{-7} respectively. The GI_{50}, TGI and LC_{50} values for compound **44j** are 3.96 x 10^{-7} – 2.16 x 10^{-6} M, 1.85 – 4.06 x 10^{-6} M, 1.0 x 10^{-4} – 9.20 x 10^{-6} M

respectively. Compound **44j** was observed to be the most effective against leukemia (SR) and colon cancer (HCT-116) cell lines with GI_{50} values of 6.96 x 10^{-7} M and 8.50 x 10^{-7} respectively. The values of GI_{50}, TGI and LC_{50} for compound **44k** are 1.50 x 10^{-6} – 2.23 x 10^{-6} M, 3.21 – 7.12 x 10^{-6} M, 1.0 x 10^{-4} – 9.9 x 10^{-6} M respectively. The compound **44k** was most effective on prostate (PC-3) cell lines with GI_{50} values of 1.50 x 10^{-6} M.

6.8 Conclusion

In this part of the chapter, some new quinolyl hydrazones substituted with alkoxy chain varying in chain length are prepared by condensation of 6-bromo/6-chloro-2-methyl-quinolin-4-yl-hydrazine with various alkoxy aldehydes and alkoxy acetophenones. All the synthesised compounds are characterized by various spectroanalytical techniques. The new compounds have been screened for their antimicrobial activity using two fungal and four bacterial strains. Some of the compounds show good to outstanding antimicrobial activity. Molecular modelling study on one of the widely studied fungal enzyme revealed that the antimicrobial activity of the active compounds could be due to their interaction with sterol 14 alpha demethylase (CYP51). Further, *in vitro* anticancer activity (single dose as well as five dose assay) on 60 different cancer cell lines was carried out at NCI, USA. Out of the twenty submitted compounds, nine compounds displayed outstanding anticancer activity with lethality value ranging from 10% to 100% for several cancer cell lines at the single dose level. All the selected nine compounds exhibit excellent anticancer activity at five dose levels as well having GI_{50} value up to 0.44 μM against some of the cancer cell lines.

6.9 Experimental

General

The chemicals were used as received from local companies without further purification. Organic solvents were purified by distillation prior to use.

Column chromatography was carried out using silica gel (60-120 mesh). Thin layer chromatography was performed on the pre-coated silica gel 60 F_{254} aluminium sheets. Melting points are determined in open capillary and are uncorrected.

FT-IR spectra were recorded on Bruker Alpha FTIR spectrometer between 4000-400 cm^{-1} in solid state as KBr discs. The NMR spectra were recorded on 400 MHz Bruker Avance-III instrument and chemical shifts are given in parts per million. In the NMR data for ^{19}F decoupled ^{1}H NMR experiments, the data for the affected signals only are included. ^{19}F chemical shift values are of ^{1}H decoupled ^{19}F signals.

ESI mass spectra were recorded on Waters' Xevo G2-XS QToF mass spectrometer at Zydus Research Centre, Ahmedabad.

General Procedure for the Synthesis of 4-alkyloxybenzaldehydes 34.[56,62]

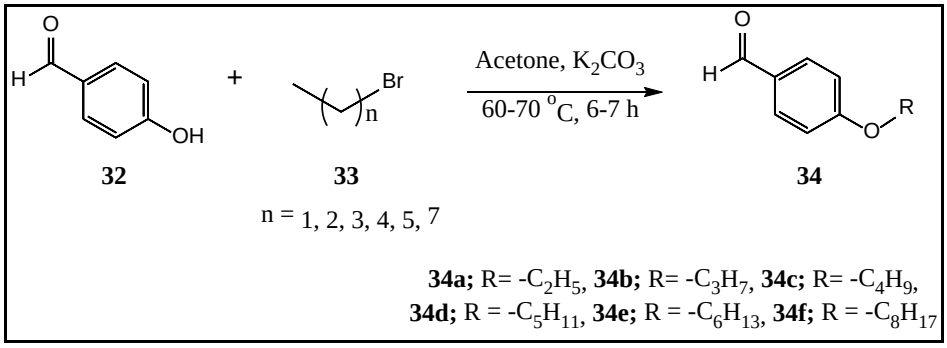

A magnetically stirred mixture of 4-hydroxybenzaldehyde **32** (0.3 mol) and an appropriate 1-bromoalkane **33** (0.1 mol) and anhydrous potassium carbonate (0.45 mol) in dry acetone (20 mL) was heated under reflux (6-7 hour). The resulting mixture was cooled to room temperature and was poured into ice water after evaporation of solvent followed by extraction with EtOAc. The combined organic layers were dried over Na_2SO_4 and the solvent was removed in vacuo. The residue was subjected to column chromatography to give the required product 4-n-alkoxy benzaldehydes **34**. Yield: 80-90%.

The boiling points of all the prepared alkoxy aldehydes and alkoxy acetophenones are in agreement with the reported once.[56,62]

Synthesis of 3,4-Bis-octyloxybenzaldehyde and 3,4,5-tris-octyloxybenzaldehyde 37, 39.[63,64]

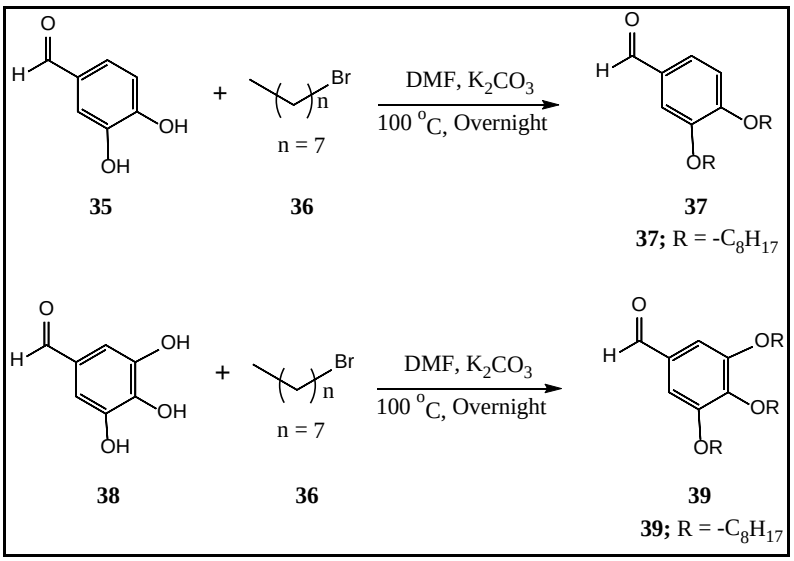

To a solution of 3,4-dihydroxybenzaldehyde **35** (0.1 mol) or 3,4,5-trihydroxy benzaldehyde **38** (0.1 mol) in DMF was added potassium carbonate (0.45 mol) followed by 1-bromooctane **36** (0.3 mol) and the reaction mixture was stirred at 90-100 °C under a nitrogen atmosphere for 12-14 hrs (overnight). The reaction mixture was cooled and poured into ice cold water with constant stirring. The organic layer was separated and the aqueous layer was extracted with DCM. The combined organic layers were dried over Na_2SO_4 and the solvent was removed in vacuo. The product was purified by column chromatography to afford the required compound **37**/**39**. Yield: 80-90%.

The boiling points of 3,4-bis-octyloxybenzaldehyde and 3,4,5-tris-octyloxy benzaldehyde were observed and found comparable with that of the reported ones.[63,64]

General Procedure for the Synthesis of 1-(4-alkoxyphenyl)-ethan-1-ones 42.[65]

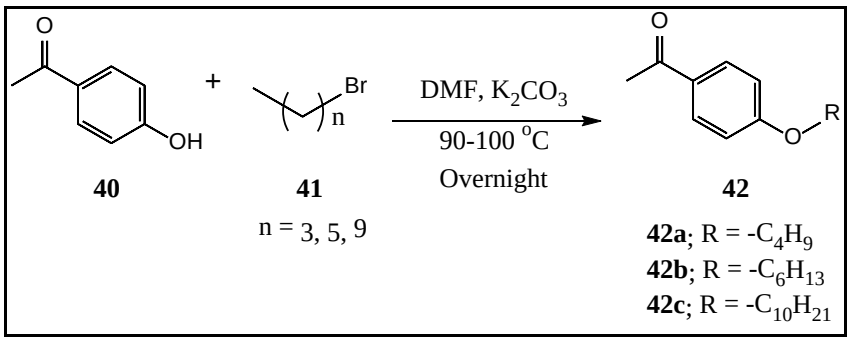

To a solution of 4-hydroxyacetophenone **40** (0.1 mol) in DMF was added potassium carbonate (0.45 mol) followed by 1-bromoalkanes **41** (0.3 mol) and the resulting reaction mixture was stirred at 90-100 °C under nitrogen atmosphere for 12-14 hrs (overnight). The reaction mixture was cooled and poured into ice cold water with stirring. The organic layer was separated and the aqueous layer was extracted with DCM. The combined organic layers were dried over Na_2SO_4 and solvent was removed in vacuo. The product was purified by column chromatography to afford the required compounds **42**. Yield: 80-90%.

The boiling points of 1-(4-alkoxyphenyl)-ethan-1-ones **42** were confirm by matching with that of the reported one.[65]

General Procedure for the Synthesis of 4-{ N'-arylidene-hydrazinyl}-6-bromo/6-chloro-2-methylquinoline 44.[54,55]

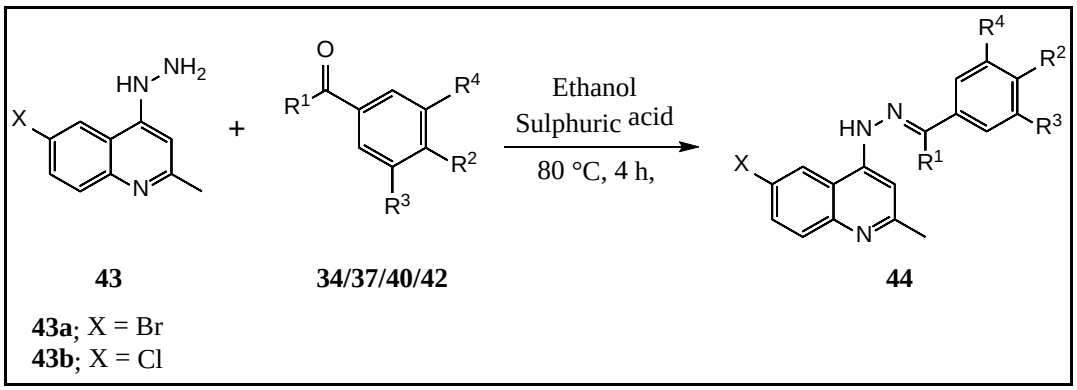

43 **34/37/40/42** **44**

43a; X = Br
43b; X = Cl

Alkyloxy benzaldehyde/acetophenone (0.46 mmol) and 6-bromo/6-chloro-2-methyl-quinolin-4-yl-hydrazine (0.46 mmol) were dissolved in ethanol (5 mL). A catalytic amount of concentrated sulphuric acid was added. The reaction mixture was heated at 80 ^{o}C for 4 h, and then kept at room temperature overnight. The resultant solid separated was filtered, washed with chilled ethanol and crystallized from ethanol to afford the pure final hydrazones. Yield: 76-82%.

[6-Bromo-4-{N'-(4-ethyloxybenzylidene)hydrazinyl}-2-methylquinoline] 44a.

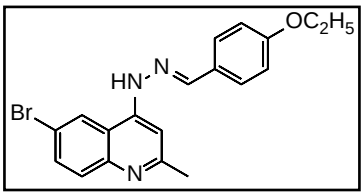

Compound **44a** was prepared by following the general procedure described above by reacting 4-ethoxybenzaldehyde **34a** (0.034g, 0.24 mmol) in ethanol with 6-bromo-2-methyl-quinolin-4-yl-hydrazine **43a** (0.05g, 0.24 mmol) using H_2SO_4 as a catalyst. Yield = 0.072g, 82%; Yellow Solid; MP = 202 ^{o}C; **IR (KBr) cm^{-1}**: 3288, 2977, 1242, 1189, 849, 771; **^{1}H NMR (400 MHz, DMSO-d$_6$, δ ppm)**: 1.1 (3H, t, *J* = 7.2 Hz, terminal -CH_3), 2.73 (3H, s, -CH_3), 4.12 (2H, q, *J* = 7.2 Hz, -OCH_2), 7.06 (2H, d, *J* = 8.4 Hz, Ar-H), 7.55 (1H, s, -N=CH-), 7.87 (2H, d, *J* = 9.2 Hz, Ar-H), 7.90 (1H, d, *J* = 9.2 Hz, Qui-H), 8.01 (1H, d, *J* = 9.2 Hz, Qui-H), 8.55 (1H, s, Qui-H), 8.70 (1H, d, *J* = 2 Hz, Qui-H), 12.22 (1H, s, -NH); **^{13}C NMR (100 MHz, DMSO-d$_6$, δ ppm)**: 15.5 (-**C**H_3), 20.6 (-**C**H_3), 63.9 (-O**C**H_2), 101.0, 115.7, 115.9, 119.4, 122.6, 125.7, 126.1, 136.6, 150.6, 155.1, 161.4; **Mass (TOF MS ES+)**: m/z 384.07 $(M+H)^+$, 386.06 $(MH+2)^+$ for M = $C_{19}H_{18}BrN_3O$.

[6-Chloro-4-{N'-(4-ethyloxybenzylidene)hydrazinyl}-2-methylquinoline] 44b.

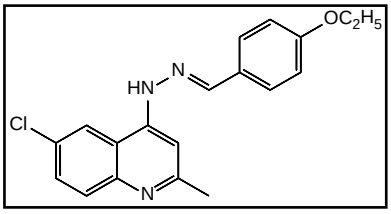

Compound **44b** was prepared by following the general procedure described above by reacting 4-ethoxybenzaldehyde **34a** (0.043g, 0.27 mmol) in ethanol with 6-chloro-2-methyl-quinolin-4-yl-hydrazine **43b** (0.05g, 0.27 mmol) using H_2SO_4 as a catalyst. Yield = 0.072g, 74%; Yellow Solid; MP = 210 °C; **IR (KBr) cm^{-1}**: 3286, 2977, 1510, 1210, 1169, 918, 771; **^{1}H NMR (400 MHz, DMSO-d$_6$, δ ppm)**: 1.10 (3H, t, *J* = 7.2 Hz, terminal -CH_3), 2.73 (3H, s, -CH_3), 4.12 (2H, q, *J* = 7.2 Hz, -OCH_2), 7.05 (2H, d, *J* = 8.8 Hz, Ar-H), 7.53 (1H, s, -N=CH-), 7.87 (2H, d, *J* = 8.4 Hz, Ar-H), 7.89 (1H, d, *J* = 9.2 Hz, Qui-H), 8.00 (1H, d, *J* = 8.8 Hz, Qui-H), 8.54 (1H, s, Qui-H), 8.69 (1H, s, Qui-H), 12.19 (1H, s, -NH); **^{13}C NMR (100 MHz, DMSO-d$_6$, δ ppm)**: 15.5 (-**C**H_3), 20.6 (-**C**H_3), 63.9 (-O**C**H_2), 101.1, 115.3, 115.5, 122.3, 122.7, 126.1, 130.1, 131.3, 134.1, 150.7, 151.1, 155.2, 161.4; **Mass (TOF MS ES+)**: m/z 340.12 $(M+H)^+$, 342.12 $(MH+2)^+$ for M = $C_{19}H_{18}ClN_3O$.

[6-Bromo-2-methyl-4-{N'-(4-propyloxybenzylidene)hydrazinyl}quinoline] 44c.

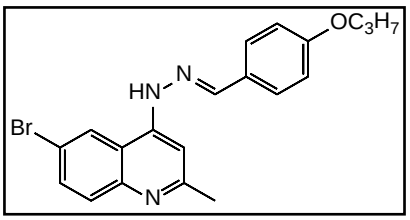

Compound **44c** was prepared by following the general procedure described above by reacting 4-propyloxybenzaldehyde **34b** (0.037g, 0.22 mmol) in ethanol with 6-bromo-2-methyl-quinolin-4-yl-hydrazine **43a** (0.05g, 0.22 mmol) using H_2SO_4 as a catalyst. Yield = 0.071g, 78%; Yellow Solid; MP = 204 °C; **IR (KBr) cm^{-1}**: 3211, 2964, 1605, 1249, 1168, 913, 845; **^{1}H NMR (400 MHz, DMSO-d$_6$, δ ppm)**: 0.99 (3H, t, *J* = 7.2 Hz, terminal -CH_3), 1.75 (2H, m, -CH_2-), 2.71 (3H, s, -CH_3), 4.01 (2H, t, *J* = 6.4 Hz, -OCH_2), 7.06 (2H, d, *J* = 8.4 Hz, Ar-H), 7.53 (1H, s, -N=CH-), 7.81 (2H, d, *J* = 8.8 Hz, Qui-H), 7.85 (2H, d, *J* = 8.4 Hz, Ar-H), 8.11 (1H, d, *J* = 9.2 Hz, Qui-H), 8.53 (1H, s, Qui-H), 8.82 (1H, s, Qui-H), 12.22 (1H, s, -NH); **^{13}C NMR (100 MHz, DMSO-d$_6$, δ ppm)**: 10.8 (-**C**H_3), 15.5 (-**C**H_3), 22.42 (-**C**H_2), 69.7 (-O**C**H_2), 101.0, 115.4, 115.8, 119.5, 122.2, 125.7, 126.1, 130.0, 136.7, 150.7, 155.0, 161.6 ; **Mass (TOF MS ES+)**: m/z 398. 09 $(M+H)^+$, 400.08 $(MH+2)^+$ for $C_{20}H_{20}BrN_3O$.

[6-Chloro-2-methyl-4-{N'-(4-propyloxybenzylidene)hydrazinyl}quinoline] 44d.

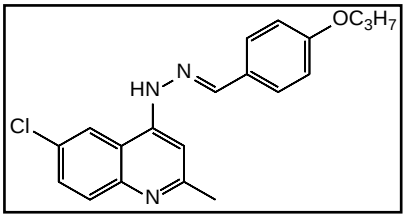

Compound **44d** was prepared by following the general procedure described above by reacting 4-propyloxybenzaldehyde **34b** (0.047g, 0.28 mmol) in ethanol with 6-chloro-2-methyl-quinolin-4-yl-hydrazine **43b** (0.05g, 0.28 mmol) using H_2SO_4 as a catalyst. Yield = 0.075g, 74%; Yellow Solid; MP = 200 °C; **IR (KBr) cm^{-1}**: 3211, 2964, 1605, 1249, 1168, 913, 845; **^{1}H NMR (400 MHz, DMSO-d$_6$, δ ppm)**: 1.10 (3H, t, *J* = 7.2 Hz, terminal -CH_3), 1.75 (2H, m, -CH_2-), 2.72 (3H, s, -CH_3), 3.73 (2H, t, *J* = 6.8 Hz, -OCH_2), 7.06 (2H, d, *J* = 8.4 Hz, Ar-H), 7.53 (1H, s, -N=CH-), 7.87 (2H, d, *J* = 8.4 Hz, Ar-H), 7.89 (1H, d, *J* = 9.2 Hz, Qui-H), 8.00 (1H, d, *J* = 8.8 Hz, Qui-H), 8.54 (1H, s, Qui-H), 8.68 (1H, d, *J* = 1.6 Hz, Qui-H), 12.21 (1H, s, -NH); **^{13}C NMR (100 MHz, DMSO-d$_6$, δ ppm)**: 10.8 (-**C**H_3), 15.5 (-**C**H_3), 22.43 (-**C**H_2), 69.7 (-O**C**H_2), 101.1, 115.4, 115.5, 122.3, 122.7, 126.1, 130.1, 131.3, 134.2, 150.7, 151.1, 155.2, 161.6; **Mass (TOF MS ES+)**: m/z 354.13 $(M+H)^+$, 356.13 $(MH+2)^+$ for M = $C_{20}H_{20}ClN_3O$.

[6-Bromo-4-{N'-(4-butyloxybenzylidene)hydrazinyl}-2-methylquinoline] 44e.

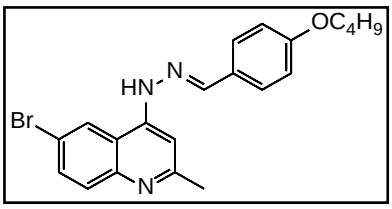

Compound **44e** was prepared by following the general procedure described above by reacting 4-butyloxybenzaldehyde **34c** (0.04g, 0.22 mmol) in ethanol with 6-bromo-2-methyl-quinolin-4-yl-hydrazine **43a** (0.05g, 0.22 mmol) using H_2SO_4 as a catalyst. Yield = 0.075g, 80%; Yellow Solid; MP = 186 °C; **IR (KBr) cm^{-1}**: 3202, 2935, 1600, 1445, 1251, 772; **^{1}H NMR (400 MHz, DMSO-d$_6$, δ ppm)**: 0.95 (3H, t, *J* = 7.2 Hz, terminal -CH_3), 1.46 (2H, m, -CH_2), 1.72 (2H, m, -CH_2), 2.72 (3H, s, -CH_3), 4.05 (2H, t, *J* = 6.4 Hz, -OCH_2), 7.06 (2H, d, *J* = 8.4 Hz, Ar-H), 7.54 (1H, s, -N=CH-), 7.82 (1H, d, *J* = 9.2 Hz, Qui-H), 7.85 (2H, d, *J* = 8.8 Hz, Ar-H), 8.35 (1H, d, *J* = 8.8 Hz, Qui-H), 8.54 (1H, s, Qui-H), 8.83 (1H, s, Qui-H), 12.23 (1H, s, -NH); **^{13}C NMR (100 MHz, DMSO-d$_6$, δ ppm)**: 14.1 (-**C**H_3), 15.5 (-**C**H_3), 19.1 (-**C**H_2), 20.6 (-**C**H_2), 31.0, 67.9 (-O**C**H_2), 101.0, 115.3, 115.8, 119.5, 122.2, 125.6, 126.0, 130.0, 136.7, 137.7, 1506, 150.9, 155.1, 161.6 ; **Mass (TOF MS ES+)**: m/z 412.10 $(M+H)^+$, 414.10 $(MH+2)^+$ for M = $C_{21}H_{22}BrN_3O$.

[4-{N'-(4-Butyloxybenzylidene)hydrazinyl}-6-chloro-2-methylquinoline] 44f.

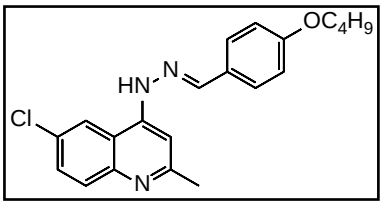

Compound **44f** was prepared by following the general procedure described above by reacting 4-butyloxybenzaldehyde **34c** (0.05g, 0.28 mmol) in ethanol with 6-chloro-2-methyl-quinolin-4-yl-hydrazine **43b** (0.05g, 0.28 mmol) using H_2SO_4 as a catalyst. Yield = 0.078g, 76%; Yellow Solid; MP = 198 °C; **IR (KBr) cm^{-1}**: 3211, 1642, 1251, 1170, 898, 773; **^{1}H NMR (400 MHz, DMSO-d$_6$, δ ppm)**: 0.94 (3H, t, *J* = 7.2 Hz, terminal -CH_3), 1.46 (2H, m, -CH_2), 1.72 (2H, m, -CH_2), 2.71 (3H, s, -CH_3), 4.04 (2H, t, *J* = 6.4 Hz, -OCH_2), 7.06 (2H, d, *J* = 8.4 Hz, Ar-H), 7.52 (1H, s, -N=CH-), 7.85 (1H, d, *J* = 8.8 Hz, Qui-H), 7.88 (2H, d, *J* = 9.2 Hz, Qui-H), 7.98 (1H, d, *J* = 9.2 Hz, Qui-H), 8.53 (1H, s, Qui-H), 8.68 (1H, s, Qui-H), 12.17 (1H, s, -NH); **^{13}C NMR (100 MHz, DMSO-d$_6$, δ ppm)**: 14.1 (-**C**H_3), 15.5 (-**C**H_3), 19.1 (-**C**H_2), 20.7 (-**C**H_2), 31.1, 67.9 (-O**C**H_2), 101.9, 115.4, 122.6, 126.1, 130.0, 131.3, 133.9, 150.9, 155.1, 161.6; **Mass (TOF MS ES+)**: m/z 368.15 $(M+H)^+$, 370.15 $(MH+2)^+$ for M = $C_{21}H_{22}ClN_3O$.

[6-Bromo-2-methyl-4-{N'-4-(pentyloxybenzylidene)hydrazinyl}quinoline] 44g.

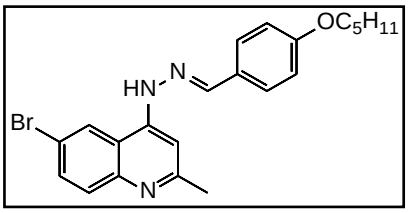

Compound **44g** was prepared by following the general procedure described above by reacting 4-pentyloxybenzaldehyde **34d** (0.04g, 0.22 mmol) in ethanol with 6-bromo-2-methyl-quinolin-4-yl-hydrazine **43a** (0.05g, 0.22 mmol) using H_2SO_4 as a catalyst. Yield = 0.066g, 68%; Yellow Solid; MP = 194 °C; **IR (KBr) cm^{-1}**: 3235, 1643, 1253, 1053, 892, 772; **^{1}H NMR (400 MHz, DMSO-d$_6$, δ ppm)**: 0.90 (3H, t, *J* = 7.2 Hz, terminal -CH_3), 1.52 (4H, m, -CH_2), 1.74 (2H, m, -CH_2), 2.70 (3H, s, -CH_3), 4.05 (2H, t, *J* = 6.4 Hz, -OCH_2), 7.06 (2H, d, *J* = 8.4 Hz, Ar-H), 7.52 (1H, s, -N=CH-), 7.81 (2H, d, *J* = 9.2 Hz, Qui-H), 7.85 (2H, d, *J* = 8.4 Hz, Ar-H), 8.08 (1H, d, *J* = 8.4 Hz, Qui-H), 8.53 (1H, s, Qui-H), 8.82 (1H, s, Qui-H), 12.18 (1H, s, -NH); **^{13}C NMR (100 MHz, DMSO-d$_6$, δ ppm)**: 14.3 (-**C**H_3), 20.5 (-**C**H_3), 22.3 (-**C**H_2), 28.0 (-**C**H_2), 28.6 (-**C**H_2), 68.2 (-O**C**H_2), 100.9, 115.3, 115.7, 119.6, 122.1, 130.0, 136.7, 137.5, 150.7, 150.8, 154.8, 161.5; **Mass (TOF MS ES+)**: m/z 426.08 $(M+H)^+$, 428.08 $(MH+2)^+$ for M = $C_{22}H_{24}BrN_3O$.

[6-Chloro-2-methyl-4-{N'-(4-pentyloxybenzylidene)hydrazinyl}quinoline] 44h.

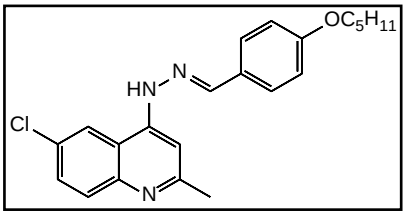

Compound **44h** was prepared by following the general procedure described above by reacting 4-pentyloxybenzaldehyde **34d** (0.05g, 0.28 mmol) in ethanol with 6-chloro-2-methyl-quinolin-4-yl-hydrazine **43b** (0.05g, 0.28 mmol) using H_2SO_4 as a catalyst. Yield = 0.079g, 72%; Yellow Solid; MP = 190 °C; **IR (KBr) cm^{-1}**: 3211, 1643, 1253, 1168, 899, 772; **^{1}H NMR (400 MHz, DMSO-d$_6$, δ ppm)**: 0.90 (3H, t, *J* = 7.2 Hz, terminal -CH_3), 1.50 (4H, m, -CH_2), 1.74 (2H, m, -CH_2), 2.72 (3H, s, -CH_3), 4.05 (2H, t, *J* = 6.4 Hz, -OCH_2), 7.06 (2H, d, *J* = 8.8 Hz, Ar-H), 7.53 (1H, s, -N=CH-), 7.88 (2H, d, *J* = 8.8 Hz, Ar-H), 7.88 (1H, d, *J* = 8.8 Hz, Qui-H), 8.00 (1H, d, *J* = 8.8 Hz, Qui-H), 8.54 (1H, s, Qui-H), 8.69 (1H, s, Qui-H), 12.20 (1H, s, -NH); **^{13}C NMR (100 MHz, DMSO-d$_6$, δ ppm)**: 14.3 (-**C**H_3), 20.7 (-**C**H_3), 22.3 (-**C**H_2), 28.1 (-**C**H_2), 28.7 (-**C**H_2), 68.2 (-O**C**H_2), 101.0, 115.3, 115.5, 122.5, 122.6, 126.1, 130.0, 131.2, 134.0, 137.7, 150.5, 151.0, 155.2, 161.5; **Mass (TOF MS ES+)**: m/z 382.13 $(M+H)^+$, 384.13 $(MH+2)^+$ for M = $C_{22}H_{24}ClN_3O$.

[6-Bromo-4-{N'-(4-hexyloxybenzylidene)hydrazinyl}-2-methylquinoline] 44i.

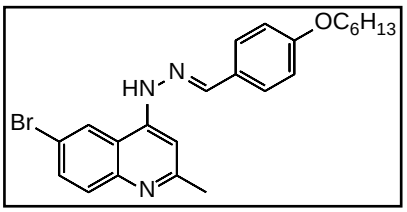

Compound **44i** was prepared by following the general procedure described above by reacting 4-hexyloxybenzaldehyde **34e** (0.04g, 0.22 mmol) in ethanol with 6-bromo-2-methyl-quinolin-4-yl-hydrazine **43a** (0.05g, 0.22 mmol) using H_2SO_4 as a catalyst. Yield = 0.072g, 72%; Yellow Solid; MP = 190 °C; **IR (KBr) cm^{-1}**: 3210, 2928, 1604, 1210, 1066, 892, 846; **^{1}H NMR (400 MHz, DMSO-d$_6$, δ ppm)**: 0.86 (3H, t, *J* = 7.2 Hz, terminal -CH_3), 1.29 (4H, d(b), -CH_2), 1.40 (2H, t(b), -CH_2), 1.72 (2H, m, -CH_2), 2.68 (3H, s, -CH_3), 4.02 (2H, t, *J* = 6.4 Hz, -OCH_2), 7.03 (2H, d, *J* = 8.8 Hz, Ar-H), 7.47 (1H, s, -N=CH-), 7.80 (3H, t, *J* = 8.8 Hz, Ar-H), 7.06 (1H, d, *J* = 8.8 Hz, Qui-H), 8.50 (1H, s, Qui-H), 8.78 (1H, s, Qui-H), 12.17 (1H, s, Ar-H); **^{13}C NMR (100 MHz, DMSO-d$_6$, δ ppm)**: 14.3 (-**C**H_3), 20.7 (-**C**H_3), 22.4 (-**C**H_2), 25.5 (-**C**H_2), 28.9 (-**C**H_2), 31.4 (-**C**H_2), 68.2 (-O**C**H_2), 101.0, 115.4, 115.9, 119.4, 122.5, 122.7, 125.6, 126.1, 130.0, 136.6, 150.5, 150.7, 161.5; **Mass (TOF MS ES+)**: m/z 440.02 $(M+H)^+$ for M = $C_{23}H_{26}BrN_3O$.

[6-Chloro-4-{N'-(4-hexyloxybenzylidene)hydrazinyl}-2-methylquinoline] 44j.

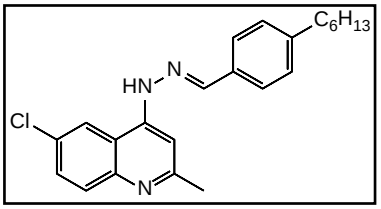

Compound **44j** was prepared by following the general procedure described above by reacting 4-hexyloxybenzaldehyde **34e** (0.05g, 0.28 mmol) in ethanol with 6-chloro-2-methyl-quinolin-4-yl-hydrazine **43b** (0.05g, 0.28 mmol) using H_2SO_4 as a catalyst. Yield = 0.086g, 76%; Yellow Solid; MP = 188 ^oC; **IR (KBr) cm^{-1}**: 3242, 2925, 1604, 1252, 1168, 846, 772; **^{1}H NMR (400 MHz, DMSO-d$_6$, δ ppm)**: 0.88 (3H, t, *J* = 7.2 Hz, terminal -CH_3), 1.38 (6H, m, -CH_2), 1.73 (2H, t(br), -CH_2), 2.72 (3H, s, -CH_3), 4.05 (2H, t, *J* = 6.4 Hz, -OCH_2), 7.06 (2H, d, *J* = 8.4 Hz, Ar-H), 7.53 (1H, s, -N=CH- proton), 7.86 (2H, d, *J* = 8.8 Hz, Ar-H), 7.89 (1H, d, *J* = 9.2 Hz, Ar-H), 7.99 (1H, d, *J* = 8.8 Hz, Qui-H), 8.54 (1H, s, Qui-H), 8.69 (1H, s, Qui-H), 12.20 (1H, s, -NH); **^{13}C NMR (100 MHz, DMSO-d$_6$, δ ppm)**: 14.3 (-**C**H_3), 20.5 (-**C**H_3), 22.4 (-**C**H_2), 25.5 (-**C**H_2), 28.9 (-**C**H_2), 31.4 (-**C**H_2), 68.2 (-O**C**H_2), 100.9, 115.3,, 122.2, 122.6, 126.0, 130.0, 131.4, 137.3, 150.7, 150.9, 155.0, 161.5; **Mass (TOF MS ES+)**: m/z 396.15 $(M+H)^+$, 398.14 $(MH+2)^+$ for M = $C_{22}H_{24}ClN_3O$.

[6-Bromo-2-methyl-4-{N'-(4-octyloxybenzylidene)hydrazinyl}quinoline] 44k.

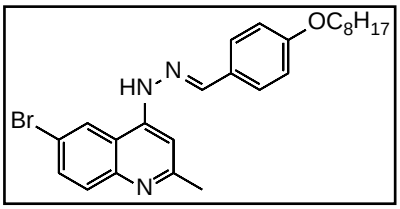

Compound **44k** was prepared by following the general procedure described above by reacting 4-octyloxybenzaldehyde **34f** (0.05g, 0.22 mmol) in ethanol with 6-bromo-2-methyl-quinolin-4-yl-hydrazine **43a** (0.053g, 0.22 mmol) using H_2SO_4 as a catalyst. Yield = 0.087g, 82%; Yellow Solid; MP = 186 ^oC; **IR (KBr) cm^{-1}**: 3244, 2926, 1604, 1250, 1066, 891; **^{1}H NMR (400 MHz, DMSO-d$_6$, δ ppm)**: 0.84 (3H, t, *J* = 7.2 Hz, terminal -CH_3), 1.25 (8H, d(b), -CH_2), 1.39 (2H, d(b), -CH_2), 1.68-1.74 (2H, m, -CH_2), 2.67 (3H, s, -CH_3), 4.02 (2H, t, *J* = 6.4 Hz, -OCH_2), 7.03 (2H, d, *J* = 8.8 Hz, Ar-H), 7.45 (1H, s, -N=CH-), 7.79 (3H, t(b), *J* = 8.8 Hz, Ar-H), 8.05 (1H, d, *J* = 8.8 Hz, Qui-H), 8.49 (1H, s, Qui-H), 8.76 (1H, s, Qui-H), 12.17 (1H, s, -NH); **^{13}C NMR (100 MHz, DMSO-d$_6$, δ ppm)**: 14.3 (-**C**H_3), 20.4 (-**C**H_3), 22.5 (-**C**H_2), 25.8 (-**C**H_2), 28.9 (-**C**H_2), 29.0 (-**C**H_2), 29.1 (-**C**H_2), 31.6 (-**C**H_2), 68.1 (-O**C**H_2), 100.4, 115.4, 115.9, 119.7, 122.3, 126.0, 130.0, 136.7, 137.6, 138.0, 150.9, 155.1, 156.5161.4 ; **Mass (TOF MS ES+)**: m/z 468.16 $(M+H)^+$, 470.16 $(MH+2)^+$ for M = $C_{25}H_{30}ClN_3O$.

[6-Chloro-2-methyl-4-{N'-(4-octyloxybenzylidene)hydrazinyl}quinoline] 44l.

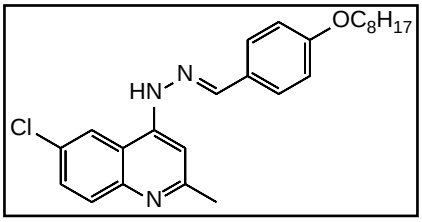

Compound 44**l** was prepared by following the general procedure described above by reacting 4-octyloxybenzaldehyde **34f** (0.06g, 0.28 mmol) in ethanol with 6-chloro-2-methyl-quinolin-4-yl-hydrazine **43b** (0.05g, 0.28 mmol) using H_2SO_4 as a catalyst. Yield = 0.098g, 79%; Yellow Solid; MP = 182 °C; **IR (KBr) cm^{-1}**: 3242, 2925, 1641, 1247, 1048, 897; **^{1}H NMR (400 MHz, DMSO-d$_6$, δ ppm)**: 0.84 (3H, t, *J* = 7.2 Hz, terminal -CH_3), 1.25 (8H, d(b), -CH_2), 1.39 (2H, d(b), -CH_2), 1.70 (2H, m, -CH_2), 2.69 (3H, s, -CH_3), 4.02 (2H, t, *J* = 6.4 Hz, -OCH_2), 7.02 (2H, d, *J* = 8.8 Hz, Ar-H), 7.46 (1H, s, -N=CH-), 7.80 (2H, d, *J* = 8.8 Hz, Ar-H), 7.86 (1H, d, *J* = 9.2 Hz, Qui-H), 7.97 (1H, d, *J* = 1.6 Hz, Qui-H), 8.50 (1H, s, Qui-H), 8.63 (1H, s, Qui-H), 12.17 (1H, s, Ar-H); **^{13}C NMR (100 MHz, DMSO-d$_6$, δ ppm)**: 14.3 (-**C**H_3), 20.4 (-**C**H_3), 22.5 (-**C**H_2), 25.9 (-**C**H_2), 28.9 (-**C**H_2), 29.0 (-**C**H_2), 29.1 (-**C**H_2), 31.6 (-**C**H_2), 68.2 (-O**C**H_2), 100.9, 115.3, 122.0, 122.5, 126.0, 130.0, 131.4, 134.1, 137.2, 150.7, 150.9, 154.9, 161.5; **Mass (TOF MS ES+)**: m/z 424.21 $(M+H)^+$, 426.47 $(MH+2)^+$ for M = $C_{25}H_{30}ClN_3O$.

4-[N'-{3,4-Bis-octyloxybenzylidene}hydrazinyl]-6-bromo-2-methylquinoline 44m.

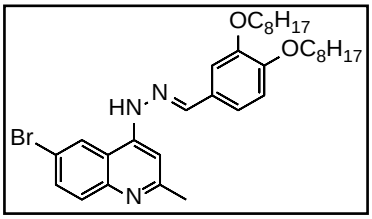

Compound **44m** was prepared by following the general procedure described above by reacting 3,4-dioctyloxybenzaldehyde **37** (0.083g, 0.22 mmol) in ethanol with 6-bromo-2-methyl-quinolin-4-yl-hydrazine **43a** (0.05g, 0.22 mmol) using H_2SO_4 as a catalyst. Yield = 0.106g, 78%; Yellow Solid; MP = 184 °C; **IR (KBr) cm^{-1}**: 3244, 2949, 1604, 1270, 1050, 959; **^{1}H NMR (400 MHz, DMSO-d$_6$, δ ppm)**: 0.85 (6H, t, *J* = 7.2 Hz, terminal -CH_3), 1.26 (16H, d(b), -CH_2), 1.46 (4H, d(b), -CH_2), 1.74 (4H, m, -CH_2), 2.66 (3H, s, -CH_3), 4.01 (2H, t, *J* = 6.4 Hz, -OCH_2), 4.06 (2H, t, *J* = 6.4 Hz, -OCH_2), 7.05 (1H, d, *J* = 8.4 Hz, Ar-H), 7.34 (1H, d, *J* = 8.0 Hz, Ar-H), 7.42 (1H, s, Ar-H), 7.46 (1H, s, -N=CH-), 7.77 (1H, d, *J* = 9.2 Hz, Qui-H), 8.01 (1H, d, *J* = 8.8 Hz, Qui-H), 8.45 (1H, s, Qui-H), 8.76 (1H, s, Qui-H), 11.97 (1H, s, -NH); **^{13}C NMR (100 MHz, DMSO-d$_6$, δ ppm)**: 14.3 (-**C**H_3), 20.6 (-**C**H_3), 22.5 (-**C**H_2), 26.0 (-**C**H_2), 26.1 (-**C**H_2), 29.24 (-**C**H_2), 29.26 (-**C**H_2),29.3 (-**C**H_2), 31.7 (-**C**H_2), 69.1 (-O**C**H_2), 101.0, 111.8, 113.4, 115.4, 122.2, 122.6, 126.3, 131.3,

134.1, 137.3, 149.2, 151.1, 155.0 ; **Mass (TOF MS ES+)**: m/z 596.29 $(M+H)^+$, 598.28 $(MH+2)^+$calculated for M = $C_{33}H_{46}BrN_3O_2$.

4-[N'-{3,4-Bis-octyloxybenzylidene}hydrazinyl]-6-chloro-2-methylquinoline 44n.

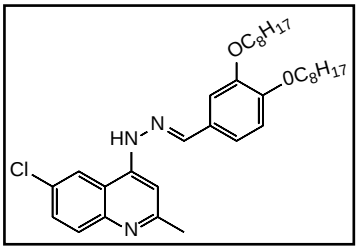

Compound **44n** was prepared by following the general procedure described above by reacting 3,4-dioctyloxybenzaldehyde **37** (0.10g, 0.28 mmol) in ethanol with 6-chloro-2-methyl-quinolin-4-yl-hydrazine **43b** (0.05g, 0.28 mmol) using H_2SO_4 as a catalyst. Yield = 0.112g, 71%; Yellow Solid; MP = 182 °C; **IR (KBr) cm^{-1}**: 3244, 2926, 1253, 1066, 891; **^{1}H NMR (400 MHz, DMSO-d$_6$, δ ppm)**: 0.85 (6H, t, *J* = 7.2 Hz, terminal -CH_3), 1.30 (16H, m, -CH_2), 1.45 (4H, t(b), -CH_2), 1.74 (4H, m, -CH_2), 2.72 (3H, s, -CH_3), 4.03 (2H, t, *J* = 6.4 Hz, -OCH_2), 4.06 (2H, t, *J* = 6.4 Hz, -OCH_2), 7.06 (1H, d, *J* = 8.4 Hz, Ar-H), 7.37 (1H, d, *J* = 8.4 Hz, Ar-H), 7.49 (1H, s, -N=CH), 7.50 (1H, d, *J* = 6.0 Hz, Ar-H), 7.89 (1H, d, *J* = 8.8 Hz, Qui-H), 7.99 (1H, d, *J* = 9.2 Hz, Qui-H), 8.50 (1H, s, Qui-H), 8.69 (1H, s, Qui-H), 12.20 (1H, s, -NH); **^{13}C NMR (100 MHz, DMSO-d$_6$, δ ppm)**: 14.3 (-**C**H_3), 20.6 (-**C**H_3), 22.5 (-**C**H_2), 26.0 (-**C**H_2), 26.1 (-**C**H_2), 29.24 (-**C**H_2), 29.26 (-**C**H_2),29.3 (-**C**H_2), 31.7 (-**C**H_2), 69.1 (-O**C**H_2), 101.0, 111.8, 113.4, 115.4, 122.2, 122.6, 126.3, 131.3, 134.1, 137.3, 149.2, 151.1, 155.0 ; **Mass (TOF MS ES+)**: m/z 552.33 $(M+H)^+$, 554.34 $(MH+2)^+$ for M = $C_{33}H_{46}ClN_3O_2$.

6-Bromo-2-methyl-4-[N'-{3,4,5-tris-octyloxybenzylidene}hydrazinyl]quinoline 44o.

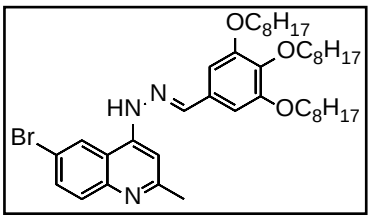

Compound **44o** was prepared by following the general procedure described above by reacting 3,4,5-trioctyloxybenzaldehyde **39** (0.11g, 0.22 mmol) in ethanol with 6-bromo-2-methyl-quinolin-4-yl-hydrazine **43a** (0.05g, 0.22 mmol) using H_2SO_4 as a catalyst. Yield = 0.122g, 74%; Yellow Solid; MP = 180 °C; **IR (KBr) cm^{-1}**: 3247, 2923, 1606, 1206, 1117, 892; **^{1}H NMR (400 MHz, DMSO-d$_6$, δ ppm)**: 0.85 (9H, t, *J* = 7.2 Hz, terminal -CH_3), 1.27 (26H, s(b), -CH_2), 1.55 (6H, d(b), -CH_2), 1.73 (4H, m, -CH_2), 2.73 (3H, s, -CH_3), 3.91 (6H, t, *J* = 6.4 Hz, -OCH_2), 7.12 (2H, s, Ar-H), 7.51 (1H, s, -N=CH), 7.83 (1H, d, *J* = 9.2 Hz, Qui-H), 7.11 (1H, d, *J* = 9.2 Hz, Qui-H), 8.49 (1H, s, Qui-H), 8.83 (1H, s, Qui-H), 12.25 (1H, s, -NH); **^{13}C NMR (100 MHz, DMSO-d$_6$, δ ppm)**: 14.3 (-**C**H_3), 20.6 (-**C**H_3), 22.5 (-**C**H_2),

26.0 (-$\mathbf{C}H_2$), 26.1 (-$\mathbf{C}H_2$), 29.24 (-$\mathbf{C}H_2$), 29.26 (-$\mathbf{C}H_2$),29.3 (-$\mathbf{C}H_2$), 31.7 (-$\mathbf{C}H_2$), 68.4 (-O$\mathbf{C}H_2$), 101.2, 107.0, 119.7, 122.3, 122.34, 127.1, 129.2, 137.6, 140.6, 151.4, 153.4, 155.6; **Mass (TOF MS ES+)**: m/z 724.34 $(M+H)^+$, 726.34 $(MH+2)^+$ for M = $C_{41}H_{62}ClN_3O_3$.

6-Chloro-2-methyl-4-[N'-{3,4,5-tris-octyloxybenzylidene}hydrazinyl]quinoline 44p.

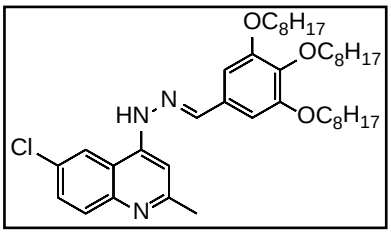

Compound **44p** was prepared by following the general procedure described above by reacting 3,4,5-trioctyloxybenzaldehyde **39** (0.14g, 0.28 mmol) in ethanol with 6-chloro-2-methyl-quinolin-4-yl-hydrazine **43b** (0.05g, 0.28 mmol) using H_2SO_4 as a catalyst. Yield = 0.141g, 72%; Yellow Solid; MP = 178 °C; **IR (KBr) cm^{-1}**: 2924, 1644, 1206, 1047, 892; **^{1}H NMR (400 MHz, DMSO-d$_6$, δ ppm)**: 0.86 (9H, t, *J* = 7.2 Hz, terminal -CH_3), 1.27 (26H, s(b), -CH_2), 1.46 (6H, d(b), -CH_2), 1.70 (4H, m, -CH_2), 2.73 (3H, s, -CH_3), 3.91 (2H, t, *J* = 6.4 Hz, -OCH_2), 4.05 (4H, t, *J* = 6.0 Hz, -OCH_2), 7.01 (2H, s, Ar-H), 7.49 (1H, s, -N=CH-), 7.90 (1H, d, *J* = 8.8 Hz, Qui-H), 8.00 (1H, d, *J* = 9.2 Hz, Qui-H), 8.48 (1H, s, Qui-H), 8.68 (1H, s, Qui-H), 12.24 (1H, s, -NH); **^{13}C NMR (100 MHz, DMSO-d$_6$, δ ppm)**: 14.3 (-$\mathbf{C}H_3$), 20.6 (-$\mathbf{C}H_3$), 22.5 (-$\mathbf{C}H_2$), 26.0 (-$\mathbf{C}H_2$), 26.1 (-$\mathbf{C}H_2$), 29.24 (-$\mathbf{C}H_2$), 29.26 (-$\mathbf{C}H_2$),29.3 (-$\mathbf{C}H_2$), 31.7 (-$\mathbf{C}H_2$), 69.0 (-O$\mathbf{C}H_2$), 101.0, 106.6, 115.5, 122.3, 122.7, 128.8, 131.3, 134.2, 137.6, 140.4, 151.2, 153.4, 155.2; **Mass (TOF MS ES+)**: m/z 680.45 $(M+H)^+$, 682.45 $(MH+2)^+$ for M = $C_{41}H_{62}BrN_3O_3$.

[6-Bromo-2-methyl-4-{N'-(1-phenylethylidene)hydrazinyl}quinoline] 44q.

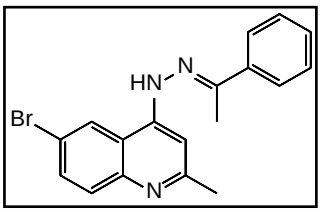

Compound **44q** was prepared by following the general procedure described above by reacting acetophenone **42** (0.02g, 0.22 mmol) in ethanol with 6-bromo-2-methyl-quinolin-4-yl-hydrazine **43b** (0.05g, 0.22 mmol) using H_2SO_4 as a catalyst. Yield = 0.045g, 56%; Yellow Solid; MP = 137 °C; **IR (KBr) cm^{-1}** : 3250, 3113, 2939, 1634, 850, 684; **^{1}H NMR : (400 MHz, CDCl$_3$, δ ppm)** : 2.62 (s, 3H, -CH_3), 2.74 (s, 3H, -CH_3), 7.50 (5H, m, Ar-H), 7.86 (1H, d, Ar-H), 8.03 (1H, d(b), Ar-H), 8.13 (1H, d, Qui-H), 8.99 (1H, s, Qui-H), 11.08 (1H, s, -NH); **^{13}CNMR : (100 MHz, CDCl$_3$, δ ppm)** : 15.7 (-$\mathbf{C}H_3$), 20.6 (-$\mathbf{C}H_3$), 101.9, 116.3, 119.5, 122.1, 126.4,

127.3, 129.0, 130.8, 136.9, 137.5, 137.6, 151.9, 155.7, 159.1; **EI-Mass**: (m/z) 353.03 for M = $C_{18}H_{16}ClN_3$.

6-Bromo-2-methyl-4-[N'-{1-(4-nitrophenyl)-ethylidene}hydrazinyl]quinoline 44r.

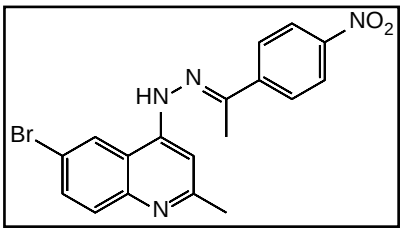

Compound **44r** was prepared by following the general procedure described above by reacting 4-nitro acetophenone **42** (0.03g, 0.22 mmol) in ethanol with 6-bromo-2-methyl-quinolin-4-yl-hydrazine **43b** (0.05g, 0.22 mmol) using H_2SO_4 as a catalyst. Yield = 0.076g, 83%; Yellow Solid; mp 143 ^oC; **IR (KBr) cm^{-1}**: 3078, 2916, 1597, 1067, 962, 590, 449; **^{1}H NMR : (400 MHz, $CDCl_3$, δ ppm)**: 2.62 (3H, s, -CH_3), 2.73 (3H, s, -CH_3), 7.55 (1H, s, Ar-H), 7.82 (1H, d, Ar-H), 8.11 (2H, d, Ar-H), 8.26 (4H, q, Qui-H), 8.95 (1H, s, Qui-H); **^{13}C NMR: (100 MHz, $CDCl_3$, δ ppm)**: 15.5 (-**C**H_3), 20.6 (-**C**H_3), 102.6, 116.5, 119.8, 122.1, 124.0, 126.5, 128.5, 136.9, 137.6, 143.6, 148.5, 151.9, 155.7; **EI-Mass**: (m/z) 398.03 for M = $C_{18}H_{15}BrN_4O_2$.

6-Bromo-2-methyl-4-[N'-{1-(4-butoxphenyl)-ethylidene}hydrazinyl]quinoline 44s.

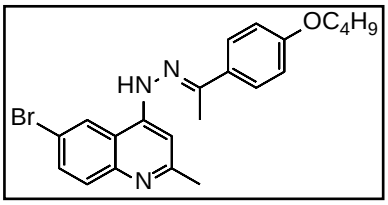

Compound **44s** was prepared by following the general procedure described above by reacting 4-butyloxy acetophenone **42a** (0.04g, 0.22 mmol) in ethanol with 6-bromo-2-methyl-quinolin-4-yl-hydrazine **43b** (0.05g, 0.22 mmol) using H_2SO_4 as a catalyst. Yield = 0.079g, 81%; Yellow Solid; mp 132 ^oC, **IR (KBr) cm^{-1}**: 3066, 2946, 1638, 1559, 1061, 890, 570; **^{1}H NMR : (400 MHz, $CDCl_3$, δ ppm)**: 0.93 (3H, t, *J* = 7.2 Hz, terminal-CH_3),1.42 (2H, m, -CH_2), 1.70 (2H, m, -CH_2), 2.54 (3H, s, -CH_3), 2.69 (3H, s, -CH_3), 4.02 (2H, t, -OCH_2), 7.01 (1H, d, Ar-H), 7.38 (1H, s, Ar-H), 8.80 (1H, d , Ar-H), 7.95 (2H, d, Ar-H), 8.08 (1H, d, Qui-H), 8.91 (1H, s, Qui-H); **^{13}CNMR : (100.61 MHz, $CDCl_3$, δ, ppm)**: 14.1 (-**C**H_3), 15.5 (-**C**H_3), 19.1 (-**C**H_3), 20.5, 31.0, 67.8, 101.4, 107.5, 114.8, 116.1, 119.5, 121.9, 126.3, 129.0, 129.6, 130.9, 136.8, 140.8, 151.6, 161.0; **EI-Mass** : (m/z) 425.08 for M = $C_{22}H_{24}BrN_3O$.

6-Bromo-2-methyl-4-[N'-{1-(4-hexyloxyphenyl)-ethylidene}hydrazinyl]quinoline 44t.

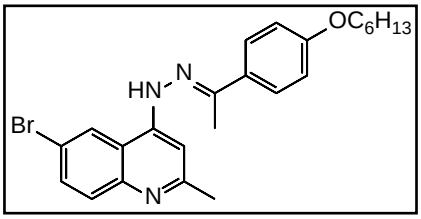

Compound **44t** was prepared by following the general procedure described above by reacting 4-hyxyloxy acetophenone **42b** (0.05g, 0.22 mmol) in ethanol with 6-bromo-2-methyl-quinolin-4-yl-hydrazine **43b** (0.05g, 0.22 mmol) using H_2SO_4 as a catalyst. Yield = 0.09g, 87%, Yellow Solid; mp 141 ^oC, **IR (KBr) cm^{-1}** : 2918, 1595, 1508, 1064, 798; **^{1}H NMR : (400 MHz, $CDCl_3$, δ ppm)**: 0.89 (3H, t (b), *J* = 7.2 Hz, terminal-CH_3), 1.31 (4H, d (b), -CH_2), 1.41 (2H, m, -CH_2), 1.74 (2H, m, -CH_2), 2.57 (3H, s, -CH_3), 2.72 (3H, s, -CH_3), 4.04 (2H, t, -OCH_2), 7.02 (2H, d, Ar-H), 7.42 (1H, s, Ar-H), 7.84 (1H, d , Ar-H), 7.98 (2H, d, Ar-H), 8.12 (1H, d, Qui-H), 8.96 (1H, s, Qui-H), 11.08 (1H, s, -NH); **^{13}CNMR : (100 MHz, $CDCl_3$, δ ppm)**: 14.4 (-**C**H_3), 15.5 (-**C**H_3), 20.6 (-**C**H_3), 22.5, 25.6, 29.0, 31.4, 68.1, 101.9, 105.2, 114.8, 116.3, 119.4, 122.1, 126.4, 129.0, 129.6, 131.8, 133.9, 136.8, 151.7, 161.0; **EI-Mass** : (m/z) 453.14 for M = $C_{24}H_{28}BrN_3O$.

6-Bromo-4-[N'-{1-(4-decylloxyphenyl)ethylidene}hydrazinyl]-2-methylquinoline 44u.

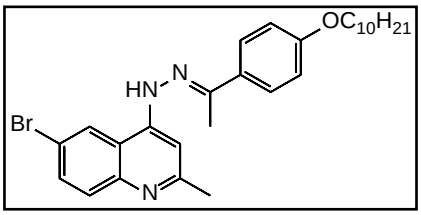

Compound **44u** was prepared by following the general procedure described above by reacting acetophenone **42c** (0.06g, 0.22 mmol) in ethanol with 6-bromo-2-methyl-quinolin-4-yl-hydrazine **43b** (0.05g, 0.22 mmol) using H_2SO_4 as a catalyst. Yield = 0.089g, 76%, Yellow Solid; mp 138 ^oC, **IR (KBr) cm^{-1}**: 3267, 2974, 1634, 1597, 1106, 765; **^{1}H NMR : (400 MHz, $CDCl_3$, δ ppm)**: 0.84 (3H, t (b), *J* = 7.2 Hz, terminal-CH_3), 1.26 (12H, d (b), -CH_2), 1.39 (2H, d (b), -CH_2), 1.71 (2H, m, -CH_2), 2.56 (3H, s, -CH_3), 2.71 (3H, s, -CH_3), 4.03 (2H, t, -OCH_2), 7.01 (2H, d, Ar-H), 7.41 (1H, s, Ar-H), 7.82 (1H, d, Ar-H), 7.97 (2H, d, Ar-H), 8.12 (1H, d, Qui-H), 8.94 (1H, s, Qui-H); **^{13}C NMR : (100 MHz, $CDCl_3$, δ ppm)**: 14.4 (-**C**H_3), 15.5 (-**C**H_3), 20.5 (-**C**H_3), 22.5, 25.9, 29.0, 29.1, 29.2, 29.3, 29.4, 31.7, 68.1, 114.8, 115.9, 116.3, 118.4, 122.0, 126.3, 129.0, 129.6, 130.4, 130.9, 135.3, 136.7, 151.6, 161.0; **EI-Mass** : (m/z) 509.20 for M = $C_{28}H_{36}BrN_3O$.

6.10 Spectral Data

Compound 44a

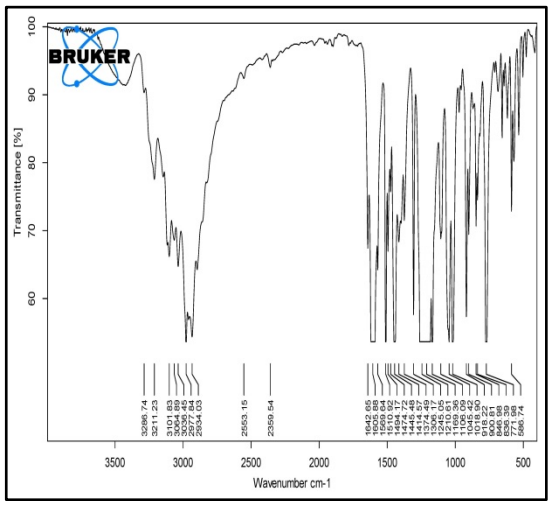

Spectrum 1. IR of compound 44a

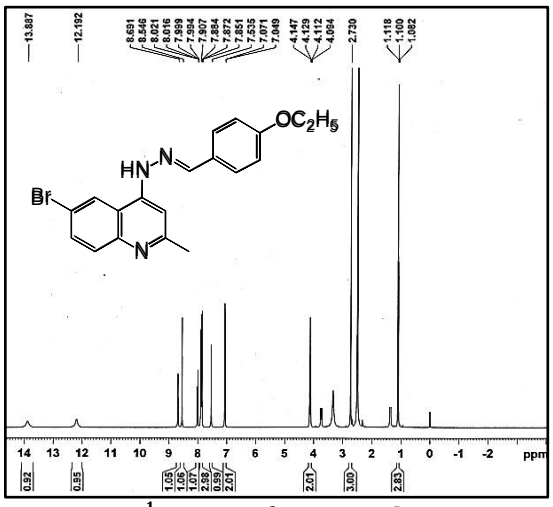

Spectrum 2. ^{1}H NMR of compound 44a

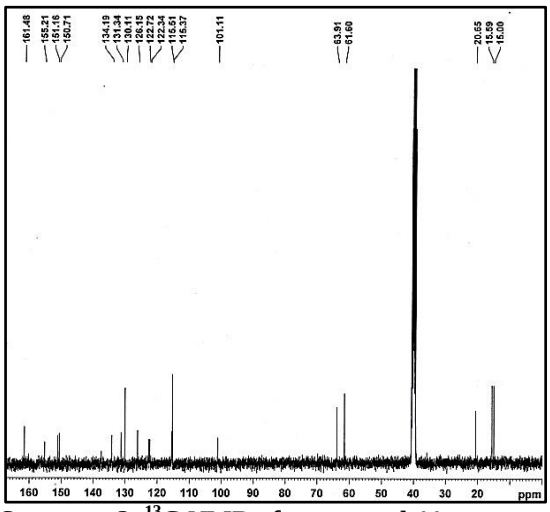

Spectrum 3. ^{13}C NMR of compound 44a

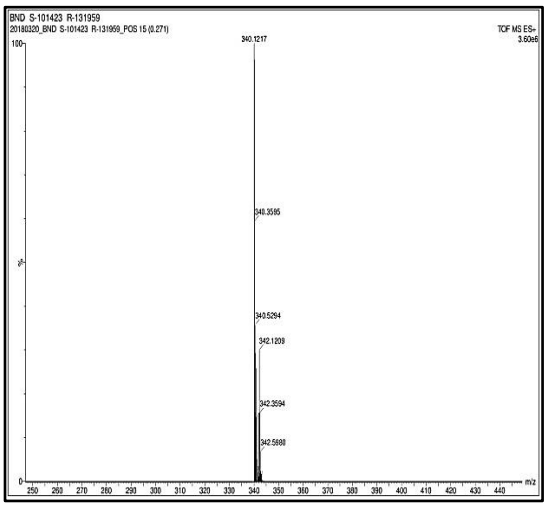

Spectrum 4. MASS of compound 44a

Compound 44b

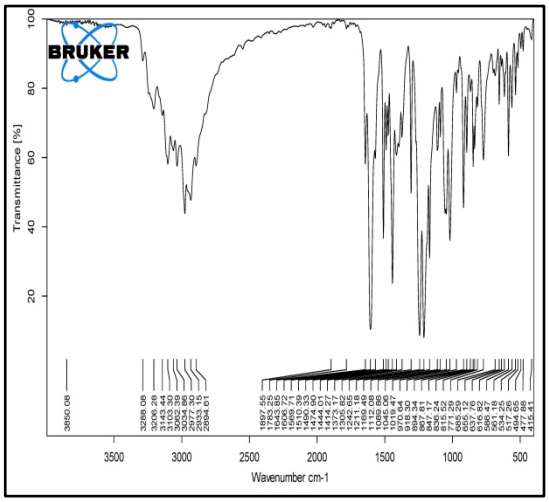

Spectrum 5. IR of compound 44b

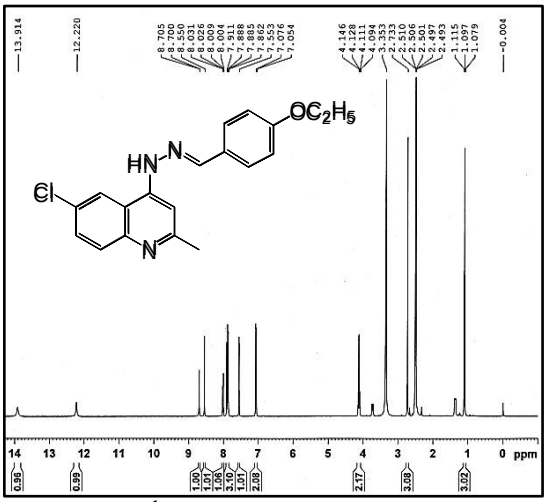

Spectrum 6. ^{1}H NMR of compound 44b

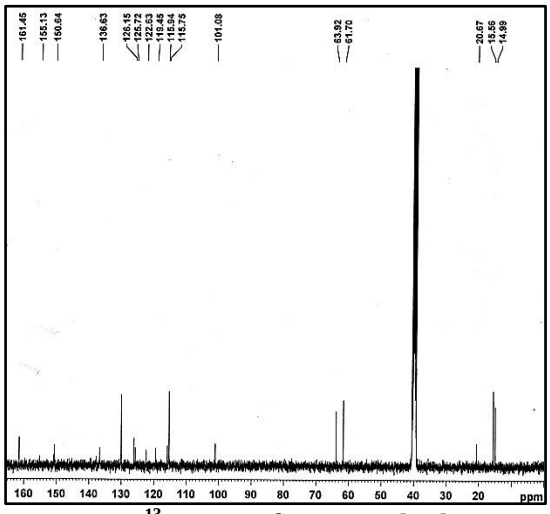

Spectrum 7. ^{13}C NMR of compound 44b

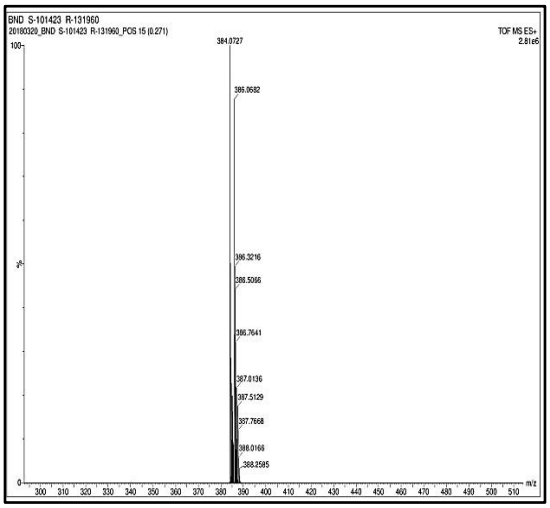

Spectrum 8. MASS of compound 44b

Compound 44c

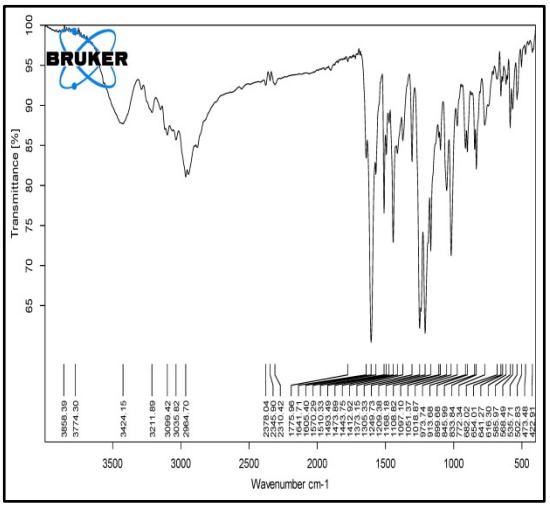

Spectrum 9. IR of compound 44c

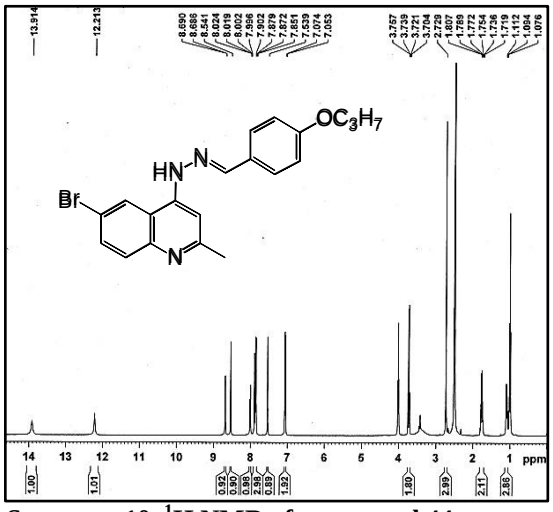

Spectrum 10. ^{1}H NMR of compound 44c

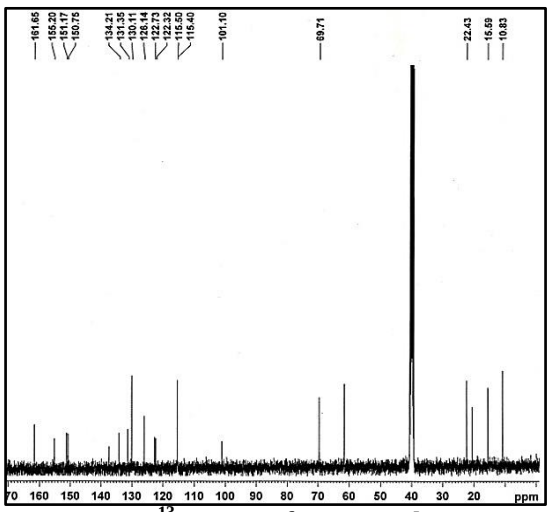

Spectrum 11. ^{13}C NMR of compound 44c

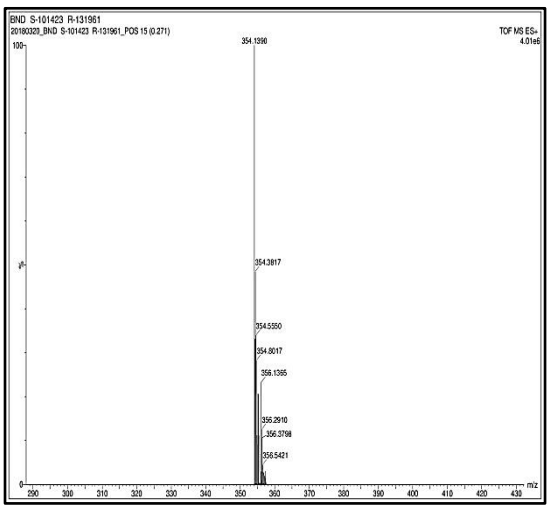

Spectrum 12. MASS of compound 44c

Compound 44d

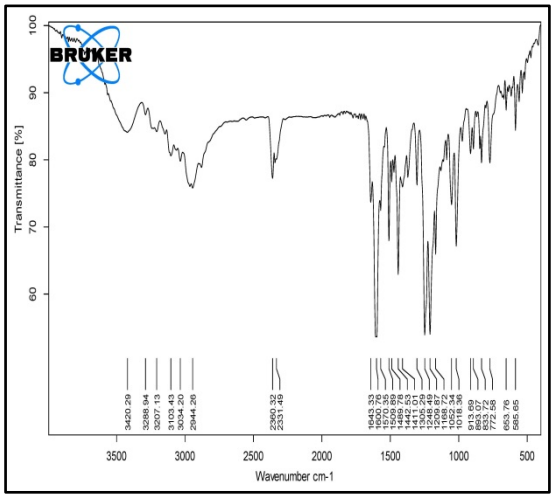

Spectrum 13. IR of compound 44d

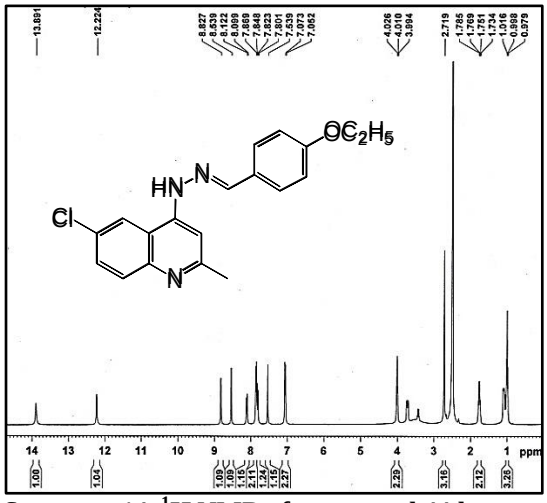

Spectrum 14. ^{1}H NMR of compound 44d

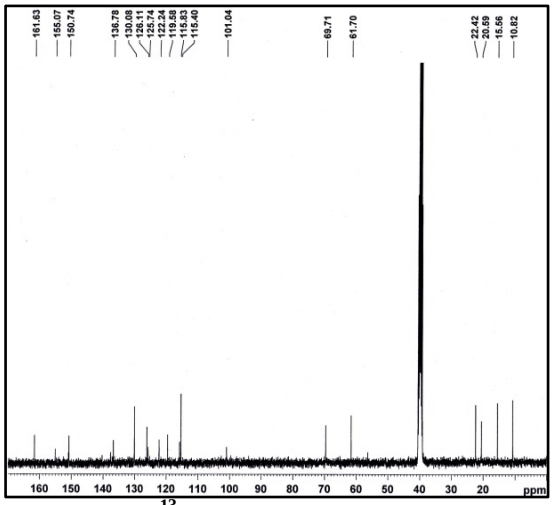

Spectrum 15. ^{13}C NMR of compound 44d

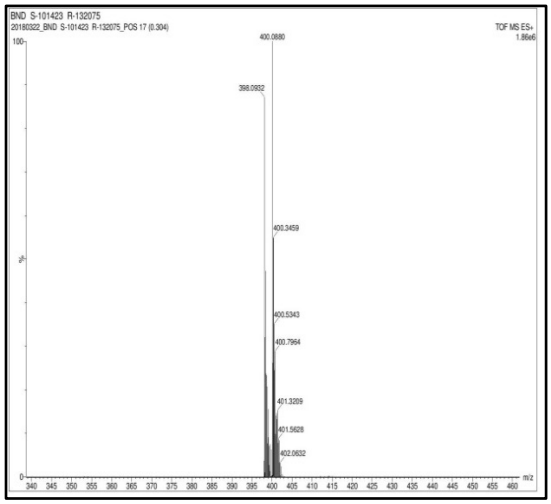

Spectrum 16. MASS of compound 44d

Compound 44e

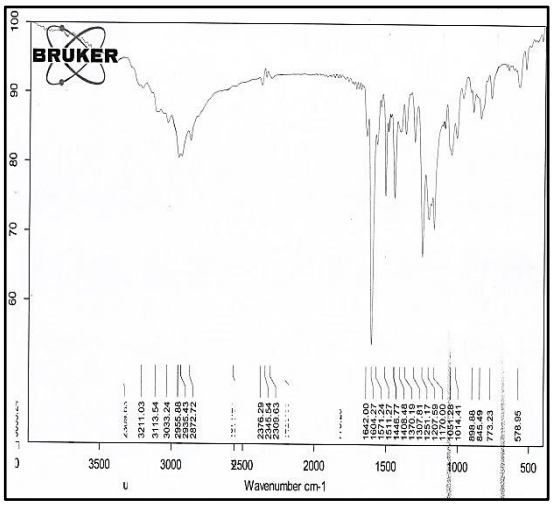

Spectrum 17. IR of compound 44e

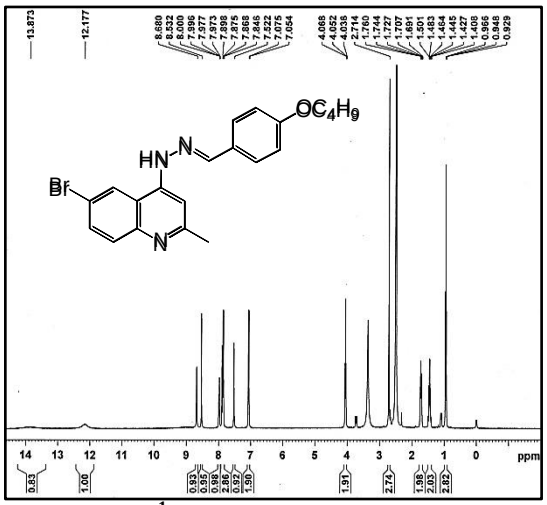

Spectrum 18. ^{1}H NMR of compound 44e

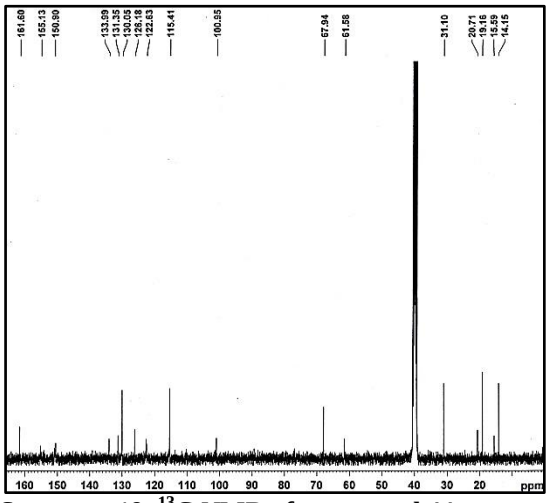

Spectrum 19. ^{13}C NMR of compound 44e

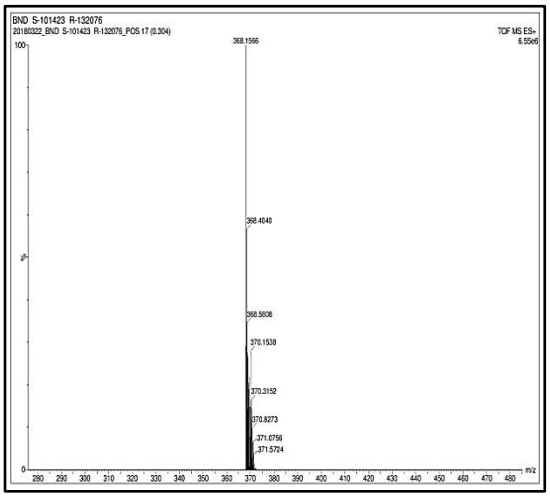

Spectrum 20. MASS of compound 44e

Compound 44f

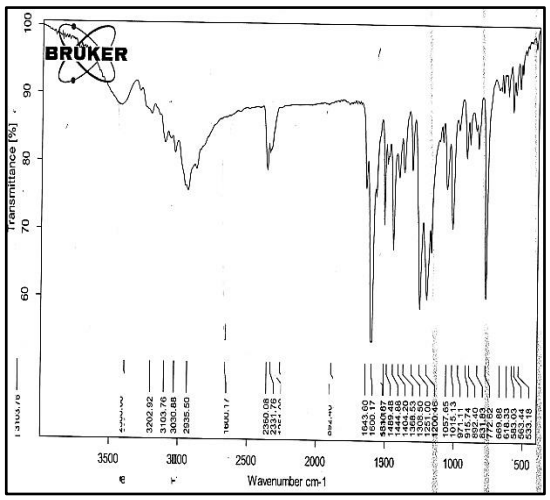

Spectrum 21. IR of compound 44f

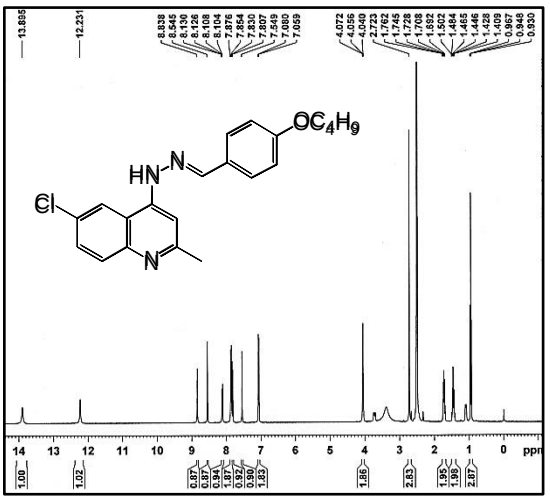

Spectrum 22. ^{1}H NMR of compound 44f

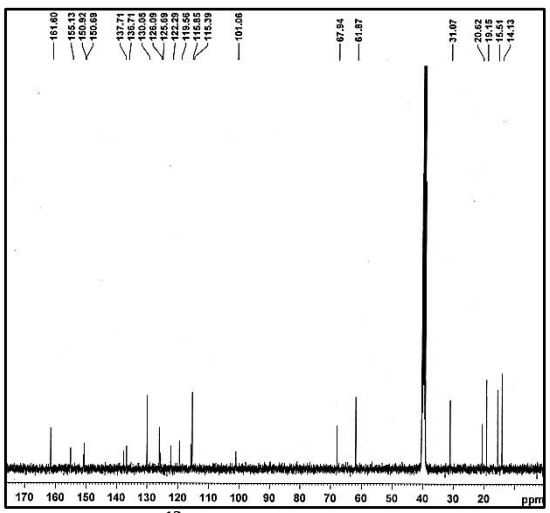

Spectrum 23. ^{13}C NMR of compound 44f

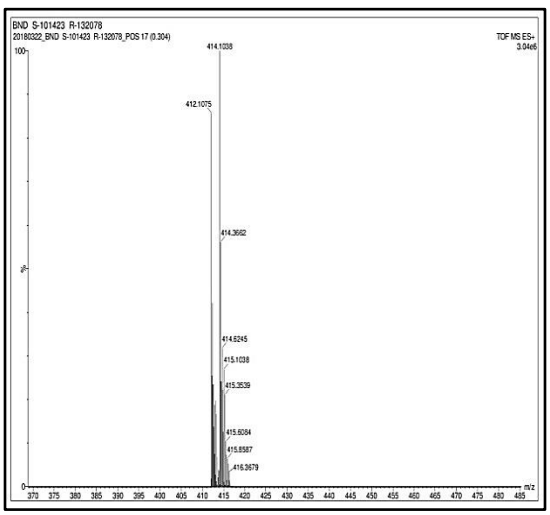

Spectrum 24. MASS of compound 44f

Compound 44g

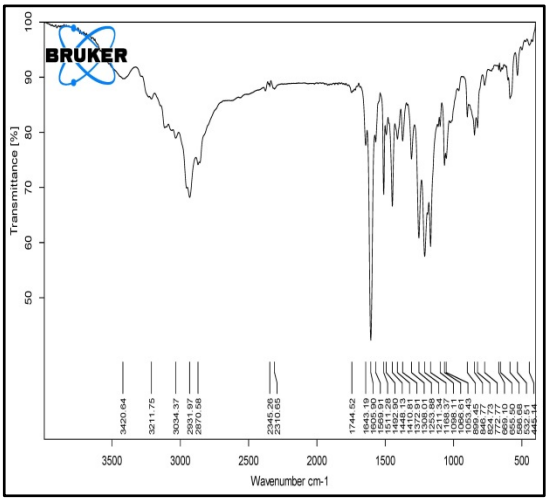

Spectrum 25. IR of compound 44g

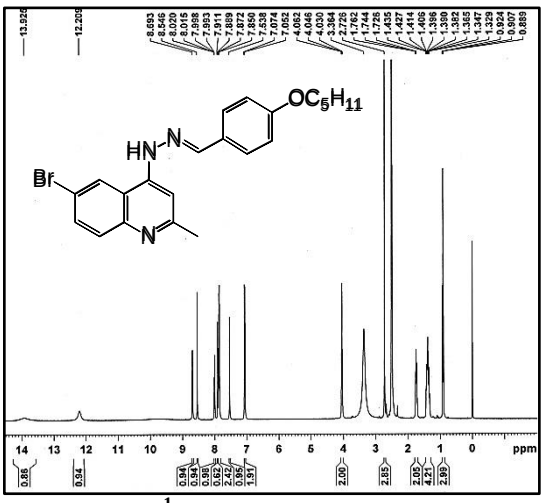

Spectrum 26. ^{1}H NMR of compound 44g

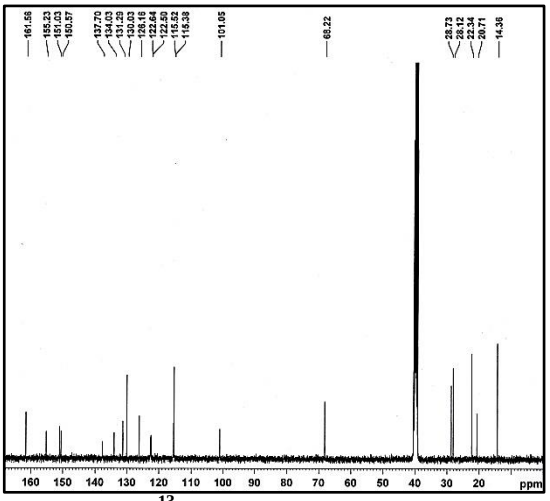

Spectrum 27. ^{13}C NMR of compound 44g

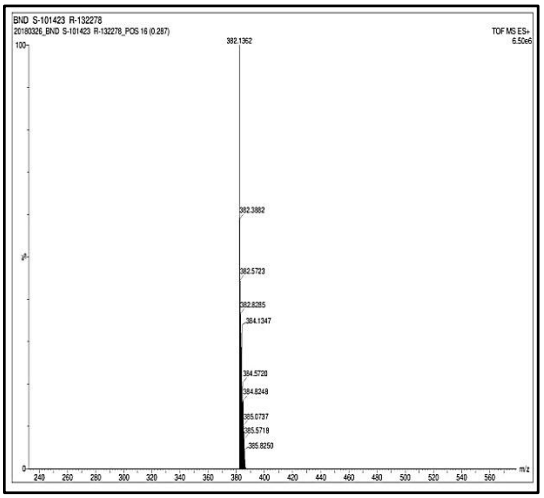

Spectrum 28. MASS of compound 44g

Compound 44h

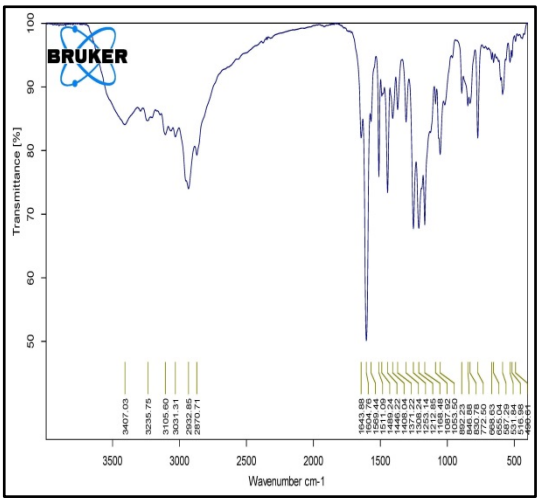

Spectrum 29. IR of compound 44h

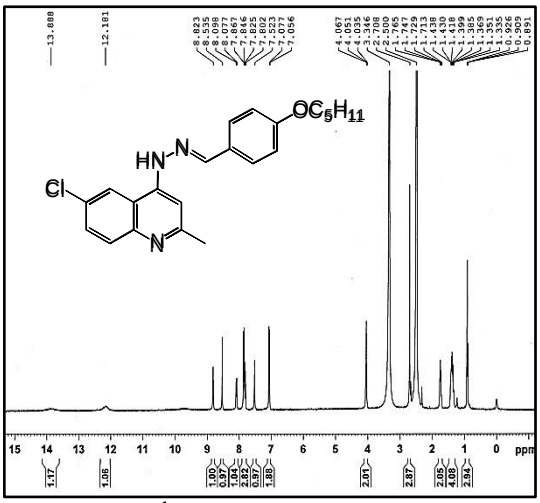

Spectrum 30. ^{1}H NMR of compound 44h

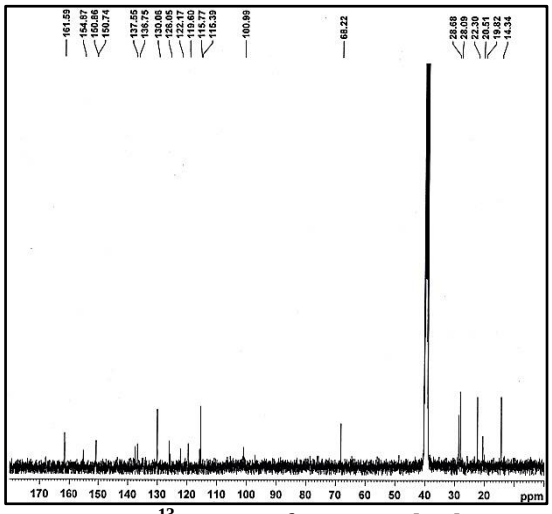

Spectrum 31. ^{13}C NMR of compound 44h

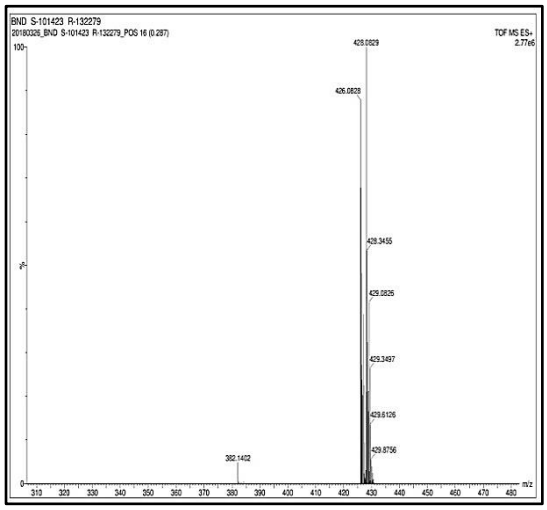

Spectrum 32. MASS of compound 44h

Compound 44i

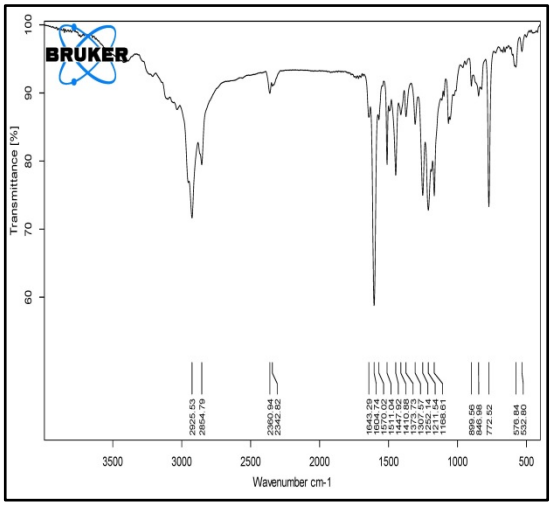

Spectrum 33. IR of compound 44i

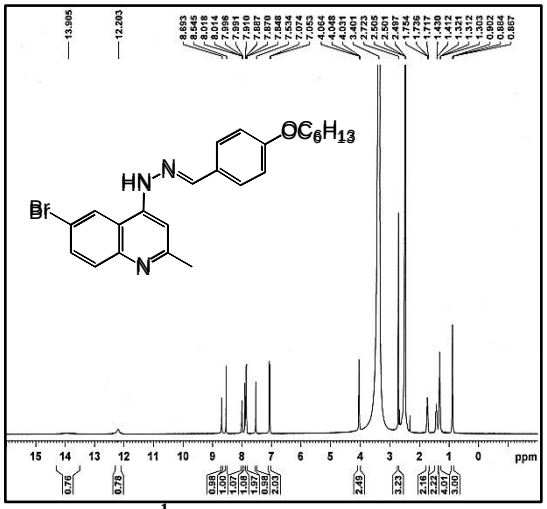

Spectrum 34. ^{1}H NMR of compound 44i

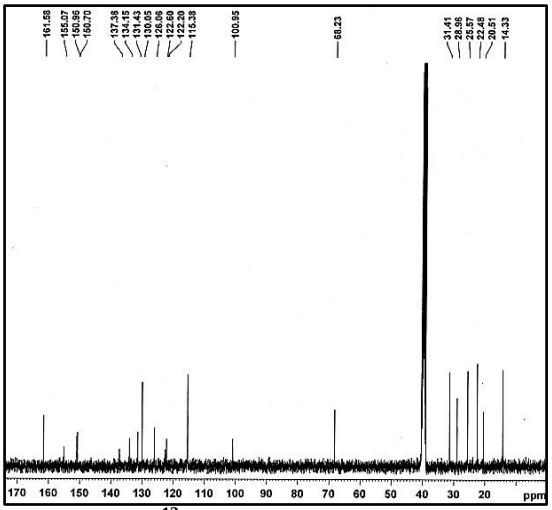

Spectrum 35. ^{13}C NMR of compound 44i

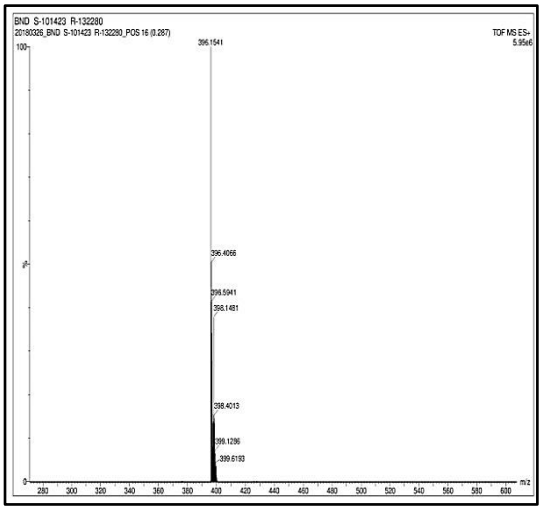

Spectrum 36. MASS of compound 44i

Compound 44j

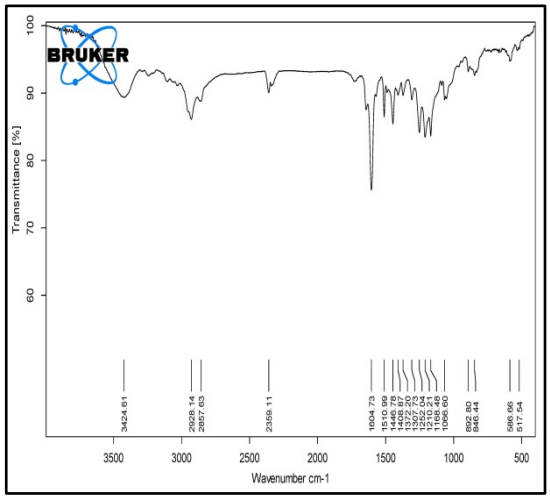

Spectrum 37. IR of compound 44j

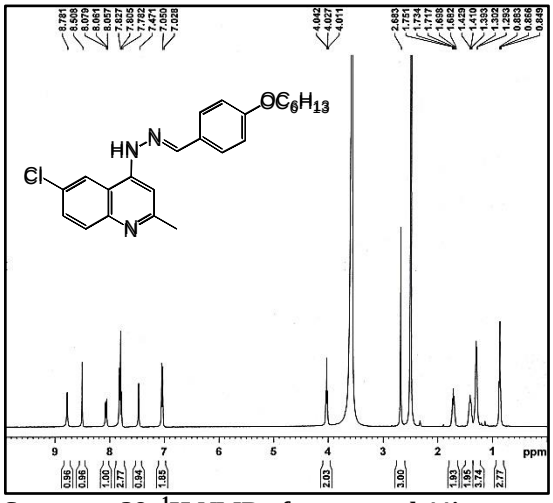

Spectrum 38. ^{1}H NMR of compound 44j

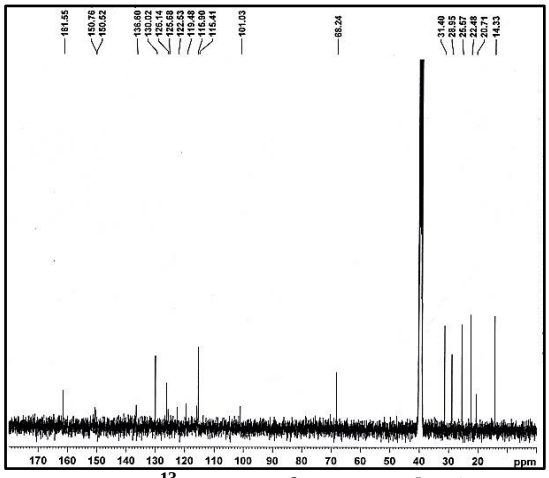

Spectrum 39. ^{13}C NMR of compound 44j

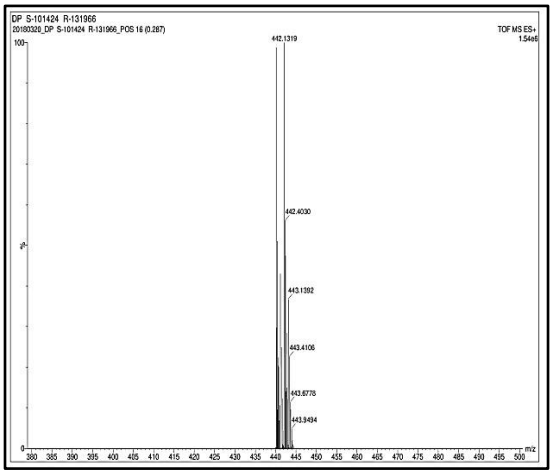

Spectrum 40. MASS of compound 44j

Compound 44k

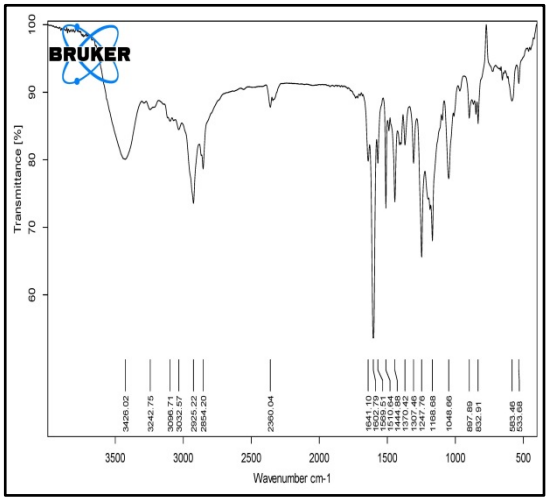

Spectrum 41. IR of compound 44k

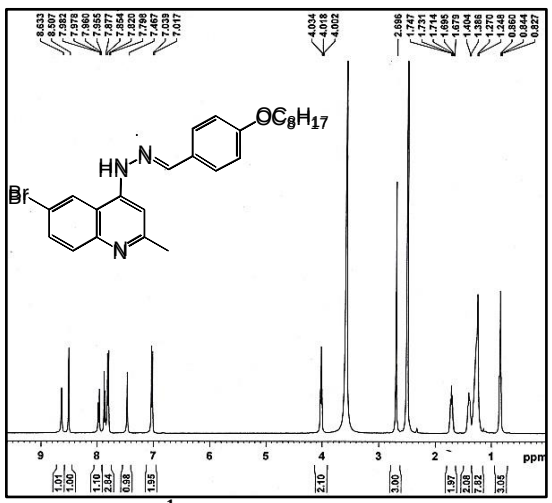

Spectrum 42. ^{1}H NMR of compound 44k

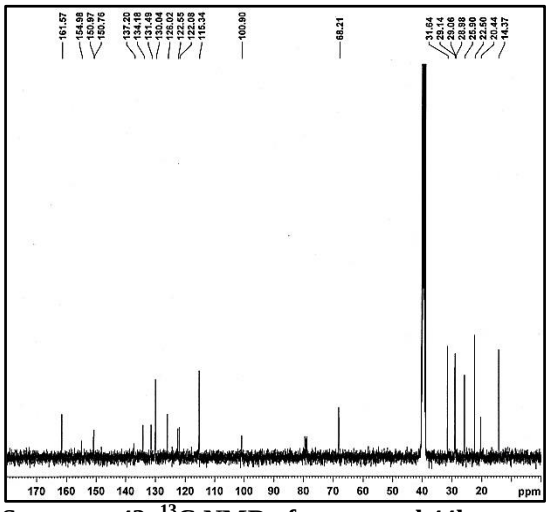

Spectrum 43. ^{13}C NMR of compound 44k

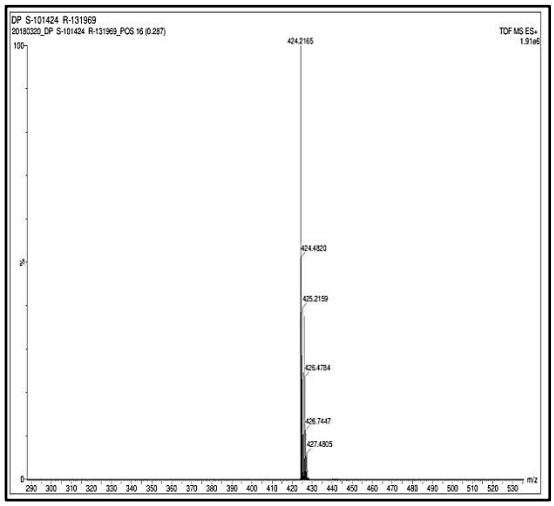

Spectrum 44. MASS of compound 44k

Compound 44l

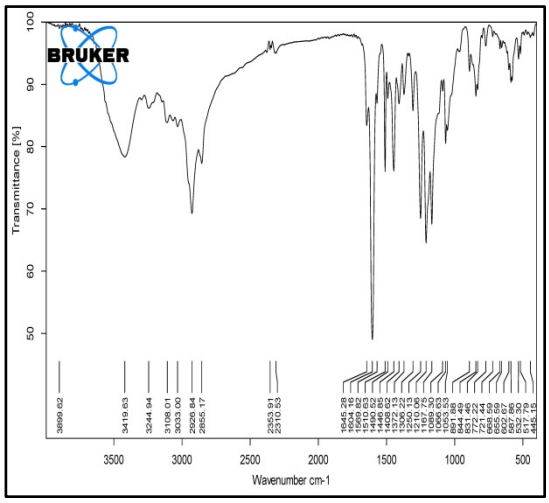

Spectrum 45. IR of compound 44l

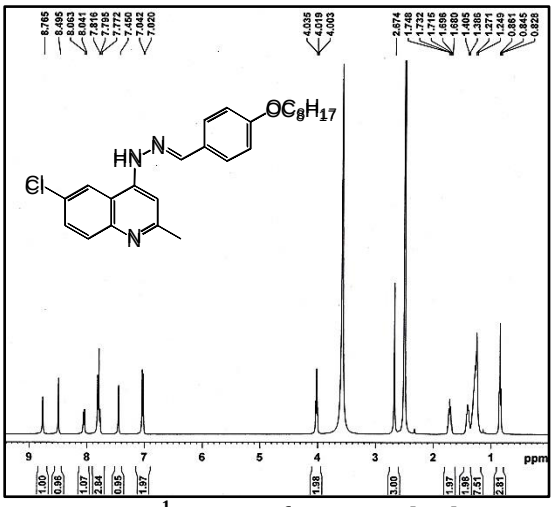

Spectrum 46. ^{1}H NMR of compound 44l

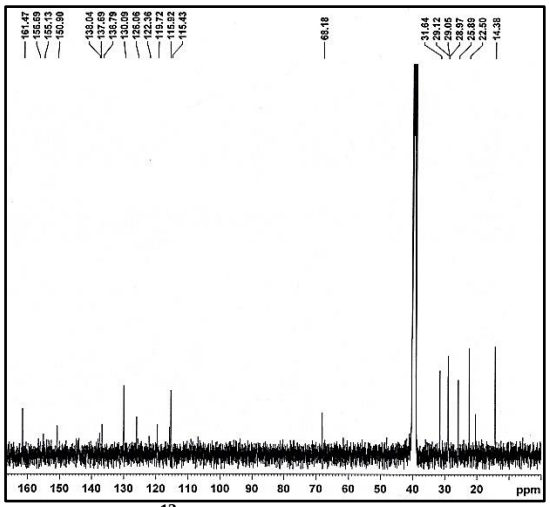

Spectrum 47. ^{13}C NMR of compound 44l

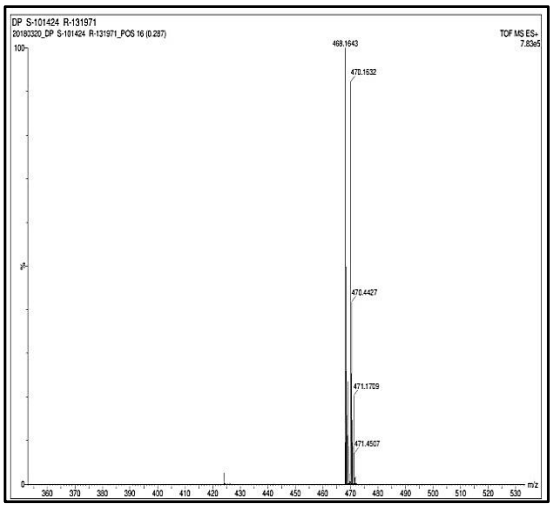

Spectrum 48. MASS of compound 44l

Compound 44m

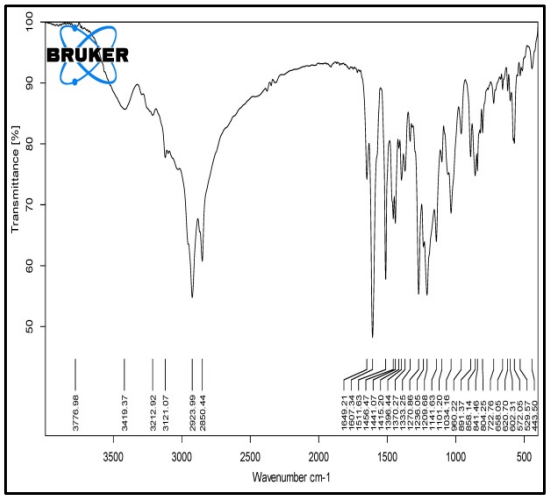

Spectrum 49. IR of compound 44m

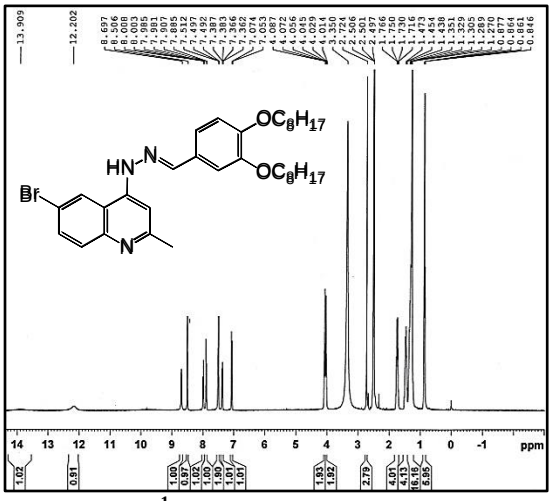

Spectrum 50. ^{1}H NMR of compound 44m

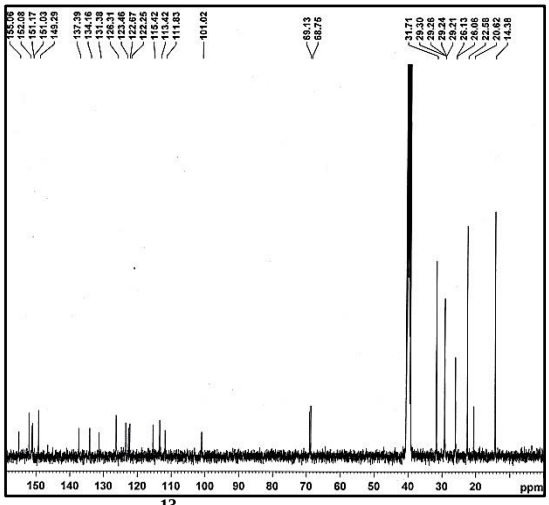

Spectrum 51. ^{13}C NMR of compound 44m

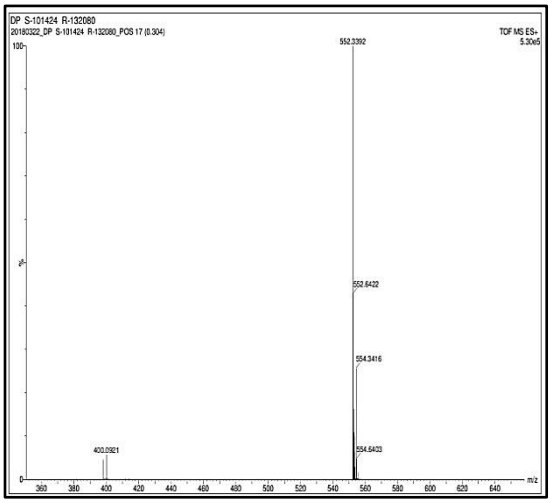

Spectrum 52. MASS of compound 44m

Compound 44n

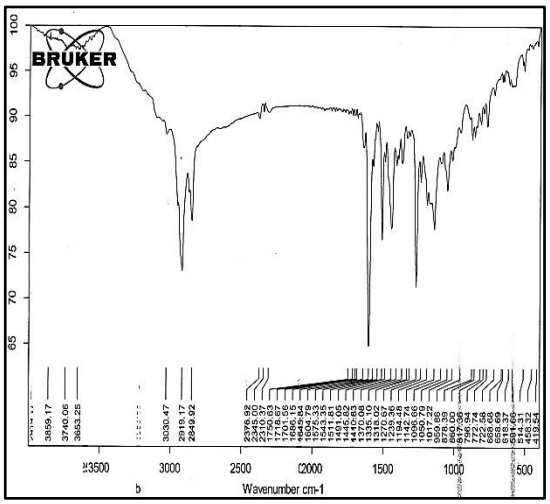

Spectrum 53. IR of compound 44n

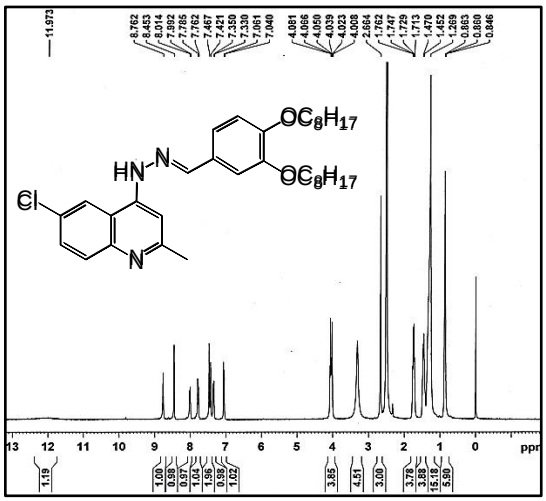

Spectrum 54. ^{1}H NMR of compound 44n

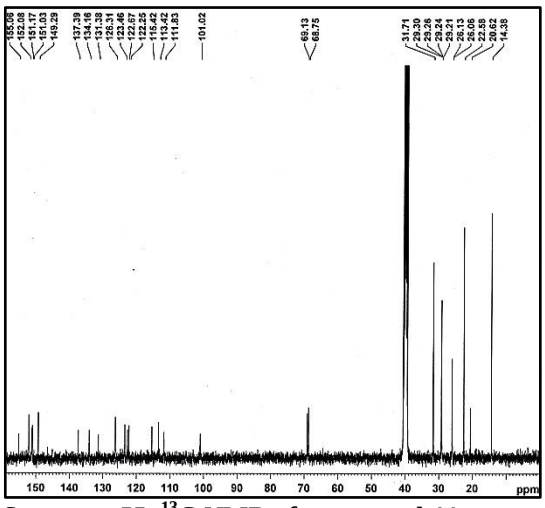

Spectrum 55. ^{13}C NMR of compound 44n

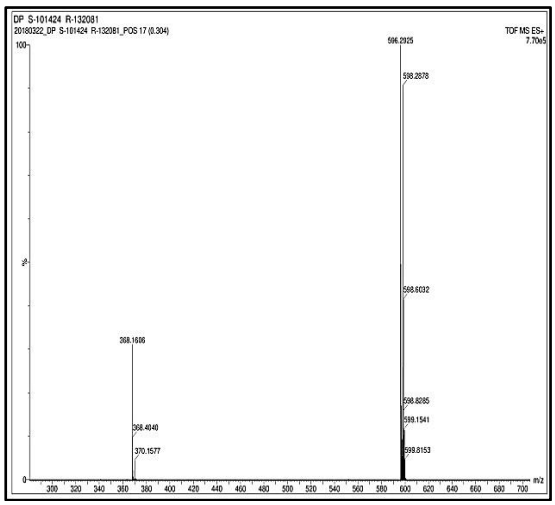

Spectrum 56. MASS of compound 44n

Compound 44o

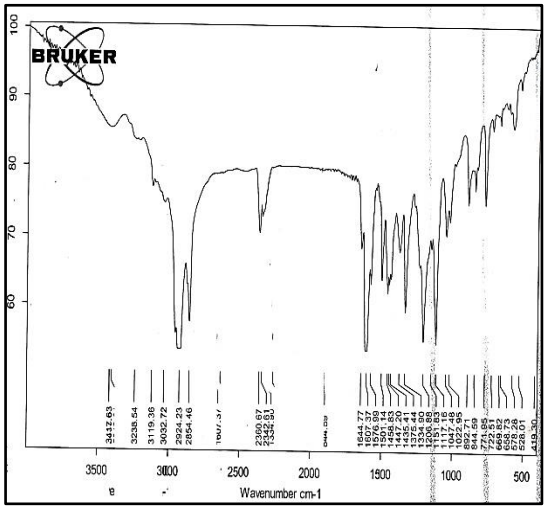

Spectrum 57. IR of compound 44o

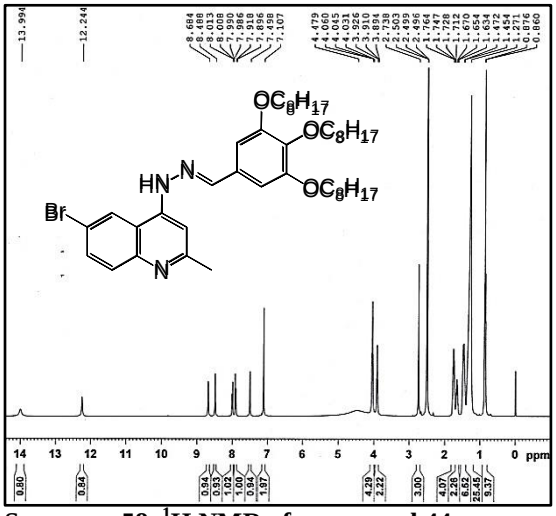

Spectrum 58. ^{1}H NMR of compound 44o

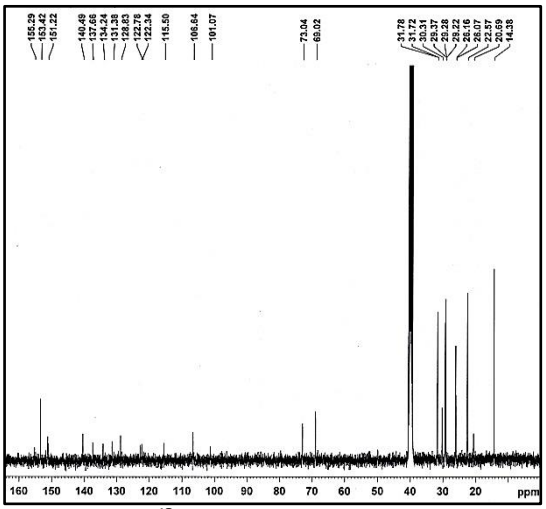

Spectrum 59. ^{13}C NMR of compound 44o

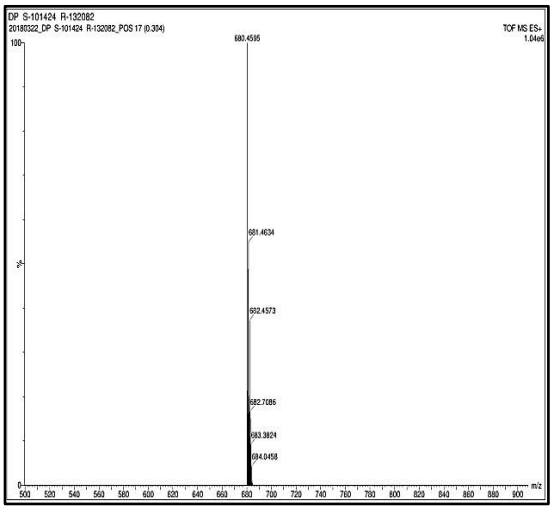

Spectrum 60. MASS of compound 44o

Compound 44p

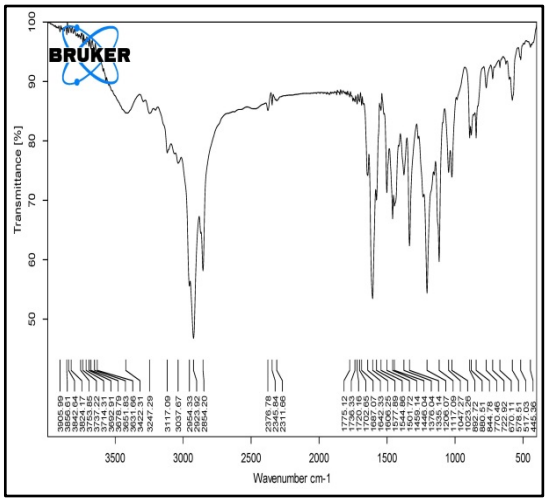

Spectrum 61. IR of compound 44p

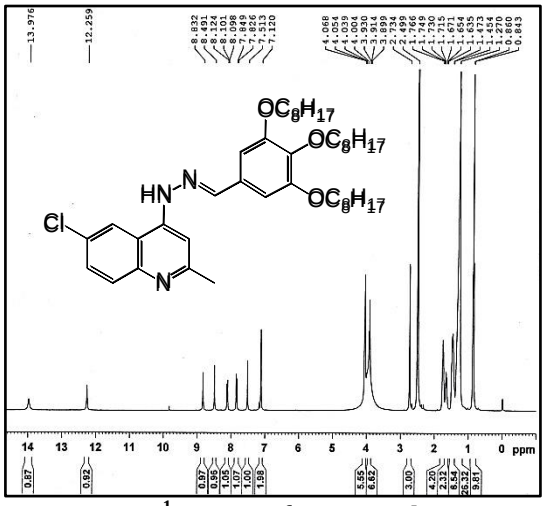

Spectrum 62. ^{1}H NMR of compound 44p

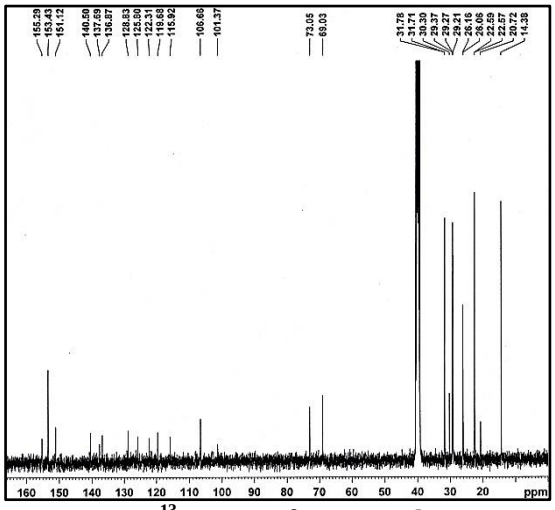

Spectrum 63. ^{13}C NMR of compound 44p

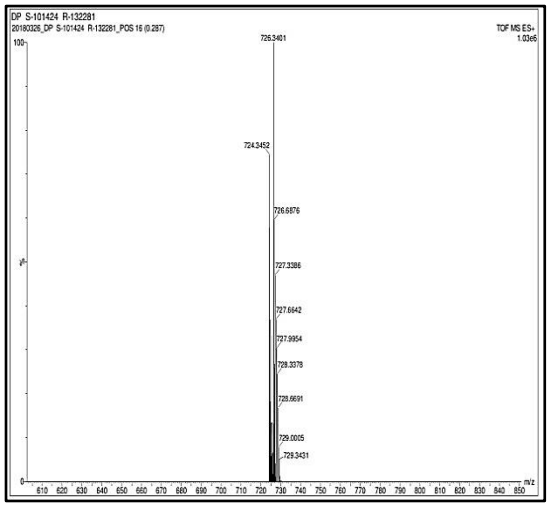

Spectrum 64. MASS of compound 44p

Compound 44q

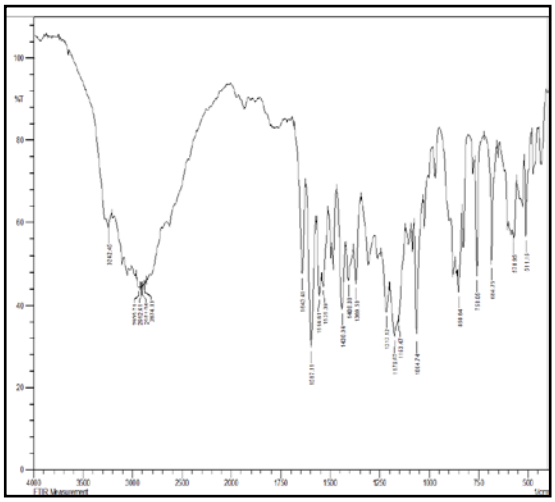

Spectrum 65. IR of compound 44q

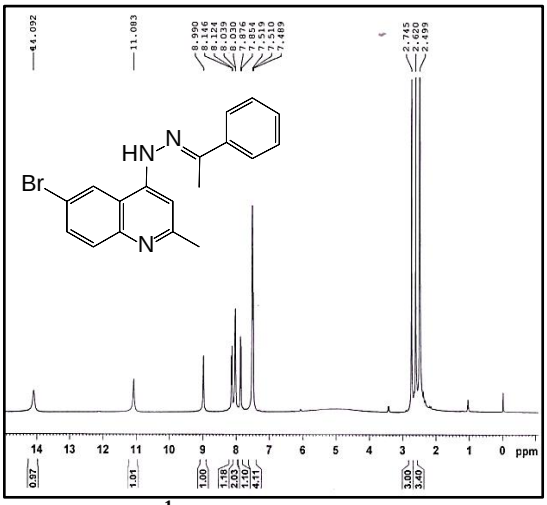

Spectrum 66. ^{1}H NMR of compound 44q

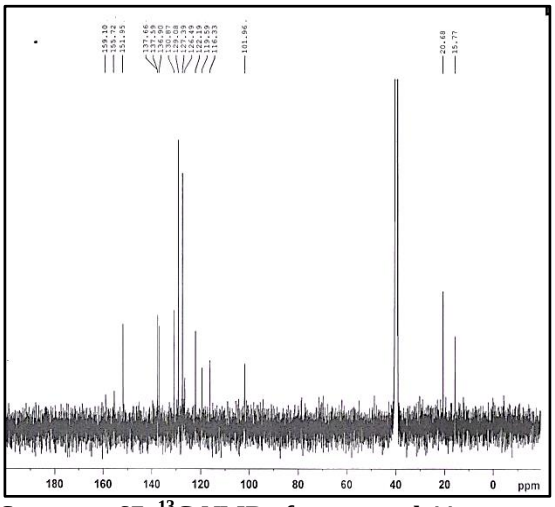

Spectrum 67. ^{13}C NMR of compound 44q

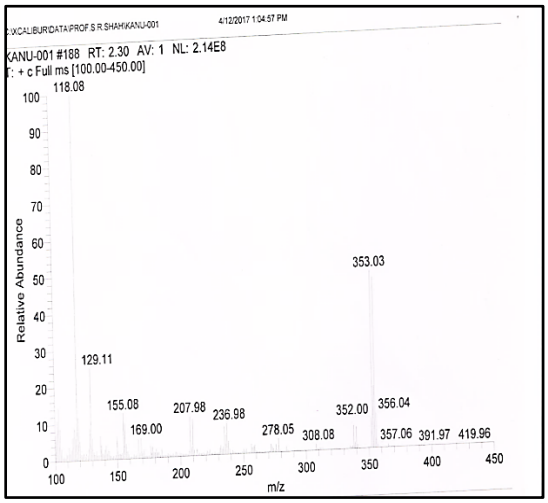

Spectrum 68. MASS of compound 44q

Compound 44r

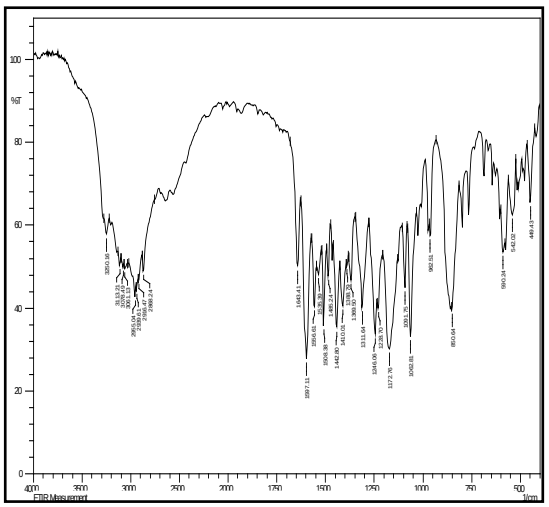

Spectrum 69. IR of compound 44r

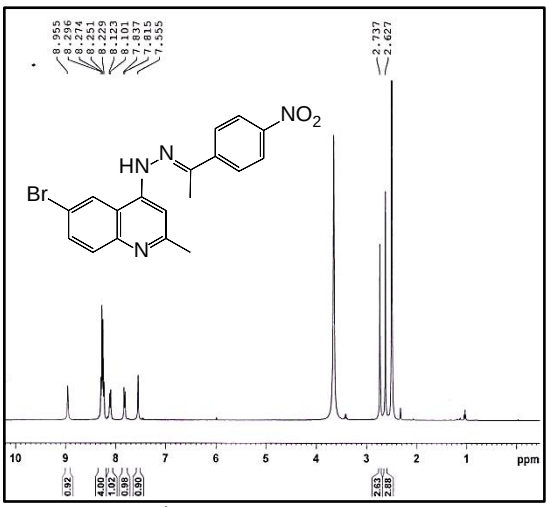

Spectrum 70. ^{1}H NMR of compound 44r

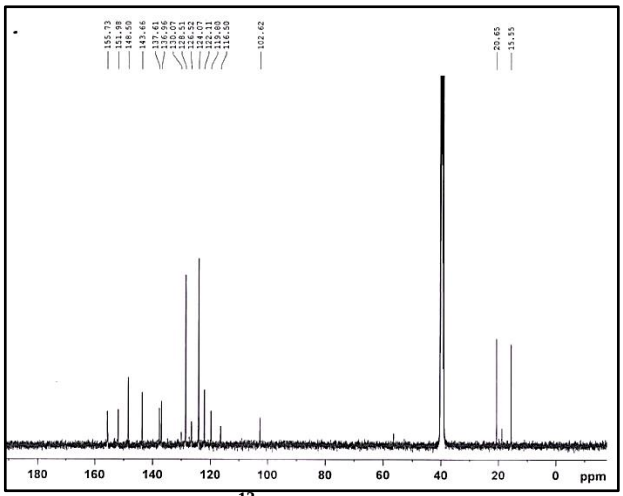

Spectrum 71. ^{13}C NMR of compound 44r

Compound 44s

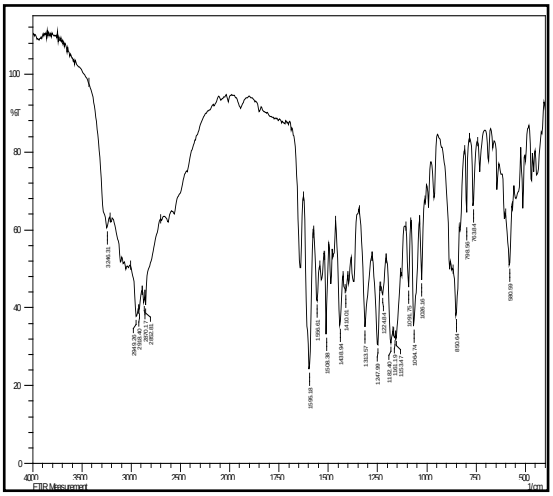

Spectrum 72. IR of compound 44s

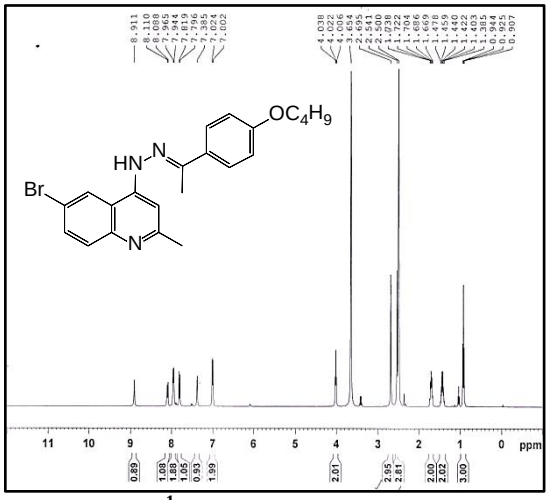

Spectrum 73. ^{1}H NMR of compound 44s

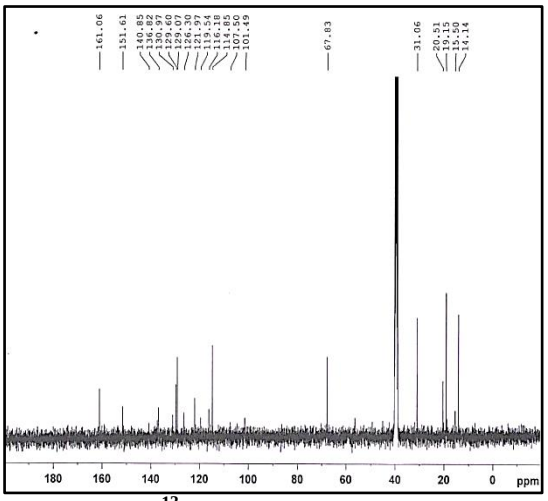

Spectrum 74. ^{13}C NMR of compound 44s

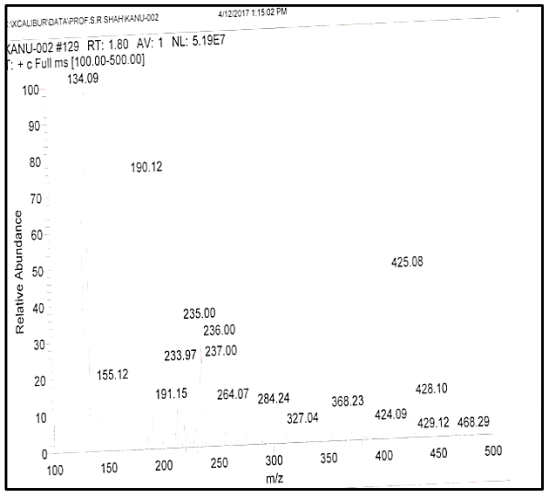

Spectrum 75. MASS of compound 44s

Compound 44t

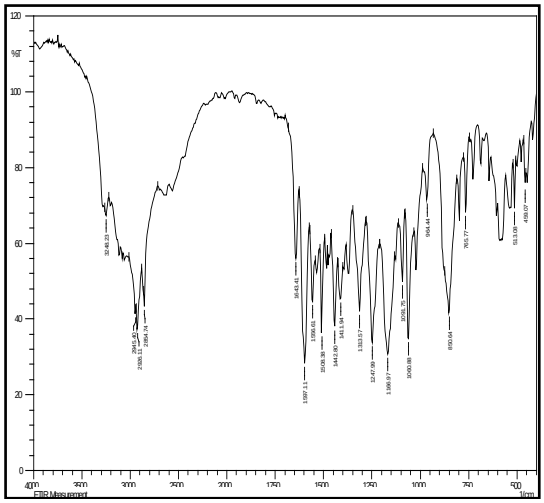

Spectrum 76. IR of compound 44t

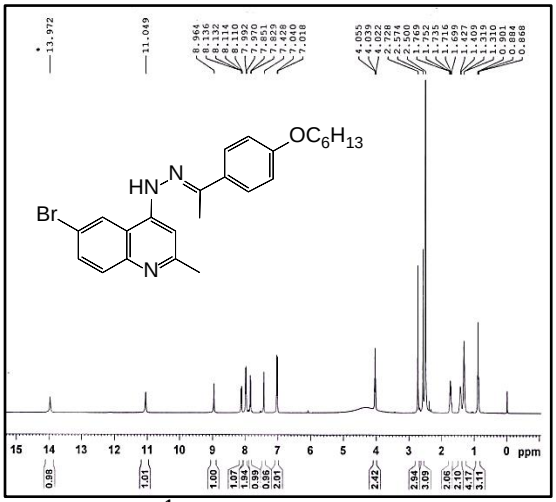

Spectrum 77. ^{1}H NMR of compound 44t

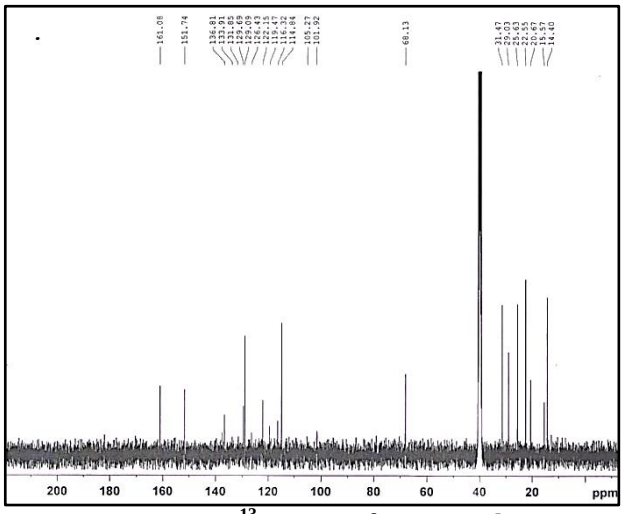

Spectrum 78. ^{13}C NMR of compound 44t

Compound 44u

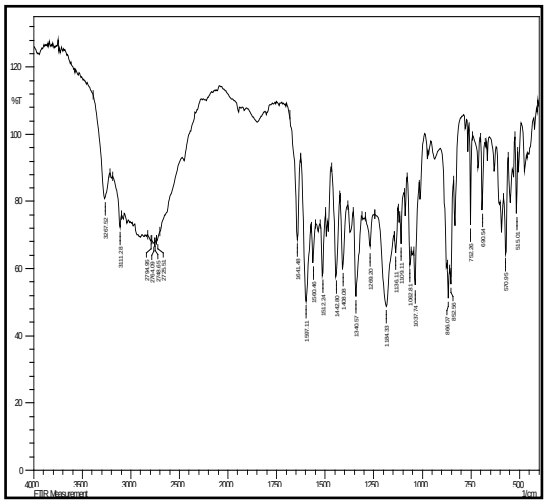

Spectrum 79. IR of compound 44u

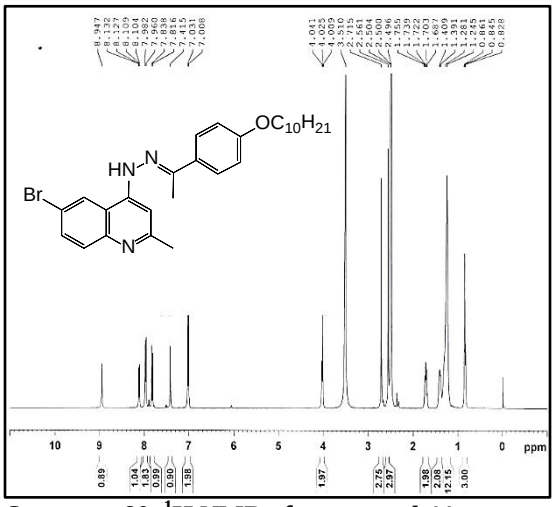

Spectrum 80. ^{1}H NMR of compound 44u

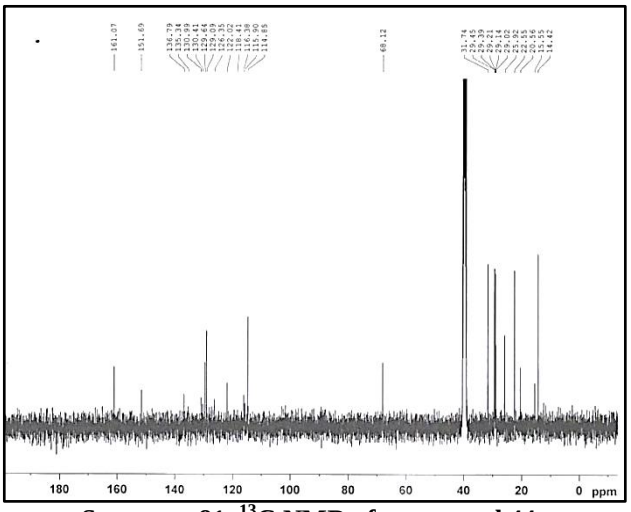

Spectrum 81. ^{13}C NMR of compound 44u

6.10 References

1 C. Avendaño and J. C. Menéndez, in *Medicinal Chemistry of Anticancer Drugs*, eds. C. Avendaño and J. C. Menéndez, Elsevier, Boston, Second Edi., 2015, p. 768.

2 J. Crombie and D. L. Longo, in *Clinical Cardio-Oncology*, ed. J. Herrmann, Elsevier, 2016, p. 416.

3 J. C. Garcia-Monco, in *Neurologic Aspects of Systemic Disease Part III*, eds. J. Biller and J. M. Ferro, Elsevier, 2014, vol. 121, pp. 1485–1499.

4 J. Heyckendorf, C. Lange and J. Martensen, in *Emerging Infectious Diseases*, eds. Ö. Ergönül, F. Can, L. Madoff and M. Akova, Academic Press, Amsterdam, 2014, pp. 420–489.

5 A. Shehzad, G. Rehman, M. Ul-Islam, W. Khattak and Y. Lee, *Brazilian J. Infect. Dis.*, 2013, **17**, 74–81.

6 C. Y. Kuo, W. H. Wang, C. H. Huang, Y. H. Chen and P. L. Lu, *J. Microbiol. Immunol. Infect.*, 2018, **51**, 88–93.

7 M. Decker, in *Design of Hybrid Molecules for Drug Development*, ed. M. Decker, Elsevier, 2017, p. 352.

8 C. Viegas-Junior, A. Danuello, V. Bolzani, E. J. Barreiro and C. Fraga, *Curr. Med. Chem.*, 2007, **14**, 1829–1852.

9 N. Kerru, P. Singh, N. Koorbanally, R. Raj, V. Kumar, P. Singh, N. Koorbanally, R. Raj and V. Kumar, *Eur. J. Med. Chem.*, 2017, **142**, 179–212.

10 Shaveta, S. Mishra and P. Singh, *Eur. J. Med. Chem.*, 2016, **124**, 500–536.

11 Y.-J. Wu, in *Progress in Heterocyclic Chemistry*, eds. G. W. Gribble and J. A. Joule, Elsevier, 2012, vol. 24, pp. 1–53.

12 T. Shiro, T. Fukaya and M. Tobe, *Eur. J. Med. Chem.*, 2015, **97**, 397–408.

13 S. Mukherjee and M. Pal, *Drug Discov. Today*, 2013, **18**, 389–398.

14 K. Kaur, M. Jain, R. P. Reddy and R. Jain, *Eur. J. Med. Chem.*, 2010, **45**, 3245–3264.

15 S. Vandekerckhove and D. Matthias, *Bioorg. Med. Chem.*, 2015, **23**, 5098–5119.

16 A. Marella, O. P. Tanwar, R. Saha, M. R. Ali, S. Srivastava, M. Akhter, M. Shaquiquzzaman and M. M. Alam, *Saudi Pharm. J.*, 2013, **21**, 1–12.

17 A. Garrido Montalban, in *Heterocycles in Natural Product Synthesis*, Wiley-Blackwell, 2011, pp. 299–339.

18 Seneca, in *Alkaloids - Secrets of Life*, ed. T. Aniszewski, Elsevier, Amsterdam, 2007, p. 334.

19 A. A. L. Gunatilaka, in *The Alkaloids: Chemistry and Biology*, ed. G. A. Cordell, Academic Press, 1999, vol. 52, p. 391.

20 J. P. Michael, in *Chemistry of Carbon Compounds*, ed. M. Sainsbury, Elsevier, Amsterdam, 1991, pp. 423–482.

21 M. Xu, T. Wagerle, J. K. Long, G. P. Lahm, J. D. Barry and R. M. Smith, *Bioorg. Med. Chem. Lett.*, 2014, **24**, 4026–4030.

22 S. Eswaran, A. V. Adhikari and N. S. Shetty, *Eur. J. Med. Chem.*, 2009, **44**, 4637–4647.

23 M. Foley and L. Tilley, *Pharmacol. Ther.*, 1998, **79**, 55–87.

24 F. Hayat, A. Salahuddin, S. Umar and A. Azam, *Eur. J. Med. Chem.*, 2010, **45**, 4669–4675.

25 A. R. Chabukswar, B. S. Kuchekar, S. C. Jagdale, P. D. Lokhande, V. V. Chabukswar, S. U. Shisodia, R. H. Mahabal, A. M. Londhe and N. S. Ojha, *Arab. J. Chem.*, 2016, **9**, 704–712.

26 S. K. Gupta and A. Mishra, *Antiinflamm. Antiallergy. Agents Med. Chem.*, 2016, **15**, 31–43.

27 M. Ferlin, G. Chiarelotto, F. Antonucci, L. Caparrotta and G. Froldi, *Eur. J. Med. Chem.*, 2002, **37**, 427–434.

28 H. Nikookar, M. Mohammadi-Khanaposhtani, S. Imanparast, M. A. Faramarzi, P. Ranjbar, M. Mahdavi and B. Larijani, *Bioorg. Chem.*, 2018, **77**, 280–286.

29 S. Singh, G. Kaur, V. Mangla and M. K. Gupta, *J. Enzyme Inhib. Med. Chem.*, 2015, **30**, 492–504.

30 H. Pun and C. Chui, *Future Med. Chem.*, 2015, **7**, 947–967.

31 V. R. Solomon and H. Lee, *Curr. Med. Chem.*, 2011, **18**, 1–21.

32 O. Afzal, S. Kumar, R. Ali, R. Kumar, M. Jaggi and S. Bawa, *Eur. J. Med. Chem.*, 2015, **97**, 871–910.

33 C. H. Tseng, C. W. Tung, C. H. Wu, C. C. Tzeng, Y. H. Chen, T. L. Hwang and Y. L. Chen, *Molecules*, 2017, **22**, 1–15.

34 N. Muruganantham, R. Sivakumar, N. Anbalagan, V. Gunasekaran and J. T. Leonard, *Biol. Pharm. Bull.*, 2004, **27**, 1683–1687.

35 K. V Sashidhara, S. Rao, V. Mishra, G. Reddy, L. R. Singh, N. Singh, Y. S. Chhonker, P. Swami and R. S. Bhatta, *Eur. J. Med. Chem.*, 2015, **89**, 638–653.

36 N. Ahmed, K. G. Brahmbhatt, S. Sabde, D. Mitra, I. P. Singh and K. K. Bhutani, *Bioorg. Med. Chem.*, 2010, **18**, 2872–2879.

37 M. C. Mandewale, U. C. Patil, S. V. Shedge, U. R. Dappadwad and R. S. Yamgar, *Beni-Suef Univ. J. Basic Appl. Sci.*, 2017, **6**, 354–361.

38 R. S. Keri and S. A. Patil, *Biomed. Pharmacother.*, 2014, **68**, 1161–1175.

39 S. M. A. Hussaini, *Expert Opin. Ther. Pat.*, 2016, **26**, 1201–1221.

40 K. Gopaul, S. Shintre and N. Koorbanally, *Anticancer. Agents Med. Chem.*, 2015, **15**, 631–646.

41 A. L. P. Candéa, M. de L. Ferreira, K. C. Pais, L. N. d. F. Cardoso, C. R. Kaiser, M. das G. M. d. O. Henriques, M. C. S. Lourenço, F. A. F. M. Bezerra and M. V. N. de Souza, *Bioorg. Med. Chem. Lett.*, 2009, **19**, 6272–6274.

42 S. Eswaran, A. V. Adhikari, I. H. Chowdhury, N. K. Pal and K. D. Thomas, *Eur. J. Med. Chem.*, 2010, **45**, 3374–3383.

43 K. D. Thomas, A. V. Adhikari, S. Telkar, I. H. Chowdhury, R. Mahmood, N. K. Pal, G. Row and E. Sumesh, *Eur. J. Med. Chem.*, 2011, **46**, 5283–5292.

44 S. Jain, A. Kumar and D. Saini, *Exp. Parasitol.*, 2018, **185**, 107–114.

45 A. Upadhyay, P. Kushwaha, S. Gupta, R. P. Dodda, K. Ramalingam, R. Kant, N. Goyal and K. V Sashidhara, *Eur. J. Med. Chem.*, 2018, **154**, 172–181.

46 I. Chaaban, O. H. Rizk, T. M. Ibrahim, S. S. Henen, E.-S. M. El-Khawass, A. E. Bayad, I. M. El-Ashmawy and H. A. Nematalla, *Bioorg. Chem.*, 2018, **78**, 220–235.

47 B. Bano, Arshia, K. M. Khan, Kanwal, B. Fatima, M. Taha, N. H. Ismail, A. Wadood, M. Ghufran and S. Perveen, *Eur. J. Med. Chem.*, 2017, **139**, 849–864.

48 P. Shah, D. Naik, N. Jariwala, D. Bhadane, S. Kumar, S. Kulkarni, K. K. Bhutani and I. P. Singh, *Bioorg. Chem.*, 2018, **80**, 591–601.

49 M. M. Ghorab, F. A. Ragab and M. M. Hamed, *Eur. J. Med. Chem.*, 2009, **44**, 4211–4217.

50 R. K. Arafa, G. H. Hegazy, G. A. Piazza and A. H. Abadi, *Eur. J. Med. Chem.*, 2013, **63**, 826–832.

51 M. Serda, D. S. Kalinowski, A. Mrozek-Wilczkiewicz, R. Musiol, A. Szurko, A. Ratuszna, N. Pantarat, Z. Kovacevic, A. M. Merlot, D. R. Richardson and J. Polanski, *Bioorg. Med. Chem. Lett.*, 2012, **22**, 5527–5531.

52 M. Bingul, O. Tan, C. R. Gardner, S. K. Sutton, G. M. Arndt, G. M. Marshall, B. B. Cheung, N. Kumar and D. S. C. Black, *Molecules*, 2016, **21**, 1–19.

53 A. Erguc, M. D. Altintop, O. Atli, B. Sever, G. Iscan and G. G. and A. Ozdemir, *Lett. Drug Des. Discov.*, 2018, 15, 193–202.

54 N. Nayak, J. Ramprasad and U. Dalimba, *J. Fluor. Chem.*, 2016, **183**, 59–68.

55 K. D. Katariya and S. R. Shah, *Der Pharma Chem.*, 2017, **9**, 94–100.

56 W. Luo, W. Q. Lu, K. Q. Cui, Y. Liu, J. Wang and C. Guo, *Med. Chem. Res.*, 2012, **21**, 3073–3079.

57 US 6,414,002 B1, 2002, 201.

58 WO 2015/008872 A1, 2015, 741.

59 WO 01/21602 A1, 2001, 362.

60 B. Hulin, D. A. Clark, S. W. Goldstein, R. E. McDermott, P. J. Dambek, W. H. Kappeler, C. H. Lamphere, D. M. Lewis and J. P. Rizzi, *J. Med. Chem.*, 1992, **35**, 1853–1864.

61 WO2004076427A1, 2004, 84.

62 G. N. Vyas and N. M. Shah, *Org. Synth.*, 1951, **31**, 90.

63 G. Nagarjuna, A. Kokil, J. Kumar and D. Venkataraman, *J. Mater. Chem.*, 2012, **22**, 16091–16094.

64 V. J. Bhanvadia, Y. J. Mankad, A. L. Patel and S. S. Zade, *New J. Chem.*, 2018, **42**, 13565–13572.

65 D. W. Bruce, V. N. Kozhevnikov, S. J. Cowling and P. B. Karadakov, *J. Mater. Chem.*, 2008, **18**, 1703–1710.